SKB TECHNICAL REPORT **97-23**

Summary of hydrogeologic conditions
at Aberg, Beberg and Ceberg

Douglas Walker[1], Ingvar Rhén[2], Ioana Gurban[1]

1 INTERA KB
2 VBB Viak

October 1997

SUMMARY OF HYDROGEOLOGIC CONDITIONS AT ABERG, BEBERG AND CEBERG

Douglas Walker1, Ingvar Rhén[2], Ioana Gurban[1]

1   INTERA KB
2   VBBViak

October 1997

SUMMARY OF HYDROGEOLOGIC CONDITIONS AT ABERG, BEBERG AND CEBERG

Douglas Walker

INTERA KB

Ingvar Rhén

VBBViak

Ioana Gurban

INTERA KB

ABSTRACT

Swedish Nuclear Fuel and Waste Management Company (SKB) is responsible for the safe handling and disposal of nuclear wastes in Sweden. This responsibility includes conducting studies into the siting of a deep repository for high-level nuclear waste. The Safety Report for 1997 (SR 97) will present a performance assessment (PA) of the overall long-term safety of a deep repository at three hypothetical sites in Sweden. These sites, arbitrarily named Aberg, Beberg and Ceberg, are based on previous SKB site characterisation programmes conducted in Sweden. This report is a compilation of existing data and descriptions for use in the hydrogeologic modelling of these hypothetical sites. It provides modelling teams with preliminary conceptual models, parameter values and uncertainties for inputs to numerical flow and transport models on the regional and site scales. Its primary objective is to provide consistent data sets and conceptual models so that the results of PA modelling will be as comparable as possible. Where possible, this report also provides alternative conceptual models that should be evaluated as part of the modeller's sensitivity analysis.

Aberg will use data from the Äspö site, which is the most recently and thoroughly investigated site in the SKB program. Äspö is also the site of the intensive investigations associated with the Äspö Hard Rock Laboratory (HRL). Beberg is based on Finnsjön, perhaps the second-most thoroughly investigated site in the SKB program. Finnsjön was also the subject of SKB 91, a previous PA modelling study. The last site, Ceberg, is based on data taken from Gideå, one of the oldest SKB site characterisation studies. Although a great deal of data exists for Gideå, it is the least thoroughly investigated site of the three sites.

The information contained in this report is taken from several key sources, including the SKB SICADA database, the Swedish Geological Survey (SGU) well database, the SKB Geographic Information System (GIS), the Swedish Land Survey (LMV) databases, and published SKB reports.

SAMMANFATTNING

SR 97 utgör en av flera redovisningar av den långsiktiga säkerheten för inkapslat bränsle och annat långlivat avfall, deponerat i djupförvar. Syftet med SR 97 är att visa säkerhetsfunktionen för de geologiska förhållanden som kan förekomma inom tre möjliga förläggningsplatser, i svensk, kristallin berggrund, och för den försvarsutformning som anpassats till dessa platser. De tre områdena har kallats Aberg, Beberg och Ceberg, vilka baserar sig på data från tidigare platsundersökningar utförda av Svensk Kärnbränslehantering (SKB). Denna rapport är en sammanställning av befintliga data och beskrivningar som ska användas i de hydrogeologiska modelleringarna av de tre hypotetiska områdena. Den syftar att ge modelleringsgrupper preliminära konceptuella modeller, parametervärden samt osäkerheter för indata till numeriska flödes- och transportmodeller, i regional och lokal skala. Det primära målet är att ge överensstämmande dataserier och begreppsmässiga modeller, så att resultaten av analyserna blir så jämförbara som möjligt. Om möjligt ger denna rapport också alternativa konceptuella modeller, vilka kan användas för känslighetsanalys.

Aberg använder data från Äspö, vilken är den senaste och mest grundligt undersökta området (Äspölaboratoriet). Beberg baseras på data från Finnsjön, som kanske är det näst mest undersökta området inom SKB programmet. SKB 91 var en platsspecifik säkerhetsanalys för just Finnsjön. Det sista området, Ceberg, baseras på data från Gideå, ett av de äldsta områdena inom SKB:s platsundersökningsprogram. Även om det finns en hel del data från Gideå, är området det minst grundligt undersökta av de tre nämnda.

Informationen i denna rapport har sitt ursprung från flera olika källor vilka inkluderar SKB:s SICADA databas, Sveriges Geologiska Undersöknings (SGU) brunnsarkiv, SKB Geografiska Informations System (GIS), Lantmäteriverkets (LMV) databaser samt publicerade SKB rapporter.

TABLE OF CONTENTS

LIST OF FIGURES

xi

LIST OF TABLES

1. INTRODUCTION

1.1. PURPOSE AND SCOPE

Swedish Nuclear Fuel and Waste Management Company (SKB) is responsible for the safe handling and disposal of nuclear wastes in Sweden. This responsibility includes conducting studies into the siting of a deep repository for high-level nuclear waste. The Safety Report for 1997 (SR 97) will present a performance assessment (PA) of the overall long-term safety of a deep repository at three hypothetical sites in Sweden. One component of these PA studies is hydrogeologic modelling to examine the possible transport of radionuclides from the emplaced waste packages through the host rock to the accessible environment.

The three hypothetical sites are named arbitrarily Aberg, Beberg and Ceberg, each of which is based on data from previous site characterisation studies conducted by SKB. These are:

- Aberg, which is based on the Äspö Hard Rock Laboratory in southern Sweden;

- Beberg, which is based on investigations at Finnsjön, in central Sweden; and

- Ceberg, which is based on investigations at Gideå, in northern Sweden.

This report is one of many in support of SR 97, and is a compilation of existing data and descriptions for each of three sites for use in the hydrogeologic modelling. It is intended to provide modelling teams with conceptual models, parameter values and uncertainties for inputs to numerical flow and transport models on the regional and site scales. Specifically, this report:

- reviews the investigations at the sites and existing reports,

- summarises the current knowledge of conditions and uncertainties regarding the hydrogeology of the sites,

- updates the data and analyses to correct known errors and inconsistencies, and

- provides estimates of the block-scale parameters for use in modelling the sites at the Regional and Site scales.

In short, this report is a data handbook for hydrogeologic modelling at the Aberg, Beberg and Ceberg sites. Its primary objective is to provide consistent data sets and conceptual models so that the results of modelling will be as comparable as possible. One limitation to comparing PA modelling studies for alternative sites is that the site characterisation studies and analyses of data are frequently conducted at different times for different

goals. Although the bias and error of site investigations are never fully known, a consistent analysis of the data and presentation of conceptual models will at least help confine the differences to the sites themselves.

The parameters reported here are summarised and adapted from the interpretations of other investigators. For example, no new measurements were taken, and the study uses the interpreted hydraulic conductivities found in the SICADA database. Where appropriate, interpretative methods used by other investigators are discussed along with the consequences of those methods. Although the complete reanalysis of basic field data is beyond the scope of this report, the scaling calculations and geostatistical modelling are original and are discussed in the appendices. The introductory sections of this report are original and were written by Doug Walker of INTERA. Much of the remaining sections have been adapted from existing reports by Doug Walker, assisted by Ioana Gurban of INTERA. Doug Walker edited and summarised Section 2.0 from Sections 6.0 and 8.0 of Rhén, et al. (1997), originally written by Ingvar Rhén of VBBViak.

Although this report briefly discusses transport parameters (e.g., porosities, dispersivities), a separate report compiles transport parameters for SR 97:

- Andersson J, Elert M, Hermanson J, Moreno L, Gylling B, and Selroos J–O, 1997. Derivation and treatment of the flow wetted surface and other geosphere parameters in the transport models FARF31 and COMP23 for use in safety assessment. SKB R-97-XX (in publication, SKB report)

1.2. APPROACH

Great uncertainty exists for all subsurface investigations and the results of PA modelling must reflect that uncertainty. To that end, this report provides a probabilistic description of the input parameters, acknowledging the observed and assumed uncertainties of the data. However, even these descriptions implicitly or explicitly include limiting assumptions (e.g., lineaments as conductive features, lognormally distributed hydraulic conductivity). Where possible, this report also provides alternative conceptual models that should be evaluated as part of the modeller's sensitivity analysis.

The material properties and concepts presented here focus mainly on 3-D numerical continuum models such as PHOENICS, NAMMU, and HYDRASTAR. Consequently this report emphasises block-scale parameters for numerical solutions such as block hydraulic conductivity, rather than transmissivity or fracture apertures. Modellers should be aware that these parameters are inherently scale dependent, and may need to be adapted for use in particular models. This scale dependency is addressed in Section 1.6, which presents and discusses scaling relationships developed from site-specific measurements. The reader should also note that this report does not specifically address parameters used by Discrete Feature (DFN) or Channel Network models (CN), even though the general hydrogeologic information may still be useful to modelling teams using such approaches.

2

1.3. PRIMARY SOURCES OF INFORMATION AND ANALOGUE DATA

The information contained in this report is taken from several key sources. Site-specific interpreted hydraulic conductivity and salinity measurements were taken directly from the SKB SICADA database. Regional specific capacity measurements were taken directly from the Swedish Geological Survey (SGU) well database. Topographic maps and digital terrain models (DTM) were taken from the SKB Geographic Information System (GIS) which includes several of the Swedish Land Survey (LMV) databases. The overall approach to analysing and modelling the data is taken from:

- Rhén, I (ed.), Gustafson G, Stanfors R, and Wikberg P., Äspö HRL - Geoscientific evaluation 1997/5. Models based on site characterisation 1986-1995. SKB TR 97-06

Aberg will use data from the Äspö site, which is the most recently and thoroughly investigated site in the SKB program. This is mostly the result of the intensive site and regional scale investigations associated with the Äspö Hard Rock Laboratory (HRL), an international centre for research related to disposal of nuclear wastes in fractured crystalline rock. It also has abundant general regional information (e.g., SGU summary reports, SMHI data, etc.).

Beberg is based on Finnsjön, perhaps the second-most thoroughly investigated site in the SKB program. Finnsjön has been the subject of two investigations, the first being the KBS site characterisation campaign (1977 to 1983) and the second being the Fracture Zone project (1985 to 1988). Like Äspö, Finnsjön general regional information is relatively abundant. Other sources of information in the region are the Dannemora iron mine and SKB studies associated with the Swedish Final Repository for reactor operational waste (SFR) at Forsmark.

The last site, Ceberg, is based on data taken from Gideå, one of the oldest SKB site characterisation studies. Although a great deal of data exists for Gideå, it is the least thoroughly investigated site of the three sites. The availability of general geologic information at Gideå is limited relative to the Finnsjön and Äspö regions because of the lower population of Northern Sweden. Although the Gissjö hydropower tunnel provides some information on fracture orientation and lineaments, its shallow depth limits its usefulness.

Modellers may require parameters that have not been measured at the site of interest. If site-specific measurements are not explicitly provided, data from analogue sites may be used for scoping calculations and alternative case models. Potentially useful analogue site data can be found in the following summary reports:

- Rhén, et al., 1997 (as sited above).

- Andersson P, 1995. Compilation of tracer tests in fractured rock. SKB Progress Report 25-95-05.

- Elert M, 1997. Retention mechanisms and the flow wetted surface – implications for safety analysis. SKB R-97-XX (in publication, SKB report).

- Olsson O (ed), 1992. Site Characterisation and Validation–Final Report. SKB Technical Report Stripa Project 91-22.

- Winberg A, 1989. Project – 90. Analysis of variability of hydraulic conductivity data in the SKB database GEOTAB. SKI TR 89:12.

Note: Analogue data should not take precedence over site-specific measurements or the base-case models provided in this report. As far as possible, analogue data should be taken only from sites that are similar to the site of interest, e.g., similar geology, hydrology, geochemistry, tectonics, etc.

1.4. REPORT STRUCTURE

As well as summarising the site characterisation studies that provide data for SR 97, this report also describes the methods used and documents the data sources for the study. This report is divided into the following sections:

1. Introduction

This section outlines the purpose and scope of SR 97 and this compilation. It also presents the modelling approach and a suggested approach to the scale dependency of hydraulic properties.

2. Aberg, 3. Beberg, and 4. Ceberg

Each of these sections summarise the regional and site scale characteristics for use in hydrogeologic modelling of Aberg, Beberg, and Ceberg, respectively.

5. Summary and Intersite Comparison

This section presents an overview of the 3 sites, and presents a brief comparison of site characteristics and site characterisation programmes.

Appendices A, B, and C

Each of these discusses the data reduction and statistical analysis performed for the Aberg, Beberg and Ceberg sites, respectively. These include the analysis of the SGU data, analysis of the on-site packer tests, and geostatistical modelling. The appendices also include SICADA log files and summary tables for parameter sources.

Appendix D

This appendix summarises the methods and software used in the analyses, including the regression relationships for upscaling and for reducing the data. It also presents a brief comparison of alternative approaches to upscaling. This is followed by parameters for the excavation disturbed zone (EDZ), which are the same for all three sites.

1.5. CONCEPTUAL MODELS

SKB has previously investigated a number of locations in Sweden for possible disposal sites and for experimentation. Most of these sites have fractured crystalline host rocks, which are broadly described as volumes of largely intact, competent rock mass (rock domains, denoted RD), interrupted by conductive fractured zones (conductor domains, or CD). It should be noted from the outset that this distinction is somewhat arbitrary, since even in the rock domain the flow of groundwater is dominated by flow in fractures. In practice, conductive fracture zones are delineated from the rock mass by contrasts in hydraulic conductivity, geophysical anomalies and topographic lineaments. This two-domain representation is well suited to continuum models, which are the focus of this report.

It is usually difficult to construct a single numerical model with sufficient extent to include the regional flow system and still have adequate detail to address site-scale variability. Consequently this report assumes a nested approach will be used for SR 97, using a site-scale model within a regional model (see Section 1.6). The regional scale models cover an area of approximately 100 to 200 km^2, and the site-scale models cover an area of approximately 1 to 6 km^2. In addition to the regional and site-scale concepts, the expected or base-case model is presented, along with suggested alternative models for uncertainty analysis. Rhén et al. (1997) introduced a system of abbreviations to organise the domains and scales of the various conceptual models. Table 1-1 summarises the domains and conceptual models at both site and regional scales.using these abbreviations.

Table 1-1. Summary of SR 97 Conceptual Models

Code	Mode
	Regional Scale (1)
	Rock Domain
RRD1	Hydraulic conductivity based on SGU data, depth zones from on-site packer tests
RRD2	Variation for hydraulic conductivity correlated to rock type
RRD3	Variation for anisotropic hydraulic conductivity
	Conductor Domain
RCD1	Regional lineaments as conductive fracture zones, properties and depth zones from on-site packer tests
RCD2	Variation case for alternative depth zonation
RCD3	Hypothetical / Alternative lineament interpretation
	Site Scale (2)
	Rock Domain
SRD1 to SRD5	Hydraulic conductivity from on-site packer test data (1-5 are regions/rock types that apply only to Äspö)
SRD6	Hydraulic conductivity from on-site packer test data
SRD7	Variation case for anisotropy
	Conductor Domain
SCD1	Mapped fractured zones, properties inferred from site packer test data and borings
SCD2	Hypothetical / Alternative fracture zones
	Excavation Disturbed Zone (EDZ)
EDZ1	Hydraulic conductivity of rock surrounding the tunnel unchanged
EDZ2	10X increase in hydraulic conductivity parallel to tunnel axis in 25cm of rock surrounding tunnel (Appendix D.8)

Notes:
(1)   Regional hydraulic conductivity upscaled to numerical model block scale using the Äspö regression equation, calibrated to observed heads and recharge/discharge patterns.
(2)   Site hydraulic conductivity upscaled to numerical block scale using Äspö regression equation, calibrated to observed heads and regional boundary fluxes. Covariance of hydraulic conductivity upscaled via INFERENS.

1.6. PROBLEMS OF SCALE

Many authors in physics and engineering have noted that properties measured at one scale are inadequate for modelling processes at a different scale. This is particularly important for numerical models because they must average or upscale the small-scale measurements of hydraulic properties to the numerical block scale, and use mixing coefficients to account for sub-scale variability. The problem is compounded by the multiscale variability of host rocks, mixed scales of measurement, the use of variable size blocks, and nested modelling approaches. The scale problem in stochastic hydrogeology focuses on hydraulic conductivity, but many media properties demonstrate scale dependency. The scale problem is widely acknowledged but its solution is not agreed upon and it remains the subject of intense research (Renard and de Marsily, 1997; Wen and Gomez-Hernandez, 1996). In spite of this ambiguity, numerical groundwater models for SR 97 require an upscaling method such that block properties will be representative of the media of interest.

This approach assumes that the available computer resources are inadequate to build regional-scale numerical models with grids of sufficient detail to represent the observed small-scale variability of hydraulic properties. The proposed solution is a nested modelling approach, where a regional model of coarse resolution provides the expected boundary fluxes and heads for a site-scale model of much finer resolution (Ward, et al. 1987). Ideally, the regional scale model could be homogeneous continuum model, providing the expected boundary fluxes via an effective hydraulic conductivity. The site scale model would be a stochastic continuum model, using conditionally simulated hydraulic conductivity fields to simulate the flow field variability for transport modelling.

1.6.1. Hydraulic Conductivity

1.6.1.1. Regional scale

Stochastic continuum theory suggests that, under certain conditions, there exists an effective hydraulic conductivity, K_e, that satisfies:

$$\langle \bar{q} \rangle = -K_e \nabla \langle \bar{h} \rangle$$

Where:

$\langle \bar{q} \rangle$ = the expected flux over the domain

$\nabla \langle \bar{h} \rangle$ = the expected gradient

This K_e is a construct of stochastic continuum theory, valid for an infinite, statistically homogeneous domain under uniform, steady flow (Dagan, 1986). In practice and in numerical experiments, the infinite domain requirement for K_e is approximately satisfied for domains $L_e > 10\lambda$, where λ is the integral scale of the spatial covariance. Note that K_e is otherwise

independent of the size of the field. K_e is useful for SR 97 in that it can be used to estimate the expected value of the flux in a smaller domain (Rubin and Gómez-Hernández, 1990). This suggests that a regional model with a uniform hydraulic conductivity of K_e could be used to determine the boundary fluxes of a site-scale model subdomain.

The problem lies in determining K_e. Several authors have offered approximate analytical solutions for K_e, including the case of 3-D flow with anisotropic, nonstationary hydraulic conductivity (Gutjahr et al., 1978; Gelhar, 1993). Such solutions were derived under a number of restrictive assumptions that include:

- uniform flow in a porous media;

- mildly nonstationary, lognormally-distributed hydraulic conductivity;

- low variance ($\sigma^2_{lnK} < 1.0$);

and others. Although these solutions have demonstrated remarkable robustness to violations of the underlying assumptions (e.g., Neuman and Depner, 1988), it is unknown if they are applicable to hydrogeologic systems of interest in SR 97. At the Äspö site, for example, the rock mass is a fractured media with non-lognormally distributed hydraulic conductivities of variance $\sigma^2_{lnK} = 16.0$ (Liedholm (ed.), 1991a). The departures from the underlying assumptions and the abrupt changes in hydraulic conductivity represented by the deterministic fracture zones may have unknown effects (Gelhar, 1993).

One alternative is suggested by the observed scale dependency of the geometric mean of hydraulic conductivity at the Äspö site. Rhén, et al. (1997) analysed the Äspö data and presented a linear relationship for the geometric mean of hydraulic conductivity versus packer test interval. For each test interval scale, L_m, they computed the geometric mean of interpreted hydraulic conductivity, K_g. This was normalised for each borehole as K_g/K_{bh}, the relative hydraulic conductivity. As shown in Figure 1-1, they plotted and regressed $Log_{10}(K_g/K_{bh})$ versus $Log_{10}(L_m)$, arriving at the regression equation:

$$Log_{10}K_{gu} = Log_{10}K_{gm} + 0.782(Log_{10}L_u - Log_{10}L_m)$$

Where:

K_g = geometric mean of hydraulic conductivity (m/s)

L = length scale (m)

The subscripts m and u refer to the measurement and upscaled values, respectively (note that K_g is identical to the arithmetic mean of the Log_{10} of hydraulic conductivity). Note that this relationship assumes that the measurement scale is equal to packer interval, L_m. It can be shown that this regression equation gives results that are weakly comparable to the approximate solutions of Gutjahr et al. (1978), commensurate with the regression's wide confidence interval (Appendix D.6). The relationship

should not be extrapolated beyond the range of measured hydraulic conductivities (approximately 3m to 300m). Such multiscale data are not available at Gideå and Finnsjön in sufficient density to establish similar relationships for those sites.
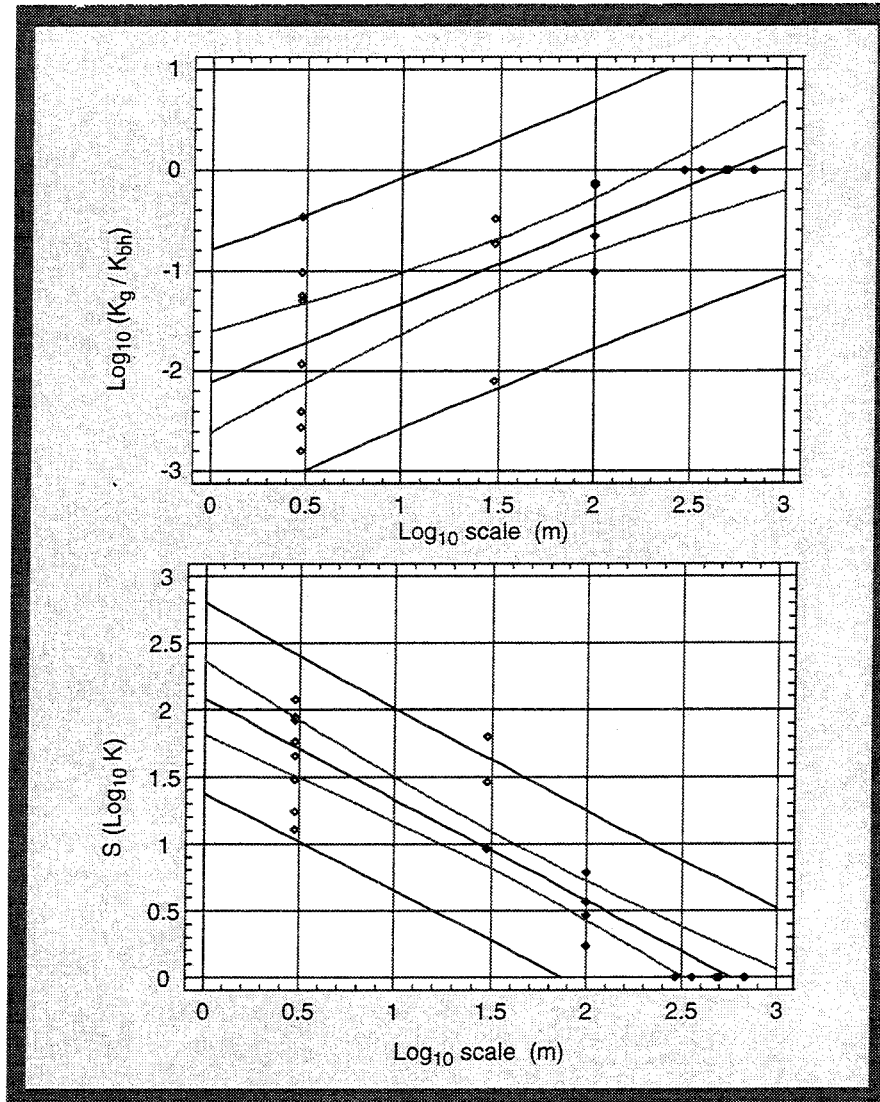
Figure 1-1. Scale dependency of the geometric mean and the standard deviation of Log_{10} hydraulic conductivities (m/s). K_{bh} is hydraulic conductivity of the largest scale test in each of the common borehole sections (from Rhén et al, 1997). Inner pair of lines is 95% CI for mean, outer pair of lines is 95% CI for prediction.

The analytical solutions of Gutjahr et al. (1978) do not explicitly require a length scale L_e for determining K_e. However, this scale is implicit in the sampling grid and in the inference of the spatial covariance of hydraulic conductivity (Gelhar, 1993). Unlike the analytical solutions, the regression approach requires an explicit length scale for K_e. If we use the previously cited practical minimum of $L_e > 10\lambda$, then the covariance model determined for Äspö (Appendix A) gives $L_e = 170m$. Similarly, the covariances cited

9

by Niemi (1995) and LaPointe (1994) give 70m $< L_e <$ 260m, suggesting that L_e be on the order of 10^2 m. Figure 1-1 appears to qualitatively agree with this estimate, since the Log_{10} (K_g/K_{bh}) and the standard deviation stabilise at approximately this length scale. However, this behaviour may be purely an artifact of the comparison: Log_{10} K_g/K_{bh} and the standard deviation stabilise because the maximum scale of K_{bh} is 300 to 500m for most of the boreholes, thus no change beyond this scale is recorded. Longer test intervals might indicate a continuously increasing K_g/K_{bh}.

This regression approach also neglects the possible anisotropy of hydraulic conductivity, which would require K_e to be treated as second rank tensor. Treating K_e as a scalar for upscaling and applying an anisotropy ratio afterwards ignores the relationship between the anisotropic covariance and anisotropic tensor of hydraulic conductivity (Gelhar, 1986). For example, it can be shown that an anisotropic covariance cannot exist without an anisotropic tensor for hydraulic conductivity (Indelman and Dagan, 1993).

Plainly, the uncertainty of the Äspö regression and the violated assumptions of the analytical solutions are unsatisfactory. As an interim solution to this problem for SR 97, this study suggests calibration of K_e by comparing the regional modelling results to observed hydraulic head distribution the patterns of recharge and discharge. Such joint use of calibration and effective parameters has been used in previous applications of the stochastic continuum approach (Gelhar, 1986; Neuman and Depner, 1988). The calibration is anticipated to be nonunique and modellers should conduct a sensitivity analysis of K_e versus the boundary fluxes of the site-scale subdomain. The Äspö regression relationship should be used as starting value for the calibration at all three sites. The depth trends and conductive structures should also be included in the regional models to include the important effects of large-scale trends and abrupt changes in hydraulic conductivity (Gelhar, 1993).

1.6.1.2. Site scale

As discussed above, the site scale numerical models are proposed to be stochastic continuum models using means and covariances (and trends, if necessary) that represent the inferred characteristics of each site. Because the scale of hydraulic conductivity variability is smaller than the anticipated numerical block sizes, we are forced to determine an appropriate block hydraulic conductivity, K_b. In addition to this, spatially correlated random variables require that the covariance be upscaled (regularised from the measurement scale to the block scale) in a manner compatible with K_b.

The available literature on this subject offers a variety of possible solutions, but presents no clear recommendation or agreement on the criteria that K_b must meet (Wen and Gómez-Hernández, 1996). Several recent proposals show promise for porous media (e.g., Indelman and Dagan, 1993), but these have not yet been thoroughly tested and may not be adequate for fractured media. Recent research using DFN approaches and inverse modelling shows promise but is still under development (LaPointe et al., 1995; Vomvoris, 1996).

The SKB stochastic continuum model, HYDRASTAR, uses a heuristic averaging rule to determine K_b. The algorithm uses an arithmetic mean of hydraulic conductivity, corrected for packer length and borehole diameter, as a moving average to upscale the hydraulic conductivity measurements to the block scale. HYDRASTAR then directly simulates conditional fields of K_b using a regularised covariance (Norman, 1992a and 1992b). A companion code, INFERENS (Geier 1993a and 1993b) uses the same regularisation algorithm with universal kriging to infer upscaled models for the spatial covariance and trends of K_b. Although innovative for its time, the HYDRASTAR upscaling algorithm has been criticised because (LaPointe, 1994; Lovius, 1994):

- The method assumes a constant test volume (support scale) derived from the packer interval, an assumption which disagrees with current understanding of test hydraulics.

- Although the method has been adapted to account for the measurement limits, the adaptation requires the data to be lognormally distributed (i.e., multivariate lognormal).

- The results may not be compatible with the Äspö scale dependency of Rhén et al. (1997)

The lack of acceptable alternatives compels using the HYDRASTAR regularisation approach to determine the trends and the regularised covariance of K_b. As suggested by Renard and de Marsily (1995), calibration is an upscaling algorithm in that it attempts to find values of K_b that satisfies the observed flow system. This study recommends using the Äspö regression relationships to determine a preliminary value of the geometric mean of K_b. This value should be adjusted so that the average boundary fluxes of the site-scale model approximately reproduce the fluxes calculated by the regional model (i.e., adjust the geometric mean of K_b so that continuity is satisfied in an average sense between the regional and site-scale models). We strongly recommend research into this problem and the development of alternatives.

1.6.1.3. Summary of Approach to Upscaling of Hydraulic Conductivity

As discussed above, this study suggests the following approach to the upscaling of hydraulic conductivity for the regional and site-scale models at all three sites:

Regional Scale:

- Large-scale discontinuities (e.g., fracture zones and rock types) should be treated as step changes (domains) in hydraulic conductivity.

- The regional scale model should have a uniform hydraulic conductivity of K_e, the effective hydraulic conductivity, within each domain.

- The preliminary values of K_e should be determined by applying the Äspö regression relationship to the on-site packer tests.

11

- This K_e should be calibrated so that the model simulates the observed heads and the patterns of recharge and discharge with reasonable accuracy.

Site-Scale:

- The site-scale model should be a stochastic continuum model, with boundary heads taken from the regional model.

- The geometric mean of K_b, the block hydraulic conductivity of the site-scale model, should be determined by applying the Äspö regression relationship to the on-site packer tests.

- This K_b should be calibrated so that the model simulates the observed heads and, as an average over model realisations, reproduces the regional model boundary fluxes with reasonable accuracy.

- The covariance of K_b should be determined by applying the HYDRASTAR regularisation algorithm (or alternatively, the INFERENS implementation of this algorithm. See Appendix D.3)

1.6.2. Lineaments and Fractures

The choice of map scale and resolution imposes arbitrary limits on the minimum detected length of lineaments and the accuracy of the mapped location. Askling (1997) estimated this to be a minimum length of 200m and a location error of 125m for the Gideå lineament map. The map scale and resolution also influence the designation as well expressed or less well expressed and the inferred widths of the lineaments.

The separation of regional, site and block scale lineaments is purely arbitrary. Some authors have suggested that a self-similar continuum of structures exist from microscopic fractures to megascopic regional fault zones (Dershowitz et al., 1992). Similarly, the mapping of fractures on outcrops and in tunnels is in many cases influenced by arbitrary lower and upper limits (Hermanson, 1995). This study is restricted somewhat by current techniques, modelling approaches and the lack of a unifying model for scaling structure and hydraulic conductivity in fractured media.

For this study, it is anticipated that some of the well-expressed lineaments might be modelled individually as conductive fractured zones forming the boundaries of the modelled domain. To be consistent with previous modelling studies, the remaining well expressed and less-well-expressed lineaments should be averaged into the model grid block hydraulic conductivities using the classical formulas (Bear, 1972).

1.6.3. Other Properties

Various other properties of interest for hydrogeologic modelling may also exhibit scale dependence, but the relationships are very poorly understood. Many of these are transport parameters that appear to be model-fitted and therefore are model-specific (Andersson, 1995). Several general relationships have been suggested but should not be used if site-specific measurements at the scale of interest are available. Compilations of

12

analogue site results are found in Andersson (1995), Winberg (1996), and Elert (1997).

Kinematic porosity (flow porosity), n_e, Rhén et al. (1997) have suggested the following regression equation:

$$n_e = 34.87K^{0.753}$$

Where:

n_e = kinematic porosity = (effective pore volume)/(total volume)

K = hydraulic conductivity (m/s)

This regression equation was based on data from tracer experiments in fractured zones at the Äspö HRL. Because K is thought to be scale dependent, the above relationship implies that so is n_e. The relationship is very uncertain, however, and was suggested as a scoping calculation to be used only if site-specific data were unavailable (Rhén et al., 1997).

Solutions of the advection-dispersion equation rely on a mixing parameter, the coefficient of hydrodynamic dispersion, D. Although models differ widely on how this parameter is treated, its definition is (2-dimensional, principal axes aligned in x and y, flow in x only, negligible diffusion):

$$D_L = \alpha_L v_x$$
$$D_T = \alpha_T v_x$$

Where:

D_L, D_T = longitudinal and transverse coefficients of hydrodynamic dispersion (m^2/s)

α_L, α_T = longitudinal and transverse dispersivities, respectively (m)

v_x = pore velocity (m/s)

(adapted from Bear, 1972). The apparent increase of α_L with increasing transport distance is well documented (Pickens and Grisak, 1981). Gelhar and Axness (1983) suggest that after a transport occurs over sufficient distance, α_L reaches an maximum value of A_L, the asymptotic macrodispersivity (isotropic covariance, $\alpha_L < \lambda$):

$$A_L = \frac{\sigma_{\ln K}^2 \lambda}{\gamma^2}$$

where γ^2 is approximately 1.0. This solution is only approximate and thought to be valid for $\sigma^2_{\ln K} < 1.0$, but has been repeatedly verified numerically and in field experiments. An extension of this approach has been made to single fractures (Gelhar, 1987), but it is unknown how well the above solution applies to 3-dimensional fractured media of high variance.

13

Flow wetted surface, a_r, is the contact area between flowing water-wetted fracture surface per unit rock volume. Elert (1997) compiled values of a_r cited by various studies, finding a range of over five orders of magnitude (0.001 to 100). It appears to be a model-dependent fitting parameter. If kinematic porosity is scale dependent, then it might be speculated that flow wetted surface must be scale dependent as well, but this is unknown.

1.6.4. Uncertainties

The hydraulic conductivity values are based on the interpretation of packer tests and well tests performed by others. These interpretations are based on assumed flow models and, if such models are inappropriate for the flow system being measured, order-of-magnitude errors may result (Geier et al., 1996). This study has not verified the hydraulic test methods and interpretations, nor made any attempt to quantify measurement errors. It is therefore possible that isolated or systematic errors in the interpreted parameter values have led to errors in the inferred models presented in this report.

The upscaled averages and regularised covariances are based on the assumption of a uniform test scale (support volume) derived from the packer interval. In practice, the volume of tested rock is a function of the hydraulic properties and test duration. This might introduce additional errors into the upscaling and regularisation. Overall the determination of K_e and K_b in the case of fractured media is still very much a research topic. Various authors have commented on the effects of boundaries on the stochastic continuum approach. It is unknown what (if any) effect the nested modelling approach will have on the stochastic continuum results as a result of introducing an additional set of boundaries.

Regional lineaments are, in reality, one-dimensional features inferred to be the topographic expression of a bedrock feature. Such features are frequently fractured rock zones with elevated transmissivity in comparison to the surrounding rock mass. However, the mapping of lineaments is highly subjective, and the ultimate geologic cause is unknown until characterised in the field. Even if a lineament can be identified as a fractured zone, factors such as rock type, age, degree of mineralisation, movement, weathering, etc. all may dramatically alter the hydraulic conductivity of fractured zones. The nature, width and extent of a lineament should therefore be considered uncertain.

2. ABERG

Aberg takes its data from the Äspö site, which is located in southern Sweden, in the northern part of Småland (Figure 2-1). It is just off the Swedish coast in Baltic Sea, near Oskarshamn nuclear power plant, in an area corresponding to LMV map sheets Vimmerby 6G SÖ and NÖ. A 25km x 25km region centred on the site is characterised by low topographic relief and a mosaic of shallow coastal waterways and islands. The altitude of the region ranges from sea level to approximately 60 masl. From a hydrogeologic perspective, the region is notable for the intrusion of saltwater from the Baltic Sea. The low relief, rate of landrise and the coastal location result in a continuously changing pattern of coastline and recharge.
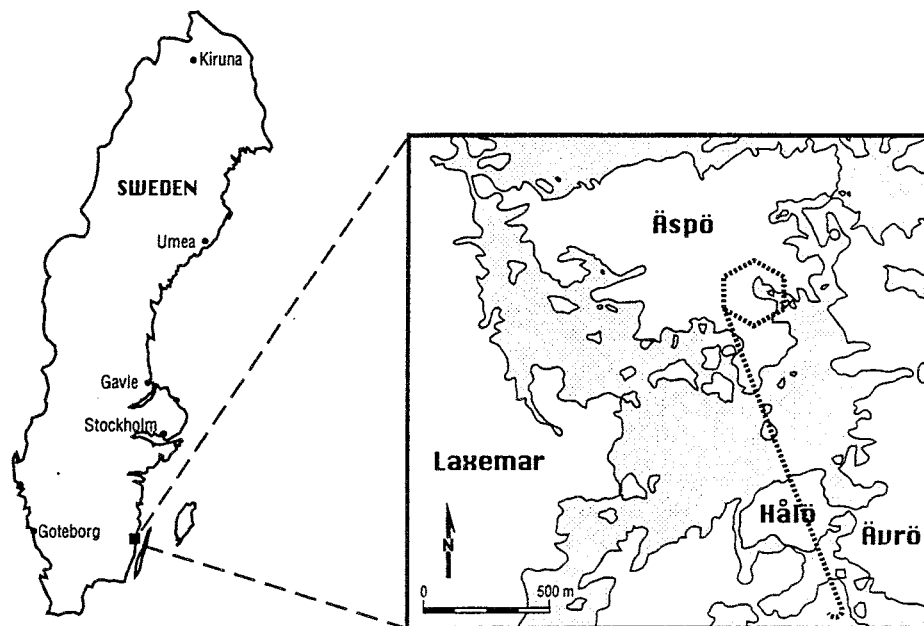
Figure 2-1. Location of the Äspö site and Hard Rock Laboratory.

The Äspö site is also the location of the Äspö Hard Rock Laboratory (HRL), an underground research facility owned and operated by SKB. The HRL lies beneath Äspö island and consists of a vertical elevator shaft and horizontal access tunnels connected to a descending spiral tunnel that extends to a depth of over 450m below ground surface (Figure 2-2). It is operated by SKB for the purpose of investigating geological, geochemical, and hydrogeological phenomena that affect the design and operation of deep repositories for underground disposal of nuclear waste. Nuclear waste management organisations and investigators from several countries participate in research conducted at this facility (SKB, 1996).
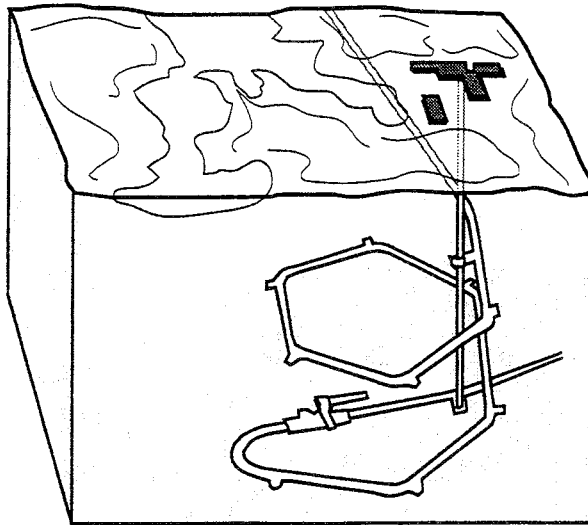
Figure 2-2. Äspö Hard Rock Laboratory.

This compilation of data and conceptual models for Äspö has taken advantage of information from the HRL tunnel in various ways. Hydraulic tests in the probeholes drilled during construction are used infer hydraulic properties of the area south of Äspö (e.g., SRD4). The probehole data and fracture mapping within the tunnel were used with borehole data to infer the direction and magnitude of anisotropy for hydraulic conductivity. The water table response to the construction of the tunnel demonstrated that the upper levels of Northern Äspö are poorly connected to the underlying and southern areas of Äspö. The construction of the tunnel also revealed an additional structure, NNW-7. Thus, the HRL tunnel has greatly contributed to the understanding of this site. Table 2-1 summarises the site characterisation studies at Äspö.

2.1. PRIMARY SOURCES OF INFORMATION

The information in this section is taken from several key sources in addition to the SKB and SGU databases. Much of the descriptions of geology, surface hydrology and hydrogeology are taken directly from the summaries of the extensive investigations of the Äspö area:

- Wikberg P, Gustafson G, Rhén I, Stanfors R. 1991. Äspö Hard Rock Laboratory. Evaluation and conceptual modelling based on the pre-investigations 1986-1990. SKB TR 91-22.

- Rhén I, Gustafson G, Stanfors R, Wikberg P. 1997. Äspö Hard Rock Laboratory – Geoscientific Evaluation 1997/5. Models based on site characterisation 1986-1995. SKB TR 97-06.

Table 2-1. Summary of Aberg (Äspö) Site Characterisation Studies.

Programme attribute	Description
Dates of field investigations	1986 to present.
Boreholes	53 boreholes, maximum depth 1700m. 275 probeholes in tunnel.
Single borehole tests	Double Packer: 1302 tests with 3m interval, 65 tests with 30m. Pumping: 100 tests with 100m interval, 19 tests with full-borehole. Single Packer: 275 full-length in tunnel probeholes (15m). Interpretation methods vary (transient or specific capacity regression).
Interference tests	20 tests, generally in fractured zones. Two additional longterm tests of 30 and 60 days.
Tracer tests	One test each in NE-1 and Redox zones, borehole dilution tests, one longterm converging tests, TRUE* project.
Tunnels/ Excavation	Äspö Hard Rock Laboratory and access tunnel, 3600m length, max depth –450 masl.
Geophysics	Aeromagnetic and aerogravimetric, seismic, VLF electromagnetic, borehole.
Other	Borehole spinner tests, geochemical sampling, geologic/fracture mapping on outcrops, trenches and cores.

* The Tracer Retention and Understanding Experiments, consisting of a series of block-scale hydraulic and tracer tests at the Äspö HRL.

17

2.2. REGIONAL SCALE

2.2.1. Topography

The region surrounding the Äspö site is gently rolling with low relief. Elevations range from sea level to approximately 60 masl. The area is generally forested, with topographic depressions filled with peat bogs and swamps. Äspö itself is an island just off the Swedish coast in the Baltic Sea (Figure 2-3).

2.2.2. Regional Geology

2.2.2.1. Quaternary deposits

The ice of the last glaciation retreated approximately 12000 BP, depositing bouldery till throughout the region. Peatlands are found in some depressions, as are fluvial sand and gravel. The soil cover is on the order of 0 to 5m with numerous bedrock outcrops.

2.2.2.2. Bedrock and Lineaments

The 1800 Ma old Småland granite suite (Figure 2-4) dominates the Äspö regional bedrock. The rocks are rather heterogeneous with some inclusions of metavulcanites, greenstone and intrusions of a brittle, light, fine-grained granite (Wikberg et al., 1991). The temperature at 500m depth is 14.6 ± 0.3°C and the temperature gradient is 15.0 ± 0.3°C/km (Ahlbom et al, 1995).

Regional lineaments have been mapped and examined by various airphoto, aerogeophysical, outcrop, seismic and borehole studies, revealing a number of major discontinuities that have been interpreted as steeply dipping fracture zones. Figure 2-5 shows these mapped regional fracture zones and their inferred dips (from Rhén et al., 1997). The geometries of the hydraulic conductor domains and coordinates are given in Rhén et al. (1997). Some of these regional structures cross the Äspö site, where they have been thoroughly investigated via the HRL tunnel and boreholes. In general, however, the locations, dips and widths have been inferred from geophysical anomalies are uncertain.
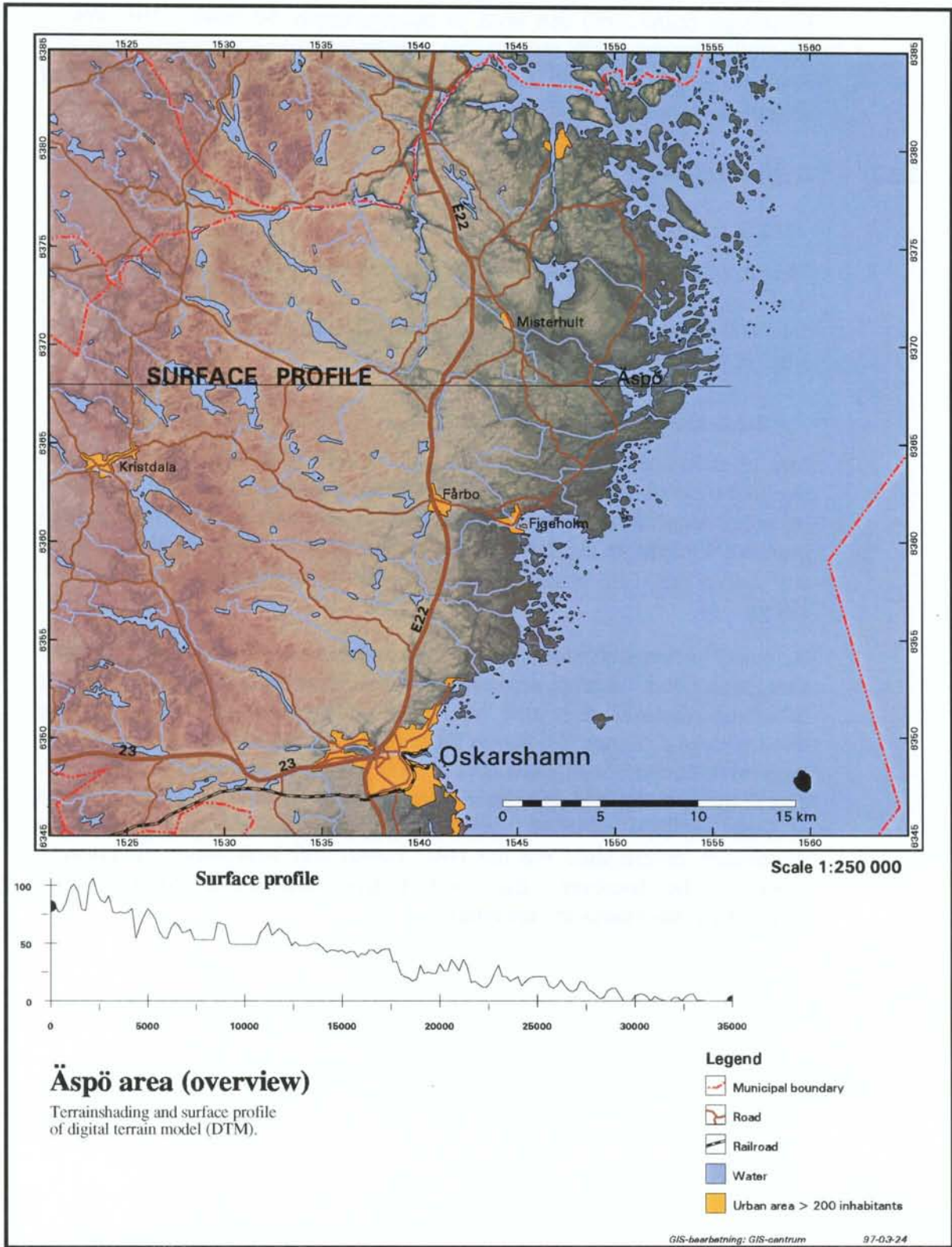
Figure 2-3. *Äspö regional topography.*
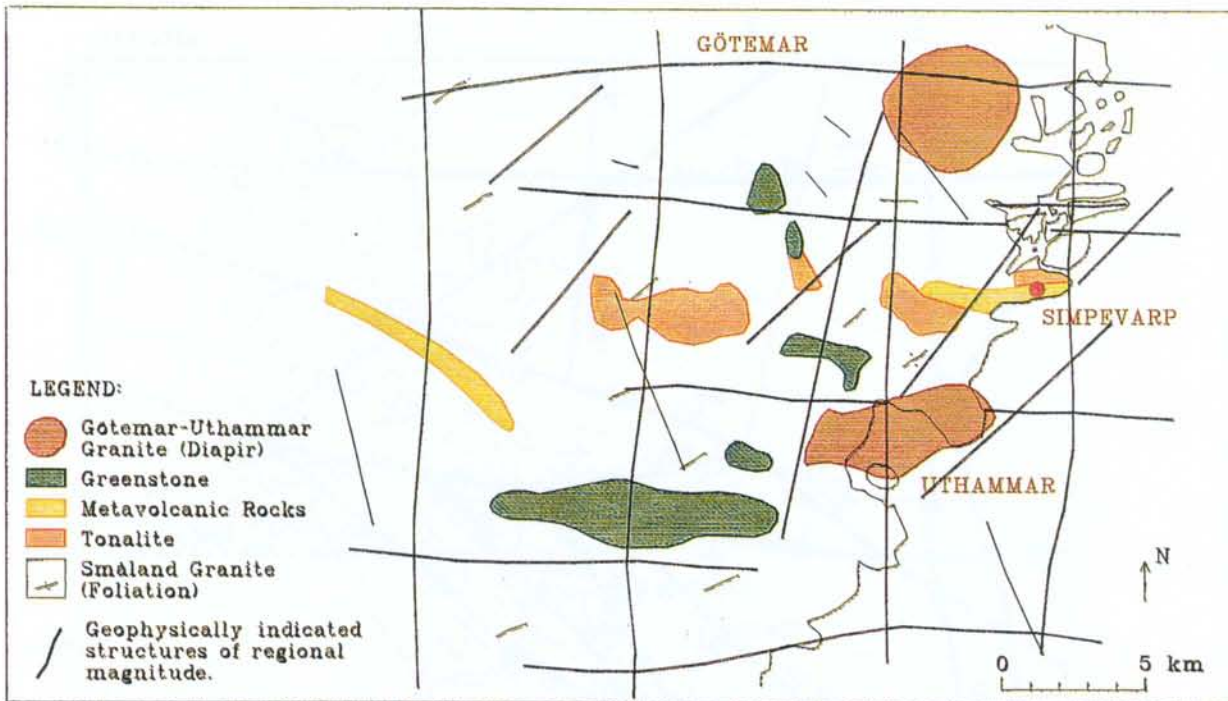
Figure 2-4. *Äspö regional geology (from Wikberg et al., 1991).*

2.2.3. Tectonics and Landrise

The Äspö shear zone cuts directly through the region, running SW-NE through Äspö Island. It corresponds roughly to site-scale structure EW-1 and SRD2. Hydraulic fracturing measurements of rock stress on site are consistent with the reported regional trends, indicating a maximal horizontal stress in approximate direction of SE-NW (Bjarnason et al., 1989; Müller et al., 1992).

The region continues to experience isostatic rebound as a consequence of the last period of continental glaciation. Because the site is near the sea and has low topographic relief, landrise has caused dramatic coastline changes. Figure 2-6 presents the shoreline displacement curve for this area (after Björk and Svensson, 1992). Rhén et al. (1997) present a sequence of shorelines over time to illustrate the changes in the upper boundary condition.
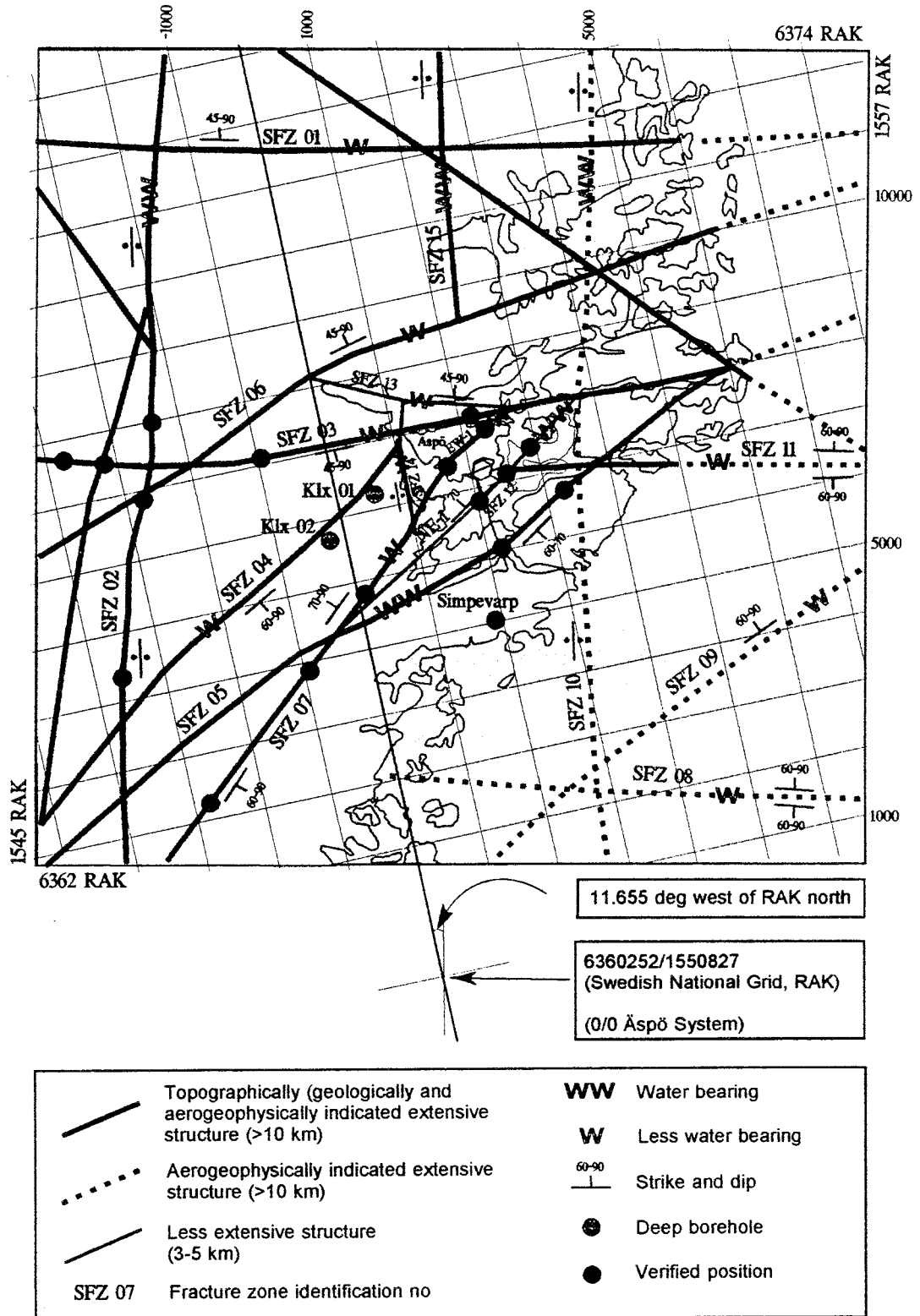
Figure 2-5. Structural model- Aberg regional scale (Coordinate systems: RAK and Äspö).
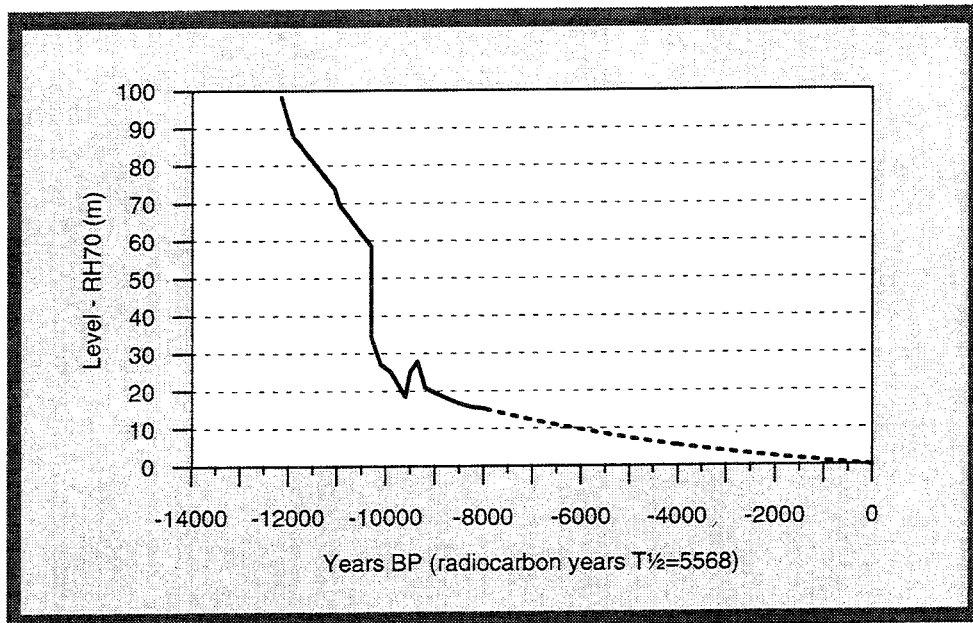
Level equation for the years - 8000 - 0 BP

$Z = 6.763 \cdot (\exp(-0.00014786 \cdot t - 1))$ (m, RH70)

Figure 2-6. Shore-displacement curve for Oskarshamn (after Björk and Svensson, 1992).

2.2.4. Geochemistry and Salinity

The salinity profile of the groundwater system is typical of islands and coastal areas: fresh groundwater near the surface rests on saline water that has intruded from the sea. The salinity or electrical conductivity of the ground water has been measured on several occasions during the pre-investigation and construction of the Äspö HRL. The undisturbed conditions are presented in Figure 2-7 for three sites, KLX01, KLX02 and Äspö. As part of investigations for the Äspö HRL near Oskarshamn, several deep wells were drilled to depths in excess of 1000m. The deepest of these, KLX02 is approximately 1.5km inland from the Baltic Sea, with a water table elevation of approximately 20m masl. That well encounters saline water at a depth of approximately 800m, as predicted by the classical Ghyben-Herzberg model for seawater intrusion. The modelling results of Svensson (1991) suggest this salinity distribution influences the pattern of groundwater flow, routing groundwater recharge on the land surface toward discharge areas under the sea near the coastline.

Appendix D.7 provides relationships developed at Äspö to convert from electrical conductivity and salinity to density.
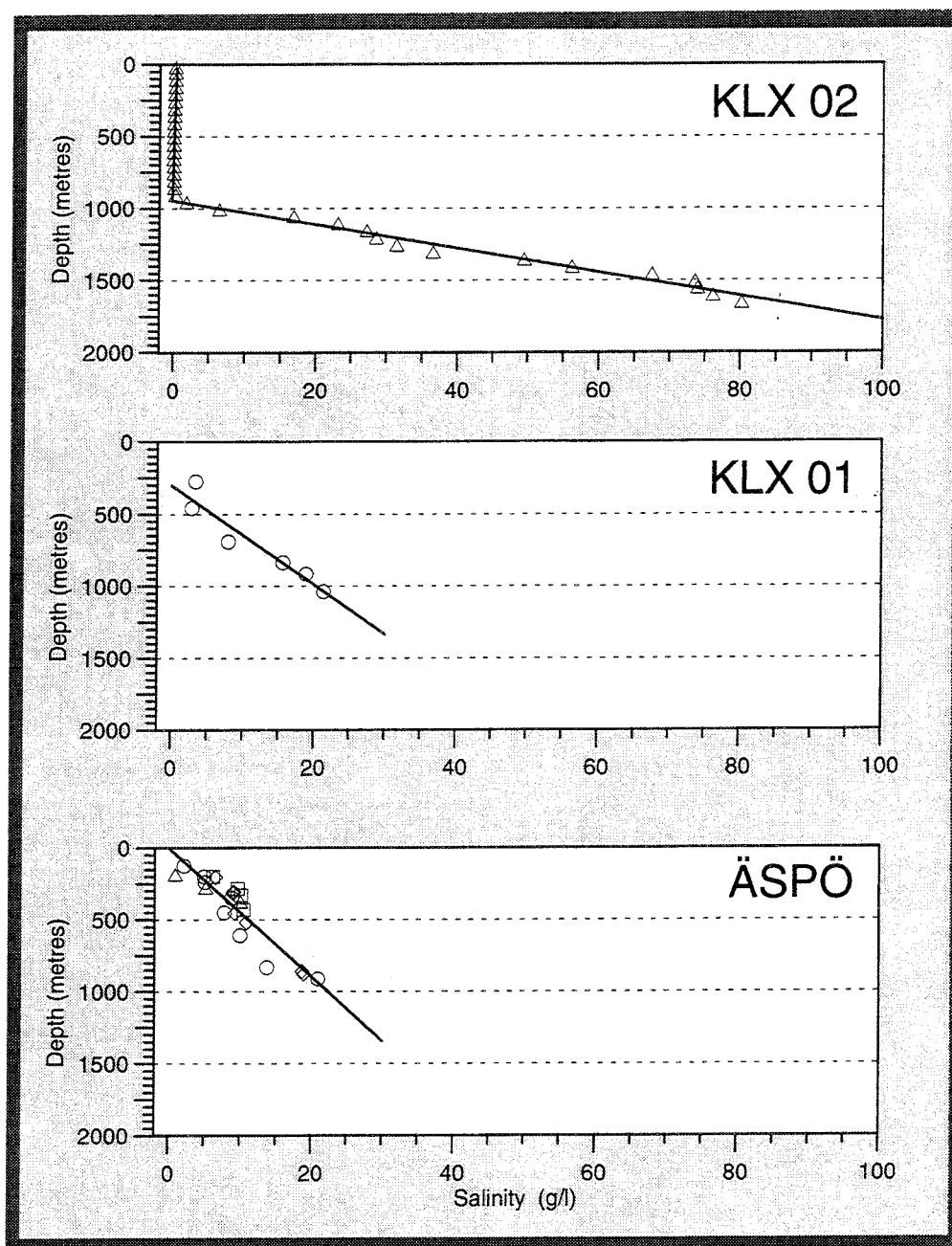
23

Figure 2-7. Salinity vs. Depth in the Äspö region.

The age and origin of the saline groundwater at the site has important implications for Performance Assessment (Ahlbom and Tirén, 1991). The sequence of glaciation and depression of the land surface followed by inundation and gradual uplift has resulted in a complex mixture of different waters in the groundwater at the site. Immediately beneath the island, meteoric water is the dominant water type. At approximately 500m depth, glacial meltwater dominates but is gradually replaced by stagnant, ancient brines with increasing depth. Figure 2-8 shows a principal component analysis of groundwater samples from 7.5 to 1002 mbgs (Laaksoharju et al., 1997)

The salinity of the Baltic Sea is approximately 7 g/l.
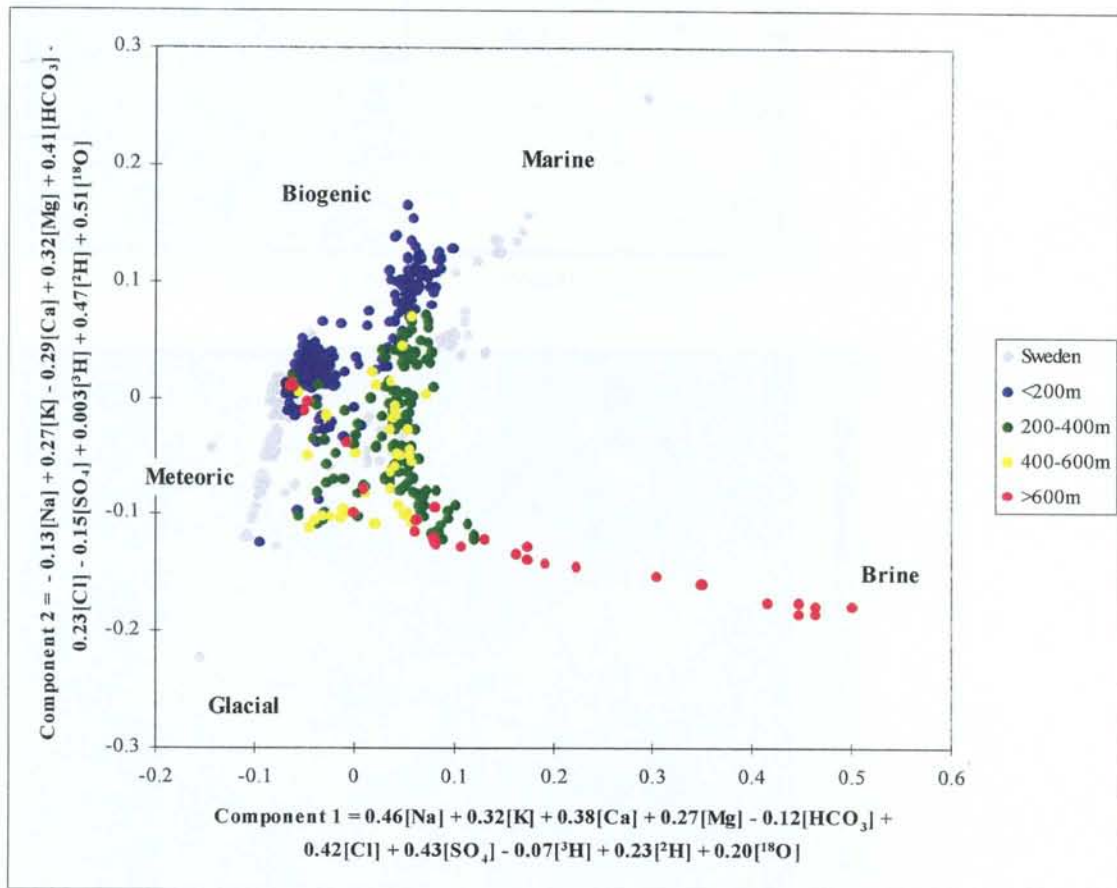
Figure 2-8. *Hydrogeochemical principal component analysis for Aberg (from Laaksoharju, 1997).*

2.2.5. Surface hydrology

The hydrology of the area around and on Äspö was compiled during 1986-1987. Figure 2-9 shows the drainage basins, rivers, lakes and peatlands that comprise the surface hydrologic features of the region. Two streams, Laxemarån and Gerseboån, were chosen to represent the coastal area. The estimated run-off per square kilometre for the two catchment areas is approximately 0.006 m³/(s km²) (Table 2-2, after Svensson, 1987).

25
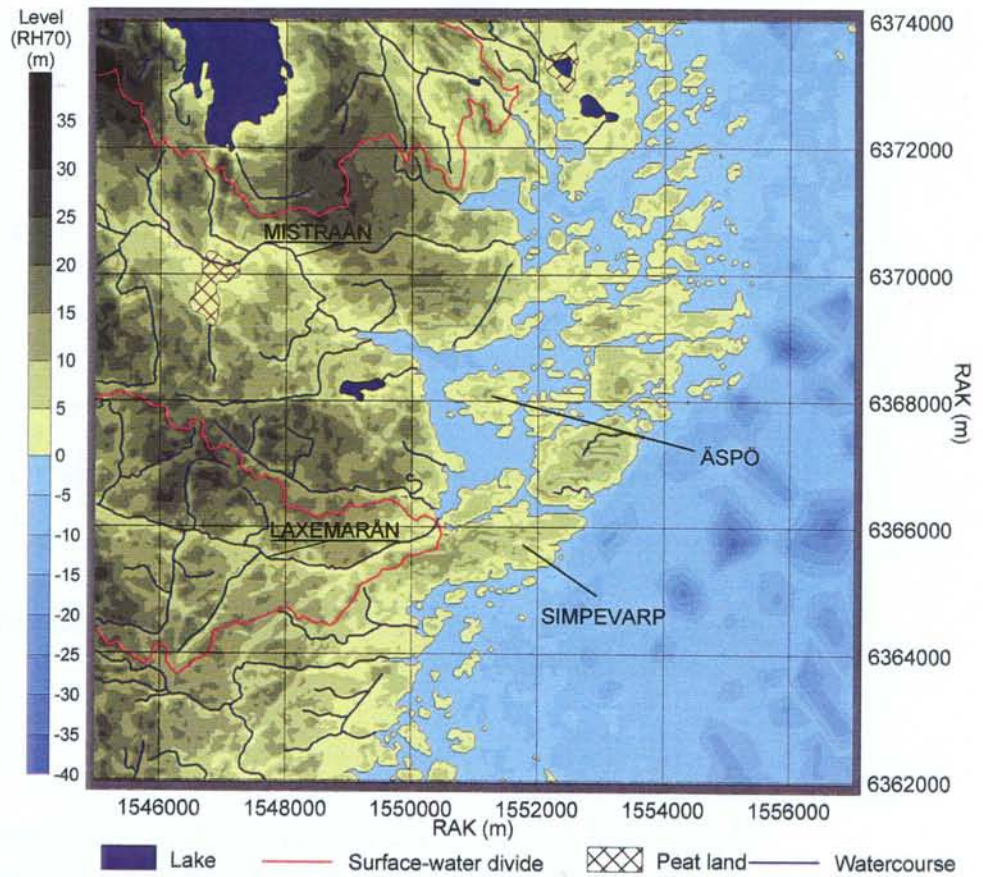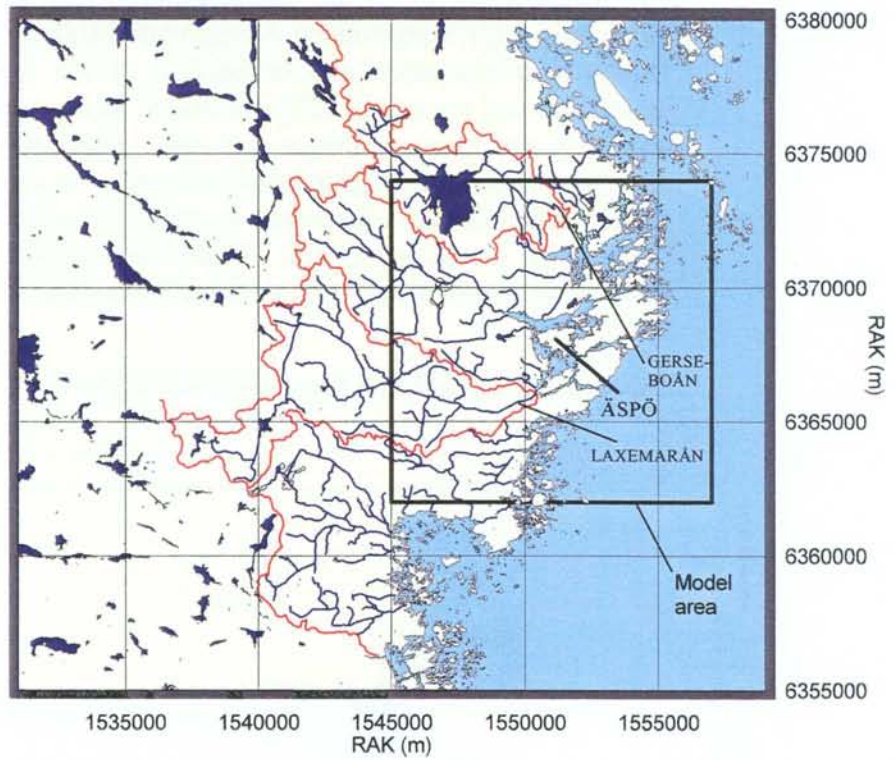
Figure 2-9. top: Hydrology of the area around Äspö (rivers outside the drainage basins are not shown). (Coordinate system: RAK).

bottom: Hydrology and topography of the area around Äspö. (Model area shown in top figure) (Coordinate system: RAK).

26

Table 2-2. Data for major catchment areas in the region around Simpevarp. Lake area as percentage of the catchment area.

Water course	Annual mean run-off (m³/s)	Catchment area (km³)	Lake area (%)
Virsboån	3.6	601	8
Marströmmen	2.9	486	7
Laxemarån	-	41	1.2
Gerseboån	-	25	12

The mean precipitation in the Kalmar County area is about 675mm/year (Svensson, 1987). About 18% falls as snow. The durability of the snow cover is on average 91 days from 30 November to 7 April. The calculated actual evapotranspiration is 490mm/year. The potential evapotranspiration of 616mm/year was calculated using SMHI meteorological data from Oskarshamn (Nyberg et al, 1995). Run-off for the Simpevarp area was estimated to be between 150 and 200mm/year. Precipitation generally exceeds evapotranspiration resulting in a net recharge on the land surface. The terrain is a mosaic of recharge and discharge areas. However, deep ground water recharge under natural conditions is thought to be small.

2.2.6. Groundwater hydrology

The Äspö regional groundwater table is strongly influenced by the topography and the level of the brackish Baltic Sea. Tidal effects and other short-term sea level variations produce water level variations in observation wells in the area. These effects are filtered out of the groundwater data using the SMHI sea level records recorded at the city of Oskarshamn. Data from SKB borings on Äspö, Bockholmen, and Ävrö indicate that the water table surface follows a subdued profile of the ground surface (Figure 2-10). The seasonal high comes in the spring and the low in late summer (Svensson, 1987).

The classical model of topographic drive suggests that recharge will occur in higher elevations and flow to discharge areas in lower elevations. This should be combined conceptually with the classical model of seawater intrusion under freshwater in coastal areas and islands. Although simplistic, this general model is consistent with the locations of streams, mires, observed hydraulic heads, salinity distributions and geochemical data available in the region. Svensson (1991) used a groundwater flow model to demonstrate that the overall pattern of groundwater flow at depth can be explained by this combination of conceptual models. However, several modelling studies suggest that the upper model boundary condition might be quite complex under certain transient conditions (Gustafson and Ström, 1995). For example, the fine sediments in the waterways around Äspö may limit recharge from the Baltic Sea in post-construction simulations. The

boundary conditions used by Svensson (1991) were: constant head on sides and bottom at hydrostatic pressure and observed salinity; top boundary as a calibrated recharge boundary. This approach was adequate to reproduce observed heads, recharge/discharge patterns and salinity, but should be evaluated for sensitivity.
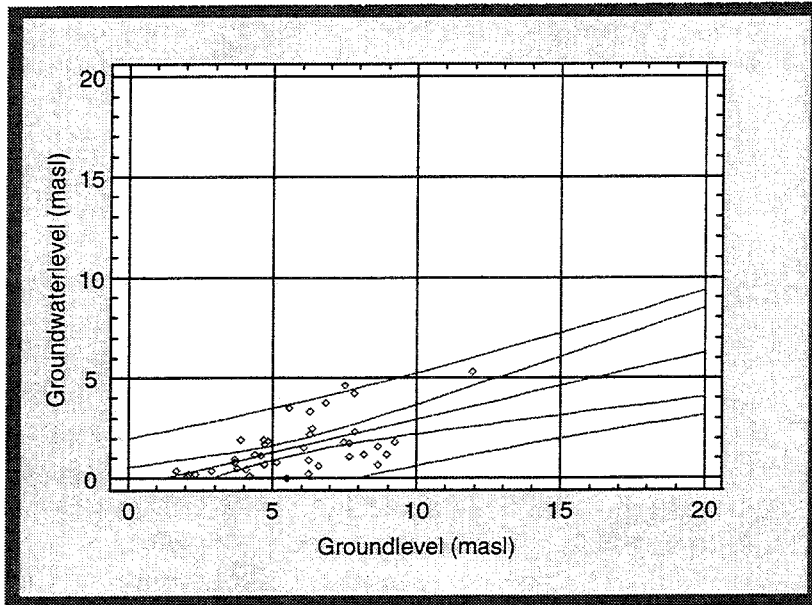
Figure 2-10. Groundwater level vs. elevation at Aberg, based on data from Äspö, Bockholmen and Ävrö. Regression equation for the fitted line is Water Table Elevation = -0.39 + 0.333masl. Inner pair of lines is 95% CI for mean. Outer pair of lines is 95% CI for prediction.

2.2.7. Hydraulic Characteristics

2.2.7.1. Rock Mass – RRD

Rhén et al. (1997) obtained and analysed SGU well data for a 25x25 km area around Äspö to infer models for the hydraulic conductivity on a regional scale (Figure 2-11). Geostatistical analysis of the SGU data suggests that hydraulic conductivity is weakly correlated over a range of approximately 800m (Appendix A.1).

Several investigations indicate that the rock becomes less permeable with depth (Ahlbom et al, 1991a, 1991b, 1992a, 1992b, 1992c; Rhén and Gustafson, 1990 and Öberg et al, 1994). Using a pooled data set of SGU data and on-site well tests of comparable length, it is possible to infer depth zones on the regional scale as presented in Table 2-3 (Appendix A.1). Note that the geometric mean hydraulic conductivity is almost constant down to a

depth of 600m, where it then decreases to approximately 10% of the value above 600m. Conceptual model RRD1 consists of depth zones for hydraulic conductivity, assuming a lognormal distribution with the means and variances given in Table 2-3.

Table 2-3. Aberg regional scale rock mass hydraulic conductivity (K) (RRD1, 100m scale down to 600m depth, 300m scale below 600m depth).

Elevation	Arithm. Mean Log_{10} K (m/s)	Variance Log_{10} K (m/s)	Sample size
0 to -200	-6.89	0.92	264
-200 to -400	-6.70	0.42	30
-400 to -600	-6.59	0.62	9
-600 to -2000	-7.33	0.51	11
0 to -2000	-6.89	0.86	314

An alternative case, RRD2, assumes that hydraulic conductivity of the Aberg rock mass is dependent on lithology. The hydraulic conductivity of different lithological units has been investigated in several studies, and the results summarised and compiled by Rhén et al. (1997). Småland granite is the dominate rock type in the region, and so the estimated properties of RRD1 are representative of Småland granite. RRD2 assumes that the geometric mean hydraulic conductivities for other rock types are determined by multiplying the values in Table 2-3 by the factors in Table 2-4. The standard deviations given in table 2-3 are unchanged for RRD2.
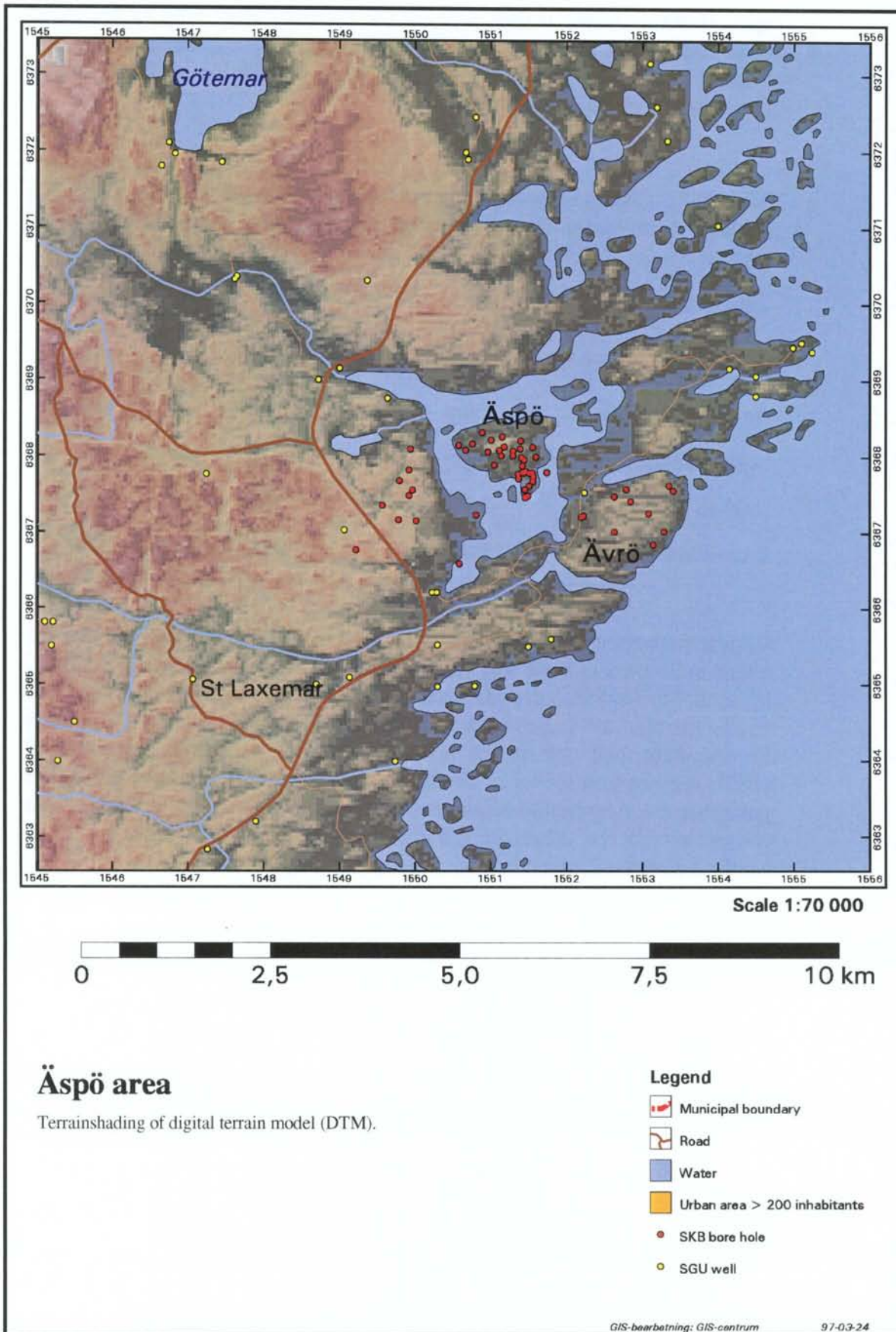
Figure 2-11. *Äspö area and borehole locations.*

Table 2-4. Aberg regional scale hydraulic Rock mass Domain (RRD2). Suggested relationships between the geometric mean value of the hydraulic conductivity (K) for different lithological units. (Geometric mean $K=10^a$, where a=arithmetic mean of $Log_{10}(K)$. Scale =test length $\approx$ 100 m.).

Lithological unit	Relationship (-)
Anorogenic granite	3
Fine-grained granite	1.8
Småland granite	1
Äspö diorite	0.5
Greenstone	0.4

2.2.7.2. Conductors – RCD

As mentioned in Section 2.2.2, only a few of the regional lineaments have been subjected to hydraulic testing. However, for assigning parameter values, Rhén et al. (1997) divided the lineaments into water bearing and less-water-bearing on the basis of expert judgement. The water-bearing lineaments (ww) are assumed to be similar to the more transmissive conductors at Äspö. The less water bearing discontinuities (w) are assumed to be similar to the less transmissive Äspö conductors. Consequently, the transmissivities for the water bearing and less water bearing lineaments are inferred to be the upper and lower quartiles of the distribution of lognormal transmissivities of the conductive zones at Äspö. The resulting parameters for the Aberg regional lineaments are given in Table 2-5.

Various studies have suggested that the transmissivity of the hydraulic conductors may decrease as much as the effective hydraulic conductivity of the rock mass. Similar to the depth zones prescribed for RRD1, the conceptual model RCD1 assumes that the transmissivity of the regional lineaments is roughly constant down to a depth of 600m. Below 600m depth, transmissivity decreases to 10% of that above 600m. An alternative case, RCD2, assumes that there is no change in the transmissivity of the lineaments with depth. Tables 2-4, 2-5 and 2-6 summarise models RCD1 and RCD2.

Other parameters for the conductors are outlined in the site scale (Section 2.3.4.2).

Table 2-5. Aberg regional scale lineament Transmissivity – RCD1 and RCD2.

Hydraulic conductor, water bearing nature	Transmissivity Mean(T) (m^2/s)
w	$0.3 \cdot 10^5$
ww	$10 \cdot 10^5$

Table 2-6. Aberg regional scale lineament (RCD) Transmissivity, depth dependence. d_b=depth to bottom level of numerical model. Transmissivity according to Table 2-5.

Spatial assignment method	Depth range (m)	Transmissivity (m^2/s)
RCD1	0-600	T
	600-d_b	0.1*T
RCD2	0-d_b	T

Uncertainties:

The regional lineaments are assumed to be uniformly conductive structures of constant width. Although this assumption is reasonable given the available data, it should be evaluated for sensitivity. Similarly, the regional boundary conditions at depth are a reasonable assumption but should be evaluated.

2.3. SITE SCALE

The Äspö site is taken as an area of approximately 1 km^2 containing the island of Äspö and the immediately surrounding shallow waterways (see Figure 2-12). The site scale description is based on data from the pre-investigation and construction phases from Rhén et al. (1997). The hydraulic properties are inferred from the interpreted hydraulic tests performed at Äspö HRL, as recorded in the SKB SICADA database.

2.3.1. Geology

The valleys are filled with peat and fine sediments while the hills consist mainly of exposed rock and till. The soil cover is usually thin (0-5m) and composed of bouldery glacial till. In the low areas fluvial deposits of clay, sand and gravel cover the till. Fine-grained fluvial deposits are found were the organic deposits are present. Sundblad et al. (1991) present detailed soil profiles for Äspö which show an upper layer of peat, occasionally underlain by unsorted gravely material, and a bottom layer of approximately 1m of clay. Samples of the sediments in the shallow strait between Äspö and Hålö show a 2-4m thick upper layer of gyttja (organic clay), occasionally underlain by a thin layer of gravel. The bottom layer is commonly 1-2m of clay.

As discussed in Section 2.2, the regional bedrock consists of the Småland granite suite. On the site scale, a more basic, denser subtype of this suite has been identified as a reddish grey diorite called the Äspö diorite. During construction, thin lenses of fine-grained granite were detected at a depth of 300 to 400m within the tunnel spiral. Because this fine-grained granite may be more hydraulically conductive and part of an extensive granitic body, it is discussed further in Section 2.3.4.

Pre-construction investigations and tunnel construction identified a number of fracture zones between 5 to 50m in width. These deterministic fracture zones and their potential influence on groundwater flow are discussed in detail in Section 2.3.4

There are, of course, fractures elsewhere in the site that are not included in the deterministic zones. Hermanson (1995) mapped fractures in the HRL tunnel and attempted to separate fractures caused by the tunnelling operations from those that are naturally present. The fractures are generally subvertical, occurring in five orientations (Figure 2-13a). The mapped grout-filled fractures are thought to be a good indication of the undisturbed conditions since grouting was performed 5-15m ahead of the tunnel face. These grout-filled fractures are dominated by a subvertical fracture set striking NW-SE (Figure 2-13c). A mapping campaign of the larger water bearing fractures in the spiral (Hermanson, 1995) showed that fractures not included in the deterministic conductive zones had widths ranging from millimetres to centimetres.
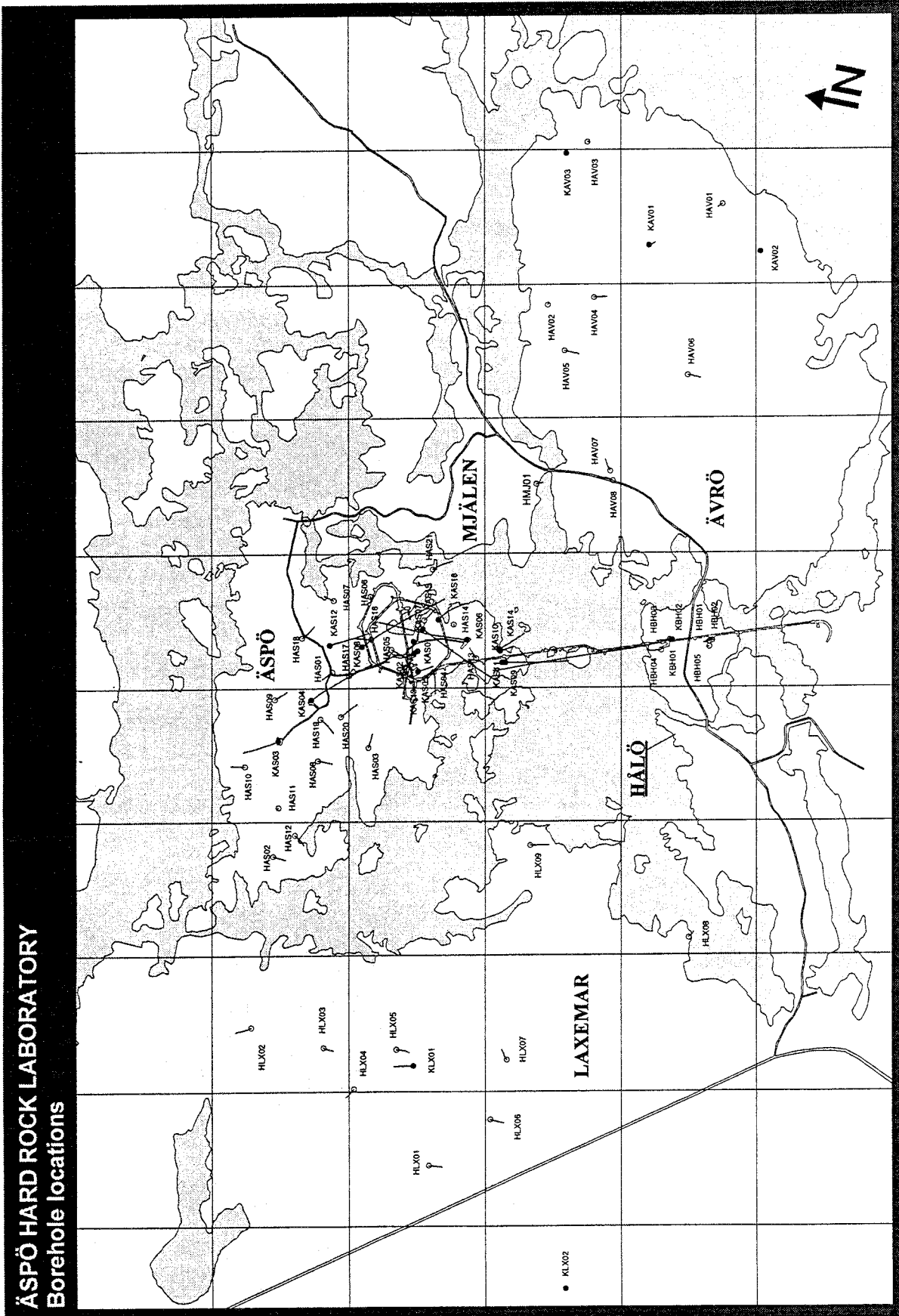
Figure 2-12. Äspö site and cored boreholes.

34
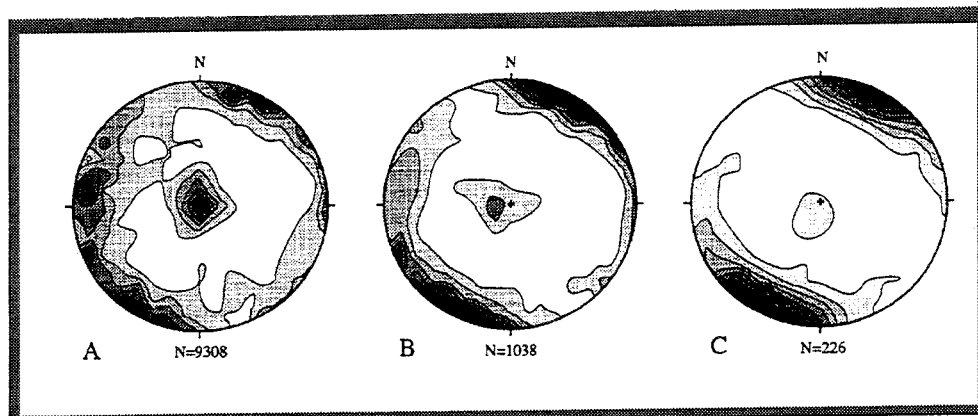
A : All fractures
B : Waterbearing fractures
C : Fractures filled with grout

Figure 2-13. *Schmidt nets for fractures from 705 m to the end of the TBM tunnel (3600m) with lower hemisphere projection of Kamb contoured poles to fracture planes. Contour interval 2.0 sigma. N= sample size. /Hermanson, 1995/.*
A: All fractures. The plot shows five concentrations of fracture orientations (one sub-horizontal set and four subvertical).
B: Water-bearing fractures.
C: Grout-filled fractures.

2.3.2. Surface hydrology

The land surface of Äspö is slightly undulating, with a maximum elevation of about 14masl. This uneven surface creates a disorganised drainage system with no perennial streams (Figure 2-14). Surface water drains to the sea through the peatlands, sediments or directly to the sea. The precipitation, temperature and potential evaporation of the area are described in the regional hydrology (Section 2.2).

2.3.3. Groundwater hydrology

Figure 2-15 shows the ground water surface levels under undisturbed conditions (before the construction of the tunnel). The maximum water table is about 4 masl for both undisturbed conditions and after the tunnel was constructed. However, deeper levels in borehole KAS03 on northern Äspö indicate a drawdown of a few metres after the tunnel was constructed. This discrepancy suggests that the upper bedrock on northern Äspö is not well connected to fracture systems deeper in the rock. The minimum measured ground water level on southern Äspö was found to be about -85 masl when the tunnel face was at chainage 2875 m.
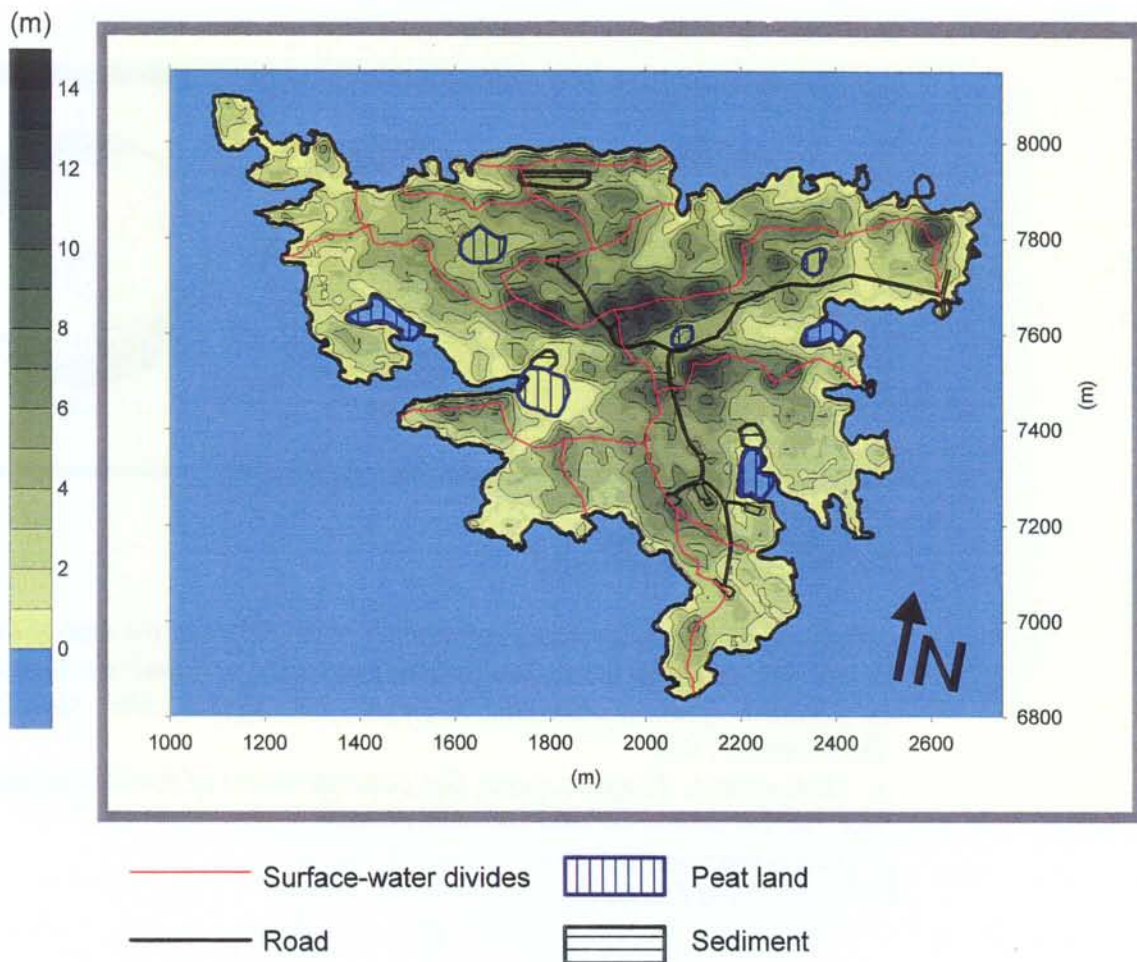
Figure 2.14. *Äspö surface hydrology.*

Svensson (1995) studied ground water recharge on Äspö via numerical modelling. The results of that study suggest that the construction of the HRL tunnel increased downward flow in southern Äspö but that much of the flow still continues to exit to the sea via the peatlands. On northern Äspö the shallow groundwater flow pattern does not change under the influence of the tunnel, suggesting that the upper levels of northern Äspö are poorly connected to both southern Äspö and the deeper groundwater system. If deep infiltration is defined as the infiltration through a horizontal surface at sea level, then the average infiltration on Äspö is calculated to be as in Table 2-7.

During the construction of the HRL tunnel, water inflows were measured via a system of weirs, humidity and airflow measurements. Details about the flow measurements are presented in Rhén (ed) (1995).
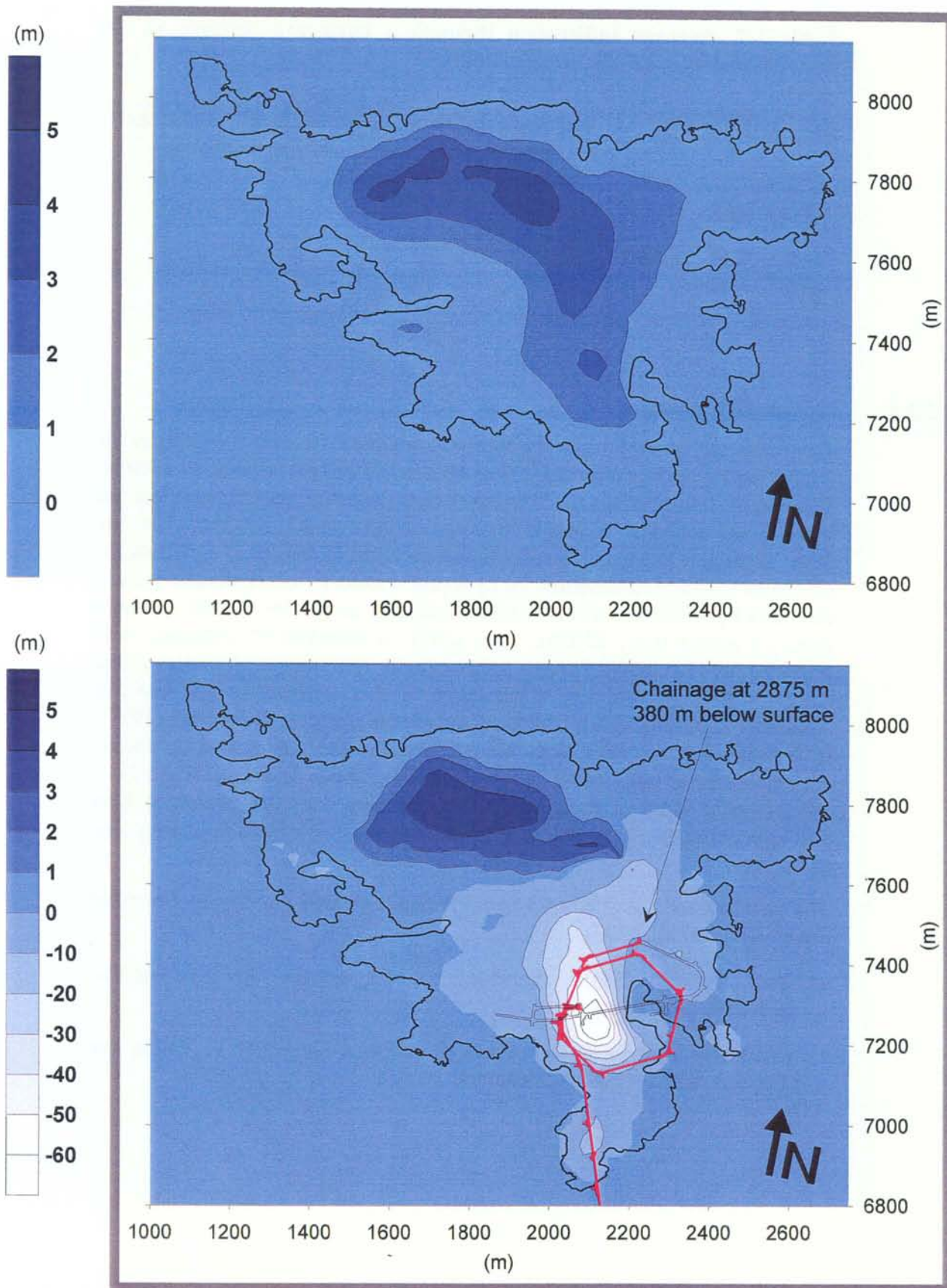
Figure 2-15. *Observed ground water table surface, before and after the construction of the HRL tunnel. (the tunnel face was at chainage 2875 m. Levels based on measured values. (Äspö coordinate system).*

Table 2-7. Average infiltration through a horizontal surface at sea surface level at Äspö (Svensson, 1995).

	Natural conditions (mm/year)	Tunnel face at chainage 2874 m (mm/year)
Entire Äspö	10	150
Above the tunnel spiral	20	180

2.3.4. Hydraulic properties

The principal source of data for hydraulic properties on the site scale is the double packer tests performed in the cored boreholes on Äspö and Laxemar. This analysis emphasises the 3m packer tests, as these have the smallest test interval and the most thorough coverage of the cored boreholes. The 3m, 30m, 100m and full-length tests in the same cored boreholes to construct the empirical scaling relationships for hydraulic conductivity. Hydraulic tests in the tunnel probeholes are used infer hydraulic properties for the southern parts of Aberg (e.g., SRD4). A series of interference pumping tests provided data for the interpreted transmissivity and storage properties of the deterministic conductors. A summary of this analysis is presented in Appendix A of this report; additional details are given in Rhén et al. (1997). It is important to note that this study uses the interpreted hydraulic conductivities as used by Rhén et al. (1997), which is not censored by a measurement limit. Consequently the summary statistics presented here will not necessarily have the same characteristics as previous interpretations of the data.

The data has been divided into two populations based on the site structural model (Rhén et al., 1997):

- Rock Domain (RD) - borehole sections outside the deterministic hydraulic conductors.

- Conductor Domain (CD) - borehole sections judged to be within the deterministic hydraulic conductors.

2.3.4.1. Rock mass – SRD1 through SRD5

On the site scale, the Aberg area is divided into five rock mass domains (SRD) each with different hydraulic properties:

- SRD 1: Northern part of Aberg, bounded to the south by the northern part of EW-1.

- SRD 2: Volume bounded by the northern and southern parts of EW-1.

- SRD 3: Southern part of Aberg bounded to the north by the southern part of EW-1 and to the south by EW-3.

- SRD 4: South of EW-3.

- SRD 5: A Fine-grained granite domain in the middle of the tunnel spiral at about 350m depth.

Outside the island, SRD1-4 are assumed to be valid within an area bounded by EW-7 to the south and some 100 m outside the island to the west, north and east (see Figure 2-16). The SRD's are thought to extend as far as the conductor domains to the north, south and to the model borders in Figure 2-16. The exceptions to this are the Laxemar and Mjälen areas, whose properties should taken as the mean of SRD1, SRD2 and SRD3.

A body of fine-grained granites are represented by SRD5, a single elliptical body centred in the HRL tunnel spiral at a depth of 350 m, with major axis length of 150m (E-W), and minor axes of 75m. The volume and shape of SRD5 are uncertain.

Svensson (personal communication, 1997) used calibration of a numerical model of Äspö to evaluate the SRD properties suggested by Rhén et al. (1997). That calibration exercise indicated that, in order to match observed heads, the hydraulic conductivity of SRD4 should be an order of magnitude lower than that of the probehole data. That is, the calibrated value of the arithmetic mean Log_{10} K (m/s) for SRD4 is approximately -7.6 at the 20m scale, more similar to SRD2.

39
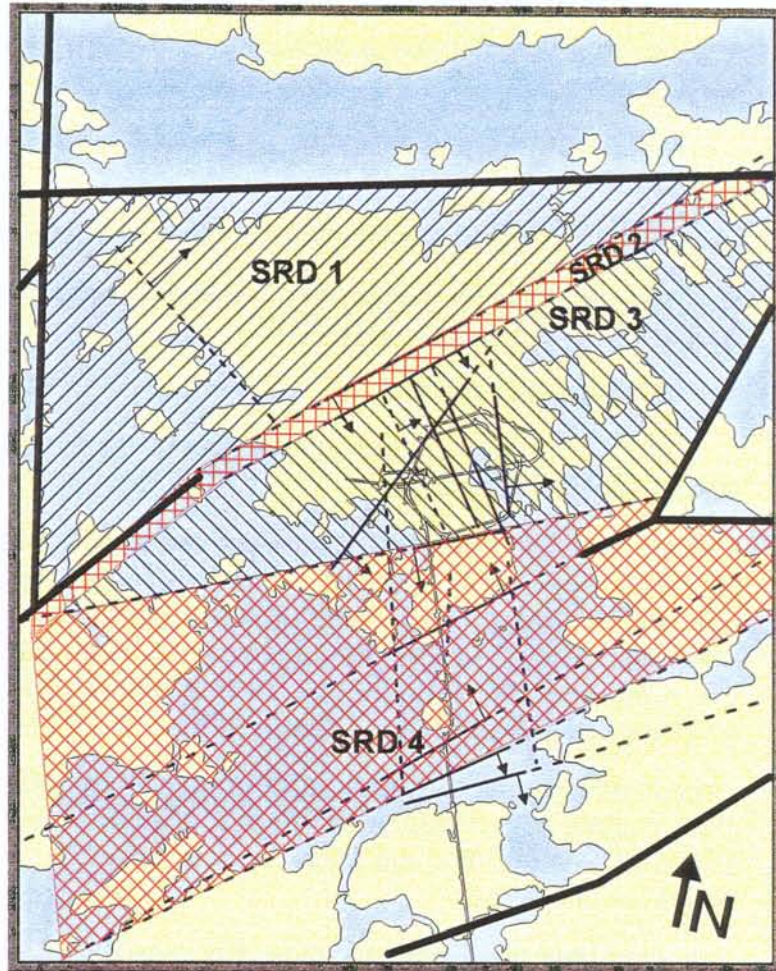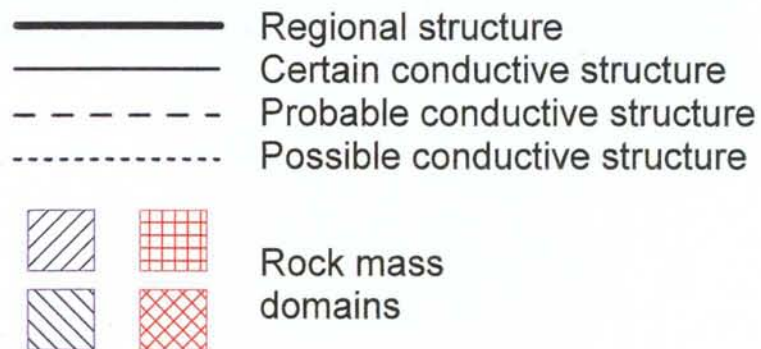
Figure 2-16. *Model of the Aberg hydraulic rock mass domains (SRD). (Äspö coordinate system).*

The statistics for the Aberg rock mass domains SRD1-5 are given in Table 2-8. The hydraulic conductivity is assumed to be lognormally distributed. The suggested means are given at the measurement scale and at the 24m scale, the proposed grid scale for the site scale models (Hans Widén, personal communication, 1997).

Table 2-8. Aberg site-scale rock domain hydraulic conductivity based on 3m data upscaled to 24m (SRD1 to SRD5).

Domain	Arithm. mean $Log_{10}K$ (m/s)	
	3m	24m
SRD1	-8.74	-8.03
SRD2	-7.82	-7.11
SRD3	-9.47	-8.76
SRD4*	-7.6*	-7.54
SRD5	-8.32	-7.61
Other**	-9.26**	-8.56

*at the 20m scale, as calibrated by Svensson (personal communication 1997). See Appendix A.2.1.
** the average of SRD1 through 3.

As discussed in Section 2.3.1, the rock mass appears to be preferentially fractured along a subvertical, NW-SE plane. This suggests that the hydraulic conductivity for a continuum model might be anisotropic with a major axis parallel to this direction. A comparison the interpreted conductivities from probeholes and boreholes of different orientations (Appendix A) suggests alternative case SRD7, which specifies that SRD1 through 5 have an anisotropy of hydraulic conductivity of 100:1:10 for major horizontal: minor horizontal: vertical. Analysis of laboratory cores indicates a lower limit for hydraulic conductivity of approximately $K=10^{-12}$ to 10^{-11} m/s.

2.3.4.2. Conductors – SCD

The hydraulic conductor domains are defined 2-D planes fitted through the ground surface and borehole observations of the major discontinuities (Figure 2-17). Appendix A provides a set coordinates for three points on the plane modelling the discontinuity. Note that one deterministic hydraulic conductor, NNW-8, is not shown in Figure 2-17 because it is not thought to reach the surface. The position and extent of NNW-5 and NNW-6 were only indicated by surface geophysical measurements and must be considered uncertain.
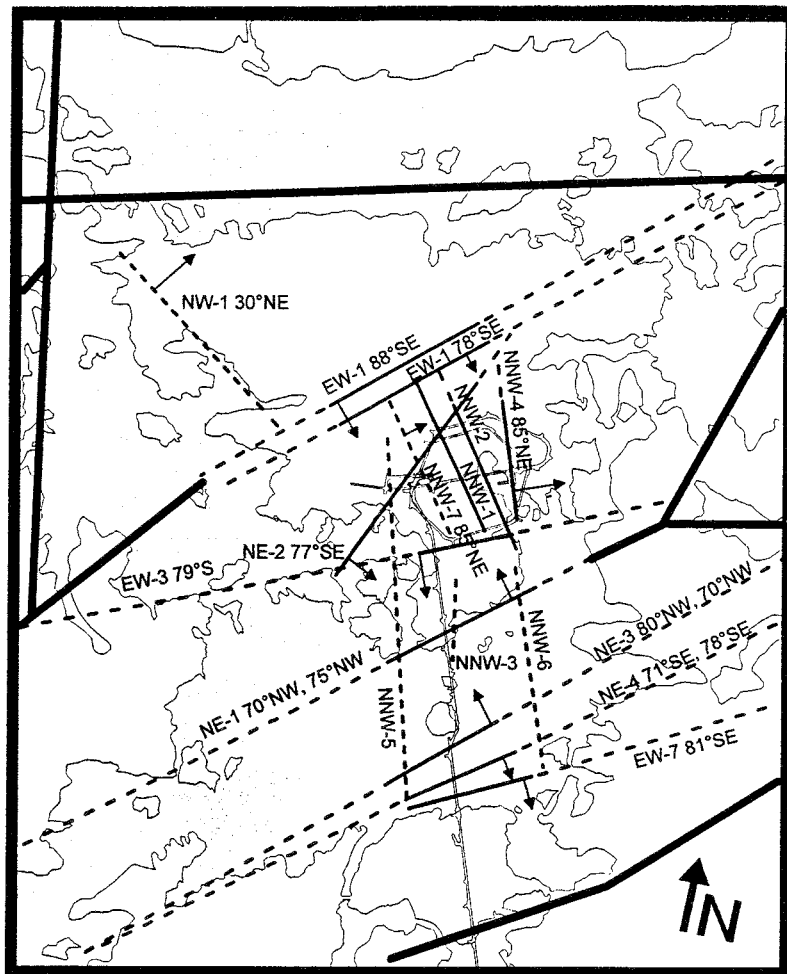
Figure 2-17. Aberg Site-scale hydraulic conductors (SCD).

Some of the conductors are also discontinuities in the geological model, while others are defined by an increased fracture density. Some of these latter conductors are rather diffuse (fracture swarms). The hydraulic conductors called NNW strike approximately N 35°W are believed to be a fracture swarm consisting of mainly subvertical fracture sets striking NW and N-S.

The hydraulic conductors EW-1 and EW-3 are complex structures. Although some the outer parts of these structures are quite conductive, interference tests and tunnel data indicate that the cores of EW-1 and EW-3 have relatively low hydraulic conductivities. This suggests that the average conductivities of EW-1 and EW-3 is anisotropic with a major axis in the E-W direction

Most of the conductors had at least one test, and several had multiple tests in several zones. The exceptions of to this are NNW-6, which was not tested, and NNW-3 and NNW-5, whose single test results are considered unreliable. In some cases discontinuities that have been identified by geological and/or geophysical investigations have not been tested hydraulically. In such cases, expert judgement was used to assign material properties. In a few cases several tests from different parts of the discontinuities are available and make it possible to assign the variability within the zone. The properties for each conductor are given in Table 2-9 (adapted from A2-7 and A2-8 of Rhén et al., 1997). Values for NNW-3 and NNW-6 can be taken as the average of all tested conductors. Measurement scale for these tests is approximately 50 to 100m (Rhén, 1988 and 1990).

Rhén, et al., suggest that conductors NW-1, NNW-3, NNW-5, NNW-6, NNW-7 and NNW8 are considered possible. Hydraulic tests have also implied additional structures between KAS03 and KAS04, near EW-1N (Rhén et al., 1997, Table A2-6). This suggests an alternative case model, SCD2, to be run once with the additional fracture zones included, and again with possible zones removed. An additional alternative case, SCD3, is suggested for increased and decreased transmissivities by a factor of 2.

Table 2-9. Aberg site-scale transmissivity of conductors (SCD1). 100m measurements from Rhén et al. (1997), scaled to 24m.

Zone	Median Log10 K (m/s)		Width (m)	Sample size
	100m	24m		
EW-1N	-7,30	-7,79	30	4
EW-1S	-6,13	-6,62	30	4
EW-3	-5,80	-6,28	15	4
EW-7	-5,17	-5,65	10	3
NE-1	-5,00	-5,48	30	16
NE-2	-7,09	-7,57	5	12
NE-3	-5,24	-5,72	50	9
NE-4	-6,12	-6,61	40	8
NNW-1	-6,26	-6,74	20	7
NNW-2	-5,55	-6,04	20	4
NNW-4	-4,82	-5,31	10	8
NNW-5	-7,00	-7,48	20	3
NNW-7	-6,62	-7,10	20	5
NNW-8	-6,30	-6,79	20	3
NW-1	-7,77	-8,25	10	3

2.3.4.3. Geostatistical model

The Aberg site-scale geostatistical model of hydraulic conductivity consists of geometric means for SRD1 through 5, SCD1 and a single covariance model. The SRD and SCD are treated as step changes in the geometric mean of block conductivities (0 order trends in Log_{10} K_b), upscaled to 24m via the Äspö regression relationships (Appendix D.5).

The spatial correlation model is inferred from the 3m packer test in the rock domain (SRD) using the SKB code INFERENS to regularise the rock mass data and apply universal kriging (Norman, 1992a). The resulting variogram model includes both the effects of the trends represented by the SRD and effects of upscaling to the numerical model grid. The fracture zones (SCD) are assumed to have the same variogram model. Results of this analysis indicated the following exponential variogram model for the 24m grid scale:

$$\gamma(h) = 0.0 + 2.72 \, Exp \, (32.3)$$

i.e., a zero nugget exponential model with a practical range of 97m. The complete geostatistical model consists of this model and the 24m scale geometric mean hydraulic conductivities given in Tables 2-7 and 2-8. The model is considered uncertain.

Details of this analysis and discussion are found in Appendix A.3.

Table 2-10. Summary of Aberg Conceptual Models.

Code	Mode
	Regional Scale (1)
	Rock Domain
RRD1	Hydraulic conductivity from SGU and Äspö borehole data with depth zones.
RRD2	As in RRD1, but hydraulic conductivity as a function of rock type
RRD3	as in RRD1, but with anisotropy in the direction of maximum horizontal rock stress
	Conductor Domain
RCD1	Regional lineaments of Rhén et al., 1997, as conductive fractured zones. T from upper and lower quartiles of on-onsite fracture zones. Depth zones as in RRD1
RCD2	as in RCD1 but constant with depth
	Site Scale (2)
	Rock Domain
SRD1 to SRD5	Hydraulic conductivity from 3m packer tests. 1 through 5 correspond to regions/rock types at Äspö.
SRD7	Variation case for anisotropy (includes SRD1 to SRD5)
	Conductor Domain
SCD1	Fracture zones with properties inferred from on-site interference tests, spinner tests.
SCD2	Extent/number of fracture zones changed with respect to uncertainties given in Rhén et al. 1997.
SCD3	Transmissivity of zones varied by a factor of 2
	Excavation Disturbed Zone (EDZ)
EDZ1	Hydraulic conductivity of rock surrounding the tunnel unchanged
EDZ2	10X increase in hydraulic conductivity parallel to tunnel axis in 25cm of rock surrounding tunnel (Appendix D.8)

Notes:
(1) Regional hydraulic conductivity upscaled to numerical model block scale using the Äspö regression equation, calibrated to observed heads and recharge/discharge patterns.
(2) Site hydraulic conductivity upscaled to numerical block scale using Äspö regression equation, calibrated to observed heads and regional boundary fluxes. Covariance of hydraulic conductivity upscaled via INFERENS.

3. BEBERG

Beberg is modelled after the Finnsjön site, which is located in central Sweden in the northern part of Uppland (Figure 3-1). It is approximately 13km inland from the Baltic Sea (Figure 3-2) in an area corresponding to LMV map sheet Östhammar 12I NV, and parts of sheets 12I NO and Österlövsta 13I SV. A 50 x 50 km region centred on the site is characterised by low relief and poorly organised drainages, with several lakes, mire and bog. The site takes its name from Lake Finnsjön, one of the largest lakes in the region. The altitude of the region ranges from sea level to approximately 62 masl. From a hydrogeologic perspective, northern Uppland is notable for the occurrence of saline groundwater at relatively shallow depths and for the presence of relatively shallow subhorizontal conductive fracture zones. These last two characteristics are thought to have profound influence on the flow patterns in the region, and might greatly inhibit releases from a repository.

Forsmark, the SKB Final Repository for Radioactive Operational Waste (SFR), is 15km northeast of the Finnsjön site. The site characterisation and modelling studies associated with the construction of the SFR provide important information on regional geology and hydrogeology. The Dannemora Mine (iron), 17 km south of the site, provides additional information on regional geology. The site characterisation studies are summarised in Table 3-1.

3.1. PRIMARY SOURCES OF INFORMATION

The information contained in this section is taken from several key sources in addition to the SKB and SGU databases. Much of the descriptions of geology, surface hydrology and hydrogeology were taken from:

- Ahlbom, K, S. Tirén 1991, Overview of geologic and geohydrologic conditions at the Finnsjön site and its surroundings, SKB TR 91-08.

- Andersson, J-E, R. Nordqvist, G. Nyberg, J. Smellie, S. Tirén 1991, Hydrogeological conditions in the Finnsjön area. Compilation of data and conceptual model, SKB TR 91-24.

- Ahlbom, K, J-E Andersson, P. Andersson, T. Ittner, C.: Ljunggren, S. Tirén 1992, Finnsjön study site. Scope of activities and main results, SKB TR 92-33.

- Stålhös, G, 1988, Bedrock Map of 12I Östhammar NV, SGU series Af nr. 166.

Table 3-1. Summary of Beberg (Finnsjön) Site Characterisation Studies.

Programme attribute	Description
Dates of field investigations	KBS site characterisation program, 1977-1983; Fracture Zone project 1985-1988.
Boreholes	18 shallow percussion, 2 shallow booster, 11 deep cored, maximum depth 691m.
Single borehole tests	Double Packer: 1377 steady-state tests with 3m interval; 830 transient tests with 2m interval (mostly in Zone 2); some 200 tests more with 0.11, 5, 10, 20m intervals. Single Packer: 2 boreholes from end-of-boring to top.
Interference tests	One test at surface and 3 in Zone 2. Series of tests during drilling of shallow booster hole BFI01.
Tracer tests	A preliminary series followed by radially converging, dipole and others. Emphasis on Zone 2.
Tunnels/ Excavation	Dannemora Mine.
Geophysics	Magnetic, seismic, slingram, resistivity, induced polarisation, VLF electromagnetic, borehole. Several experimental methods.
Other	Geochemical sampling, geologic/fracture mapping on outcrops, trenches and cores. Chernobyl project in 1986. Forsmark SFR studies in 1986.

REGIONAL AREA

SEMI-REGIONAL AREA

FINNSJÖN SITE

Borehole
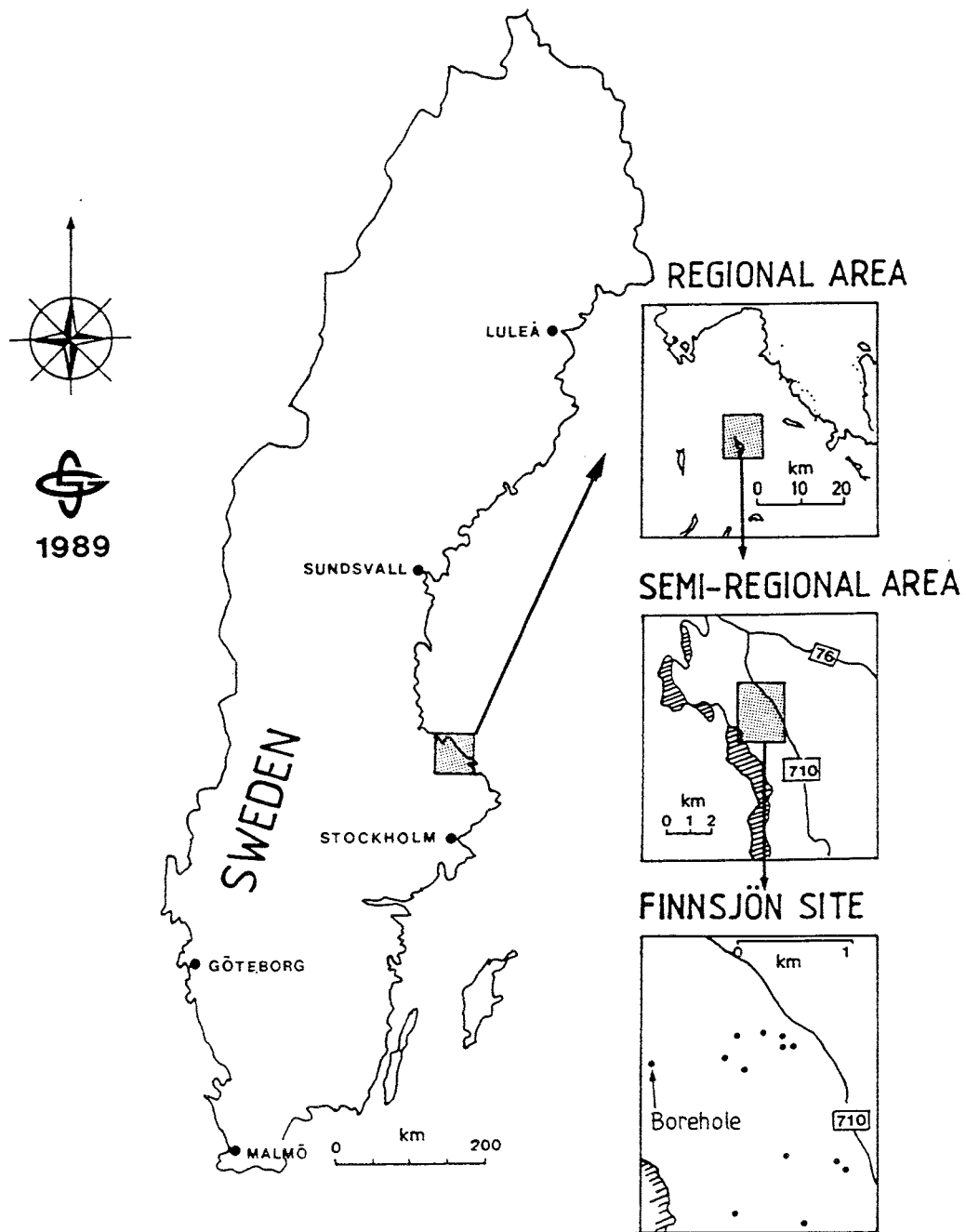
Figure 3-1. Map of Sweden showing Finnsjön site (from Ahlbom and Tirén, 1991).

49

3.2. REGIONAL SCALE

3.2.1. Topography

The ground surface of the region has little relief, and is characterised by flat rock outcrops, lakes, bogs and mires (Figure 3-2). Regional streams follow poorly organised drainages to the east, emptying into the Baltic Sea. The average elevation of the Finnsjön region is 30 masl, and varies ± 30 m. Extensive mire lies west of Lake Finnsjön and comprises the Florarna Nature Preserve (Carlsson and Gidlund, 1983).

3.2.2. Regional Geology

3.2.2.1. Quaternary Geology and Soils

The ice of the last glacial moved north to northeastward in this region, leaving behind a maximum of a few meters of Quaternary clay and glacial moraine. A thin cover of soil overlies these glacial deposits, interrupted by bedrock outcrops over approximately 15% of the region. Depressions are typically filled with peat. Approximately 25% of the region is covered by mire, 45% by till with the proportion of mire decreasing to the south and east. Within the Finnsjön site, about 20% are mire. Bogs are found in depressions in recharge areas and swamps are located in depressions in discharge areas (Carlsson and Gidlund, 1983).

3.2.2.2. Bedrock Geology and Lineaments

A generalised map showing the rock distribution is presented in Figure 3-3. The oldest rocks (2,200-1,850 Ma) are acid volcanics (leptites) and metasediments with intercalated mineralised beds. These rocks have irregular boundaries and constitute 25% of the bedrock. During the Svecokarelian orogeny (approximately 1,850 Ma) granitoids belonging to a magmatic suite of gabbroic rocks intruded the bedrock transforming the granites into gneiss. This was followed by emplacements of the youngest rocks in the region, reddish to greyish-red granites approximately 1,700 Ma in age. More than 50% of the bedrock consists of Svecokarelian granodioritic-granitic intrusive rocks. The basement rocks have not been identified (Ahlbom et al. 1992).

51
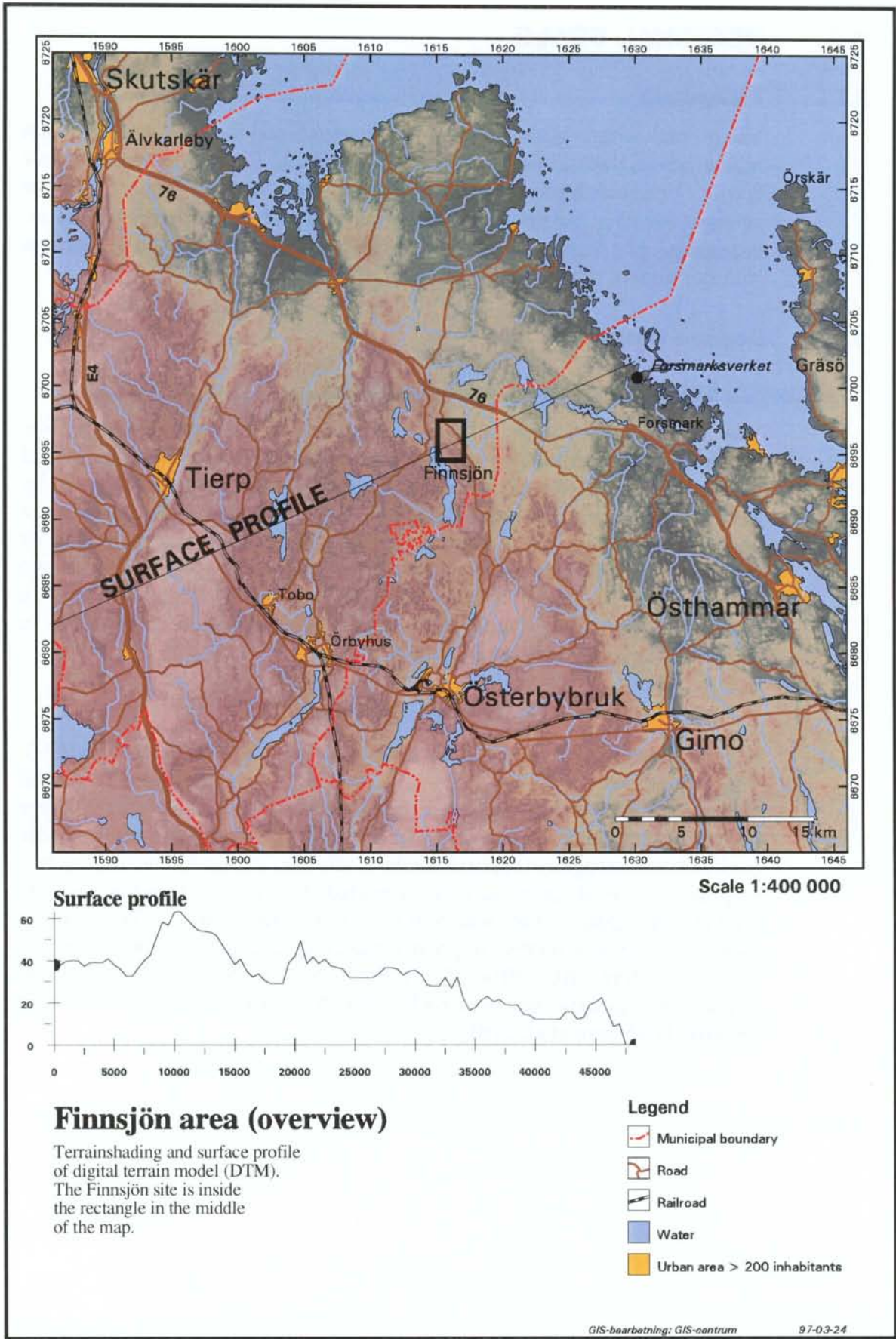
Figure 3-2. *Finnsjön Site Location Map.*
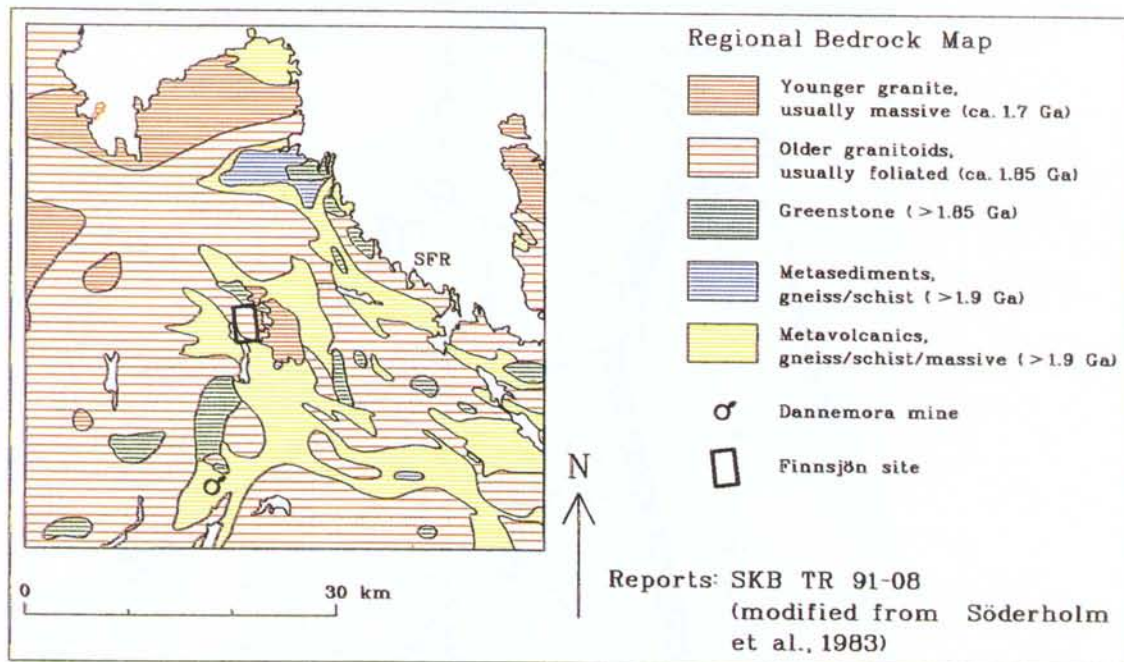
Figure 3-3. *Geology of northeastern Uppland, Finnsjön regional area (from Ahlbom et al., 1992).*

The rocks in the northern area of Figure 3-3 exhibit a pronounced NW-SE orientation, parallel to the Singö fault. The oldest rocks are downfolded at great depths near the Dannemora mine south of the site. Intruding Svecokarelian granitoids are thought to have caused this deformation. Large intrusions of younger granites (1,700 Ma) occur in the northern part of the map, accompanied by pegmatite and aplite dykes. The Finnsjön site is located within a granodioritic intrusion (Stålhös, 1988; Ahlbom et al. 1992). The temperature at 500m depth is 12.3 °C and the thermal gradient is 13 °C/km depth. The thermal conductivity for the Finnsjön granodiorite is between 3.0-3.5 Wm°C (Olkiewicz and Arnefors, 1981; Sundberg et al., 1985).

Lineaments in northeast Uppland have been interpreted from topographic maps at a scale of 1:250 000 (Ahlbom and Tirén, 1991). Figure 3-4 shows that these curved lineaments form a network of blocks, which suggests that the lineaments are shear structures. At least two sets of lineaments are present, one trending north to northeast and the other trending northwest. It is not known that the two shear sets have been active simultaneously, forming a conjugate shear configuration. An interesting feature of this region is the systematic tilting of major blocks (up to 2 degrees), as indicated in Figure 3-4. The ground surface of the north–northeast trending rock blocks are tilted towards the east and southeast while the ground surface of northwest trending rock blocks dips toward the northeast. The tilting is interpreted as listric (spoon-shaped) faults with steep dips near the ground surface.
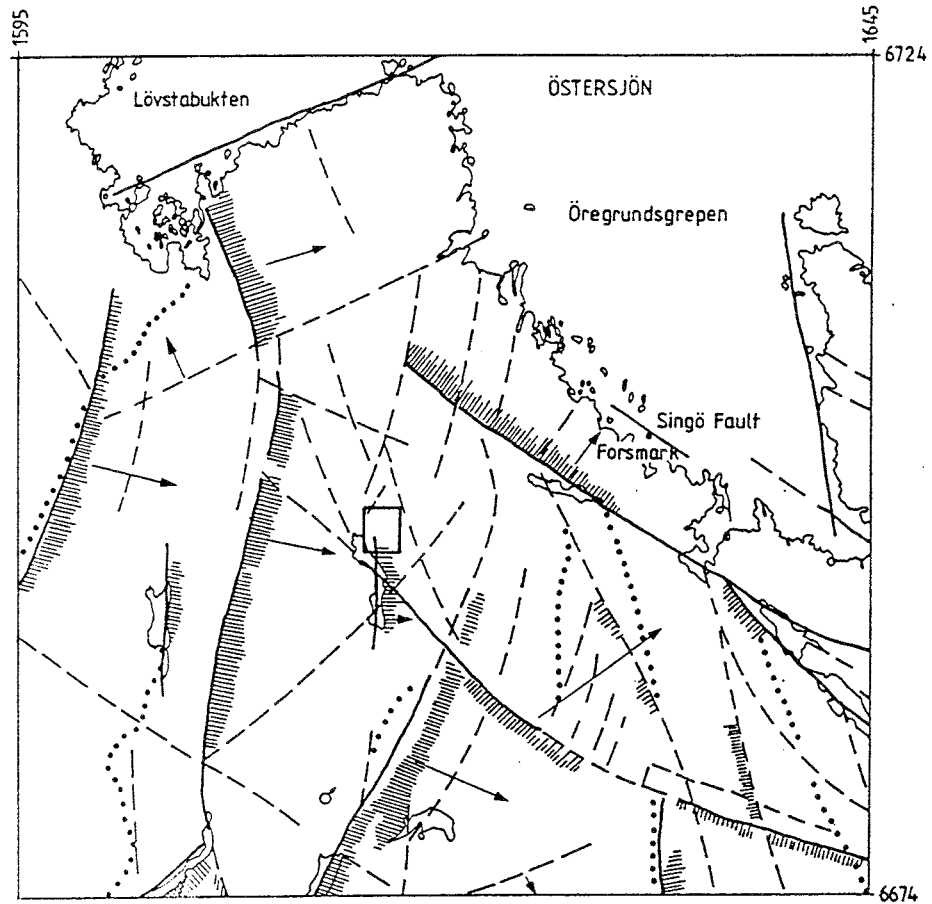
LINEAMENT MAP, NORTHEASTERN UPPLAND

REGIONAL AREA

⌐⌐⌐	Lineament, well expressed
⁻ ⁻ ⁻	Lineament, less well expressed
▨	The elevated side of the structure is marked with a line screen
⟶	Dip direction of the ground surface
••••••	Glaciofluvial deposits, eskers
♂	Dannemora mine
☐	Finnsjön site

The glacial striation is north-south

N

Division of Engineering Geology
S.A.TIRÉN, Uppsala 1987

0   10 km

Figure 3-4. *Northeastern Uppland lineament map (from Ahlbom and Tirén, 1991).*

Only one lineament in northeastern Uppland has been investigated in detail, the Singö fault, studied in connection with the Forsmark SFR. Near Forsmark, the northwesterly trending Singö fault is 100-200 m wide and subvertical, with a complex structure. It has approximately 100 m of altered and mylonitized bedrock with 15 m of crushed bedrock in the core of the fault. The hydraulic conductivity varies widely, with the core having an average hydraulic conductivity of 4×10^{-6} m/s, and the peripheral part is 5×10^{-7} m/s (Carlsson et al., 1986).

On the regional scale (approximately 10 x 10km), a gridwork pattern of lineaments can be seen running northwest–southeast, northeast–southwest, and north–south (Figure 3-5, from Ahlbom and Tirén, 1991). Several of these lineaments cross through or form the boundaries of the Finnsjön site, where several boreholes provide information on their characteristics. This lineament map forms the basis of the Beberg regional scale fracture zone model, RCD1, as is discussed in section 3.2.7.2. Extensions of lineaments beyond those shown in Figure 3-5 may be taken from Ahlbom and Tirén, (1991, Figure 5).

3.2.3. Tectonics and landrise

Results of hydraulic fracturing stress measurements at the Finnsjön site suggested thrust faulting stress conditions down to 500m, changing to strike-slip conditions below this depth. The results also suggested a 3 MPa discontinuity of the stress field occurring over Zone 2, a subhorizontal zone within the Northern Rock Block (Bjarnason and Stephansson, 1988; Ahlbom et al., 1992. See also Figure 3-17). Vertical hydrofractures indicated that the direction of maximum horizontal stress is N 48 W with a standard deviation of ± 10 degrees. This is almost parallel to the strike of the oldest set of fractures. The measured stresses at Forsmark and at the Finnsjön site generally agree in magnitude and orientation.

A shear lens runs northwesterly through the Finnsjön region. Several of the northwest-southeast trending regional lineaments have been mapped as vertical faults, including the Singö fault near Forsmark. Earthquakes of magnitude 3-4 have been reported in this region within last 100 years (Fredén, 1994)

Björk and Svensson (1992) describe sea level changes and present several shore-displacement curves for Sweden. Figure 3-6 shows the historic landrise in the area near the site, based on radiocarbon dating of paleoshoreline sediments. The present rate of landrise is 5.7 mm/yr.
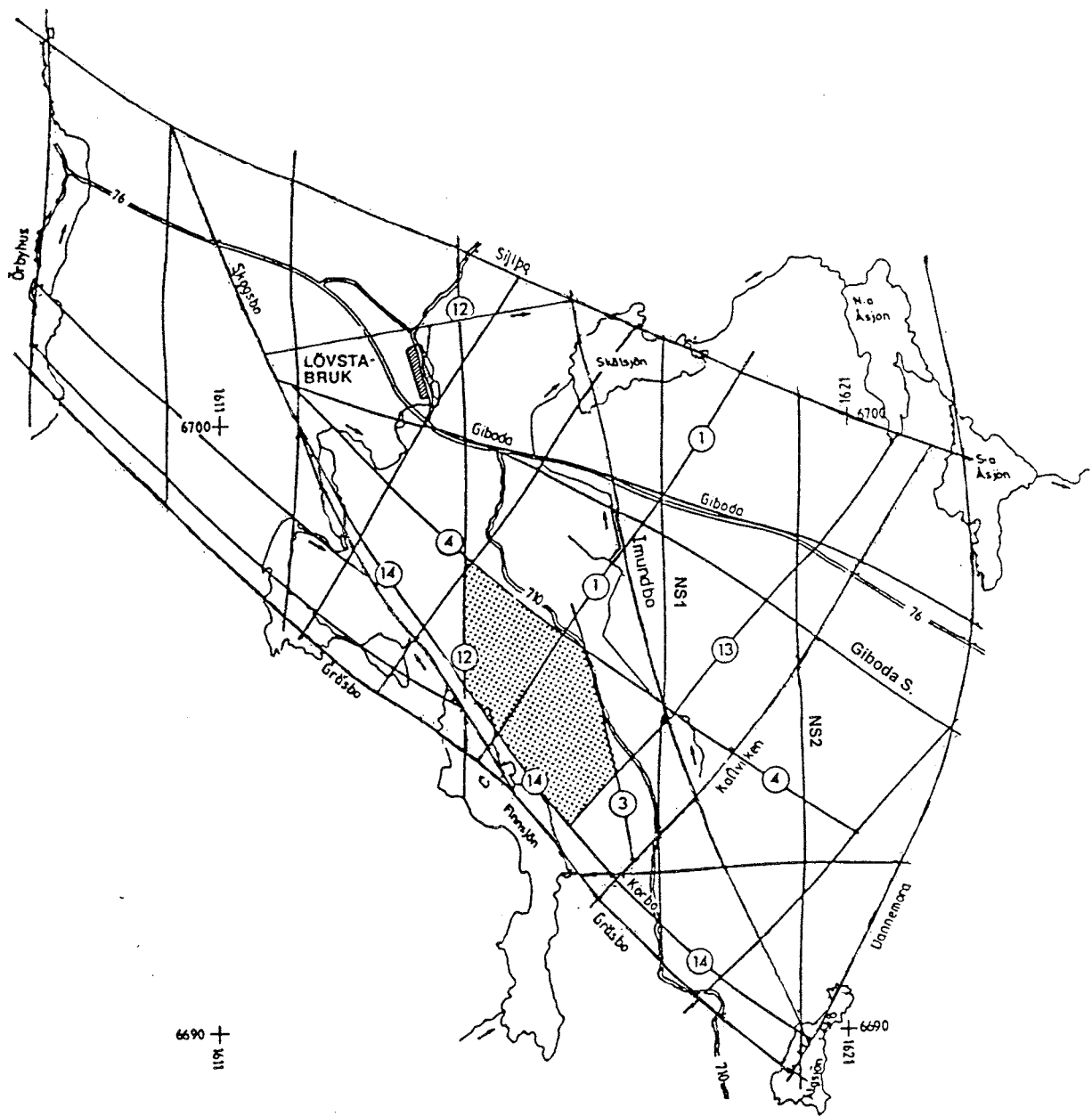
SIMPLIFIED ROCK BLOCK MAP , LÖVSTABRUK AREA
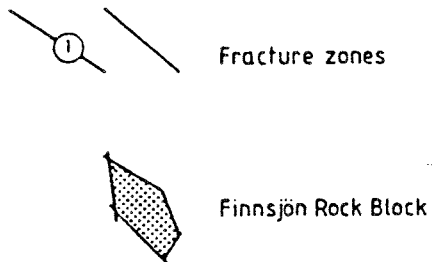
Fracture zones

Finnsjön Rock Block

The glacial striation is north-south

0   2   4 km
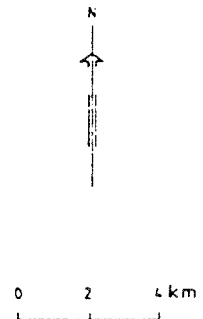
SWEDISH GEOLOGICAL CO
DIVISION OF ENGINEERING
GEOLOGY, Uppsala 1989
S A Tirén

Figure 3-5. Beberg Regional Lineaments (after Ahlbom and Tirén, 1991).
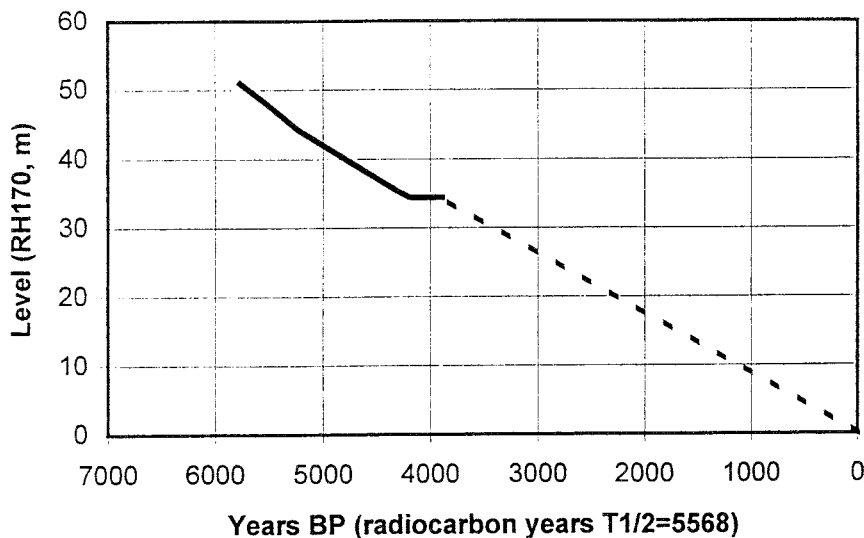
Figure 3-6. *Landrise in Beberg region (after Björk and Svensson, 1992).*

3.2.4. Geochemistry and Salinity

Groundwater with salinity in excess of 300 mg/l of chloride is common in shallow wells (up to 100 m deep) in northeast Uppland. It is estimated that at least 10% of all shallow water wells (50-100 m deep) in this region encounter saline water (Lindewald, 1985). Most of the saline wells are located near the Baltic Sea but many are encountered inland (Figure 3-7).

Saline groundwater is also quite common in deep bedrock wells in the region. Saline groundwater of 7000 mg/l of chloride occurs at 420m depth in the Dannemora Mine and saline groundwater of up to 6000 mg/l of chloride has been encountered in the SFR. Saline groundwater is present in several boreholes in the Finnsjön site. The salinity is about 0.8%, or 5000-6000 mg/l of chloride, at depths ranging from 90-300m. Since saline groundwater inland can indicate older, stagnant groundwater, the presence of saline groundwater in the bedrock at the site has important implications for Performance Assessment (Ahlbom and Tirén, 1991). Appendix D.7 provides relationships for electrical conductivity and salinity versus density.

The presence of saline groundwater at the site has been explained as resulting from the depression and uplift as a consequence of the latest glaciation period. The load of the ice depressed the land surface approximately 500 m in the Finnsjön region. Immediately after deglaciation the Finnsjön site was covered by the brackish Yoldia Sea about 9 600 years BP. As the area rebounded and the land rose, the connection to the Atlantic was closed and a non-saline water covered the area (Ancylus Lake at 9000 years BP). Between 7500-7000 years BP the seawater became saline (Litorina Sea), which gradually transformed into the present brackish Baltic Sea. The Finnsjön site rose above sea level between years 5000-3000 BP (Almén et al., 1978). Smellie and Wikberg (1989) concluded that Finnsjön saline water is dominantly marine in origin, originating from the Yoldia and Litorina seawaters but clearly has been modified by interacting with the

rock. Figure 3-8 shows a principle component analysis of groundwater samples from 71 to 539 mbgs. The plot indicates that the groundwater at the site is a mixture of meteoric, marine and brine waters, increasing in salinity with depth. This complex mixture is consistent with the recent hydrogeologic history of the site. (Laaksoharju et al., 1997).

The salinity of the brackish water of the Baltic Sea at SFR is approximately 5.5 g/l (Sjöberg, 1994).
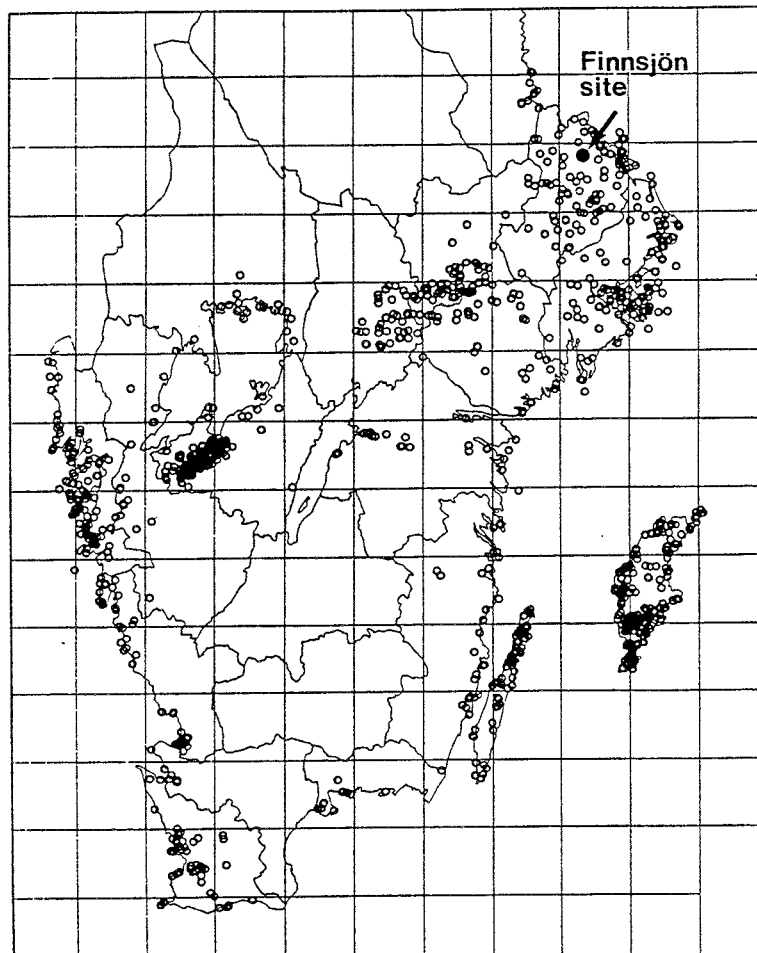
Figure 3-7. *Wells with saline groundwaterin Southern Sweden (from Lindewald, 1985).*

3.2.5.   Surface Hydrology

. The rivers Dalälven, Tämnarån, Forsmarksån and Olandsån drain surface water in the northern part of the region. The southern part of the region drains into Lake Mälaren via the rivers Örsundaån and Fyrisån. The major lakes in the region are shown in Figure 3-9. Within the Finnsjön study area there is a drained lake, Tannsjön, whose surface area is 0.01 km^2. Lake Finnsjön belongs to the run-off area of the river Forsmarksån. The size of the catchment area of the lake Finnsjön is 93km^2 at the inlet and 117km^2 at

the outlet. Lake Finnsjön is oriented north-south with a length 6.5 km, a width of 1 km and a maximum depth is 4.1 m.
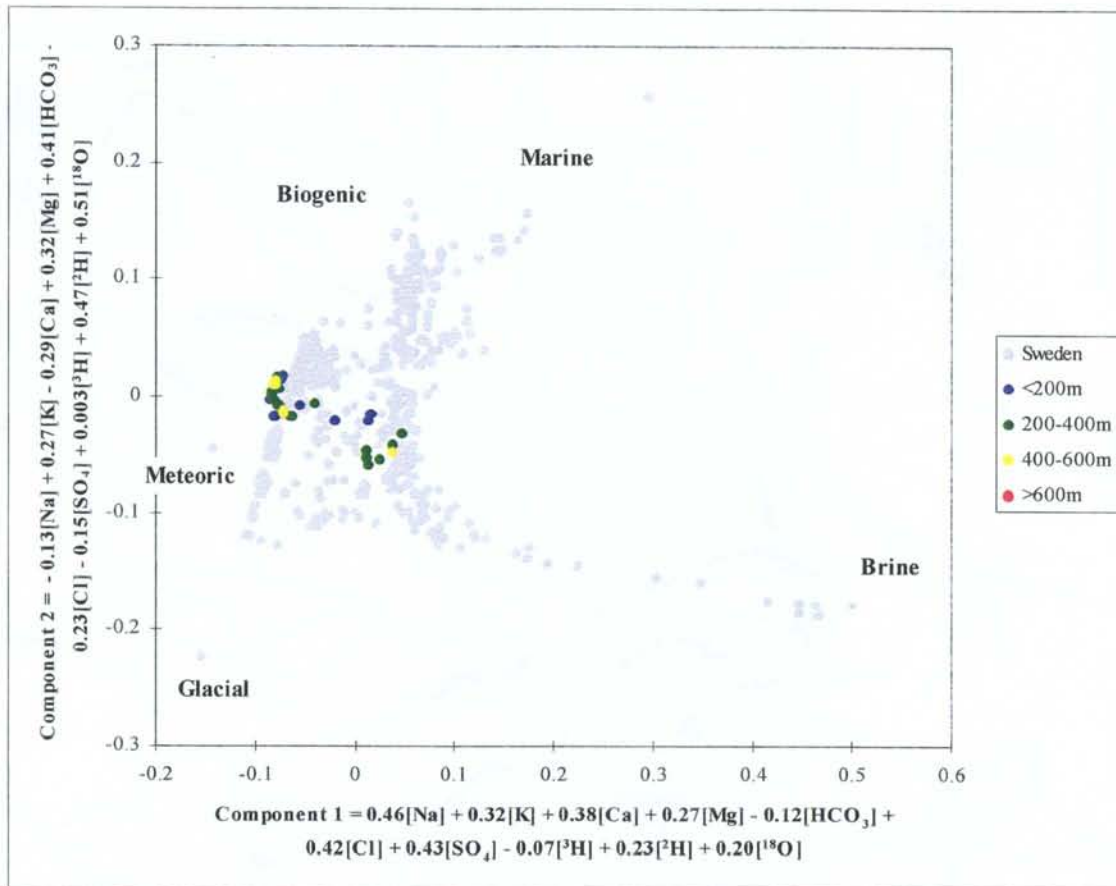
Figure 3-8. *Hydrogeochemical principal component analysis for Beberg (from Laaksoharju et al., 1997).*

Carlsson and Gidlund (1983) estimated the overall water balance for the northern Uppland. The proportion of groundwater discharge areas was estimated as about 30%, and recharge areas as 70%. In the discharge areas the potential evapotranspiration was used while the actual evapotranspiration was used in the recharge areas. The resulting water balance terms are shown in Table 3-2. The potential groundwater recharge to the surface soils was estimated to be about 180 mm/year. Other estimates by Andersson and Olsson (1978) and Carlsson et al. (1986) indicate that a reasonable estimate of the recharge to the shallow groundwater system in the Forsmark area would be 100-125 mm/year. Axelsson (1986) suggested that the actual deep recharge to the bedrock may be much smaller, and has been estimated to be 10-20 mm/year (Carlsson et al., 1986).

59
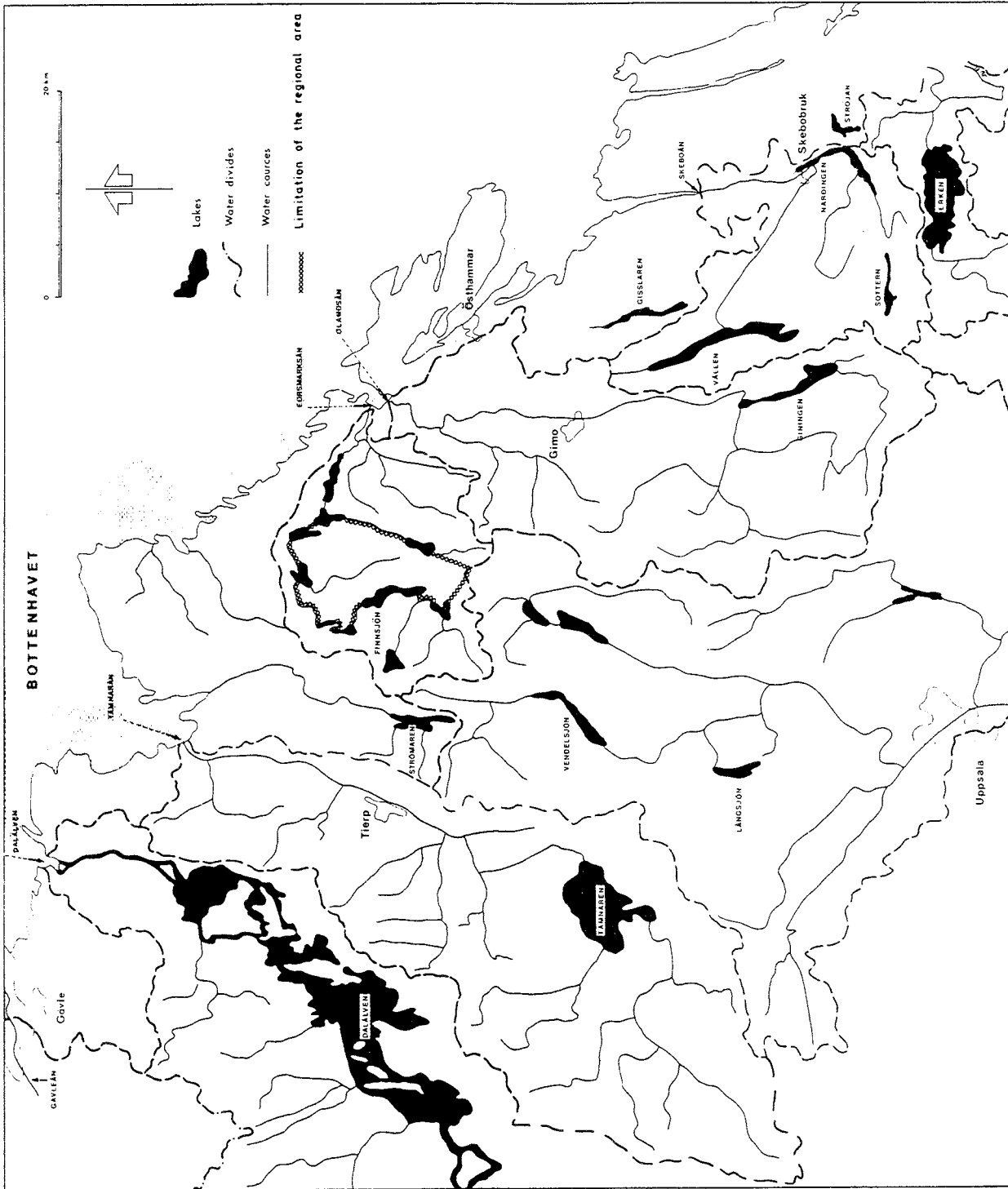
Figure 3-9. Lakes and watercourses, Northern Uppland (from Carlsson and Gidlund, 1983.

Table 3-2. Estimated water balance and groundwater recharge in northern Uppland, expressed in mm/year (long-term). From Carlsson and Gidlund (1983).

Water Balance Component	Rate (mm/yr)
Precipitation	670
Run-off	240
In discharge areas (30%)	
Evaporation	540
Groundwater discharge	420
Available run-off precipitation	130
In recharge areas (70%)	
Evaporation	380
Groundwater recharge	180
Snowmelt run-off water	105

3.2.6. Groundwater Hydrology

Andersson et al. (1991) presented a contour map of the groundwater table within the Finnsjön region (Figure 3-10). The water table coincides with surface water and wetlands elevations, and is assumed to follow a subdued profile of the ground surface. The groundwater table is relatively flat, with a general shallow groundwater flow from the southwest to northeast. Local, minor discharge areas are found in low-lying parts within the area. The regional hydraulic gradient is about 0.2-0.3% for the shallow groundwater.

The deep regional groundwater flow system is poorly understood, since water supply wells are generally shallow in this region. Based on the classical topographic drive model, recharge will enter the groundwater system from the upland lakes of Finnsjön, Lissvass and Åkerbysjön, then flow northeast to discharge areas around Skålsjön. Regional numerical modelling studies generally confirm this pattern, and suggest that local flow systems may also develop (Boghammar et al., 1993). On-site borings indicate little site-wide, consistent pattern of groundwater flow at depth (Section 3.3.3). In the Northern block, upward flow of saline groundwater is observed in Zone 2. Other subhorizontal zones under similar conditions may be present elsewhere in the region.

Several previous modelling studies have been conducted for this site as part of the SKB 91 performance assessment studies. An initial PA model by Lindbom et al. (1991) was criticised for having too limited of a domain, and was later extended by Lindbom and Boghammar (1992). The extended domain PA model showed that the Imundbo fracture zone would intercept particle tracks from all locations with the planned repository. A later 2-D

regional cross-sectional model of Boghammar et al. (1993) confirmed that the extended domain was adequate to accommodate the particle paths, even in the case of hypothetical subhorizontal fracture zones. An extended domain similar to that of Lindbom and Boghammar (1992) is proposed but should be evaluated via sensitivity analysis (Figure 3-11).
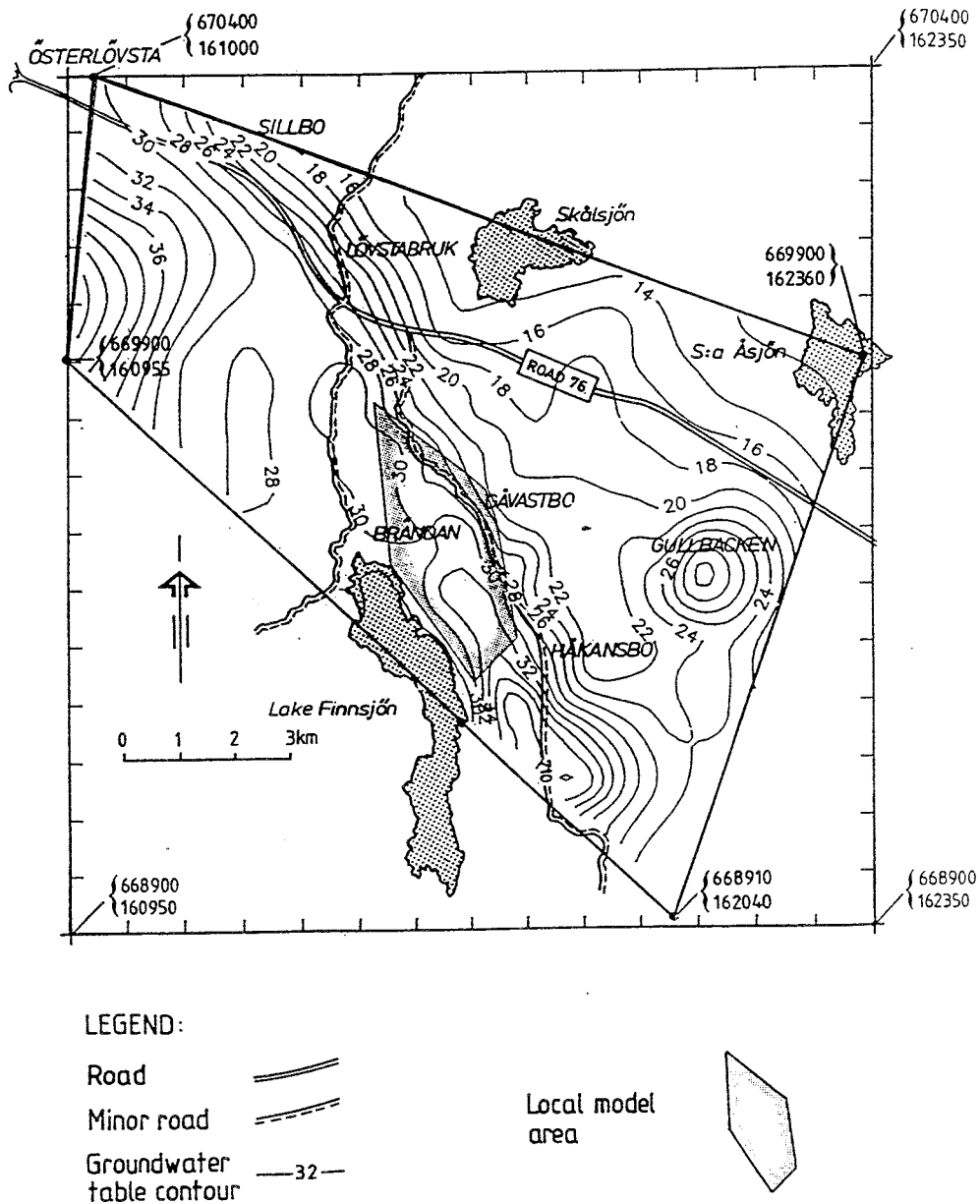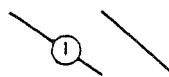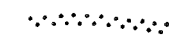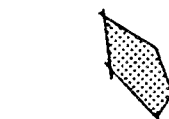
Figure 3-10. Beberg regional groundwater table map (from Andersson et al. 1991).
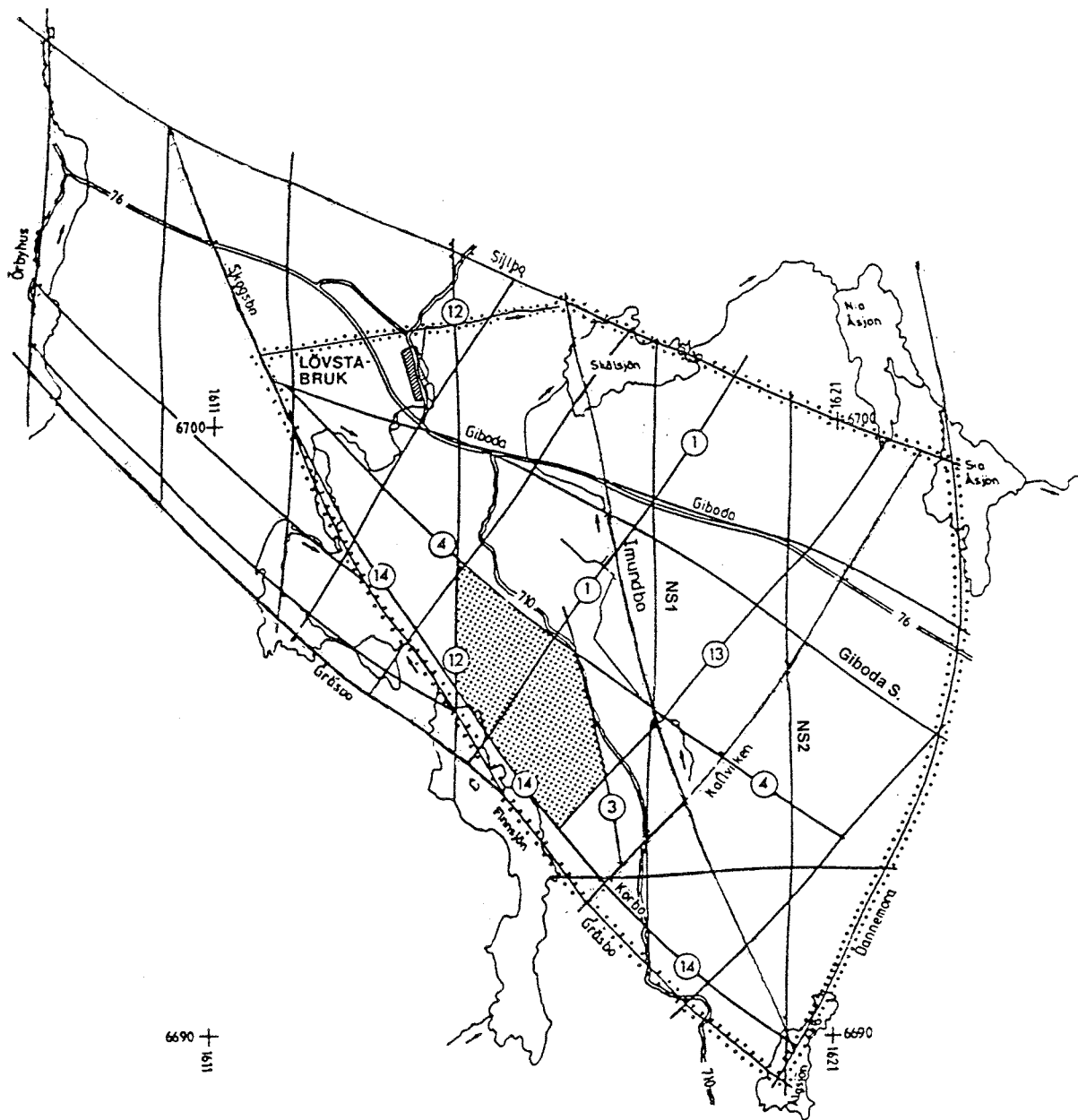
SIMPLIFIED ROCK BLOCK MAP, LÖVSTABRUK AREA

Fracture zones

Proposed extent
of regional model

Finnsjön Rock Block

The glacial striation is north-south

SWEDISH GEOLOGICAL CO
DIVISION OF ENGINEERING
GEOLOGY, Uppsala 1989
S A Tirén

Figure 3-11. Proposed Beberg regional modelling domain (after Lindbom
and Boghammar, 1992).

63

3.2.7. Hydraulic Properties

This study obtained and analysed the SGU well data for wells within a 25km radius of the site in an attempt to infer models of hydraulic conductivity on the regional scale. The SGU well archive data comes primarily from water supply wells, which are typically less than 200m total depth. Consequently, the trend of hydraulic conductivity with depth on the regional scale must be inferred from the on-site packer test data. Similarly, the 3m data on-site is used to determine the contrast between the rock mass versus fracture zones. This is combined with the SGU data to produce models for the Beberg regional scale hydraulic conductivities. Details are presented in Appendix B.2.

The SGU data appears to be spatially clustered near communities (Figure 3-12) but cluster analysis did not indicate that the data is preferentially clustered in areas of high hydraulic conductivity. Geostatistical analysis suggests that the hydraulic conductivities are spatially correlated over a practical range of 2.3km. Subsequent crossvalidation indicates that including this correlation results in limited improvement in the estimation of unknown values due to the high nugget value.

3.2.7.1. Rock Mass – RRD

The mean of the SGU data is used to determine the hydraulic conductivity of the upper elevations of the Beberg rock domain. However, the on-site packer tests are used to infer the trend with depth. The 3m packer test data can be separated into fracture zone data and rock mass data. Appendix B.3 provides the details of the determination of elevation zones for hydraulic conductivity. The regional rock domain model (RRD1) should use the elevation zones defined for this 3m rock mass data, upscaled as necessary. Table 3-3 presents the hydraulic conductivity for RRD1, the 3m data elevation zones upscaled to 100m:

Table 3-3. Beberg rock mass domain hydraulic conductivity values based on SGU data and on-site 3m tests, upscaled to 100m (RRD1).

Elevation (masl)	Arithmetic Mean $\mathrm{Log_{10}}$ K(m/s)	Variance	Number of Samples
Above -100	-6.81	0.210	142
-100 to -200	-7.67	0.151	119
-200 to -400	-8.07	0.0970	325
Below -400	-7.80	0.0424	265

Finnsjön area (overview)

Terrainshading of digital terrain model (DTM).
The Finnsjön site is inside the rectangle
in the middle of the map.

Legend

- Municipal boundary
- Road
- Railroad
- Water
- Urban area > 200 inhabitants
- ○ SGU well

GIS-bearbetning: GIS-centrum   97-03-24

Scale 1:400 000
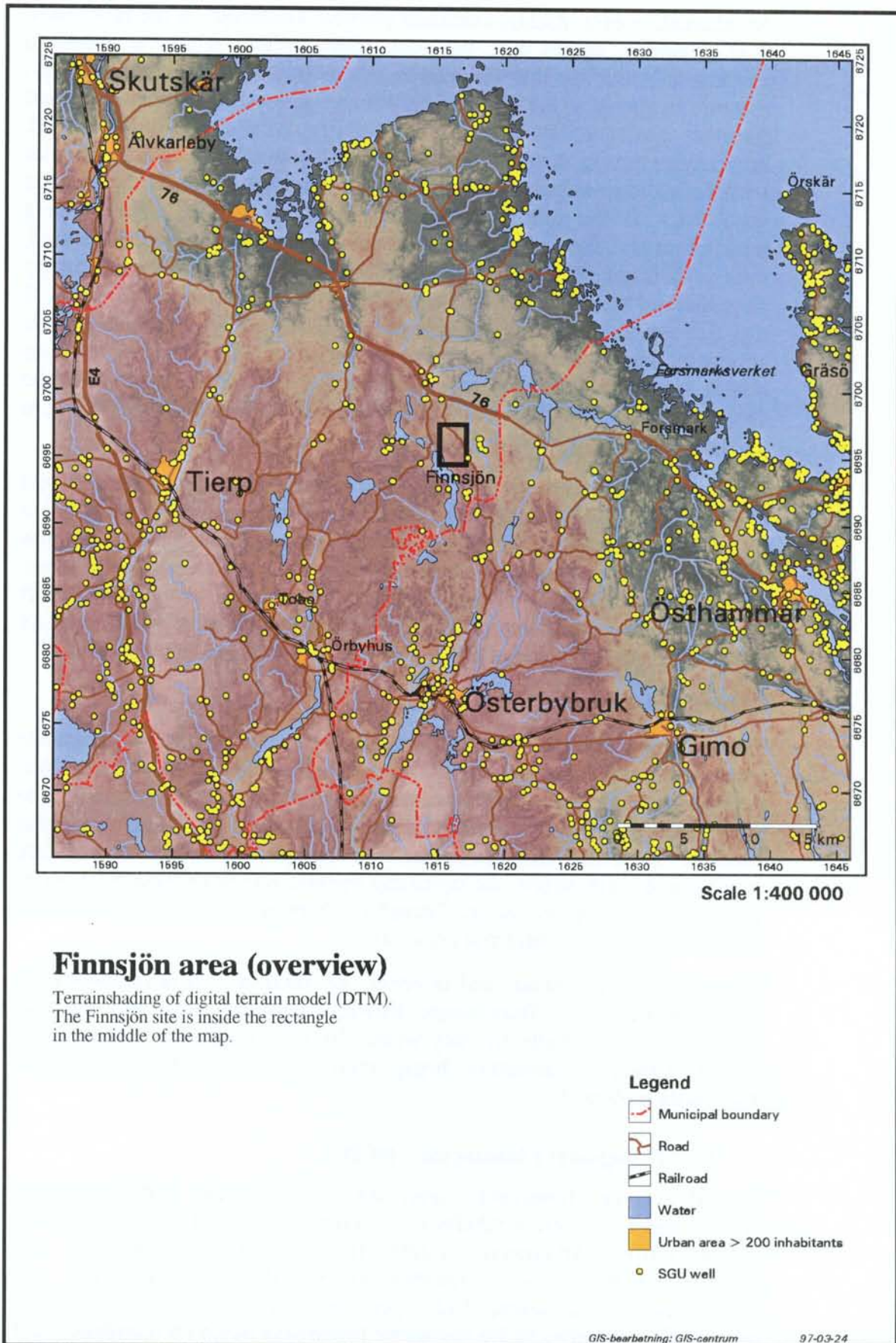
Figure 3-12. Finnsjön overview and SGU well data.

An alternative case, RRD3, examines possible anisotropy in the rock mass. It is generally agreed that the rock mass in this region is fractured preferentially and that this will lead to anisotropy of hydraulic conductivity. Fracture mapping at the site indicates that fractures in the rock mass are oriented northwest-southeast, which agrees with the regional trend. Interference tests in Zone 2 indicated isotropic transmissivity for the zone as a whole but some anisotropy of the hydraulic fracture conductivity with the major axis to the northwest (Andersson et al., 1991). For scoping calculations and alternative case models, analogue site studies may be used, such as Carlsson, et al. (1986) suggested a hydraulic conductivity anisotropy magnitude of 10:1 in the horizontal plane for the SFR studies. For the Äspö site, Rhén et al. (1997) suggested a ratio of 100:1:10 for horizontal major: horizontal minor: vertical minor. For the Gideå region, Ericsson and Ronge (1986) suggested that major axis of anisotropy should be aligned with the direction of maximum horizontal rock stress. In northern Uppland, this is in the direction of N 48 W with a standard deviation of $\pm$ 10°.

Beberg porosity values are inferred from tracer tests in the uppermost part of Zone 2, suggesting a range of kinematic (flow) porosities of 8×10^{-4} to 1×10^{-2} (Andersson et al., 1991). These values might be biased high because Zone 2 is more intensely fractured than the surrounding rock mass. Brandberg and Skagius (1991) present a compilation of other transport properties based on laboratory testing of Finnsjön core samples. Andersson et al. (1997) present a compilation of transport parameters for use in SR 97.

Uncertainties:

The reduction of SGU well archive data for water capacity to hydraulic conductivity should be considered only a rough approximation. Also, since the wells were generally drilled for water supply and not for exploration, the SGU data may be a biased sample. Although the mean hydraulic conductivity of the SGU data agrees with the upscaled 3m-packer test data at comparable elevations, the upscaling method was developed from Äspö and may not be appropriate for Finnsjön. Therefore the mean and variance of RRD1 should be considered uncertain.

The anisotropy magnitude and direction are uncertain. It is impossible to determine anisotropy from single borehole injection tests, and the few interference tests on site are only within Zone 2. Similarly, the kinematic porosity values are uncertain, being inferred on the regional scale from tracer tests in Zone 2.

3.2.7.2. Regional Lineaments – RCD

Several regional lineaments cross the Finnsjön site, and have been investigated by several boreholes (see section 3.2.2, Figure 3-5; compare to Figure 3-16). Additional information is provided by the SFR site characterisation studies. Andersen, et al. (1991) and Lindbom and Boghammar (1992, citing Tirén, personal communication, 1992) have inferred the properties of the remaining lineaments based on orientation and similarity to other lineaments in the region. Table 3-4 summarises the properties of these lineaments.

Table 3-4. Beberg regional conductor domain properties based on on-site 3m test data, upscaled to 100m (RCD1).

Zone	Inferred from	Dip	Width	Median Log_{10} K (m/s)	Variance Log_{10} K	Sample Size
1*	1 borehole	75SE	20	-4.33	0.0896	14
2**	9 boreholes	16SW	100	-5.14	0.299	82
3	1 borehole	80SW	50	-5.63	0.180	37
4	zone 5	60SW	10	-5.16	0.122	
12	Singö	90	25	-4.91	0.289***	
13	zone 1	90	20	-4.33	0.0896	
14	Singö	90	100	-4.91	0.289***	
Skogbo	zone 5	90	100	-5.16	0.122	
Giboda	zone 5	90	100	-5.16	0.122	
Giboda S.	Giboda & 4	90	50	-5.16	0.122	
Imundbo	zone 5	90	100	-5.16	0.122	
Gräsbo	Singö	90	100	-4.91	0.289***	
Dannemora	Singö	90	100	-4.91	0.289***	
Källviken	zone 1	90	100	-4.33	0.0896	
Örbyhus	Singö	90	100	-4.91	0.289***	
Sillbö	Singö	90	100	-4.91	0.289***	
NS1	Singö	90	50	-4.91	0.289***	
NS2	Singö	90	25	-4.91	0.289***	

Lineaments in **bold** also appear in the site-scale model.

*also known as the Brändan fracture zone

** Not actually in regional set, but included to address RCD3. Also the subject of many interference tests

***variance inferred from all Finnsjön 3m data in CD

RCD1 assumes that the unnamed lineaments in Figure 3-5 have properties that are the same as other regional lineaments with similar orientations and tectonic origins. Unnamed lineaments trending northeast–southwest will assume the same properties as the Singö fault or Zone 1. Northwest – southeast trending unnamed lineaments will assume the same values as Zone 5. The properties of the remaining unnamed lineaments, trending north –south and east –west, are highly uncertain. Because of their age and orientation, RCD1 assumes that these will have the same properties as Zone 12 (i.e., the Singö fault) (Andersson, et al. 1991).

Similar to the rock mass hydraulic conductivity, the trend in conductor hydraulic conductivity is inferred from the on-site packer tests. A separation of 3m packer test data into Conductor Domains indicated that there was no trend in hydraulic conductivity with depth for the conductors (See Appendix B.2.3 for details). Porosities should be assumed to be the same as in RRD1, with sensitivity analysis.

An alternative case, RCD2, is proposed to examine the possibility of a decreasing trend in fracture zone hydraulic conductivity with depth. For this case, the same relative step decrease in conductor hydraulic conductivity may be used as was suggested for the rock mass in RRD1.

An additional alternative case, RCD3, is suggested by the presence of the extensive subhorizontal conductive zone, Zone 2. Similar zones are observed at SFR and Dannemora, suggesting that additional subhorizontal zones may exist in the area but have not yet been discovered. The possible occurrence of such a zone should be evaluated for its impact on the modelling results. At SFR, one such zone is observed (15m thick at -100 to - 160 masl) and at Dannemora several zones are observed (at 300 to 500m intervals). Dips are toward the south, inclined between 0 to 30 degrees from horizontal (Ahlbom et al., 1988; Ahlbom and Tirén, 1991; Andersson et al., 1991).

Uncertainties:

It should be noted that the Beberg regional lineaments are assumed to be conductive fracture zones whose width can be inferred from topographic expression or orientation. Experience suggests that this is much too simplistic of a model; mineralised fractures can have very low hydraulic conductivities. The designation of lineaments as conductive fracture zones therefore should be considered uncertain and be evaluated by deterministic sensitivity analysis. In general, the properties given in RCD1 are based on tests in lineaments with similar tectonic origin and similar orientation. In the case of the north –south and east –west trending lineaments, no test data is available in similar lineaments. Consequently, the properties of the north –south and east –west trending lineaments should be considered uncertain.

3.3. SITE SCALE

The Finnsjön site is defined as a 6km² rectangular area immediately to the north of Lake Finnsjön (Figure 3-13). The basis for the Beberg site-scale model is the hydrogeologic information found in Andersson et al. (1991) and the interpreted hydraulic properties found in the SKB SICADA database.

3.3.1. Geology

85% of the surficial geology at the Finnsjön site consists of Quaternary sediments (till and peat), with the remaining 15% as by rock outcrops. Rock outcrops dominate in the higher elevations of the site. The till surface has been reworked by the retreating shoreline of the Baltic Sea. Fluvial sands are found in some depressions (e.g., Gåvastbo) (Gustafsson et al., 1987; Ahlbom et al., 1992).

The Finnsjön site is located in the Finnsjön Rock Block, situated in a regional WNW trending shear belt (Figure 3-14). A steep fracture zone running northeast to southwest, Zone 1 (the Brändan zone) divides the Finnsjön Rock Block into the Northern and Southern blocks. As shown in Figure 3-15, the site is located within a folded, greyish granodioritic intrusion, and approximately 12km² in size. Foliation strikes northwest to southeast with vertical to subvertical dips. Dykes of pegmatite, metabasite and aplite can be found within the granodiorite, and small bodies of granite and greenstone are found at the margins of the site (Ahlbom et al., 1992).

Site investigations identified a number of relatively conductive fracture zones between 5 and 100m in width. The rock blocks are further divided into third order blocks by northwesterly trending fracture zones, dipping 60 degrees southwest. Several boreholes on site penetrate these features and provide data for the inference of hydraulic properties, orientations and widths (Andersson et al., 1991).

Zone 2, a wide, gently dipping fracture zone, separates the Northern block into an upper low-fractured bedrock and a lower, more fractured bedrock (Figures 3-16 and 3-17). The groundwater in the upper Northern block is fresh water, while the groundwater in the lower Northern block is saline. This groundwater below Zone 2 is thought to be very old in origin and therefore the flow system in the lower Northern block is believed to be relatively stagnant. A similar subhorizontal, wide fracture zone, Zone 11, is found in the Southern block, but that zone is not saline.
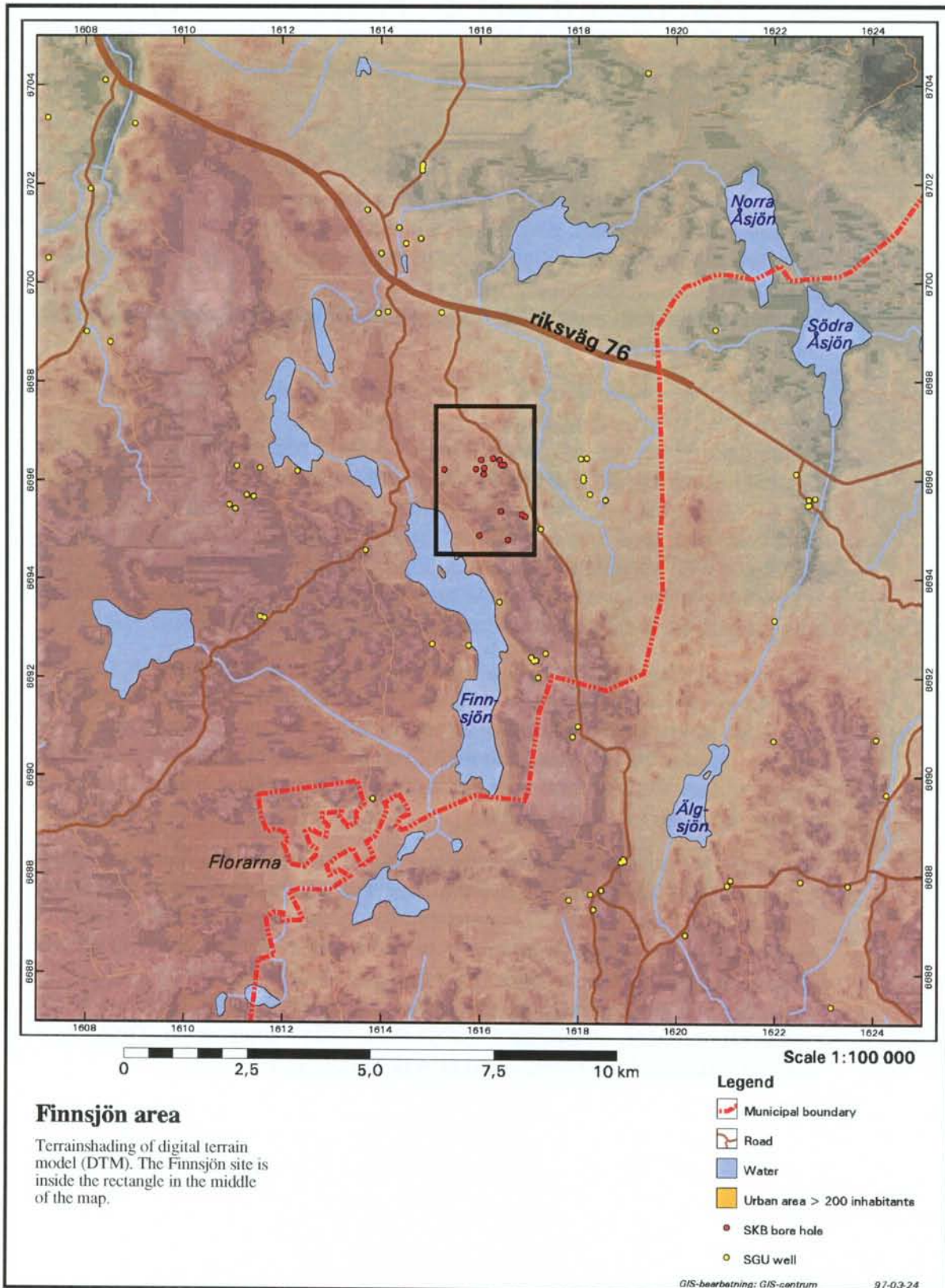
Figure 3-13. *Finnsjön Area.*
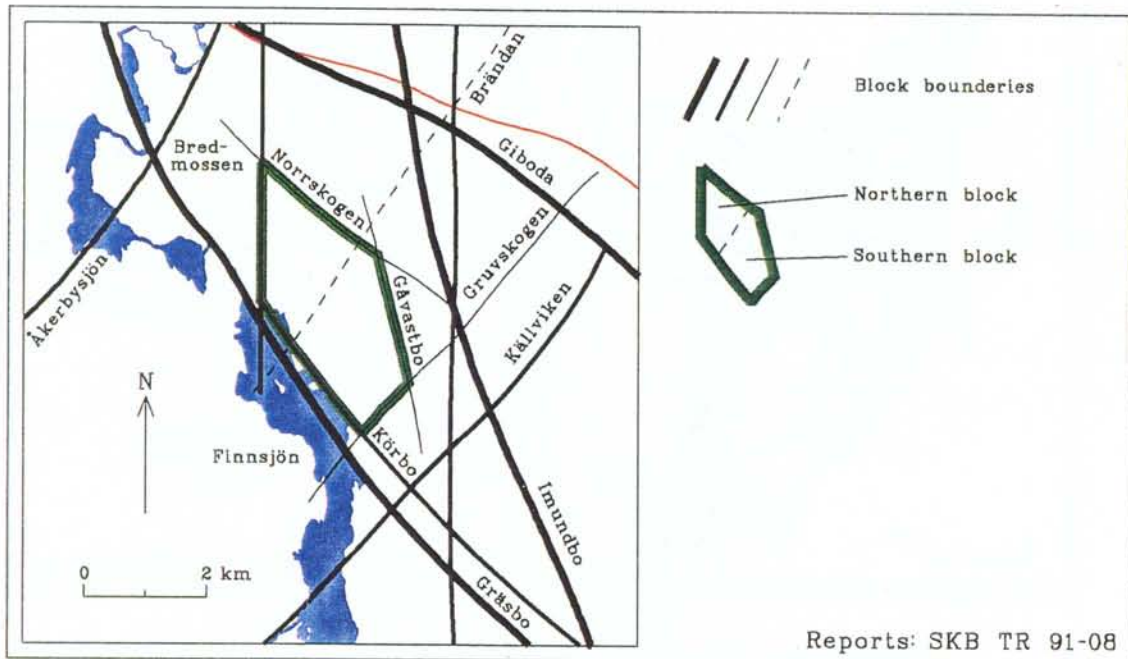
Figure 3-14. *The Finnsjön rock block (from Ahlbom et al., 1992, citing Ahlbom and Tirén, 1991).*
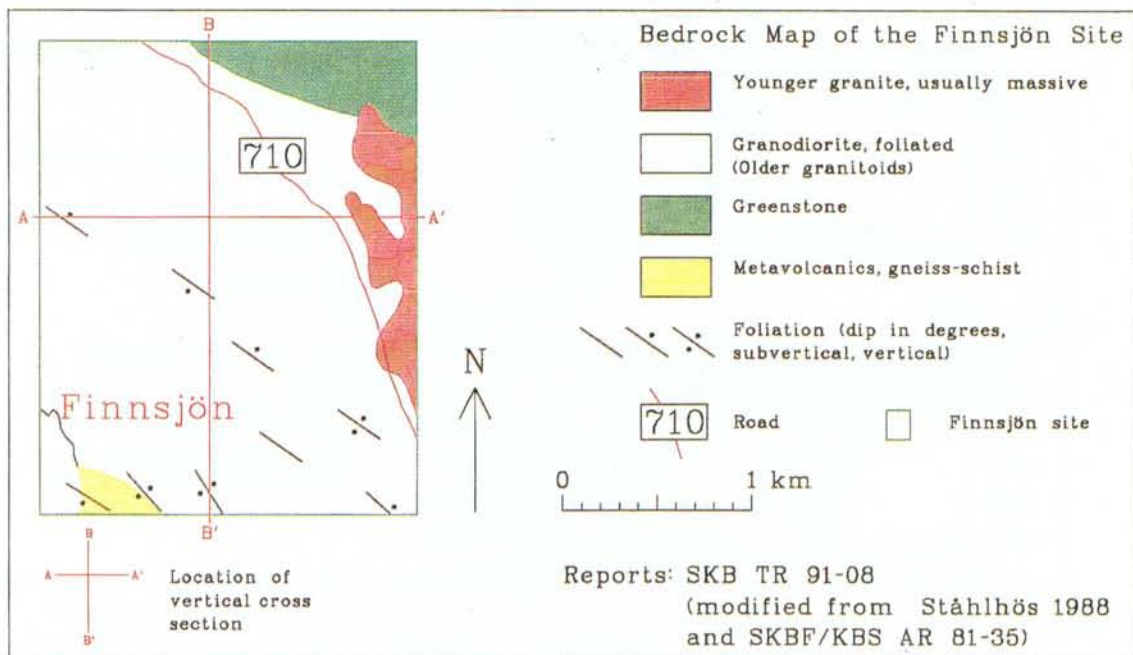
Figure 3-15. *Finnsjön bedrock geology (from Ahlbom et al., 1992, citing Stålhös, 1988).*

71
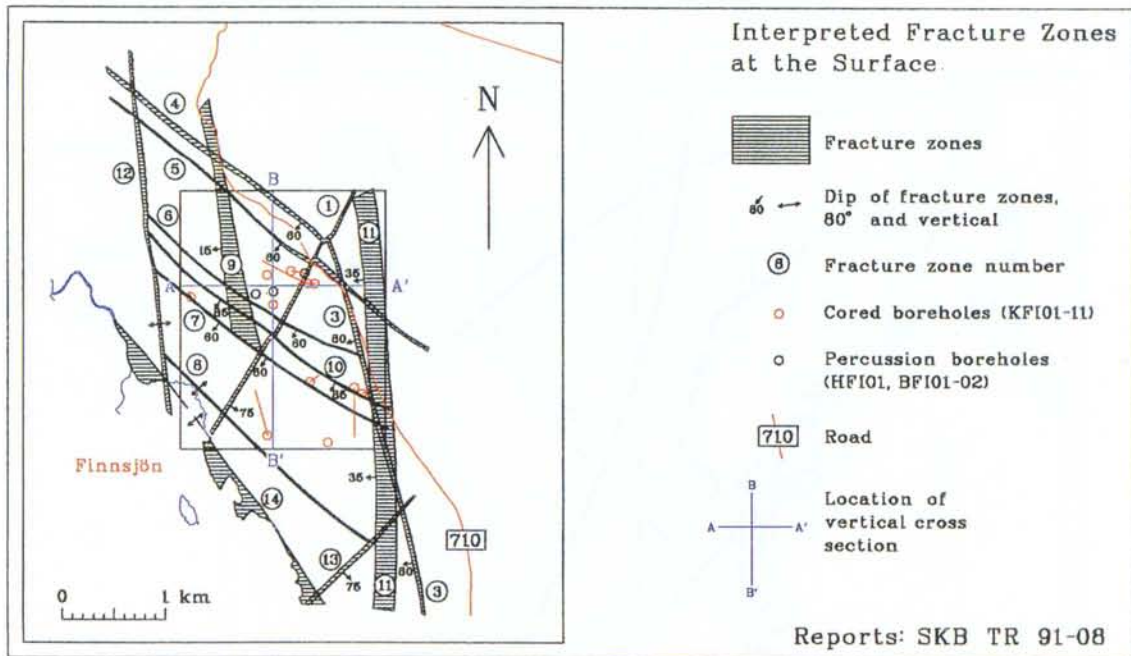
Figure 3-16. *Beberg site-scale interpreted fracture zones (from Ahlbom et al., 1992, citing Ahlbom and Tirén, 1991).*
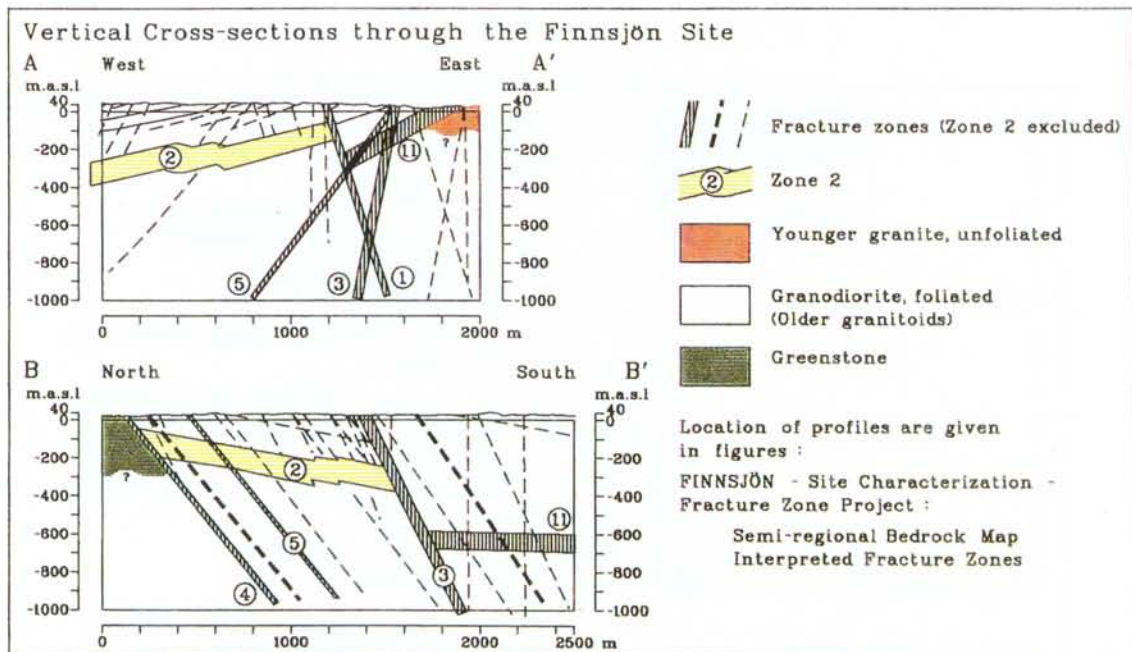
Figure 3-17. *Cross-sections through Beberg site-scale interpreted fracture zones (from Ahlbom et al., 1992, citing Stålhös, 1988).*

Fracture orientations are inferred from detailed fracture mapping in a 5 x 90m long trench in the Northern block, near KFI11. Figure 3-18 presents a stereonet plot for fractures mapped in the trench and in a 1 x 48m cell within the trench. The fractures can be assigned to two groups, one N20-75°E/70-90° and another N30-80°W/60-90° (Andersson et al., 1991). Including fracture zones, the average fracture frequency in the boreholes is 2.9 per metre, with no trend in depth (Carlsson and Gidlund, 1983).
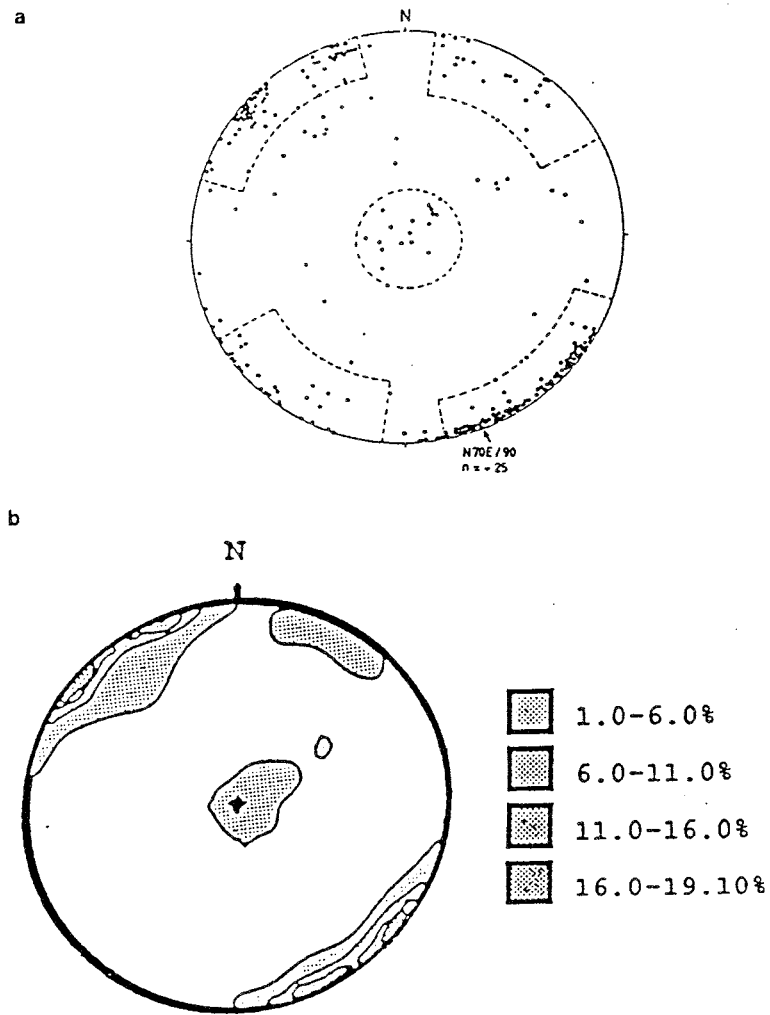
Figure 3-18. Fracture orientations at Finnsjön, a) inside 1x 48m cell, n=272, and b) in 90m trench, n=335 (from Andersson et al., 1991).

3.3.2. Surface Hydrology

The land surface within the site has an average elevation of approximately 25 masl and is flat, varying ± 15m. The area is mostly forested, with some swamplands. Peat deposits are common, dominating the central area of the site. Exposed bedrock outcrops are common, comprising as much as 60% of the Northern block and 40% of the southern block

The entire site (and much of the region) belongs to the Forsmarksån watershed. The surface water system of the Southern block is divided into two systems, one draining northeast, the other to the southwest. The Northern block drains to the northeast. The systems merge northeast of the site. The site surface hydrologic modelling parameters are otherwise as described for the regional scale in Section 3.2.5 (Ahlbom et al., 1992; Gustafsson et al., 1987).

3.3.3.   Groundwater Hydrology

Within the Finnsjön site, the groundwater table surface is a subdued reflection of the topography, slightly deeper in uplands and shallow-to-ground surface in lowlands (Figure 3-19). Using on-site head measurements, Andersson et al. (1991) mapped a mean water table surface, as shown in Figure 3-20). The shallow groundwater flow pattern is complex, with flow both to the northeast and to the southwest. Low-lying areas are typically groundwater discharge zones, while upland areas are groundwater recharge zones. It is not known how deep this pattern may persist. The annual maximum water table level is in November to December, and the minimum is in August to September.
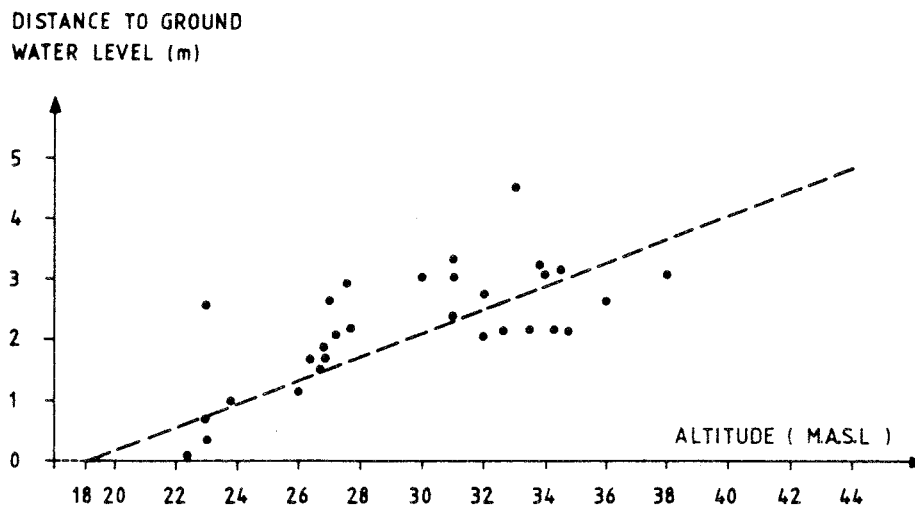
Figure 3-19. Depth to water versus elevation at Beberg site (masl, from Carlsson and Gidlund, 1983).

The deep groundwater system is a relatively complex system of subhorizontal fracture zones and abrupt salinity variations. The site characterisation programme included eleven cored borings penetrating to a depth of over 690m. In addition to the hydraulic and geophysical testing programmes, hydraulic heads were recorded in packed-off intervals of each borehole. The pressures were corrected for the varying salinity along the boreholes and converted to overpressures relative to hydrostatic pressure at depth (Figure 3-21). The overpressures are generally small, both above and below Zone 2, making any conclusions rather uncertain. The potential error in the pressure differences of the pressure transducers is estimated to about ±1 kPa (0.1 m). Furthermore, errors may also result from insufficient time allowed for the section pressure to stabilise after packer inflation. However, the gradients indicate that where Zone 2 is deep below the surface, it is recharged by nonsaline groundwater from above. Where Zone 2 is located closer to the ground surface, the gradient is reversed implying that saline groundwater is discharged from Zone 2. However, because Zone 2 is relatively transmissive, is thought to discharge laterally to Zone 1 (Gustafsson and Andersson, 1989). This conceptual model is summarised in Figure 3-22. The model is also supported by borehole piezometric measurements.

Elsewhere in the site and in the region, the groundwater hydrology is equally as complex as in the Northern block. In the Southern block, the salinity and flow patterns appear to be quite different, where a non-saline, subhorizontal zone, Zone 11, is found. In fact, saline water is not encountered in the Southern block down to the maximum borehole depth of approximately 600mbgs. This suggests that the groundwater system in the Southern block is well connected to freshwater sources, allowing a more thorough flushing of older saline water. In contrast, saline groundwater is encountered in KFI08, where it crosses Zones 3 and 11 to penetrate the rock block east of the Finnsjön rock block. This is thought to be the result of the overlying 7-8m of glacial clay, which restricts precipitation recharge to the rock block below (Ahlbom et al., 1992c).

Detailed salinity measurements in the on-site boreholes are available in SICADA
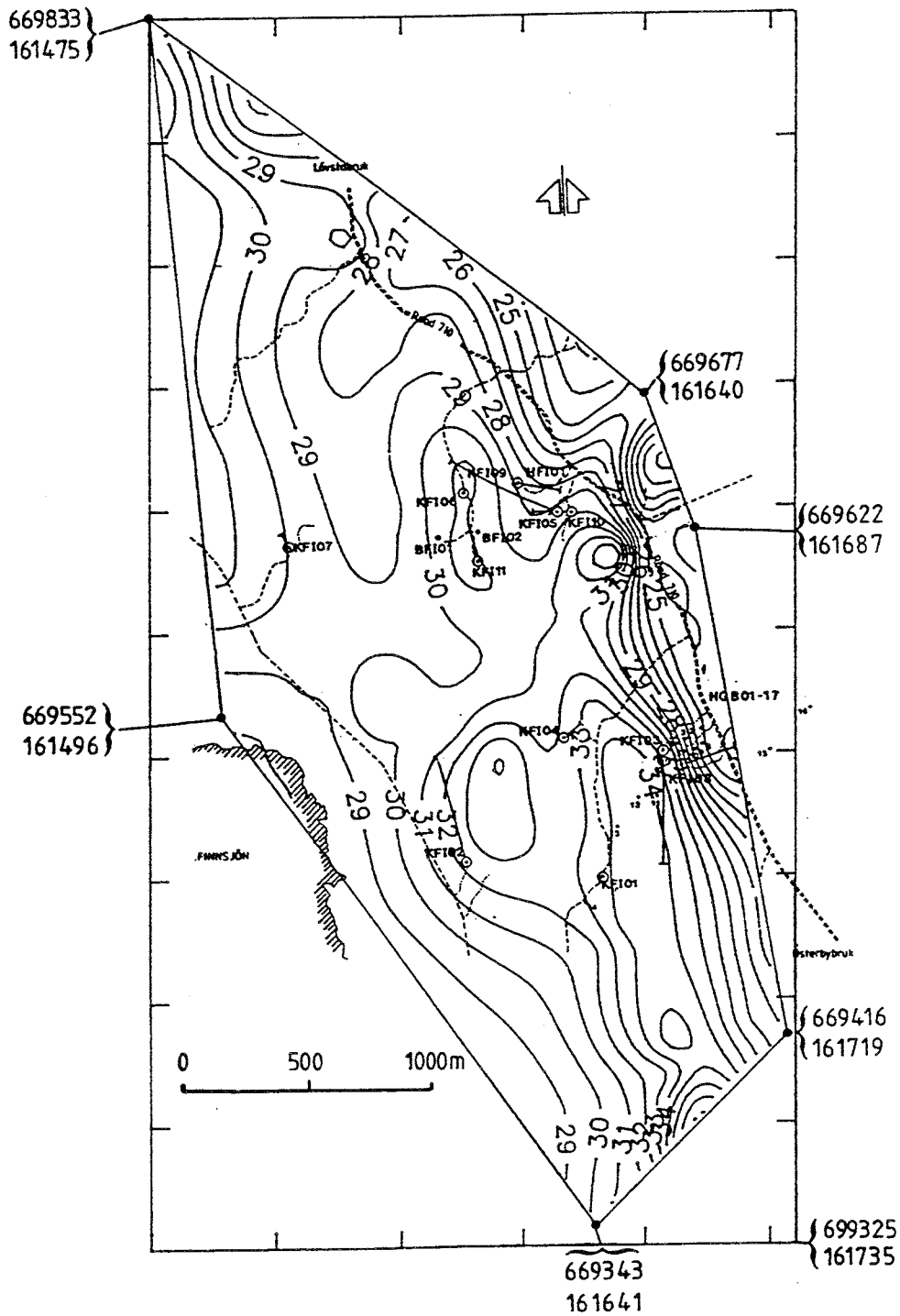
Legend:

LEGEND:

Road   = = = = = = = =

Minor road   - - - - - - -

Core borehole   ⊙

Percussion borehole   ●

Groundwater table contour   —32

Figure 3-20. *Water table surface at Beberg site, (masl, from Andersson et al. (1991).*

76
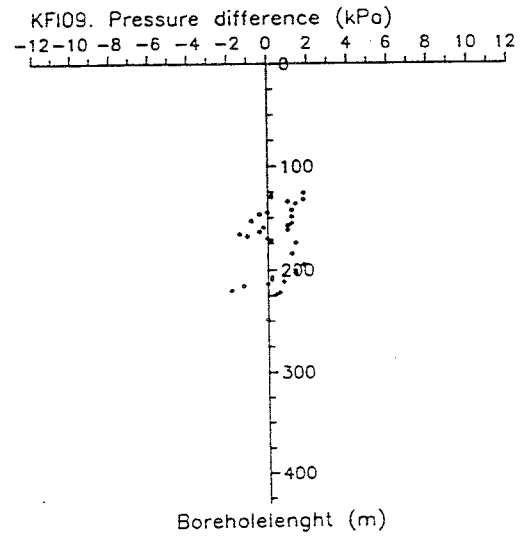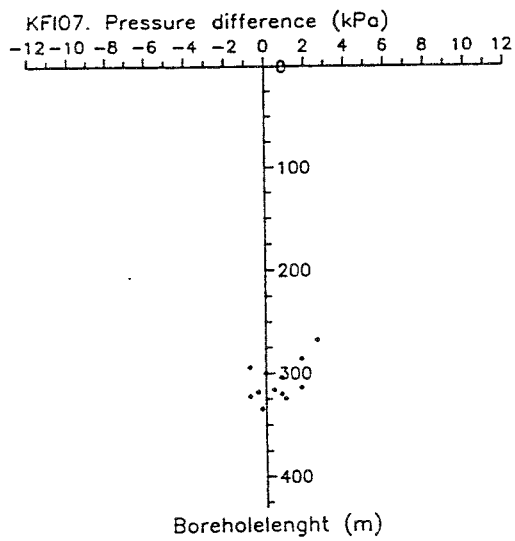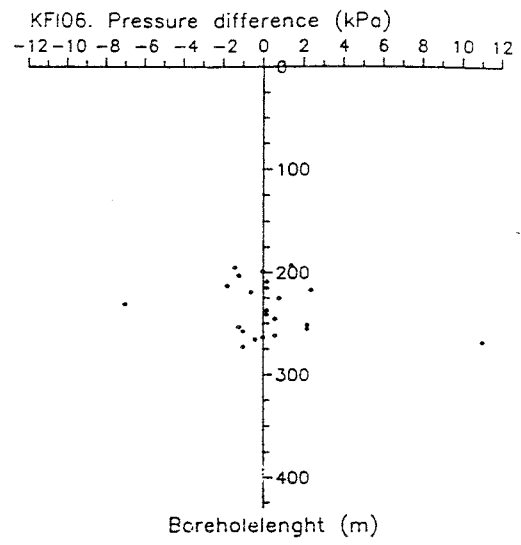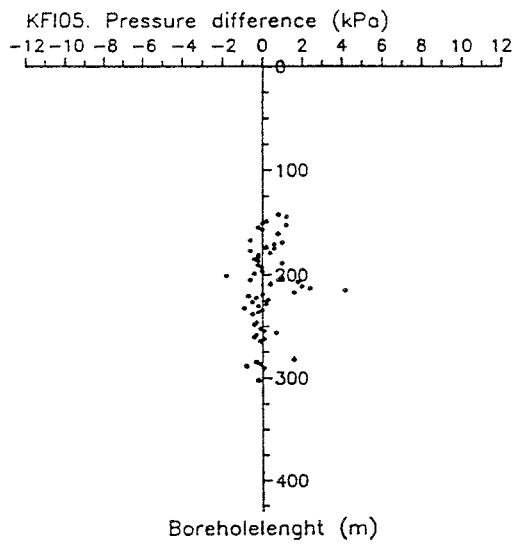
Figure 3-21. Overpressure vs. depth at Finnsjön site, (from Andersson et al. (1991).
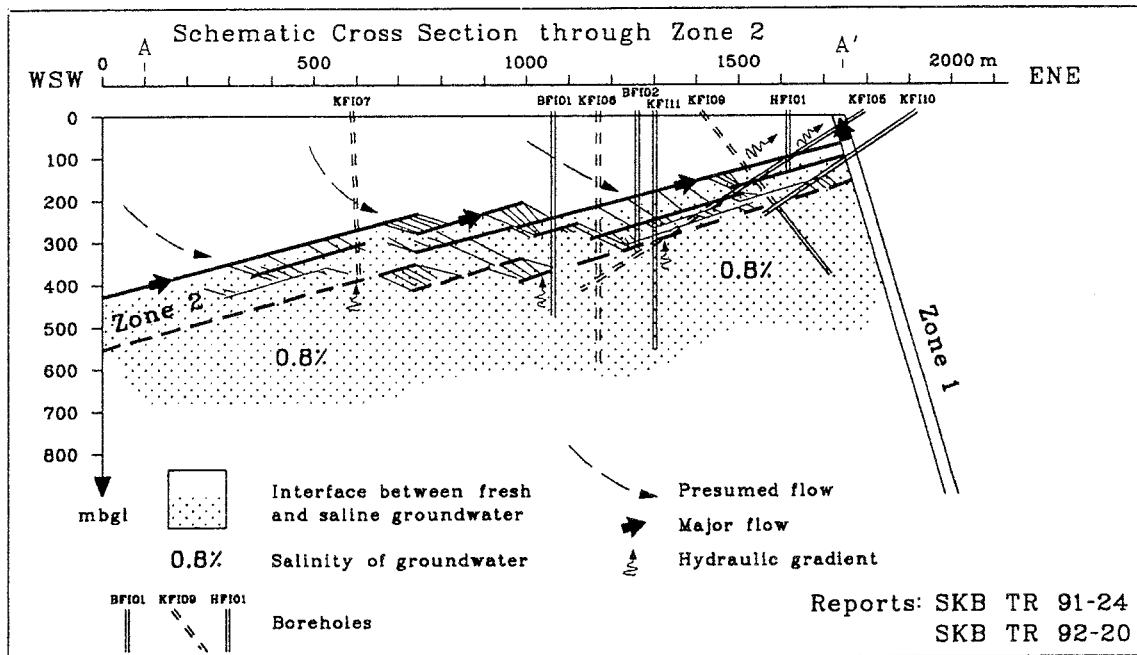
Figure 3-22. *Conceptual Hydrogeological model of Zone 2, in the Northern Rock Block of Finnsjön (from Ahlbom et al., 1991).*

3.3.4. Hydraulic Properties

The first site characterisation campaign used a test section length of 3m throughout the boreholes. In the Fracture Zone Project, the intervals of Zone 2 were generally tested in 2m sections and a few boreholes in 20m sections. A few tests with 5 m and 10 m have also been performed. Finally, a special survey was made over a total length of 10m in borehole BFI02 using injection tests in 0.11m borehole sections. The total borehole length covered by continuous double-packer tests with a section length of 20 m at Finnsjön is 1550 m, with 2m-length 1660 m and with 3m-length 4131 m.

Similar to the regional model (Section 3.2.7), the model domain is separated into a low-conductivity rock mass domain and a higher-conductivity conductor domain. This separation is based on the structural geologic model in Table 4.3 of Andersson et al. (1991). The rock domain differs from the conductor domain only by the relatively low hydraulic conductivity.

Beberg site-scale hydraulic properties are inferred from the interpreted hydraulic conductivities of the 3m packer test data, as discussed in Appendix B.3. The hydraulic conductivities are upscaled to 24m, which is the proposed grid scale for site-scale modelling (Hans Widén, personal communication, 1997).

3.3.4.1. Rock Mass – SRD

The Beberg rock mass hydraulic properties are inferred from the Finnsjön 3m packer test data. SRD6 assumes that the hydraulic conductivity has a constant geometric mean and variance within elevation zones inferred from

the 3m packer test data. The means and variances should be upscaled as necessary to the model grid scale (Table 3-5). Similar to the regional rock domain, no separation of rock mass is made on the basis of rock type. However, the domain should be separated as Northern and Southern blocks, as suggested in Andersson et al. (1991) and Axelsson et al. (1991). Note that the occurrence of the elevation zones and the form of the trend functions are deterministic.

Table 3-5. Beberg site-scale rock mass domain hydraulic conductivity values based on 3m tests upscaled to 24m (SRD6).

Elevation (masl)	Arithmetic Mean Log_{10} K(m/s)		Number of Samples
	3m	24m	
Northern Block			
above -100	-7,35	-6,64	93
-100 to -200	-7,89	-7,18	52
-200 to -400	-8,50	-7,79	177
Below -400	-8,35	-7,64	175
Southern Block			
above -100	-7,50	-6,79	60
-100 to -200	-8,54	-7,83	81
-200 to -400	-8,80	-8,09	208
Below -400	-8,59	-7,88	90
All SRD, All depths	-8,47	-7,76	828

Andersson et al. (1991) reported that preferential fracturing could be observed on outcrops and in trenches (see Section 3.3.1), which suggests that the hydraulic conductivity of the rock domain may be anisotropic. Hydraulic tests in Zone 2 suggest that the anisotropy within that fracture zone is consistent with the regional stresses. However, no formal tests for anisotropic hydraulic conductivity of the type advocated by Hsieh and Neuman (1985) were conducted. An alternative case, SRD7, is suggested to include anisotropy in the rock mass hydraulic conductivity with a magnitude of 10:1 in the horizontal plane and major axis in the direction of N 48° W with a standard deviation of ± 10° (as in RRD3; see Section 3.2.7.1). Note that the overall magnitude of the hydraulic conductivity should not change under this transformation.

Uncertainties:

The depth zone means and variances are relatively sensitive to the choice of depth interval, and should considered uncertain. Rigorous tests for hydraulic anisotropy have not been conducted at this site, and the given anisotropy ratio is considered uncertain. Transport parameters in the Rock domain outside of Zone 2 are uncertain.

3.3.4.2. Conductors – SCD

SCD1 represents the mapped fracture zones as hydraulically conductive features, with the locations and orientations as given in Andersson et al. (1991). Figures 3-16 and 3-17 show the location of these features. The extent of the zones outside of the area covered by site investigations is uncertain. Hydraulic conductivities of SCD1 are based on the 3m packer test data corresponding to conductive fracture zones identified by Anderson et al., (1991, Table 4.3). Because Zone 1 has no 3m test data, the 2m data of KFI10 was used to infer properties for this zone. Similar to RCD1, the geometric mean and variance are not indicated to change with depth. As described in Section 1.6, the SCD geometric means are upscaled from 3m to 24m using the Äspö regression relationships (Appendix D.5). Table 3-6 presents the results of this upscaling, which forms the base case model for hydraulic conductors at Beberg (SCD1).

Two additional alternative cases address the uncertainties of the conceptual model for the site-scale conductor domain. The first alternative case is SCD2, which allows the hydraulic conductivity to decrease in depth zones with the same relative changes as in SRD6. The second alternative model is that additional subhorizontal zones may exist below the maximum bored depth of 691mbgs. Properties for such a hypothetical zone should be inferred from Zones 2 and 11 (see also Section 3.2.7.2).

Andersson et al. (1991) summarise the series of tracer tests performed in Zone 2 as part of the Fracture Zone project. Although the data represents an important source of information, the parameters for Zone 2 might not be representative of the entire site. Brandberg and Skagius (1991) present a compilation of other transport properties based on laboratory testing of Finnsjön core samples. Andersson et al. (1997) present a compilation of transport parameters for use in SR 97.

Uncertainties:

The properties for untested fracture zones have been inferred from structures with similar tectonic origins and orientations. Consequently the properties of such fracture zones should be considered uncertain.

Table 3-6. Beberg site-scale conductor domain properties based on 3m tests, upscaled to 24m (SCD1).

Zone	Inferred from	Dip	Width	Median Log_{10} K (m/s) 3m	Median Log_{10} K (m/s) 24m	Sample Size
1*	2 boreholes	75SE	20	-5.66	-4,81	14
2	9 boreholes	16SW	100	-6.34	5,63	82
3	1 borehole	80SW	50	-6.82	-6,11	37
4	zone 5	60SW	10	-6.35	-5,64	
5	3 boreholes	60SW	5	-6.35	-5,64	15
6	1 borehole	60SW	5	-8.39	-7,68	2
7	Ave. 5,6,10	70SW	5	-7.39	-6,68	
8	Ave. 5,6,10	90	5	-7.39	-6,68	
9	1 borehole	15SW	50	-7.94	-7,23	18
10	1 borehole	85SW	5	-8.34	-7,63	2
11	4 boreholes	35SW	100	-7.22	-6,51	100
12	Singö	90	25	-6.10	-5,39	
13	zone 1	90	20	-5.66	-4,81	
14	Singö	90	100	-6.10	-5,39	

Fracture zones in **bold** also appear in the regional scale model

*also known as the Brändan fracture zone

3.3.4.3. Geostatistical model

The Beberg site-scale geostatistical model of hydraulic conductivity consists of the elevation zones and rock blocks described for SRD6, SCD1 and a single covariance model. The elevation zones for the Northern and Southern rock blocks are treated as step changes in the geometric mean of block conductivities (0 order trends in Log_{10} K_b), upscaled to 24m via the Äspö regression relationships (Appendix D.5).

The spatial correlation model is inferred from the 3m packer test in the rock domain (SRD6) using the SKB code INFERENS to regularise the rock mass data and apply universal kriging (Norman, 1992a). The resulting variogram model includes both the effects of the trends represented by the SRD and effects of upscaling on the numerical model grid. The fracture zones (SCD) are assumed to have the same variogram model. Results of this analysis indicate the following exponential variogram model for the 24m grid scale:

$$\gamma(h) = 0.0 + 0.77 \, Exp \, (62.67)$$

i.e., a zero nugget exponential model with a practical range of 188m. The complete geostatistical model consists of this variogram model and the 24m scale geometric mean hydraulic conductivities given in Tables 3-4 and 3-5. The sill of the variogram model has been increased slightly (from 0.64 to 0.77) to account for the censoring effect of the measurement limit on the variance. Details of this analysis and discussion are found in Appendix B3.

Uncertainties:

It is uncertain that upscaling via the Äspö scale dependency relationships is appropriate at this site. Consequently, the hydraulic conductivities may require adjustment to be consistent with the regional model boundary fluxes (see Section 1.6). The assumption of lognormally distributed hydraulic conductivities is not well supported for this data, given the measurement limits and the skewness of the univariate distribution. The validity of correcting the sill of the variogram using the univariate statistics is unknown and the variogram model is considered uncertain.

Table 3-7. Summary of Beberg Conceptual Models.

Code	Model
	Regional Scale (1)
	Rock Domain
RRD1	Hydraulic conductivity from SGU data, depth zones from on-site packer test data.
RRD3	as in RRD1, but with anisotropy in the direction of maximum horizontal rock stress
	Conductor Domain
RCD1	Mapped lineaments of SKB-91 as fractured zones. Hydraulic conductivity of individual zones inferred from packer tests. No trend with depth.
RCD2	As in RCD1 but with depth zonation as in RRD1.
RCD3	Hypothetical subhorizontal fracture zone
	Site Scale (2)
	Rock Domain
SRD6	Hydraulic conductivity from on-site 3m packer test data, with depth zonation. Rock mass separated into Northern and Southern rock blocks
SRD7	As in SRD6, but with anisotropy in the direction of maximum horizontal rock stress.
	Conductor Domain
SCD1	Fractured zones as in SKB-91, properties inferred from 3m packer tests. No trend with depth
SCD2	Fracture zones as in SCD1 but with depth zones as in SRD6
SCD3	Fractured zones as in SCD1 but with hypothetical subhorizontal fracture zone
	Excavation Disturbed Zone (EDZ)
EDZ1	Hydraulic conductivity of rock surrounding the tunnel unchanged
EDZ2	10X increase in hydraulic conductivity parallel to tunnel axis in 25cm of rock surrounding tunnel (Appendix D.8)

Notes:
(1) Regional hydraulic conductivity upscaled to numerical model block scale using the Äspö regression equation, calibrated to observed heads and recharge/discharge patterns.
(2) Site hydraulic conductivity upscaled to numerical block scale using Äspö regression equation, calibrated to observed heads and regional boundary fluxes. Covariance of hydraulic conductivity upscaled via INFERENS.

4. CEBERG

Ceberg is modelled after the Gideå site, located in northern Sweden in the northern part of Ångermanland. The site is approximately 8km inland from the Baltic Sea (Figure 4-1). The area corresponds to LMV map sheet 19J NV Husum and parts of sheets 20J SV and 19I NO. Unlike Aberg and Beberg, the region has significant topographic relief, ranging from sea level to over 300masl (Figure 4-2). This characteristic creates a regional groundwater flow pattern of recharge in the upland areas and discharge to streams in the fault valleys. This dominant flow pattern also contributes to the low salinity in the site. Another notable characteristic of the site is the comparatively low hydraulic conductivity at repository depth. As discussed in Section 1.4, the 25m packer tests indicated hydraulic conductivities an order of magnitude lower than the Äspö or Finnsjön packer tests at comparable depths (after accounting for scale effects).

The Gissjö hydropower tunnel lies approximately 2km to the southeast of the site, with its inlet near the village of Gideå and its outlet on Gideå brook 3km south of the site (Figure 4-2). It is a relatively shallow tunnel (10 to 20mbgs), lined with shotcrete in some sections. Although it is of limited use for site characterisation, Ericsson and Ronge (1986) mapped fractures within the tunnel as part of investigations into the tectonics of the area. This study and that of Hermanson et al. (1997) utilise that fracture data information to infer fracture orientation and fracture zone thickness. Table 4-1 summarises the site characterisation studies at Gideå.
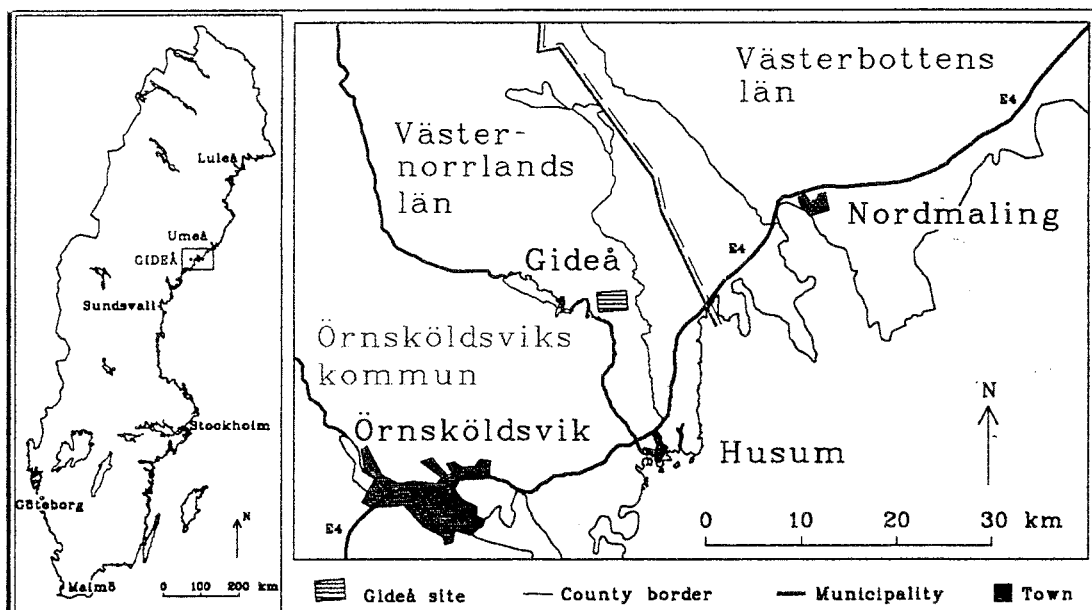
Figure 4-1. Gideå Site location map (from Ahlbom, et al, 1991).

Table 4-1. Summary of Ceberg (Gideå) Site Characterisation Studies.

Programme attribute	Description
Dates of field investigations	1981-1983.
Boreholes	24 shallow percussion, 13 deep cored, max. Depth 701m.
Single borehole tests	<u>Double Packer</u>: 308 tests with 25m interval; 144 tests with 2m interval (2 boreholes); some 150 tests with 3, 5, and 10m. <u>Single Packer</u>: 3 boreholes in intervals ranging from 107 to 287m. Interpretation methods vary (steady state or transient).
Interference tests	One at surface.
Tracer tests	None.
Tunnels/ Excavation	Gissjö Hydropower tunnel (private, 2km south).
Geophysics	Magnetic, seismic, slingram, resistivity, VLF electromagnetic, borehole.
Other	Geochemical sampling, geologic/fracture mapping on outcrops, and cores. Chernobyl project in 1986.
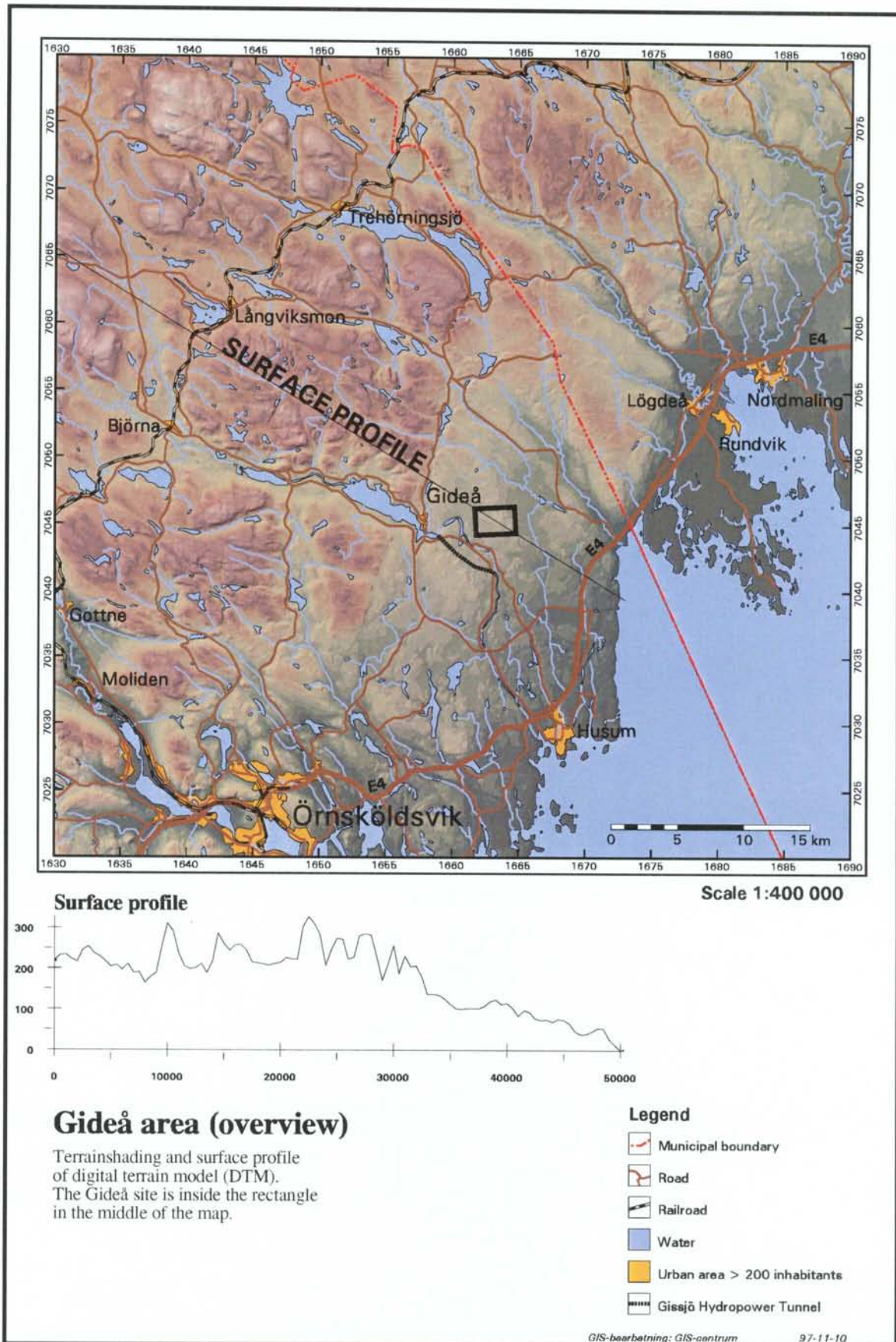
Figure 4-2. *Gideå regional topography.*

4.1. PRIMARY SOURCES OF INFORMATION

The information for this site is taken from several key sources. For an overall view of the hydrogeology and summary of site characterisation, two reports are the most useful:

- Ahlbom, K, J-E Andersson, R. Nordqvist, C. Ljunggren, S. Tirén and C. Voss, 1991a, Gideå study site. Scope of activities and main results, SKB TR 91-51.

- Ahlbom, K, B. Albino, L. Carlsson, G. Nilsson, O. Olsson, L. Stenberg and H. Timje, 1983, Evaluation of the geological, geophysical and hydrogeological conditions at Gideå, SKBF/KBS TR 83-53.

Ahlbom et al. (1991a) recommended that a 3-D model of structural geology be constructed for the Gideå site. Hermanson et al. (1997) constructed that model, including several new features and corrections to the model of Ahlbom et al. (1991a). This study uses the revised model of fractured zones, rock types and dykes as presented in:

- Hermanson, J., Hansen, L.M., and S. Follin 1997, Update of the Geological Models of the Gideå Study Site, (SKB R-97-05).

The previous site lineament maps of Ahlbom et al. (1983) were restricted to the limits of map sheet 19J NV Husum. As part of the SR 97 studies, Askling (1997) revised the lineament map and extended it to the north. The resulting maps and digitised lineaments are presented in:

- Askling, P., 1997, Lineament Map: Gideå, (SKB PR U-97-06).

Site surface hydrology and soils are described in:

- Timje, H. 1983, Hydrogeological Investigations at Study Site Gideå, SKBF/KBS AR 83-26 (in Swedish).

4.2. REGIONAL SCALE

4.2.1. Topography

The topography of the Gideå region is generally hilly, although the site itself is on a relatively flat plateau between two streams, the river Gideälven and the stream Husån (Figure 4-2). Both of these streams follow fracture valleys running north-northwest. There are numerous lakes in the region, the largest of which is Gissjön. The land surface varies between sea level and 300 masl. The land is forested with peat bogs in low-lying areas (Ahlbom et al., 1983).

4.2.2. Regional Geology

4.2.2.1. Quaternary geology and soils

Varying depths of quaternary age glacial moraine overlies the bedrock. Peat fills some surface depressions and bedrock outcrops occur throughout the region. The soils are generally thin, but there are extensive bogs and mires in the region (Ahlbom et al., 1983).

4.2.2.2. Bedrock geology and lineaments

The bedrock in the region is a migmatised veined gneiss of sedimentary origin (Figure 4-3), approximately 1.8 Ga of age. The dominant rock type is a greywacke with subordinate schist, phyllite and slate with varying degrees of metamorphosis. Foliation is generally steeply dipping to the north-northwest, with areas to the west and southwest of the site having shallow to moderate dips to the south and southwest. South of the Gideå site is a body of granite gneiss and to the west is a body of granite (Hermanson et al., 1997). Intrusive doleritic dykes and sheets 1.2 Ga of age interrupt these rock masses. The dykes are spaced approximately every 200 to 300 meters, and are 0.5 to 15 meters wide with east-west strikes and steep dips. The sheets are lopolithic, semicircular sheets, and 100 to several hundred meters thick. They have gentle dips to the east (Welin and Lundqvist, 1975; Larson, 1980). The regional temperature gradient with depth is 15.9 degrees C/km, confirmed by onsite borings (Ahlbom and Karawacki, 1983).

Regional lineaments have been interpreted from airphotos and topographical maps at a scale of 1: 50 000 (Ahlbom et al., 1983). This map was extended slightly north and south for the purposes of this study (Askling, 1997; Lundqvist et al., 1990). Figure 4-4 presents the resulting lineament map that corresponds to the Ceberg base case of RCD1. These lineaments have been interpreted as subvertical fractured zones, striking primarily west-northwest and northwest. Lineaments striking west-northwest are extensive and have surface expressions greater than 100m. Those striking northwest have surface expressions 50 to 100m wide. One of the less-well-expressed northwest-southeast striking regional lineaments appears to cross the northeast corner of the site, but no site boreholes penetrate this lineament and geophysical surveys on site fail to confirm or deny its existence. A few less-well expressed lineaments cross the site and can be roughly correlated

to fracture zones mapped on the site scale (Appendix C.1). Several boreholes penetrate these features and provide a minimal amount of data on regional lineaments. In general, however, very little information is available for the regional lineaments and the interpretation of them as hydraulically conductive should be regarded as uncertain (Ahlbom et al., 1983; Askling, 1997, Hermanson, et al. 1997). The hydraulic properties of these lineaments for RCD1 are discussed in Section 4.3.4.2.
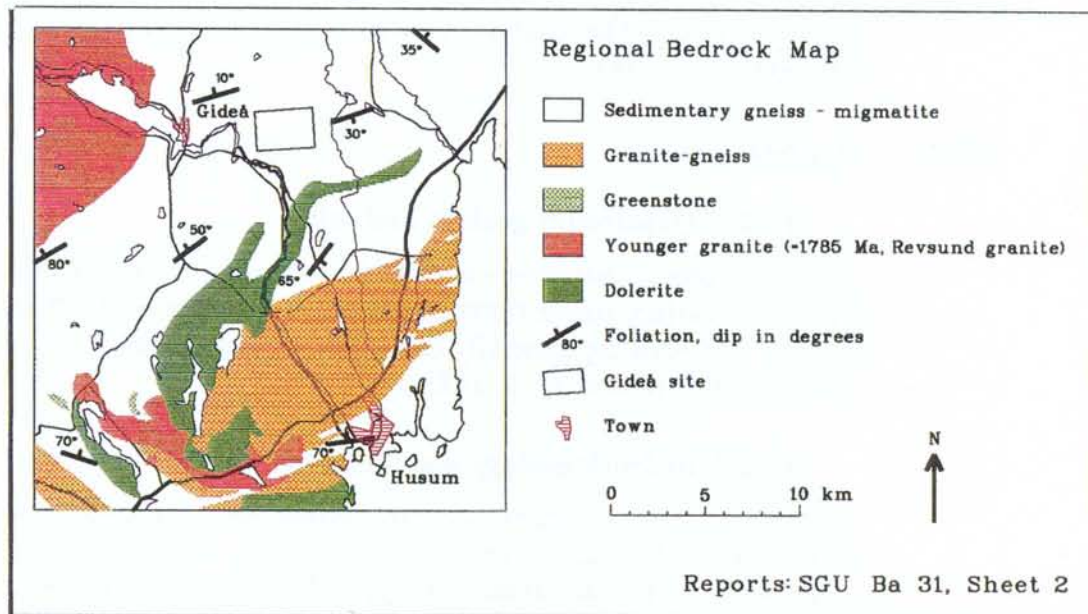
Figure 4-3. *Gideå regional geology (from Ahlbom, et al, 1991).*

Because of the uncertainties regarding the regional lineaments in Figure 4-4, a second lineament map was drawn for the purposes of SR 97. Askling (1997) used LMV digital terrain models on a 50 by 50m grid to create an alternative regional lineament map (Figure 4-5). This map is the basis for RCD3, a variation case for the Ceberg regional flow modelling (Appendix C.1). One of the well-expressed northwest-southeast striking regional lineaments of this revised map crosses the northeast corner of the site, and may have important consequences for PA modelling. Several thin, poorly expressed lineaments are quite extensive, striking east-west and northeast-southwest. Several of these thin lineaments cross the site, roughly corresponding to fracture zones and doleritic dikes mapped on the site scale. (Askling, 1997, Hermanson, et al. 1997).

4.2.3. Tectonics and Landrise

On-site measurements indicate that the major component of regional horizontal rock stress is in the direction N67° E, with a standard deviation of ± 19°. This agrees with the reported regional trend and measurements in the nearby Gissjö hydropower tunnel. However, the regional east-west lineaments and doleritic dikes suggest an EW paleostress (Hermanson et al., 1997).
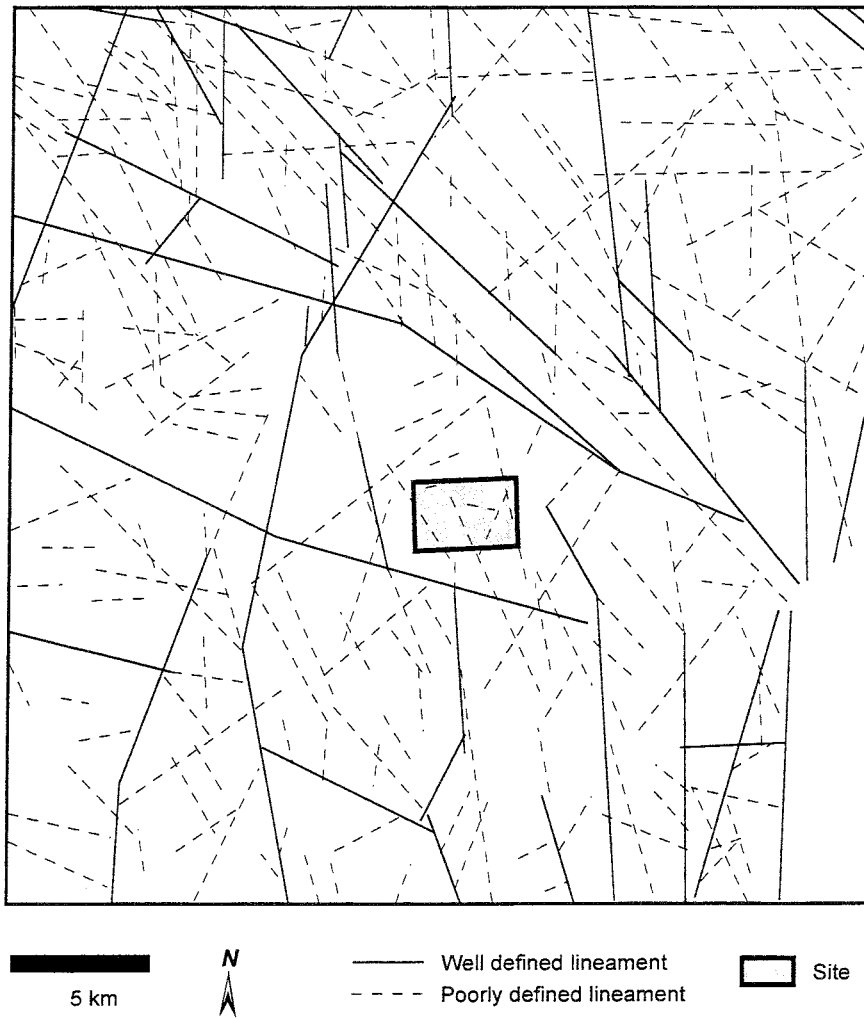
Figure 4-4. Gideå regional lineaments (after Ahlbom et al., 1983).

Some of the north-south striking regional lineaments have been interpreted as normal faults. Earthquakes up to magnitude 5 have been reported in this area, some as recent as 1983 (Kulhálnek and Wahlström, 1985; Fredén, 1994). Hermanson et al. (1997) suggest that movement has occurred along the fractured zones within the site as evidenced by offsets in the doleritic sheets where the site-scale fracture zones cross.

The site lies in the centre of post-glacial isostatic rebound in the Fennoscandian shield and exhibits landrise rates amongst the fastest in Sweden. Figure 4-6 shows the historic landrise in the area near the site, based on radiocarbon dating of paleoshoreline sediments. The present rate of landrise is 7.7 mm/yr (Björk and Svensson, 1992).
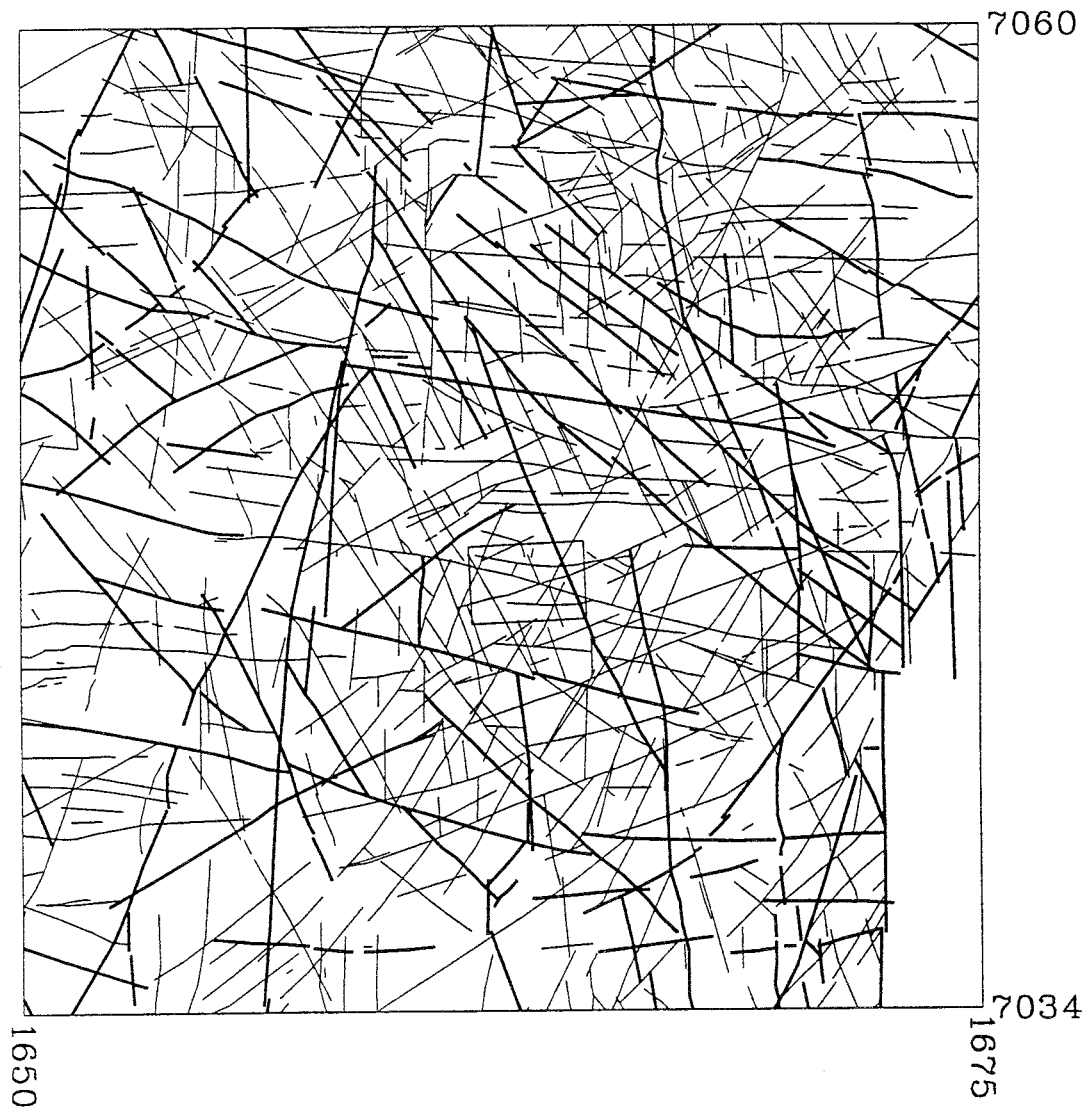
Figure 4-5. Alternative interpretation of Ceberg regional lineaments. Bold lines are well expressed lineaments, thin lines are less-well expressed lineaments (from Askling, 1997).

4.2.4. Geochemistry and Salinity

The groundwater chemistry of this area is greatly influenced by the depression, inundation and uplift resulting from the last ice age, beginning approximately 10,000 years BP. The consequent mixing of connate water, glacial meltwater, seawater and modern precipitation creates a dynamic system that is still evolving under the influence of continued landrise.
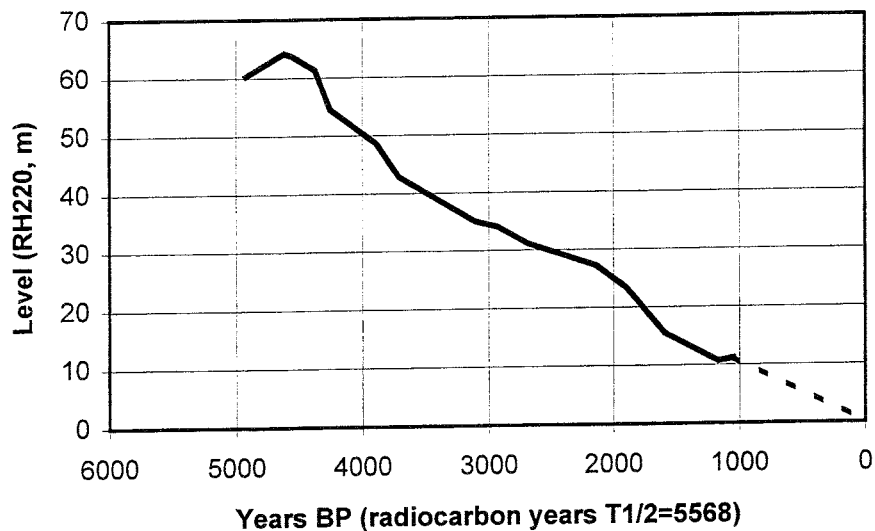
Figure 4-6. Shoreline displacement at Ceberg (after Björk and Svensson, 1992).

SKB site characterisation studies have included groundwater sampling from site boreholes, ranging from depths of 96 to 619 mbgs. Subsequent principal component analysis of the geochemistry indicates that the groundwater is meteoric in origin (Figure 4-7). This suggests an overall downward recharge of precipitation at the site, typical of upland areas with strong topographic drive.

No site-specific geochemical data exists for the groundwater system below 700m, and no saline water is encountered in the site borings. The classical model for saltwater intrusion suggests that saltwater will not be found at this site except at great depth. However, such a simple model ignores the cycle of depression, inundation and uplift seen in most of Sweden. It is possible that saline water may be encountered at the site, but at unknown depths.

The present-day salinity of the Baltic Sea is approximately 4 to 4.5 g/l in this region (Sjöberg, 1992, Carlsson, 1997).

4.2.5. Surface Hydrology

Timje (1983) summarised the Swedish Meteorological and Hydrological Institute (SMHI) data from 8 stations in the immediate area of the site. The weather station at the Örnsköldsvik airport, approximately 10 km southwest of the site has the longest period of record and is regarded as most representative of the area.

$$\text{Component 2} = -0.13[Na] + 0.27[K] - 0.29[Ca] + 0.32[Mg] + 0.41[HCO_3] - 0.23[Cl] - 0.15[SO_4] + 0.003[^3H] + 0.47[^2H] + 0.51[^{18}O]$$

$$\text{Component 1} = 0.46[Na] + 0.32[K] + 0.38[Ca] + 0.27[Mg] - 0.12[HCO_3] + 0.42[Cl] + 0.43[SO_4] - 0.07[^3H] + 0.23[^2H] + 0.20[^{18}O]$$
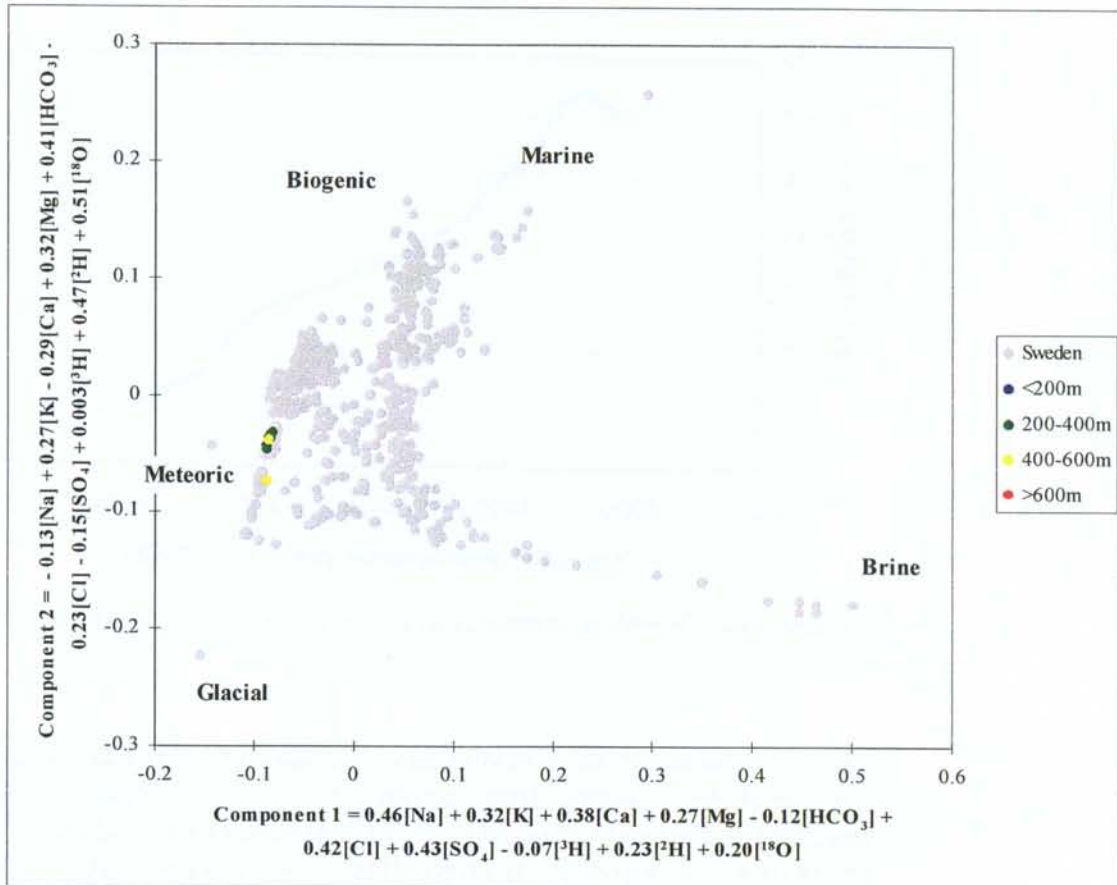
Figure 4-7. Hydrogeochemical principal component analysis for Ceberg (after Laaksoharju et al., 1997).

Stream gauging stations are sparse in this region of Sweden; only two can be found within a 50km radius of the site. They are at Björna on the Gideälven above lake Gissjön, and at Kvarnbacken on the Saluån. Timje (1983) constructed a rainfall-runoff model for this region using the Gideälven gauging station, the Örnsköldsvik weather station and data for the watershed above Björna. The resulting simulations suggest that the run-off for this region is 345mm/yr ±10mm/yr, with the peak runoff occurring in May. Therefore the mean annual net distributed recharge to the regional groundwater system is 10mm, but may vary locally depending on topography.

4.2.6. Groundwater hydrology

Timje (1983) used SGU data and 24 percussion drilled boreholes on site to assess the regional groundwater table, resulting in the regional map shown in Figure 4-8. This map represents an estimated mean groundwater level and assumes that the groundwater table follows a subdued, smoothed version of the ground surface. Some subjective judgement was used to account for recharge areas, etc. The seasonal fluctuation in water table elevations are between 0.2 to 3.9m, with the annual lows occurring in January through March and the annual highs occurring in April and October

96

(Ahlbom et al., 1983). The water table map contours indicate that the shallow groundwater system is dominated by recharge on the plateau and discharge to the streams in the fracture valleys.

Wells clustered on-site and the site-scale water table map are consistent with the classical pattern of recharge in upland areas, discharging to streams and bogs in lowlands. Surface topography and vegetation maps suggest that this pattern persists over the much of the region.

Little is known about the deep regional groundwater system, since water supply wells rarely exceed 200m depth. The deep flow system can only be inferred from on-site wells, on-site geochemistry and classical models of regional flow patterns. The classical model of topographically driven regional groundwater flow suggests that larger scale flow systems may underlie the shallow system beneath the site, flowing from the uplands north and west of the site toward the Baltic Sea. Section 4.3 discusses this in further detail.
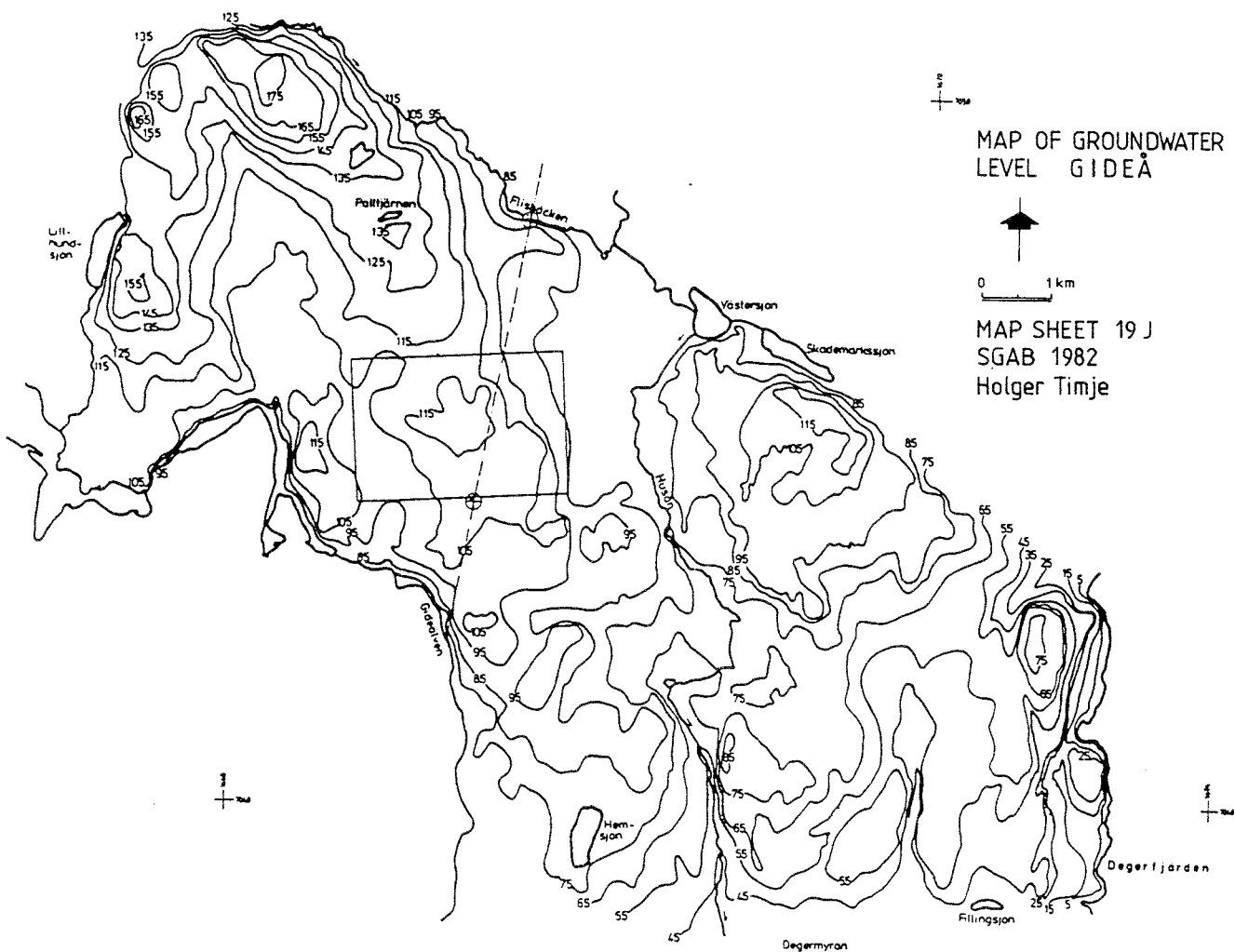
Figure 4-8. Ceberg regional water table surface map (from Timje, 1983).

For the shallow groundwater system, one choice of boundary conditions would be the fracture valleys occupied by rivers on either side of the plateau. However, this pattern of recharge from the plateau to the streams may not persist at depth. On a larger scale, the regional lineaments might reasonably be considered highly transmissive and thus as streamlines in a steady state regional model. Figure 4-9 suggests one such choice of model boundaries. These should, however, be analysed for their sensitivity.
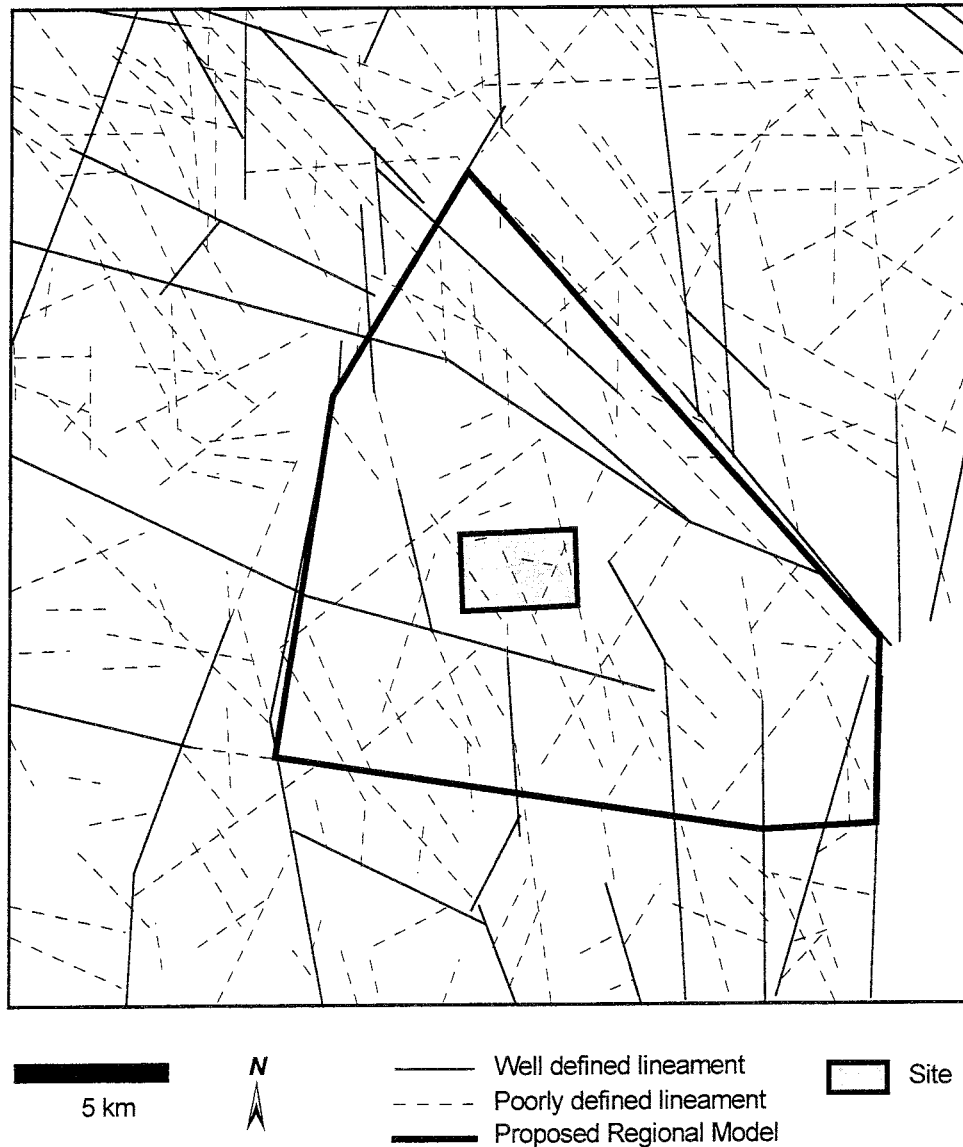
Figure 4-9. Proposed Ceberg regional modelling domain.

4.2.7. Hydraulic Properties

This study obtained and analysed the SGU well data for wells within a 25km radius of the site in an attempt to infer models of hydraulic conductivity on the regional scale. The SGU well archive data comes primarily from water supply wells, which are typically less than 200m total depth. Consequently, the trend of hydraulic conductivity with depth on the

regional scale must be inferred from the on-site packer test data. Similarly, the on-site data is used to determine the contrast between the rock mass versus fracture zones. This is combined with the SGU data to produce regional scale models for the Ceberg hydraulic conductivities. Details are presented in Appendix C.2.

The SGU data appears to be spatially clustered near communities and in the fracture valleys (Figure 4-10), but cluster analysis did not indicate that the data is preferentially clustered in areas of high transmissivity. On the other hand, the wells tend to fall in the lineaments that are thought to be fault valleys, suggesting that virtually all the SGU data is biased.

Additional analysis suggests that the hydraulic conductivities calculated from the SGU wells showed noticeable spatial correlation. Subsequent crossvalidation of the variogram and kriging models indicates that including this correlation results in limited improvement in the estimation of unknown values due to the high nugget value.

4.2.7.1. Rock Mass – RRD

The mean of the SGU data is used to determine the hydraulic conductivity of the upper elevations of the rock domain. However, the on-site packer tests are used to infer the trend with depth. Hermanson et al. (1997) analysed the on-site packer tests to determine if rock type or rock contacts could be used to explain the variations in hydraulic conductivities. They concluded that rock type seemed to have no influence on the hydraulic conductivity values but also suggested that the 25m packer test intervals had inadequate resolution to be conclusive.

The 25m packer test data can be separated into fracture zone data and rock mass data. Appendix C.3 and Section 4.3 provide the details of separating out this data and the determination of elevation zones for hydraulic conductivity. The Ceberg regional rock domain model (RRD1) should use the elevation zones defined for this 25m rock mass data, upscaled to the regional scale. Table 4-2 presents the results of this zonation of the 25m data upscaled to the 100m scale (for RRD1).

Table 4-2. Ceberg regional scale rock mass depth zonation for hydraulic conductivity at the 100m scale (RRD1).

Elevation (masl)	Arithm. Mean Log_{10} K (m/s)	Variance Log_{10} K (m/s)
+110 to 0	-7.16	0.380
0 to -100	-8.65	0.704
-100 to -300	-9.63	0.707
Below -300	-9.83	0.986

Gideå area (overview)

Terrainshading of digital terrain model (DTM).
The Gideå site is inside the rectangle
in the middle of the map.

Scale 1:400 000

Legend

Municipal boundary

Road

Railroad

Water

Urban area > 200 inhabitants

○ SGU well

GIS-bearbetning: GIS-centrum   97-03-25
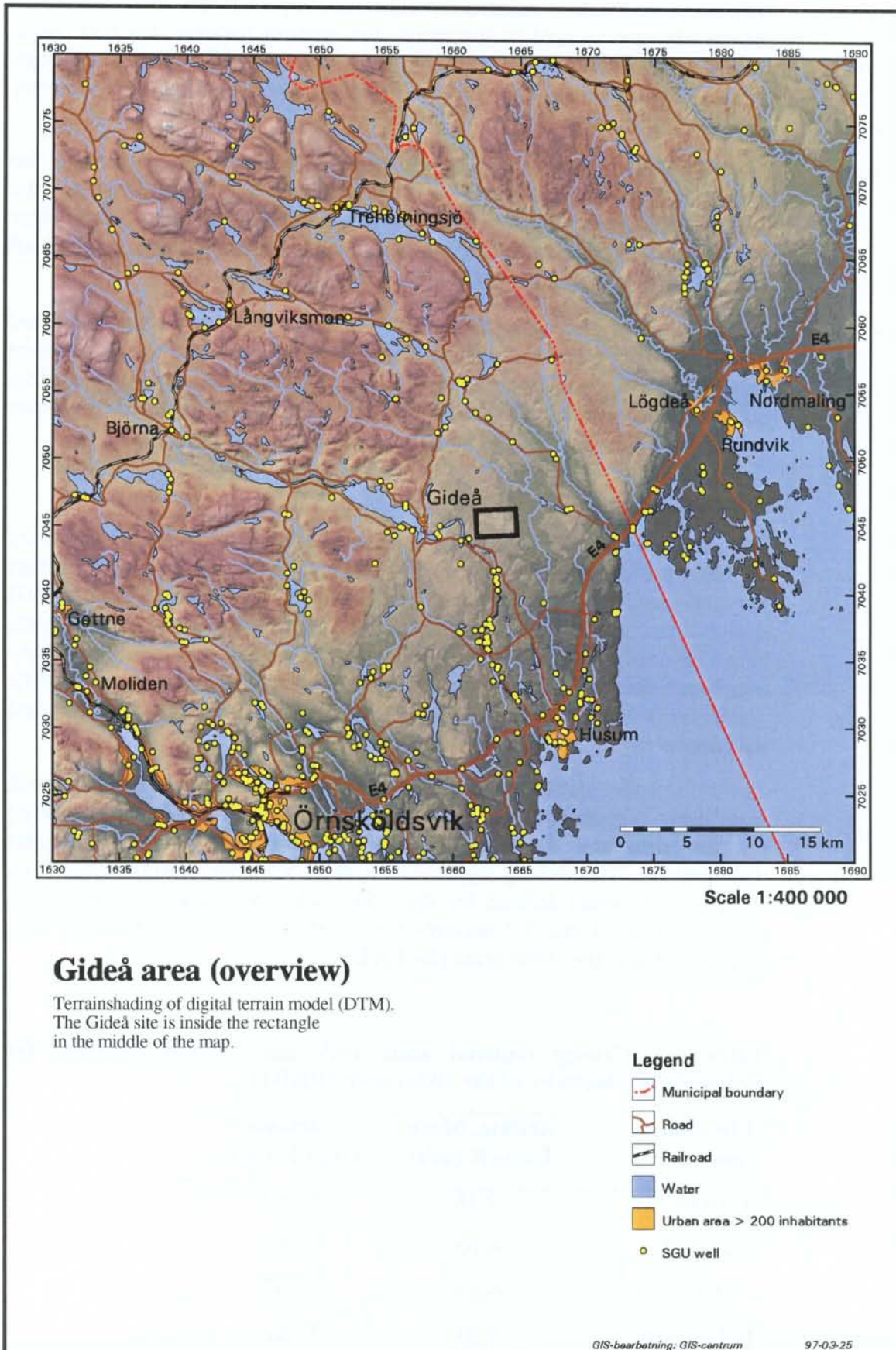
Figure 4-10. SGU wells in Gideå region.

An alternative case, RRD3, may be used to evaluate anisotropic hydraulic conductivity in the Ceberg rock mass. Ericsson and Ronge (1986) suggested a regional hydraulic conductivity anisotropy in the direction of maximum horizontal rock stress. This would be in the approximate direction of N67° E, with a standard deviation of ± 19°. Based on their analysis of SGU data, they also suggested a range of magnitudes of 30:1 to 80:1 for major versus minor directions for hydraulic conductivity. Note that for the Äspö site, Rhén et al. (1997) suggested a ratio of 100:1:10 for horizontal major : horizontal minor : vertical minor. For scoping calculations and alternative case models, analogue sites provide an anisotropy ratio of 10:1:1 for horizontal major : horizontal minor : vertical (Carlsson et al., 1986; Winberg, 1991). The overall magnitude of the hydraulic conductivity should not change under this transformation.

Ahlbom et al. 1983 suggested that the doleritic dikes and sheets might have increased hydraulic conductivity based on an increased degree of fracturing observed in the cores. Reinterpretation of that model by Hermanson et al. (1997) suggests that the dolerite intrusions may instead have comparatively low permeabilities. As stated above, there seems to be no evidence for a model of hydraulic conductivity separated by rock type, and therefore an alternative case for hydraulic conductivity by rock type (RRD2) is not suggested.

Porosity data are unavailable at depth for this site. Analogue site data (Äspö, Finnsjön) suggests a possible range of kinematic (flow) porosity of 2×10^{-4} to 1×10^{-3} (Ahlbom et al., 1983)

4.2.7.2. Regional Lineaments – RCD

The base case model for regional conductive structures, RCD1, is based on the lineament map of Figure 4-4 (Section 4.2.2.2). Little is known regarding the hydraulic characteristics of the regional lineaments. Appendix C.2 attempts to separate the SGU well data with respect proximity to the regional lineaments, but found little difference between the separated populations. This conceptual model therefore relies on the onsite 25m packer tests (see also section 4.3 and Appendix C.2). After upscaling, elevation zones can be determined for the Ceberg fracture zone hydraulic conductivities as presented in Table 4-3.

Assuming that the regional lineaments are hydraulically similar and a median width of 20m, we can assign properties to the mapped lineaments for RCD1 (Figure 4-4). Porosities should be assumed to be the same as in RRD1, with sensitivity analysis. The alternative lineament interpretation of Askling (1997) forms RCD3, an alternative case for lineament locations and extent (Figure 4-5; see also Appendix C.1). On the basis of the available data, no alternative case is provided for a specification of properties of individual zones.

101

Table 4-3. Ceberg regional scale conductor domain hydraulic conductivity at 100m scale (RCD1). (Interquartile range of 3.21 should be used for sensitivity analysis).

Elevation (m masl)	Mean Log$_{10}$ K (m/s)
+110 to 0	-6.40
0 to -100	-7.89
-100 to -300	-8.87
Below -300	-9.06

Uncertainties:

It should be noted that regional lineaments have been assumed to be conductive fracture zones whose width can be inferred from topographic expression or orientation. Experience suggests that this is much too simplistic of a model; dolerite commonly intrudes into east-west trending lineaments in this region, and mineralised fractures can have very low hydraulic conductivities. The designation of lineaments as conductive fracture zones should therefore be considered highly uncertain and be evaluated by deterministic sensitivity analysis.

4.3. SITE SCALE

The Gideå site is defined as a 3km by 2km area on a relatively flat plateau between two streams, the river Gideälven and the stream Husån (Figure 4-11). The basis for the Ceberg site-scale model is the hydrogeologic information found in Ahlbom et al., (1983) and Timje, 1983. The updated structural geologic model is taken from Hermanson et al. (1997) and the interpreted hydraulic properties are from the SKB SICADA database.

4.3.1. Geology

Surficial deposits at the Gideå site are a mixture of glacial and fluvial sediments, exposed rock and peat. Approximately 40% of the site area is glacial till whose surface has been reworked by the retreating shoreline of the Baltic Sea. In depressions, the till is overlain fluvial sand in as much as 30% of the site area. Rock outcrops are common on the site plateau, occurring in 25% of the site area. The remaining area of the site consists of low-lying areas where the till is overlain by peat (Gustafsson et al., 1987).

The site is located in the dominant rock type of the region, a migmatised veined gneiss unit which includes greywacke with subordinate schist, phyllite and slate. Doleritic dykes 0.5 to 15m thick are found on exposures and in boreholes within the site as subvertical dykes striking E-W (Figure 4-17). Subhorizontal doloritic sheets are found in the region and at one time may have overlain the Gideå site. Such subhorizontal zones might have increased hydraulic conductivity, and if present, would have important consequences for Performance Assessment. The summary of characterisation and modelling of the site by Ahlbom et al. (1991a) suggested a re-evaluation and extension of the site geologic model. That re-evaluation was addressed by Hermanson et al. (1997) as part of SR 97. Although the update of Hermanson et al. (1997) did revise previously mapped fracture zones and included several new fracture zones, they found no evidence of subhorizontal doleritic structures. Hermanson et al. (1997) suggested several corrections to the model of Ahlbom et al. (1991a) to explain the geophysical anomalies, topographical lineaments and borehole observations.

The site investigations identified a number of relatively conductive fracture zones between 5 to 50m in width. Preliminary reports by Ahlbom et al. (1983) and Ahlbom et al. (1991a) suggested that some fractured zones are clay-altered with very low hydraulic conductivity, while others are highly conductive. Thus the assumption that the fracture zones are uniformly conductive features is uncertain at Ceberg. The location and properties of the fracture zones are discussed further in Section 4.3.4.

103
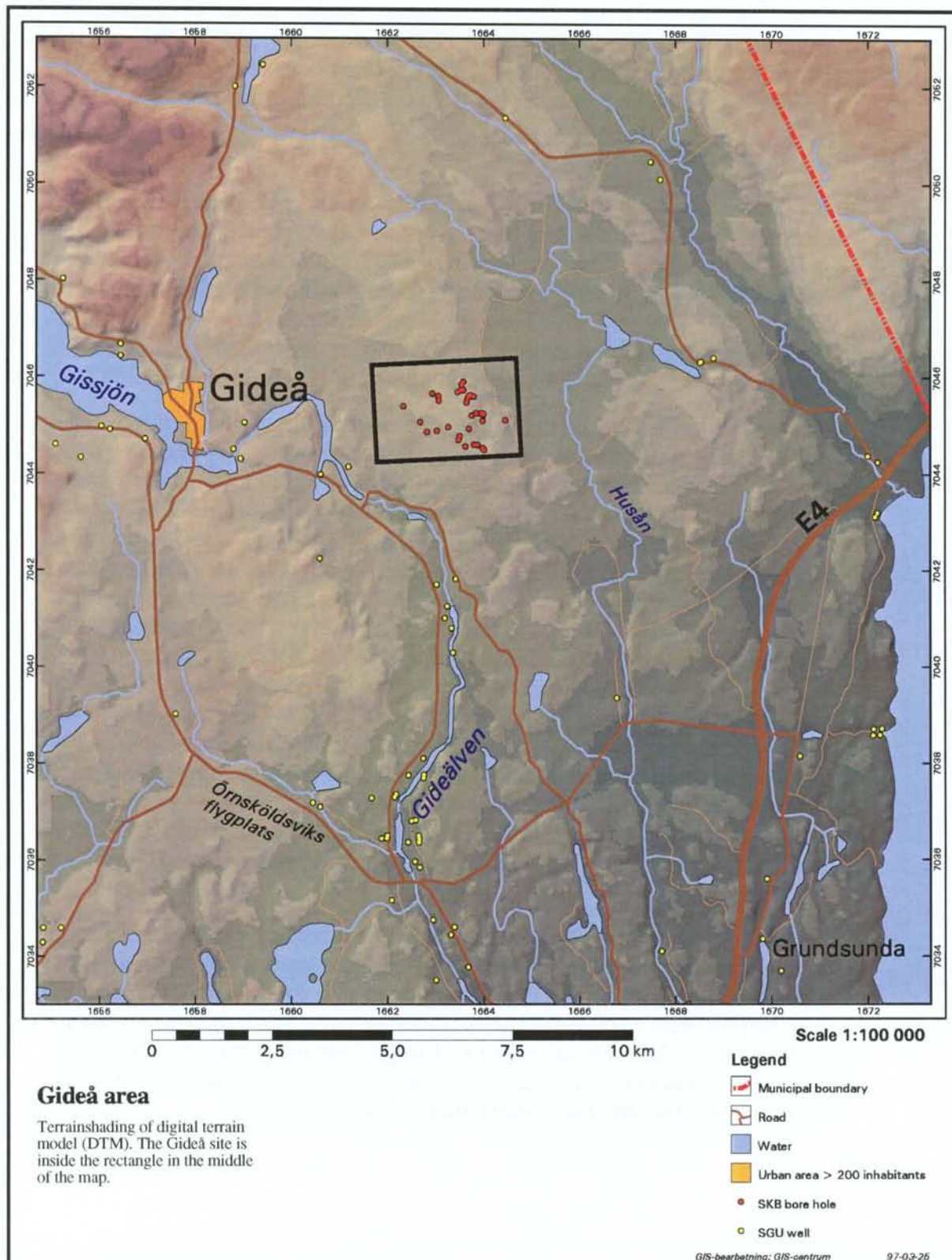
Figure 4-11. *Gideå site and boreholes.*

104

Ericsson and Ronge (1996) mapped fractures on rock outcrops at the site and in the Gissjö hydropower tunnel. Their analysis indicated four sets of subvertical fractures, oriented N-S, E-W, N60°W, and N30°E (Figure 4-12). For fractures longer than 0.5m, the frequency is 1.2 fractures per metre. Borehole data suggests that fracture frequency declines sharply at 400m depth, from 4.0 fractures per metre to 2.0 fractures per metre. (Figure 4-13).

N

13138 Fractures
838 Fractures correspond to radius

60°W   0°   ca 30°E

fol.

Noise level

N90W   0   N90E

13138 Fractures
591 Fractures correspond to maximum peak
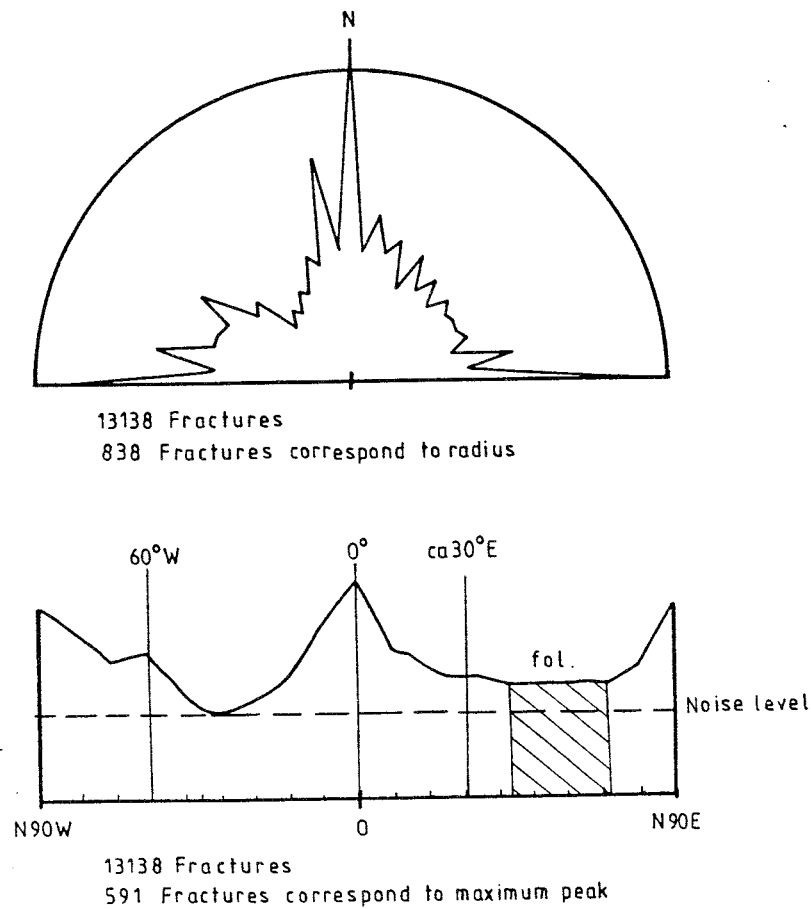
Figure 4-12. Mapped rock outcrop fracture orientations, Gideå site (from Ericsson and Ronge, 1986).

105
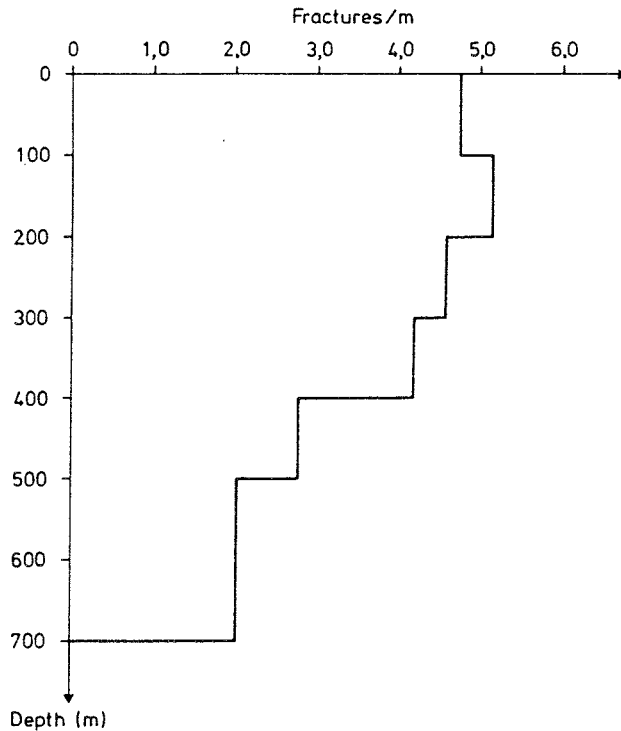
Figure 4-13. *Fracture frequency versus depth at Gideå site (from Ahlbom et al., 1983).*

4.3.2. Surface hydrology

The land surface within the site varies between 100 and 130 masl, except for the northeast corner where the land surface drops to approximately 80masl. The site is forested with a few peat bogs in low-lying areas. Part of an extensive peat bog, Stormyran, lies in the northeastern part of the site (Ahlbom et al., 1983). Three small watersheds divide the site, one draining south and west to the Gideälven, another draining north and then west into Gideälven and a third north and east into Stormyran bog and the stream Husån. Part of this latter watershed is the Orrmyrberget catchment area used by Gustafsson et al. (1987) as part of SKB studies of Chernobyl fallout. The study of Gustafsson et al. (1987) was brief (approximately 6 months) but provided useful site-specific runoff data that confirm the regional estimates given in Section 4.2.

4.3.3. Groundwater hydrology

Gustafsson et al. (1987) reported that the groundwater surface ranged from zero to 10m below ground surface for lowlands and uplands, respectively. Timje (1983) mapped an assumed mean water table surface at the Gideå site using the on-site boreholes and assuming that the groundwater table follows a subdued profile of surface topography. Figure 4-14 shows an overall pattern of recharge on the site plateau and discharge to streams in fault valleys. Local discharge and runoff is observed in peatlands within the site.
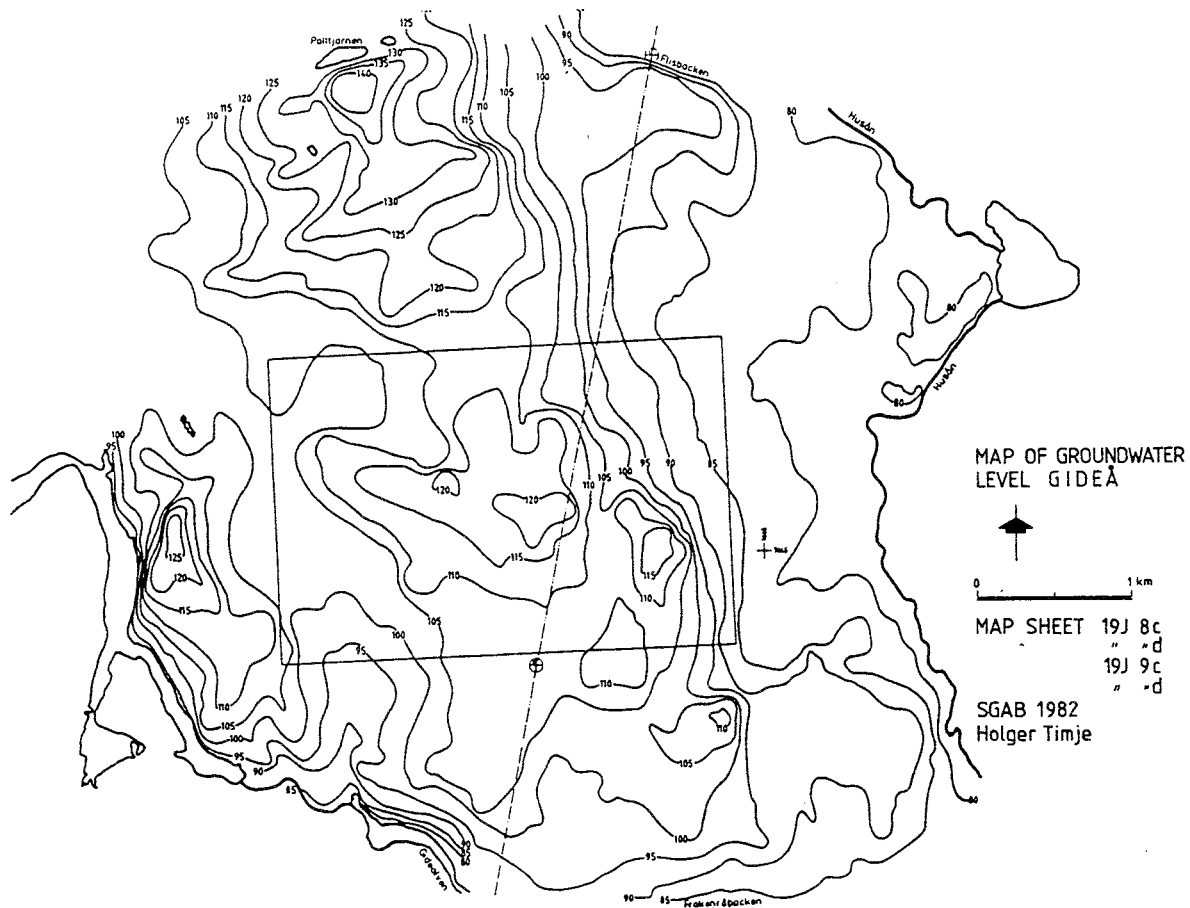
Figure 4-14. *Ceberg site groundwater table surface (from Timje, 1983).*

The variation of the groundwater system with depth has been explored on site by 13 cored borings that reach to a maximum depth of 700m. These borings have been divided into monitoring intervals by inflatable packers to provide some information on the changes of hydraulic head with depth. Figure 4-15 presents the results for these monitoring intervals as overpressure relative to hydrostatic conditions. These pressures might not reflect static conditions, since the drilling and testing operations may have created pressure transients that might not have dissipated at the time of measurement. However, a plot of overpressure versus time since packer inflation for Gi 7 (Figure 4-16) indicates that the system is relatively stable after 10 days. The observations show a pattern of overpressure above 200m depth and underpressure below 200m depth. This net downward gradient indicates that the site is in a groundwater recharge zone, confirming the patterns observed in the water table map. This also suggests that the downward flow may persist for several hundred metres depth. In several boreholes underpressures return to hydrostatic pressure by 500m depth, indicating that the deep flow system may become more complex with depth.

Gi 1   Gi 2   Gi 3

-10   0   +10   -10   0   +10   -10   0   +10
mwc   mwc   mwc   mwc   mwc   mwc

0
100
200
300
400
500
600
700

Borehole length (m)

Gi 4   Gi 5   Gi 6

-30 -20 -10   0   +10   -10   0   +10   -10   0   +10
mwc   mwc   mwc   mwc   mwc   mwc

0
100
200
300
400
500
600
700

Borehole length (m)
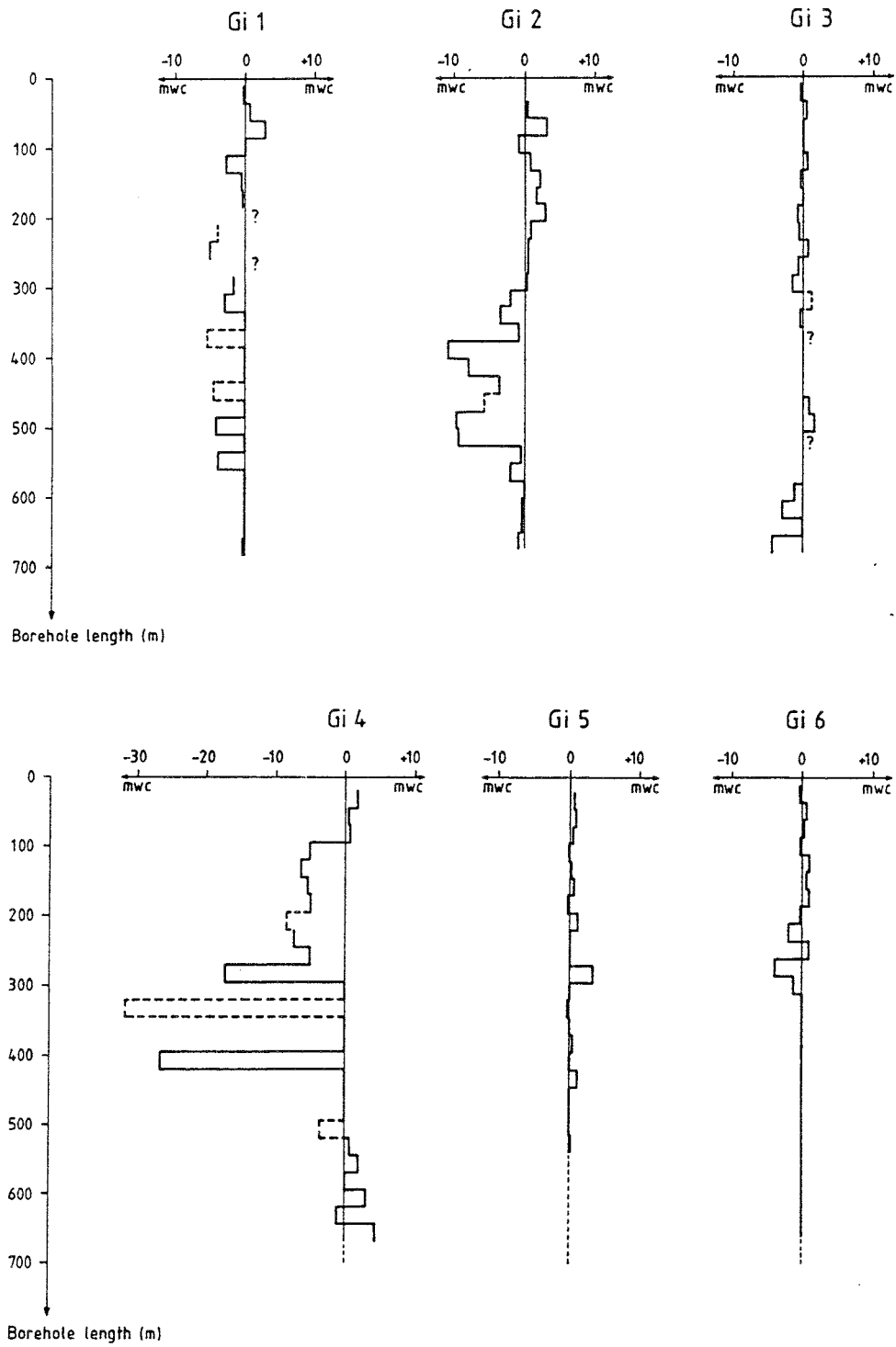
Figure 4-15. Gideå site borehole hydraulic head (metres of water column relative to hydrostatic pressure) (from Timje, 1983).
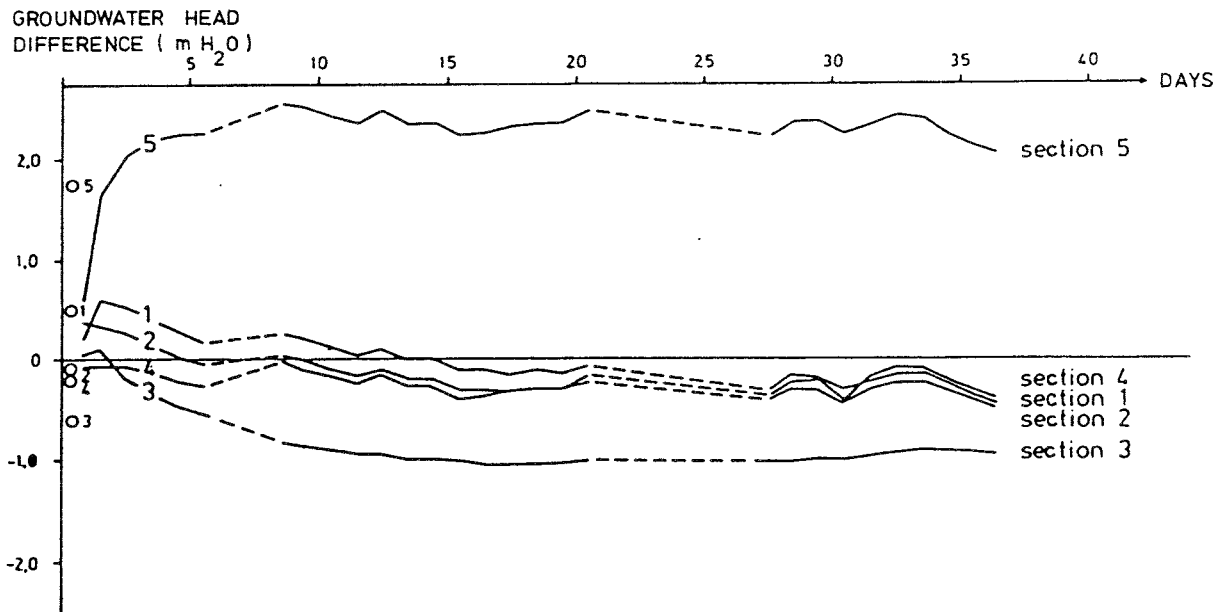
Figure 4-16. *Gideå site borehole GI07, differences in hydraulic head versus time (metres of water relative to initial pressure) (from Timje, 1983).*

4.3.4. Hydraulic Properties

Similar to the Ceberg regional model (Section 4.2.7), the site-scale model domain is separated into a low-conductivity rock mass domain and a higher-conductivity conductor domain. This separation is based on the structural geologic model of Hermanson et al. (1997). The rock domain differs from the conductor domain only by the relatively low hydraulic conductivity. In many cases, the contrast is small and masked by the depth dependence of hydraulic conductivity.

Hydraulic properties at the site scale are inferred from the interpreted hydraulic conductivities of the 25m packer test data (Appendix C.3). Except for a brief study of Chernobyl fallout (Gustafsson, et al., 1987), tracer tests have not been conducted at this site to estimate transport parameters . Andersson et al. (1997) present a compilation of transport parameters for use in SR 97.

4.3.4.1. Rock Mass – SRD

The Ceberg rock mass hydraulic properties are inferred from the Gideå 25m packer test data. In SRD6, hydraulic conductivity is assumed to have a constant geometric mean and variance within elevation zones inferred from the 25m packer test data. The means and variances should be upscaled as necessary to the model grid scale (Table 4-4). Similar to the regional rock domain, no separation of rock mass is made on the basis of rock type. Note that the occurrence of the elevation zones and the form of the trend functions are deterministic.

109

Table 4-4. Ceberg site-scale rock mass depth zonation for hydraulic conductivity at 25m scale (SRD6).

Elevation (masl)	Arithm. Mean Log_{10} K (m/s)*
+110 to 0	-7.55
0 to -100	-9.04
-100 to -300	-10.03
Below -300	-10.25

* corrected assuming normally distributed data, after Wen (1994)

Ericsson and Ronge reported that preferential fracturing can be observed in the Gissjö hydropower tunnel and on rock outcrops in the Gideå site (1986; see also Section 4.3.1). This preferential fracturing suggests that the hydraulic conductivity of the rock domain may be anisotropic, but no formal anisotropy tests of the type advocated by Hsieh and Neuman (1985) were conducted. However, since anisotropy is possible and is seen at analogue sites, SRD7 is suggested for anisotropy with the major axis in the direction of N67° E, with a standard deviation of 19°. For scoping calculations and alternative case models, analogue sites provide an anisotropy ratio of 10:1:1 for horizontal major : horizontal minor : vertical (as in RRD3; see Section 4.2.7.1). Note that the overall magnitude of the hydraulic conductivity should not change under this transformation.

4.3.4.2. Conductors – SCD

SCD1 represents the mapped fracture zones as hydraulically conductive features, with the locations and orientations as given in Hermanson et al. (1997). Figure 4-17 shows the location of these features and their inferred relative hydraulic properties. The extent of the zones outside of the area covered by site investigations is uncertain. As a base case, the Ceberg site-scale conductor domain model SCD1 allows the on-site fracture zones corresponding to the regional lineaments to extend beyond the site boundaries the same as suggested in the regional scale model, RCD1 (see Appendix C.1).

Hydraulic conductivities of SCD1 are based on the 25m packer test data corresponding to conductive fracture zones identified by Hermanson et al., (1997). Because the data is relatively sparse, the zones are assumed to have the same mean hydraulic conductivity, but varying widths as given in Table 4-5. Similar to RCD1, the geometric mean and variance will vary within elevation intervals as given in Table 4-5, upscaled as necessary (i.e., a planar feature of constant thickness for each mapped fracture zone, each with additional horizontal planes to describe the decrease in hydraulic conductivity with decreasing elevation).

110

Table 4-5. Ceberg site-scale conductor domain hydraulic conductivity at 25m scale (SCD1).

Elevation (m masl)	Mean Log_{10} K (m/s)*
+110 to 0	-7.03
0 to -100	-8.51
-100 to -300	-9.50
Below -300	-9.73

* corrected assuming normally distributed data, after Wen (1994)

As discussed in Section 4.2.2.2, the RCD1 model for the regional scale conductor domain is highly uncertain. This uncertainty is addressed by RCD3, an alternative regional conductor model based on the lineament interpretation of Askling (1997). A complementary site-scale case, SCD2, is proposed to include the Askling (1997) lineament interpretation (similar to RCD3, see Appendix C.3). This alternative lineament interpretation includes a lineament that crosses the northeast corner of the site (i.e., NW-SE w.e. 29) which may have important consequences for PA.

Two additional alternative cases address the possibility of conductive features in addition those described in SCD1. The first is SCD3, which examines the possibility that the subvertical dolerites are conductive features. The occurrence of these features is as given in Hermanson et al. (1997). The hydraulic conductivities should have the same geometric mean and elevation zonation as the fractures in SCD1. The second alternative case is SCD4, which examines the possibility that conductors I, II a, II b, XI a, XI b, and XII may have elevated hydraulic conductivities as was indicated by high yields during drilling and increased fracturing (Ahlbom et al. 1983; and Hermanson et al. 1997). As an alternative case, SCD4 assumes that the above-named zones have hydraulic conductivities 2 orders of magnitude greater than those provided in RCD1.

4.3.4.3. Geostatistical model

The Ceberg site-scale geostatistical model of hydraulic conductivity consists of SCD1, the elevation zones described for SRD6, and a single covariance model. The elevation zones are treated as step changes in the geometric mean of block conductivities (0 order trends in Log_{10} K_b). The model is presented at the measured scale of 25m, which is approximately the same as the proposed HYDRASTAR grid resolution of 30m. As explained in Appendix C.4, the HYDRASTAR upscaling algorithm is best suited to integer multiples of the measurement scale (e.g., 25, 50, 75m, etc.). If the proposed model grid scale is not an integer multiple of the measurement scale, then linear interpolation should be used to adjust the variogram model parameters. It is possible, that the K_b will require adjustment to be consistent with the expected regional boundary fluxes (Section 1.6).
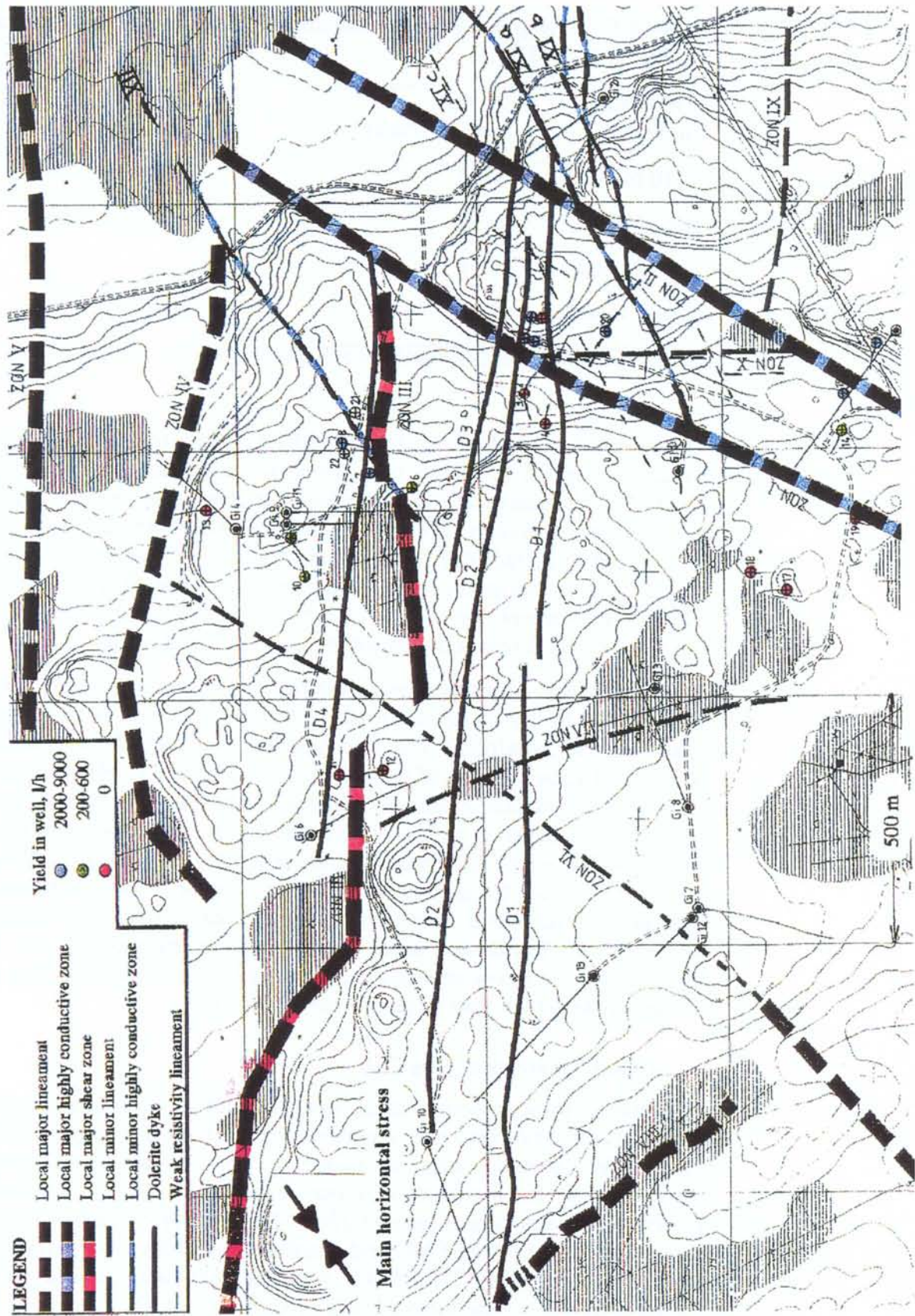
Figure 4-17. *Ceberg site-scale interpreted fracture zones (from Hermanson et al., 1997).*

112

The inference of this model is based on the 25m packer test in the rock domain and the elevation zones as described above. The SKB code INFERENS was used to apply universal kriging to determine the geometric mean of K_b for each elevation zone and model the rock mass variogram. The fracture zones, SCD, are assumed to have the same covariance. Results of this analysis indicated the following exponential variogram model for the 25m scale:

$$\gamma(h) = 0.0 + 1.56 \, Exp \, (28)$$

i.e., a zero nugget exponential model with a practical range of 84m. The complete geostatistical model consists of this variogram model and the 25m scale geometric mean hydraulic conductivities given in Tables 4-3 and 4-4. The sill of the variogram model has been increased (from 1.08 to 1.56) to account for the censoring effect of the measurement limit on the variance. The validity of such a correction is unknown and the model is considered uncertain.

Details of this analysis are found in Appendix C.4.

Table 4-6. Summary of Ceberg Conceptual Models.

Code	Model
	<u>Regional Scale (1)</u>
	Rock Domain
RRD1	Hydraulic conductivity from SGU data, depth zonation from on-site packer tests.
RRD3	as in RRD1, but with anisotropy in the direction of maximum horizontal rock stress
	Conductor Domain
RCD1	Lineaments of Ahlbom et al.(1983) as fracture zones, with width and depth zonation from on-site packer test data. Uniform hydraulic conductivity for all zones.
RCD3	Alternative lineament interpretation based on Askling (1997).
	<u>Site Scale (2)</u>
	Rock Domain
SRD6	Hydraulic conductivity from 25m packer test data, with depth zonation.
SRD7	As in SRD6, but with anisotropy in the direction of maximum horizontal rock stress
	Conductor Domain
SCD1	Fractured zones of Hermanson et al.(1997) as fracture zones, properties and depth zonation from 25m packer test data. Uniform hydraulic conductivity for all zones.
SCD2	Additional fracture zone in NE, after lineaments of Askling (1997).
SCD3	Subvertical doleritic dykes as conductive features.
SCD4	Zones I, II, XI, and XII as highly conductive.
	Excavation Disturbed Zone (EDZ)
EDZ1	Hydraulic conductivity of rock surrounding the tunnel unchanged
EDZ2	10X increase in hydraulic conductivity parallel to tunnel axis in 25cm of rock surrounding tunnel (Appendix D.8)

Notes:
(1)   Regional hydraulic conductivity upscaled to numerical model block scale using the Äspö regression equation, calibrated to observed heads and recharge/discharge patterns.
(2)   Site hydraulic conductivity upscaled to numerical block scale using Äspö regression equation, calibrated to observed heads and regional boundary fluxes. Covariance of hydraulic conductivity upscaled via INFERENS.

114

5. SUMMARY AND INTERSITE COMPARISON

This study has compiled hydrogeologic information for use in SR 97, a performance assessment study conducted by SKB using data from three sites in Sweden. These sites, arbitrarily named Aberg, Beberg and Ceberg, are based on previous SKB site characterisation programmes. The primary objective of this report is to provide conceptual models and consistent analyses of interpreted data so that the results of PA modelling will be as comparable as possible. This study has reviewed the site investigations, summarised hydrogeologic conditions, updated the analyses, and provided parameter estimates.

This final section of the report summarises the suggested modelling approach, followed by a summary of the overall site characteristics. This section also compares the site characteristics and the site characterisation programmes. Finally, this section briefly summarises the conclusions of this study.

5.1. STUDY APPROACH

As was discussed in the preliminary sections of this report, this study is a compilation of existing data and descriptions for use in hydrogeologic modelling. It provides preliminary conceptual models, parameter values and uncertainties at the regional and site scales. Where possible, this report also provides alternative conceptual models that should be evaluated as part of the modeller's sensitivity analysis. The parameters were summarised and adapted directly from the SKB SICADA database, the Swedish Geological Survey (SGU) well database, the SKB Geographic Information System (GIS), the Swedish Land Survey (LMV) databases, and published SKB reports. Where appropriate, interpretative methods and their consequences are discussed. Only the scaling calculations and geostatistical modelling are original, as discussed in the appendices.

The material properties and concepts presented focus on 3-D numerical continuum models. Consequently, numerical block-scale parameters such as block hydraulic conductivity are emphasised. Because these parameters are scale dependent, scaling relationships were developed and presented. Where possible, this report has provided a probabilistic description of the input parameters, acknowledging the observed and assumed uncertainties of the data.

The suggested conceptual model for these hypothetical sites is a two-domain representation of the host rock as one domain for the relatively conductive fracture zones, and another domain for the less-conductive rock mass. A nested modelling approach is suggested: an extensive regional scale model to address the regional flow system, and a site-scale model to address site-scale variability. Because hydraulic conductivity is inherently scale-dependent, this study suggests:

- The domains of the regional scale model should have uniform hydraulic conductivities of K_e, the effective hydraulic conductivity, to be calibrated to observed data.

- The site-scale model should be a stochastic continuum model, with boundary heads taken from the regional model and the geometric mean of K_b, the block hydraulic conductivity, to be adjusted to preserve continuity of the regional fluxes to the site-scale model.

- Preliminary estimates of K_e and K_b should be determined by applying the Äspö regression relationship to the on-site packer tests, with the covariance of K_b determined by applying the HYDRASTAR regularisation algorithm

5.2. SITE SUMMARY

Aberg takes its data from the Äspö site, which is located in southern Sweden. The region is characterised by low topographic relief and a mosaic of shallow coastal waterways and islands. From a hydrogeologic perspective, the region is notable for the intrusion of saltwater from the Baltic Sea. The low relief, rate of landrise and the coastal location result in a continuously changing pattern of coastline and recharge. Data is abundant at Äspö, and of very good quality as a consequence of the Äspö Hard Rock Laboratory (HRL). The HRL is an underground research facility owned and operated by SKB, for the purpose of investigating geological, geochemical, and hydrogeological phenomena that affect the design and operation of deep repositories for underground disposal of nuclear waste. Compared to previous studies of Äspö, this study has revised the geostatistical model of the hydraulic conductivity to reflect the revised measurement limits of the interpreted hydraulic conductivities.

Beberg is modelled after the Finnsjön site, which is located in central Sweden. The region is characterised by low relief and poorly organised drainages, with several lakes, mire and bog. From a hydrogeologic perspective, the region is notable for the occurrence of saline groundwater at relatively shallow depths and for the presence of relatively shallow subhorizontal conductive fracture zones. Similar to Äspö, data is readily available as a result of several SKB site characterisation programs. Additional geologic and hydrogeologic information is provided by investigations at Forsmark, the SKB Final Repository for Radioactive Operational Waste (SFR), and the Dannemora Mine. Compared to previous studies, this study has revised the following analyses:

- Depth dependency of hydraulic conductivity

- Geostatistical model of hydraulic conductivity

Ceberg is modelled after the Gideå site, located in northern Sweden. In comparison to Aberg and Beberg, the region has greater topographic relief, which creates a regional groundwater flow pattern of recharge in the upland areas and discharge to streams in the fault valleys. Another notable characteristic of the site is the comparatively low hydraulic conductivity at repository depth (see Section 5.3). Data is less available here than the other

two sites. The nearby Gissjö hydropower tunnel is of limited use for site characterisation but does provide some information on fracture orientation. Compared to previous studies, this study has revised the following analyses:

- Regional Lineaments

- Depth dependency of hydraulic conductivity

- Geostatistical model of hydraulic conductivity

5.3. INTERSITE COMPARISON

When comparing the three hypothetical sites, it is important to note that the characterisation methods and data types are quite different among the sites, for a number of reasons. The three site characterisation studies were each carried out at different times, with different goals, equipment and degrees of thoroughness. These differences might bias the parameter estimates at both the regional and site scales, consequently biasing the PA modelling studies. Therefore, we should try to distinguish between differences among the site characterisation methods as well as the differences among the sites themselves. The following sections briefly summarise differences between the site characterisation studies at the regional and site scales.

5.3.1. Regional Scale Information

At the regional scale, inferences for Aberg, Beberg and Ceberg are supported by studies of varying degrees of thoroughness and quality. This is partly a consequence of the relative availability of general hydrologic, geologic and hydrogeologic information in each region. Äspö and Finnsjön are located in the southern half of Sweden, where general regional information (e.g., SGU summary reports, SMHI data, etc.) is relatively abundant. At Finnsjön, the nearby Dannemora mine and the SKB studies at the Forsmark SFR augment the regional data. Gideå is in northern Sweden, a less-populated area with a consequently lower mapping priority. The Gideå region thus has no SGU hydrogeologic summary report and less regional data than the other sites. Although regional geologic reports are available for Gideå, the regional conceptual models and hydraulic parameters are almost entirely based on SKB studies.

The regional scale conductive features have been inferred from a lineament map for each region. These lineament maps are interpreted from several types of images depending on the analyst and the availability of airphotos, topographic maps, satellite imagery, LMV digital terrain models, etc. Lineaments are linear topographic features that may indicate bedrock features such as fracture zones, intrusive dykes, etc. Lineament mapping is subjective, and the geologic cause of a lineament is somewhat speculative (Askling, 1997). Although it is tempting to infer that a lineament is a conductive fracture zone, subsurface investigations and hydraulic testing should verify such an inference. In general, the existing interpretations of lineaments and regional scale structural geology were used for this study, without revision. The exception to this is the alternative case model for Ceberg, as discussed below.

The available data for the inference of regional scale conductive features has varied widely for the three sites. At Äspö, lineament maps were based on a wide array of imagery, assisted by aerogeophysical measurements. Interpretation of the Äspö lineaments as regional conductive features is based on extensive ground-based geophysical measurements and borings. Where the regional structures cross the site, borings, on-site hydraulic testing and the Äspö tunnel (SKB, 1996) provide detailed hydraulic information. At Finnsjön, the lineament map was based on topographic maps, airphotos and satellite imagery, assisted by aerogeophysical measurements. Investigations at Forsmark SFR and on-site have identified many of the lineaments as conductive fracture zones (Carlsson and Gidlund, 1983; Ahlbom and Tirén, 1991; Andersson et al., 1991). Where the lineaments cross the Finnsjön site, various borehole tests have provided estimates of hydraulic properties. At Gideå, the lineament interpretation presented in Ahlbom et al. (1983) was based on topographic maps and air photos, but there was no aerogeophysical data outside the site to confirm the regional lineaments (Ahlbom et al., 1991a). The consequent uncertainty in the lineament map may represent the greatest uncertainty in the Gideå regional-scale model. This uncertainty is addressed with a variation case for regional conductive zones based on an alternative regional lineament interpretation (Askling, 1997). On-site boreholes and ground-based geophysics were able to confirm that some of the less-well expressed regional lineaments are conductive fracture zones.

Regional scale hydraulic conductivity has been inferred using a combination of on-site measurements and SGU well archive data. SGU data consists of basic well data for public and private wells and includes drillers' estimates of water capacity. This water capacity can be transformed into a rough approximation of hydraulic conductivity as described in Appendix D. The quality of this data is low, but the estimated hydraulic conductivities generally agree with the on-site measurements at comparable scales and depths. The regional hydraulic conductivity is assumed to follow the same trend with depth as the on-site measurements.

Surface hydrology is important since the pattern of recharge and discharge areas can have deep effects, particularly in regions with strong topographic relief. The Äspö surface water and meteorological data has good period of record, and several gauging stations. Finnsjön is relatively flat, with disorganised watersheds dominated by mire, a hydrologic system whose runoff and recharge terms are difficult to quantify. On the other hand, the various SKB investigations at the site have included weather and stream gauging stations, and several studies have examined the interaction of groundwater and surface water. In contrast, Gideå has little runoff data and much of the surface hydrology needs to be inferred from soil type and the mapped locations of mires and streams.

5.3.2. Site Scale Information

The overall goals of the hydraulic testing programmes are to confirm and identify conductive features, and to determine hydraulic properties for use in subsequent quantitative modelling. However, the methods and equipment

used for borehole testing have varied widely, so that the volume of rock measured, the data spacing, measurement limits, etc. differ from site to site. These differences can effect the inferred hydraulic properties and consequently the results of groundwater flow and transport modelling. This section summarises the hydraulic testing programs at each site, and comments on the differences among the testing programmes and the sites.

5.3.2.1. Comparison of Testing Programmes

Each of the sites was explored by a series of boreholes, which were then subjected to hydraulic tests and tracer tests. As shown in Figure 5-1, the intensity of the investigation varies among the sites, with the greatest intensity at Aberg. Although more boreholes were drilled at Ceberg than at Beberg, subsequent testing in these boreholes was much extensive at Beberg. In general, each site is thoroughly and consistently tested by at least one set of single borehole packer tests with a constant packer interval (i.e., the entire length of all site cored boreholes were tested using a constant straddle packer interval and test type). Where multiple packer intervals were used, the smallest interval was chosen under the assumption that it would provide the greatest resolution. Figure 5-2 summarises these exhaustive test sets, which provide the support for the site geostatistical models of hydraulic conductivity. This analysis assumes that these exhaustive sets with a constant packer interval have a constant sample volume and therefore a common support scale. However, the volume of rock sampled by such hydraulic tests varies with the hydraulic properties and test duration (Oliver, 1990; Follin, 1992b). Classical sampling theory suggests that variations in the support scale may increase measurement error and bias (Journel and Huijbregts, 1978; Beckie, 1996). To minimise the effects of mixed support scales, only the interpreted hydraulic conductivities from tests of a common packer interval are used to support the geostatistical model at each site. It must be noted, however, that this is a subject for further research.

The test types, test scales, test durations and interpretation methods vary among the sites, as can be seen in Figure 5-2. At Äspö, the exhaustive packer test set consists of injection tests with 3m packer intervals of 10-minute duration, interpreted as transient tests. For tests below the measurement limit, Rhén et al. (1997) used specific capacity data to estimate the lowest values of hydraulic conductivity. At Finnsjön, the exhaustive set consists of 3m packer tests of 15-minute injection, interpreted as steady state. Many tests were reported as below a measurement limit, but specific capacity data for estimating such tests was unavailable. At Gideå, the tests used 25m packer intervals of 2hr injection and 2hr recovery interpreted as either transient or steady state models at the analysts' discretion. Here, as at Finnsjön, many tests were reported as below a measurement limit, but specific capacity data for re-evaluating such tests was unavailable (Ludvigson, personal communication, 1997). Differences in test methods and test interpretations can easily result in order of magnitude differences in the estimates of hydraulic conductivity (Geier et al., 1996).
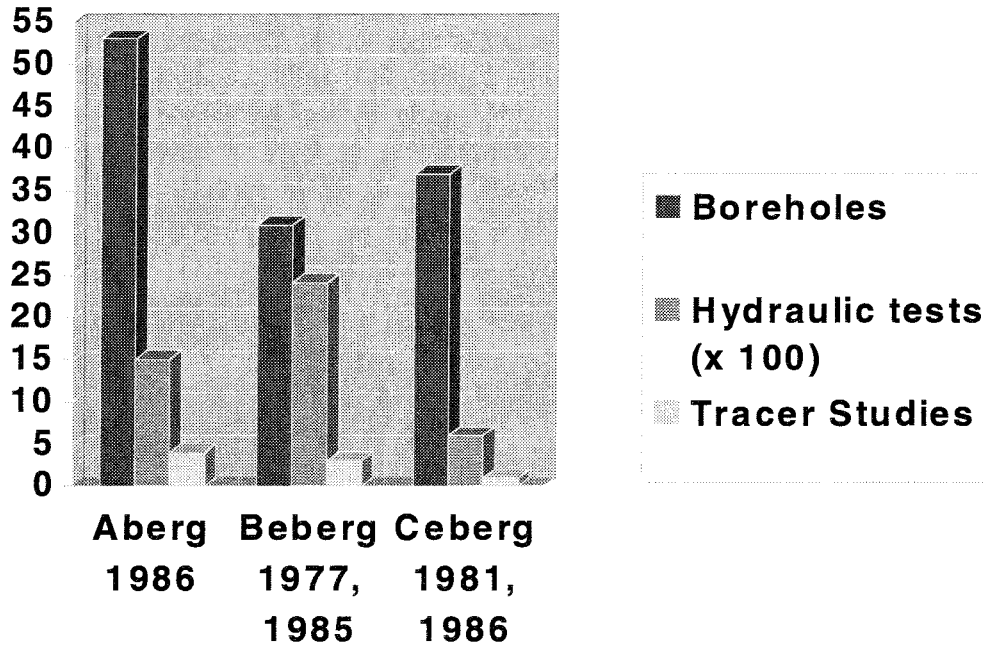
Figure 5-1. Summary of site characterisation programmes, Aberg, Beberg and Ceberg (year refers to dates of initiation of field programme).
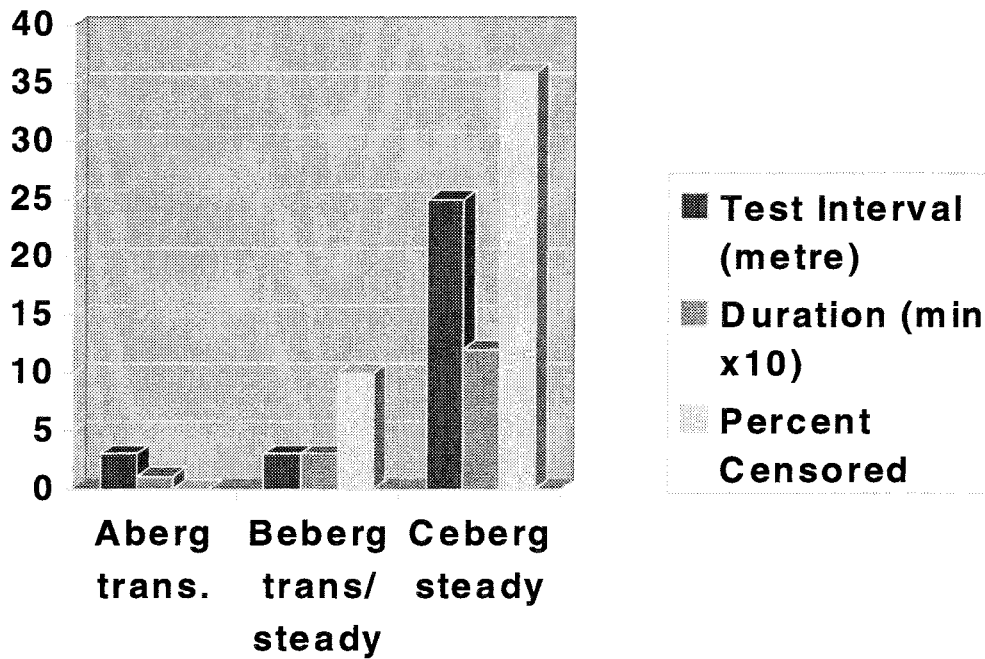
Figure 5-2. Summary of exhaustive hydraulic test data, Aberg, Beberg and Ceberg.

The set of parameters measured by the tests also differs among the sites. At Äspö and Finnsjön, several combined tracer and multiple-well interference tests were conducted. These tests analysed very large volumes of rock and have yielded estimates of hydraulic conductivity, storage and transport parameters. In contrast, at Gideå only single borehole packer tests were conducted (excluding a single, shallow interference test). Such single-hole tests provide no estimate of storage or transport parameters, so that no site-specific estimates of storage or transport parameters are available at Gideå. As for transport parameters (e.g., porosity, dispersivity, etc.), a few measurements are available at Äspö, fewer still at Finnsjön and none at Gideå. There may also be a bias in the location of the samples that reflects the emphasis on the fracture zones. At Finnsjön, for example, an extensive study was made of a subhorizontal fracture zone, Zone 2. Although the data from that study is extremely valuable, it is quite intentionally clustered on that single feature and might result in a biased perspective of that site.

Ideally, several test intervals and durations would be used in all boreholes to investigate the effects of scale on the measurements. Such multiscale data with thorough coverage is available for the Äspö site, and allows us to infer scaling relationships for hydraulic conductivity, porosity and dispersivity. At Finnsjön and Gideå, however, a complete, exhaustive set of measurements was performed with only one packer interval. The data necessary to infer a relationship of measurement scale versus measured property does not exist at these two sites. For the purposes of this report, the Äspö regression relationship for the scale dependency of hydraulic conductivity will be used at the other two sites (Section 1.6).

5.3.2.2. Comparison of Sites

Comparing the hydraulic properties of the sites is difficult, given the tremendous differences in the testing programmes and the apparent depth dependence of hydraulic conductivity. We might pick a common depth and then attempt to rescale the packer test results to account for the difference in test interval length. However, such rescaling ignores the test duration and the storage properties that also control the measured volume. Furthermore, comparing only the hydraulic properties ignores other important aspects of the hydrogeologic system (e.g., gradients, transport properties, etc.) Incorporating all these aspects to determine their net effect is, in fact, the purpose of the groundwater flow and transport modelling of these sites. Given these difficulties, a simple intersite comparison of hydraulic conductivities at Äspö, Finnsjön and Gideå may be misleading.

It is possible, however, to compare the hydrogeologic *representations* of these sites as they are to be used in SR 97. That is, it is possible to make a limited comparison of the hydrogeologic models of Aberg, Beberg and Ceberg, with the understanding that measurement interpretation, analysis and inference have filtered the data. This comparison is constructed for the proposed repository depth in the KBS-3 disposal concept (approximately 500m below ground surface). The exhaustive packer test set for each site is separated into rock mass (SRD) and conductive fracture zones (SCD). In an attempt to reduce the measurement scale differences, the arithmetic means

121

of log hydraulic conductivity for this depth zone is upscaled to 100m (see Section 1.6). The resulting statistics for the 500m depth are presented in Table 5.1.

For the three sites, Table 5-1 and Figure 5-3 present the scaled geometric means and variances of hydraulic conductivity for the conductor domain and rock domain at each site. The table also includes the test durations, scales, and percentage of data below the measurement limits (ML). Note that the means and variances have been corrected for measurement limits using the method of Wen (1994; see also Appendix D.4). As discussed in Appendix D.4, censoring severely effects the estimates of the variance and these estimates are regarded as uncertain. The upscaled variance estimates are included only for the sake of completeness.

Table 5-1. Intersite comparison of Log_{10} hydraulic conductivities upscaled to 100m (approximately 500m depth). ML = measurement limit.

Site	Log_{10} K (m/s) Mean [Variance]		Packer Interval	Duration	% of all data < ML
	Rock Mass (SRD)	Fracture zone (SCD)			
Aberg (1)	-8.0 [0.29]	-6.1 [1.3]	3m	10 min injection transient	None
Beberg (2)	-7.2 [0.042]	-5.9 [0.29]	3m	15 min injection transient or steady	10%
Ceberg (3)	-9.8 [0.99]	-9.1 [1.6]	25m	120 min injection steady	36%

(1) SRD: statistics of Log_{10} K in SRD1 through 3, depth zone 0 to 600m
SCD: statistics of Log_{10} K in SCD, approximately 50 to 100m scale measurements, depth zone 0 to 600m.

(2) Statistics of Log_{10} K in SRD and SCD, respectively, below 430m depth. At this depth, approximately 9% of the SRD data fall below the measurement limit.

(3) Statistics of Log_{10} K in SRD and SCD, respectively, below 410m depth. At this depth, approximately 58% of the SRD data fall below the measurement limit.
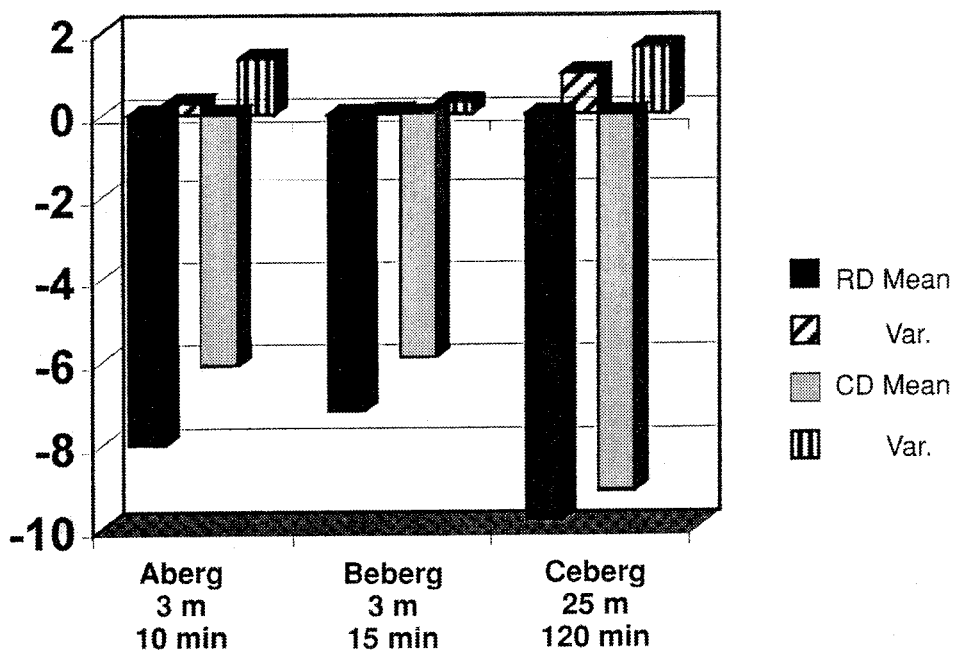
Figure 5-3. Comparison of Log_{10} hydraulic conductivities in the hydrogeologic representations of Aberg, Beberg and Ceberg. Values presented are the mean and variance of Log_{10} hydraulic conductivities at repository depth, upscaled to 100m. The values have been corrected for the effects of censoring.

The immediately obvious difference is that Ceberg has a lower hydraulic conductivity at repository depth than both Aberg and Beberg. The amount of data censored by a measurement limit also varies among the sites. This censoring effect is particularly severe at Ceberg, where 36% of entire data set is below the measurement limit and, at 500m depth, 58% of the data is below the measurement limit. Less obvious is that the tests sets are of dramatically different duration, which might lead to different tested volumes and consequently bias the estimates of the mean and variance of Log_{10} K.

Ceberg appears to have a lower contrast between rock mass and fracture zones, but this may be an artifact arising from several causes. One cause may be that the difference in the packer test intervals creates differences in the resolution of testing programmes. Another cause may be that all fracture zones in the Ceberg geologic structural model are included in the set of as conductive features, even though several have very low hydraulic conductivities. This is reflected in the high variance for the fracture zone hydraulic conductivity at Ceberg. An alternative case model for Ceberg addresses the possibility that the contrast between the fracture zones and rock mass is more similar to that inferred for Aberg and Beberg.

5.4. SUMMARY OF FINDINGS

This study is essentially a compilation of existing reports, but a number of observations can be made regarding the site characterisation programmes and the site characteristics. In spite of the differences in characterisation programmes, some qualitative comparisons can be made of the site characteristics:

- The hydraulic conductivities of Aberg and Beberg appear to be more similar to each other than to Ceberg.

- The contrast of fracture zones to the surrounding rock mass appears to be lower at Ceberg than at Aberg or Beberg.

- The differences between the hydrogeologic characteristics of these sites may be their general hydrologic features, e.g., recharge vs. discharge areas, low vs. high topographic relief, saline vs. nonsaline environments.

The primary objective of this study has been the compilation of data and parameter estimates for continuum models such as HYDRASTAR. Consequently, this study is limited in scope, e.g.:

- The study does not address parameters strictly for discrete feature models or channel network models.

- The study assumes lognormally distributed hydraulic conductivity, even though the data distributions and measurement limits might be better represented by an alternative assumption.

- The study does not compile soft data relationships such as are used in indicator approaches to geostatistics.

- The study relies on an empirical relationship for the scale dependency of hydraulic properties. Current research provides little alternative to this approach, and further investigation is recommended.

The site characterisation studies are quite different at both the regional and site scales, limiting the validity of comparisons of site properties. In particular:

- Regional conductive features have been inferred from lineament maps at all three sites, but confirmation of these structures via geophysics and borings have not been performed for all three sites.

- Site drilling and hydraulic testing programmes have varied, which might lead to bias in the estimates of hydraulic properties.

- Data with sufficient spatial coverage at multiple scales are not available to infer site-specific scaling relationships at all three sites.

- Site-specific knowledge of transport parameters is limited to tracer tests in specific fracture zones at Aberg and Beberg.

ACKNOWLEDGEMENTS

REFERENCES

Ahlbom K, Albino B, Carlsson L, Nilsson G, Olsson O, Stenberg L, Timje H, 1983. Evalutation of the geological, geophysical and hydrogeological conditions at Gideå, SKBF/KBS Technical Report TR 83-53.

Ahlbom K, Andersson J-E, Andersson P, Ittner T, Ljunggren C, Tirén S, 1992a. Klipperås study site. Scope of activities and main results, SKB Technical Report TR 92-22.

Ahlbom K, Andersson J-E, Andersson P, Ittner T, Ljunggren C, Tirén S, 1992b. Kamlunge study site. Scope of activities and main results, SKB Technical Report TR 92-15.

Ahlbom K, Andersson J-E, Andersson P, Ittner T, Ljunggren C, Tirén S, 1992c. Finnsjön study site. Scope of activities and main results. SKB Technical Report TR 92-33.

Ahlbom K, Andersson J-E, Nordqvist R, Ljunggren C, Tirén S, Voss C, 1991a. Gideå study site. Scope of activities and main results. SKB Technical Report TR 91-51.

Ahlbom K, Andersson J-E, Nordqvist R, Ljunggren C, Tirén S, Voss C, 1991b. Fjällveden study site. Scope of activities and main results, SKB Technical Report TR 91-52.

Ahlbom K, Andersson P, Ekman L, Tirén S, 1988. Characterization of fracture zones in the Brädan area, Finnsjön study site, central Sweden. SKB Progress Report PR 88-09.

Ahlbom K, Karawacki E, 1983. Thermal properties measured on core samples from Fjällveden, Gideå, Kamlunge and Svartboberget. SKBF/KBS Arbets Rapport AR 83-36.

Ahlbom K, Olsson O, Sehlstedt S, 1995. Temperature conditions in the SKB study sites. SKB Technical Report TR 95-16.

Ahlbom K, Svensson U, 1991. The groundwater circulation in the Finnsjön area – the impact of density gradients. SKB Technical Report TR 91-57.

Ahlbom K, Tirén S, 1991. Overview of geological and geohydrologic conditions at the Finnsjön site and its surroundings. SKB Technical Report TR 91-08.

Almén K-E, Ekman L, Olkiewicz A, 1978. Försöksområdet vid Finnsjön. Beskrivning till berggrunds- och jordarts kartor.

Andersson J-E, Nordqvist R, Nyberg G, Smellie J, Tirén S, 1991. Hydrogeological conditions in the Finnsjön area. Compilation of data and conceptual model. SKB Technical Report TR 91-24.

Andersson J-E, Olsson T, 1978. Forsmark Nuclear Power Plant – freshwater supply by groundwater extraction in bedrock. Swedish Geological Survey. In Swedish.

Andersson J, Elert M, Hermanson J, Moreno L, Gylling B, Selroos J–O, 1997. Derivation and treatment of the flow wetted surface and other geosphere parameters in the transport models FARF31 and COMP23 for use in safety assessment. SKB Report R-97-XX (in publication, SKB report)

Andersson P, 1995. Compilation of tracer tests in fractured rock. SKB Progress Report PR 25-95-05.

Askling, P., 1997. Gideå lineament map. An interpretation based on elevation data models. SKB Progress Report PR U-97-06.

Axelsson C-L, Byström J, Eriksson Å, Holmén J, Haitjema H M, 1991. Hydraulic evaluation of the groundwater conditions at Finnsjön. The effects on dilution in a domestic well. SKB Technical Report TR 91-54.

Bear J, 1972. Dynamics of fluids in porous media. Dover Publications, Inc., New York.

Beckie R, 1996. Measurement scale, network sampling scale, and groundwater model parameters. Water Resources Research, Vol. 32:1.

Bergman S, Isaksson H, Johansson R, Lindén A, Persson C, Stephens M, 1996. Förstudie Östhammar. Jordarter, bergarter och deformationszoner. SKB Djupförvar Projekt Rapport PR D-96-016.

Bjarnason B, Klasson H, Leijon B, Strindell L, Öhman T, 1989. Rock stress measurements in boreholes KAS02, KAS03, and KAS05 on Äspö. SKB Progress Report PR 25-89-17.

Björck S, Svensson N-O, 1992. Climatic changes and uplift patterns - past, present and future. SKB Technical Report TR 92-38.

Brandberg F, Skagius K, 1991. Porosity, sorption and diffusivity data compiled for the SKB 91 study. SKB Technical Report TR 91-16.

Boghammar A, Grundfelt B, Widén H, 1993. Analysis of the regional groundwater flow in the Finnsjön area. SKB Technical Report TR 93-15.

Carlsson L, Gidlund G, 1983. Evaluation of the hydrogeological conditions at Finnsjön. SKBF KBS Technical Report TR 83-56.

Carlsson L, Gustafson G, 1984. Provpumpning som geohydrologisk undersökningsmetodik, (Byggforskningsrådet), R41:1984, Stockholm.

Carlsson L, Winberg A, Arnefors J, 1986. Hydraulic modeling of the final repository for reactor waste (SFR). Compilation and conceptualization of available geological and hydrogeological data. SKB Progress Report SFR 86-03.

Carlsson L, Winberg A, Grundfelt B, 1983. Model calculations of the groundwater flow at Finnsjön, Fjällveden, Gideå and Kamlunge. SKBS KBS Technical Report TR 83-45.

Carlsson M, 1997. Sea level and salinity variations in the Baltic Sea – an oceanographic study using historical data. Dept. of Oceanography, Göteboreg Univ., Sweden.5.

Cohen A C Jr, 1959. Simplified estimators for the normal distribution when samples are single censored or truncated. Technometrics 1.

Dagan G, 1986. Statistical theory of groundwater flow and transport: pore to laboratory, laboratory to formation, and formation to regional scale. Water resources Research, Vol. 22:9.

Dershowitz W, Redus K, Wallmann P, LaPointe P, Axelsson C-L, 1992. The implication of fractal dimension in hydrogeology and rock mechanics. Verision 1.1. SKB Technical Report TR 92-17.

Dershowitz W, Thomas A, Busse R, 1996. Discrete fracture analysis in support of the Äspö tracer retention understanding experiment (TRUE-1). SKB, (in press).

Deutsch C, 1989. DECLUS: a Fortrab 77 program for determining optimum spatial declustering weights. Computers & Geoscience 15:3.

Deutsch C V, Journel A G, 1992. GSLIB Geostatistical software library and user's guide. Oxford University Press, Inc., New York.

Domenico P A, Schwartz F W, 1990. Physical and Chemical Hydrogeology, (John Wiley & Sons), New York.

Elert M, 1997. Retention mechanisms and the flow wetted surface – implications for safety analysis. SKB Report R-97-XX (in publication, SKB report).

Englund E, Sparks A, 1991. GEO-EAS 1.2.1. Geostatistical environmental assessment software. User's guide. Environmental monitoring systems laboratory office of research and development, U.S. Environmental Protection Agency EPA, Las Vegas Nevada.

Ericsson L O, and Ronge B, 1986. Correlations between tectonic leneaments and permeability values of crystalline bedrock in the Gideå area, SKB Technical Report TR 86-19.

Eriksson B, 1980. The water balance of Sweden. Annual mean values (1931-60) of precipitation, evaporation and run-off (in Swedish), SMHI Nr RMK 18 and Nr RHO 21 (1980), SMHI, Norrköping.

Follin S, 1992a. Numerical calculations on heterogeneity of groundwater flow. SKB Technical Report TR 92-14.

Follin S, 1992b. On the interpretation of double-packer tests in heterogeneous porous media: Numerical simulations using the stochastic continuum analogue. SKB Technical Report TR 92-36.

Forsmark T, 1992. Hydraulic tests at Äspö in KAS16. SKB Progress Report PR 25-92-15.

Forsmark T, Stenberg L, 1993. Supplementary investigations of fracture zones in the tunnel. Hydrogeology. Measurements performed during con-

struction of chainage 1475-2265 m. Compilation of Technical Notes. SKB Progress Report PR 25-94-06.

Fredén C, (Ed) 1994. National atlas of Sweden. Geology. SNA Publ., Sveriges nationalatlas, Almqvist & Wiksell International, Stockholm.

Geier J, 1993a. Verification of the geostatistical inference code INFERENS Version 1.1 and demonstration using data from Finnsjön. SKB Technical Report TR 93-09.

Geier J, 1993b. Version 1.0. Users guide to INFERENCE 1.1. SKB Arbets Rapport AR 93-24.

Geier J E, Doe T W, Benabderrahman, Hässler L, 1996. SITE-94. Generalized radial flow interpretation of well tests for the SITE-94 Project. SKI Report 96:4.

Gelhar L W, 1986. Stochastic subsurface hydrology from theory to applications. Water Resources Research, Vol. 22:9.

Gelhar L W, 1987. Applications of stochastic models to solute transport in fractured rocks. SKB Technical Report TR 87-05.

Gelhar L W, 1993. Stochastic subsurface hydrology. Prentice Hall, New Jersey.

Gelhar L W, Axness C L, 1983. Three-dimensional stochastic analysis of macrodispersion in aquifers. Water Resources Research, Vol. 19:1.

Gottschalk L, 1982. Hydrologi. Hydrology compendium (in Swedish), Lund.

Gustafsson E, Nordqvist R, 1993. Radially converging tracer test in a low-angle fracture zone at the Finnsjön site, central Sweden. The Fracture Zone Project - Phase 3 SKB Technical Report TR 93-25.

Gustafsson E, Skålberg M, Sundblad B, Karlberg O, Tullborg E-L, Ittner T, Carbol P, Eriksson N, Lampe S, 1987. Radionuclide deposition and migration within the Gideå and Finnsjön study sites, Sweden: A study of the fallout after the Chernobyl accident. Phase I, initial study. SKB Technical Report TR 87-28.

Gustafsson G, Ström A, 1995. The Äspö task force on modelling of groundwater flow and transport of solutes. Evaluation report on Task No 1, the LPT2 large scale field experiments. SKB International Cooperation Report 95-05.

Gutjahr A L, Gelhar L, Bakr A A, MacMillan J R, 1978. Stochastic analysis of spatial variability in subsurface flows. 2. Evaluation and Application. Water Resources Research, Vol. 14:2.

Hermanson J, 1995. Structural geology of water-bearing fractures. SKB Progress Report PR 25-95-23.

Hermanson J, 1996. Visualization of the fracture network in rock blocks along the Äspö HRL tunnel using a DFN model approach. SKB PR HRL 96-08.

Hermanson J, Hansen L M, Follin S, 1997. Update of the Geological Models of the Gideå Study Site, SKB Report R-97-05.

Hsieh P A, Neuman S P, 1985. Field detrmination of the Three-Dimensional Hydraulic Conductivity Tensor of Anisotropic Media. 1. Theory. Water Resources Research, Vol. 21:11.

Indelman P, Dagan G, 1993. Upscaling of permeability of anisotropic heterogenous formations. 1. The general framework. Water Resources Research, Vol. 29:4.

Ittner T, 1990. Long term sampling and measuring program. Joint report for 1987, 1988 and 1989. Within the project: Fallout studies in the Gideå and Finnsjön areas after the Chernobyl accident in 1986. SKB Technical Report TR 91-09.

Ittner T, Gustafsson E, Nordqvist R, 1991. Radionuclide content in surface and groundwater transformed into breakthrough curves. A Chernobyl fallout study in a forested area in Northern Sweden. SKB Technical Report TR 91-28.

Jibao He, 1992. Lined underground openings. Rock mechanical effects on high internal pressure. Doctoral Thesis. Chalmers University of Technology.

Johansson J, Stille H, Sturk R, 1995a. Dept. of Geotechnical Engineering, Gothenburg, Sweden.

Johansson J, Stille H, Sturk R, 1995b. Pilotanläggning för inklädda gaslager i Grängesberg. Fördjupad analys av försöksresultaten. Kungliga Tekniska Högskolan. Inst för anläggning och miljö. Avd för jord och bergmekanik. ISRN KTH/ AMI/REPORT-3004-SE (Pilot plant for lined gas installations in Grängesberg. Deep analyses of test results. School of Civil engineering and the environment - in Swedish) ISRN KTH/ AMI/REPORT-3004-SE. Stockholm, Sweden.

Journel A G, Huijbregts Ch J, 1978. Mining geostatistics. Academic press, London.

Jönsson P, Wallroth T, Wladis D, 1997, Statistical analysis of hydraulic conductvity at Gideå and Fjällveden, unpublished draft, SKB, Stockholm, Sweden.

Kickmaier W, 1993. Definition and characterisation of the N-S fracture system - tunnel sections 1/600m to 2/400m. Relationships to grouted sections - some remarks. SKB ICR 95-02.

Kroll C N, Stedinger J R, 1996. Estimation of moments and quantiles using censored data. Water Resources Research, Vol. 32:4.

Kulhánek O, Wahlström R, 1985. Macroseismic observations in Sweden 1980-1983. SGU ser. C 808.

La Pointe P R, 1994. Evaluation of stationary and non-stationary geostatistical models for inferring hydraulic conductivity values at Äspö. SKB Technical Report TR 94-22.

131

La Pointe P R, Wallmann P, Follin S, 1995. Estimation of effective block conductivities based on discrete network analyses using data from the Äspö site. SKB Technical Report TR 95-15.

Laaksoharju M, Skårman C, Gurban I. 1997. SR97: Summary of Hydrogeochemical conditions at Aberg, Beberg and Ceberg. SKB Technical Report Report R 97-XX.

Larson S-Å, 1980. Layered intrusions of the Ulvö dolerite Complex, Ångermanland, Sweden. PhD Thesis, Publ. A 36, Geologiska institutionen, Chalmers Tekniska Högskola/Göteborgs Universitet.

Liedholm M, 1987a. Regional Well Data Analysis. SKB Progress Report PR 25-87-07.

Liedholm M, 1987b. Regional Well Water Chemistry. SKB Progress Report PR 25-87-08.

Liedholm M (ed), 1991a. Conceptual Modelling of Äspö. Technical Notes 1-17. General geological, hydrogeological and hydrochemical information, SKB Progress Report PR 25-90-16 a.

Liedholm M (ed), 1991b. Conceptual Modelling of Äspö. Technical Notes 18-31. General geological, hydrogeological and hydrochemical information, SKB Progress Report PR 25-90-16 b.

Liedholm M, 1992. The hydraulic properties of different greenstone areas. A comparative study, SKB Progress Report PR LOK 92-07.

Lindbom B, Boghammar A, 1992. Numerical groundwater flow calculations at the Finnsjön study site – extended regional area. SKB Technical Report TR 92-03.

Lindbom B, Boghammar A, Lindberg H, Bjelkås J, 1991. Numerical groundwater flow calculations at the Finnsjön site. SKB Technical Report TR 91-12.

Lindewald H, 1985. Galt grundvatten i Sverige. SGU, Rapporter och Meddelanden nr 39.

Lovius L, 1994. Suggestions for estimation of conductivity statistics when data below the measurement limit is present. SKB Arbetsrapport AR 94-26.

Lundqvist T, Gee D, Karis L, Kumpulainen R, Kresten P, 1990. Beskrivning till berggrundskartan över Västernorrlands Län (in Swedish with an English summary). SGU ser. BA 31. Geological Survey of Sweden, Uppsala.

Müller B, Zoback M L, Fucha K, Mastin L, Gregersen S, Pavoni N, Stephansson O, Ljunggren C, 1992. Regional patterns of tectonic stress in Europe. J. Geoph. Res. 97, B.

Neuman S P, 1994. Generalized scaling of permeabilities: Validation and effect of support scale. Geophysical Research Letters, Vol. 21:5.

Neuman S P, Depner J S, 1988. Use of variable-scale pressure test data to estimate the log hydraulic conductivity covariance and dispersivity of

fractured granites near Oracle, Arizona. Journal of Hydrology, 102.

Neuman S P, Jacobson E A, 1984. Analysis of Nonintrisic Spatial Variability by residual kriging with Application to Regional Groundwater levels. Math. geol., Vol. 16:5.

Niemi A, 1995. Modelling of Äspö hydraulic conductivity data at different scales by means of 3-dimensional Monte Carlo simulations. SKB ICR 95-08.

Nilsson L, 1989. Hydraulic tests at Äspö and Laxemar. SKB HRL Progress Report PR 25-88-14.

Nilsson L, 1990. Hydraulic tests at Äspö, KAS05-KAS08, HAS13-HAS17, Evaluation. SKB HRL Progress Report PR 25-89-20.

Norman S, 1992a. Statistical inference and comparison of stochastic models for the hydraulic conductivity at the Finnsjö site. SKB Technical Report TR 92-08.

Norman S, 1992b. HYDRASTAR - a code for stochastic simulation of groundwater flow. SKB Technical Report TR 92-12.

Nyberg G, Jönsson S, Ekman L, 1995. Groundwater level program. Report for 1994. SKB Progress Report PR 25-95-08.

Olivier D S, 1990. The averaging process in permeability estimation from well-test data. SPE Formation Evaluation.

Olkiewicz A, Arnefors J, 1981. Berggrundsbeskrivning av undersöknings området vid Finnsjön i norra Uppland. SKBF/KBS Arbets Rapport AR 81-35.

Olsson O (ed), 1992. Site Characterisation snd Validation–Final Report. SKB Technical Report Stripa Project 91-22

Olsson O (ed), 1994. Localization of experimental sites and layout of turn 2. Results from core mapping, radar and hydraulic investigations. Compilation of Technical Notes 2. SKB Progress Report PR 25-94-15.

Olsson O, Emsley S, Bauer C, Falls S, Stenberg L, 1996. Zedex, a study of the zone of excavation disturbance for blasted and bored tunnels. SKB ICR 96-03

Olsson O, Stanfors R, Ramqvist G, Rhén I. 1994. Localization of experimental sites and layout of turn 2. Results of investigations. SKB Progress Report PR 25-94-14.

Olsson O, Winberg A, 1996. Current understanding of the extent and properties of the excavation disturbed zone and its dependence of excavation. Unpublished SKB project memo, September 19, 1996.

Pickens J F, Grisak G E, 1981. Scale-dependent dispersion in a stratified ganular aquifer. Water Resources Research, Vol. 17:4.

Poteri A, 1996. Analysis of bedrock fracturing at Äspö. SKB ICR 96-01.

Priest, S. D., 1985. Hemispherical projection methods in rock mechanics, George Allen and Unwin, London.

Renard Ph, de Marsily G, 1997. Calculating equivalent permeability: a review. Advance Water Resource 1997.

Rhén I. 1988. Transient interference tests on Äspö 1988. Evaluation. SKB Progress Report PR 25-88-13.

Rhén I. 1990. Transient interference tests on Äspö 1989 in KAS06, HAS13 and KAS07. Evaluation. SKB Progress Report PR 25-90-09.

Rhén I (ed), 1995. Documentation of tunnel and shaft data, tunnel section 2874 - 3600 m, hoist and ventilation shafts 0 - 450 m. SKB Progress Report PR 25-95-28.

Rhén I, Danielson P, Forsmark T, Gustafson G, Liedholm M, 1993a. Geohydrological evaluation of the data from section 700-1475 m. SKB Progress Report PR 25-93-06.

Rhén I, Danielsson P, Forsmark T, Gustafson G, Liedholm M, 1993b. Geohydrological evaluation of the data from section 1475 - 2265 m. SKB Progress Report PR 25-93-11.

Rhén I, Danielsson P, Forsmark T, Gustafson G, Liedholm M. 1994a. Geohydrological evaluation of the data from section 2265-2874 m. SKB Progress Report PR 25-94-20.

Rhén I, Forsmark T, Danielsson P. 1994b. Piezometric levels. Evaluation of the data from section 2265-2874 m. SKB Progress Report PR 25-94-22.

Rhén I, Forsmark T, Nilsson L, 1991. Hydraulic tests on Äspö, Bockholmen and Laxemar 1990 in KAS09, KAS11-14, HAS18-20, KBH01-02 and KLX01. Evaluation. SKB Progress Report PR 25-91-01.

Rhén I, Gustafson G, 1990. DDP evaluation of hydrogeological data, Report U(G) 1990/59.

Rhén, I (ed), Gustafson G, Stanfors R, and Wikberg P., 1997. Äspö HRL - Geoscientific evaluation 1997/5. Models based on site characterization 1986-1995. SKB Technical Report TR 97-06.

Rhén I, Stanfors R, 1995. Supplementary investigations of fracture zones in Äspö tunnel. SKB Progress Report PR 25-95-20.

Rhén I, Svensson U, Andersson J-E, Andersson P, Eriksson C-O, Gustafsson E, Ittner T, Nordqvist R, 1992. Äspö Hard Rock Laboratory. Evaluation of the combined long-term pumping and tracer test (LPT2) in borehole KAS06. SKB Technical Report TR 92-32.

Rosen L, Gustafsson G, 1996. A Bayesian Markov geostatistical model for estimation of hydrogeological properties. Ground Water, Vol. 34:5.

Rubin Y, Gómez-Hernández J J, 1990. S stochastic Approach to the problem of Upscaling of conductivity in disordered media: Theory and unconditional numarical simulations. Water Resourches Research, Vol. 26:4.

Serafin J L, Pereira J P, 1983, Consideration on the geomechanical classification of Bieniawski, Proc.Int. Symp. On Engr. Geology and Underground Construction, Lisbon, vol. 1.

Shan K C, Huan W X, Cvetkovic V, Winberg A, 1992. Stochastic continuum simulation of mass arrival using a synthetic data set. The effect of hard and soft conditioning. SKB Technical Report TR 92-18.

Sjöberg B (Ed), 1992. National atlas of Sweden. Sea and coast. SNA Publ., Sveriges nationalatlas, Almqvist & Wiksell International, Stockholm.

SKB, 1995. Äspö Hard Rock Laboratory. Annual Report 1994. SKB Technical Report TR 95-07.

SKB, 1996. Äspö Hard Rock Laboratory. 10 years of research. SKB.

Smellie J A T, Wikberg P, 1989. Characterization of fracture zone 2, Finnsjön study site. In: Ahlbom and Smellie (eds). SKB Technical Report TR 89-19.

Stille H, Olsson P, 1996. Summary of rock mechanical experiences from the construction of Äspö Hard Rock Laboratory. SKB Progress Report PR HRL 96-07.

Stålhös, G, 1988. Bedrock Map of 12I Östhammar NV, SGU series Af nr. 166 (in Swedish).

Sundberg J, Thunholm B, Johnsson J, 1985. Värmeöverförande egenskaper i svensk berggrund. BFR rapport R97:1985.

Sundblad B, Mathiasson L, Holby O, Landström O, Lampe S, 1991. Chemistry of soil and sediments, hydrology and natural exposure rate measurements at the Äspö Hard Rock Laboratory. SKB Progress Report PR 25-91-08.

Svensson, U, 1991. Groundwater flow at Äspö and changes due to the excavation of the laboratory, SKB Progress Report PR 25-91-03.

Svensson U, 1995. Modelling the unsaturated zone at Äspö under natural conditions and with the tunnel front at 2874 metres. SKB Progress Report PR 25-95-24.

Svensson T, 1987. Hydrological conditions in the Simpevarp area. SKB Progress Report PR 25-87-09.

Timje, H. 1983. Hydrogeological Investigations at Study Site Gideå, SKBF/KBS Arbetsrapport AR 83-26 (in Swedish).

Tsang Y YW, 1996. SITE-94. Stochastic Continuum Hydrological Model of Äspö for the SITE-94 Performance Assessment Project.

Uchida M, Doe T, Dershowitz W, Thomas A, Wallmann P, Sawada A, 1994. Discrete-fracture modelling of the Äspö LPT-2, large-scale pumping and tracer test. SKB ICR 94-09.

Vomvoris S, Andrews R W, Lanyon G W, Voborny O, Wilson W, 1996. Methodology for deriving hydrogeological input parameters for safety-

analysis models – application to fractured crystalline rocks of northern Switzerland. NAGRA Technical Report TR 93-14.

Ward D S, Buss D R, Mercer J W, and Hughes S S, 1987. Evaluation of a Groundwater Corrective Action at the Chem-Dyne Hazardous Waste Site using a telescopic mesh refinement modeling approach, Water Resour. Res., vol 23, no 4, pp603-617.

Wellin E, Lundqvist T, 1975. K-Ar ages of Jotnian dolerites in Västernorrland County, central Sweden. Geologiska Föreningen i Stockholm Förhandlingar, Vol. 97.

Wen, X-H, 1994. Estimation of statistical parameters for censored lognormal hydraulic conductivity measurements. Mathematical Geology, Vol. 26:6.

Wen X-H, Gómez-Hernández J J, 1996. Upscaling hydraulic conductivities in heterogeneous media: An overview. Journal of Hydrology 183.

Wikberg P, Gustafson G, Rhén I, Stanfors R. 1991. Äspö Hard Rock Laboratory. Evaluation and conceptual modelling based on the pre-investigations 1986-1990. SKB Technical Report TR 91-22.

Winberg A, 1989. Project – 90. Analysis of variability of hydraulic conductivity data in the SKB database GEOTAB. SKI Technical Report TR 89:12.

Winberg A, 1991. Analysis of spatial correlation of hydraulic conductivity data from the Stripa Mine. SKB Technical Report Stripa Project 91-28.

Winberg A, 1996. First TRUE stage – tracer retention understanding experiments. Descriptive structural-hydraulic models on block and detailed scales of the TRUE-1 site. SKB International Cooperation Report 96-04.

Öhberg A, Saksa P, Ahokas H, Routsalainen P, Snellman M, 1994. Summary report of the experiences from TVO's site investigations, SKB Technical Report TR 94-17.

APPENDIX A. ABERG

A.1 ANALYSIS OF SGU DATA IN ÄSPÖ REGION

The Swedish Geological Survey (SGU) provided well data from the SGU well archive for a 25 x 25km area in the Äspö region. As discussed in Appendix D.1, it is possible to estimate the well's specific capacity, Q/dh, and use a regression relationship for Q/dh versus T to determine the transmissivity. The effective hydraulic conductivity (K) was estimated by dividing T by the test length. This SGU data is pooled with Äspö HRL borehole tests of comparable length to determine the hydraulic conductivity distribution in the region. Figure A-1 shows the statistics for the entire sample and for depth ranges (SGU wells within the regional model area plus the Äspö HRL superficial boreholes). The sample statistics of specific capacity show that the means are about the same but the standard deviation of the Äspö HRL data (see Table A-1).

Geostatistical analysis of SGU estimated hydraulic conductivities indicated that two wells with relatively low hydraulic conductivity should be excluded as they had a very strong impact on the correlation range. An isotropic variogram model was fitted by eye using the following spherical model:

$$\gamma(h) = 0.3423 + 0.3307 \text{ Sph}(825)$$

That is, a spherical model with a range of 825m and approximately 50% nugget. Figure A-2 shows the regional hydraulic conductivity field as estimated by kriging with the above variogram model. Note that the distance between wells generally exceeds the range of the variogram model (825m). Given the wide confidence band for the T vs. Q/dh relationship (Appendix D.1) and the SGU data spacing, including spatial correlation will have little impact on the estimation of the regional hydraulic conductivity field.

Figure A-1 also illustrates the depth dependence of hydraulic conductivity. The Äspö borehole data indicates that hydraulic conductivity is roughly constant down to 600 m. The limited data below 600m suggests that below 600m the hydraulic conductivity decreases by a factor of 10 (after accounting for the measurement scale). If data from deeper levels than 200 m are included, there are only smaller changes of the statistics for the sample.
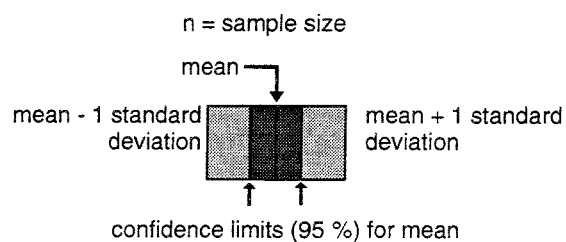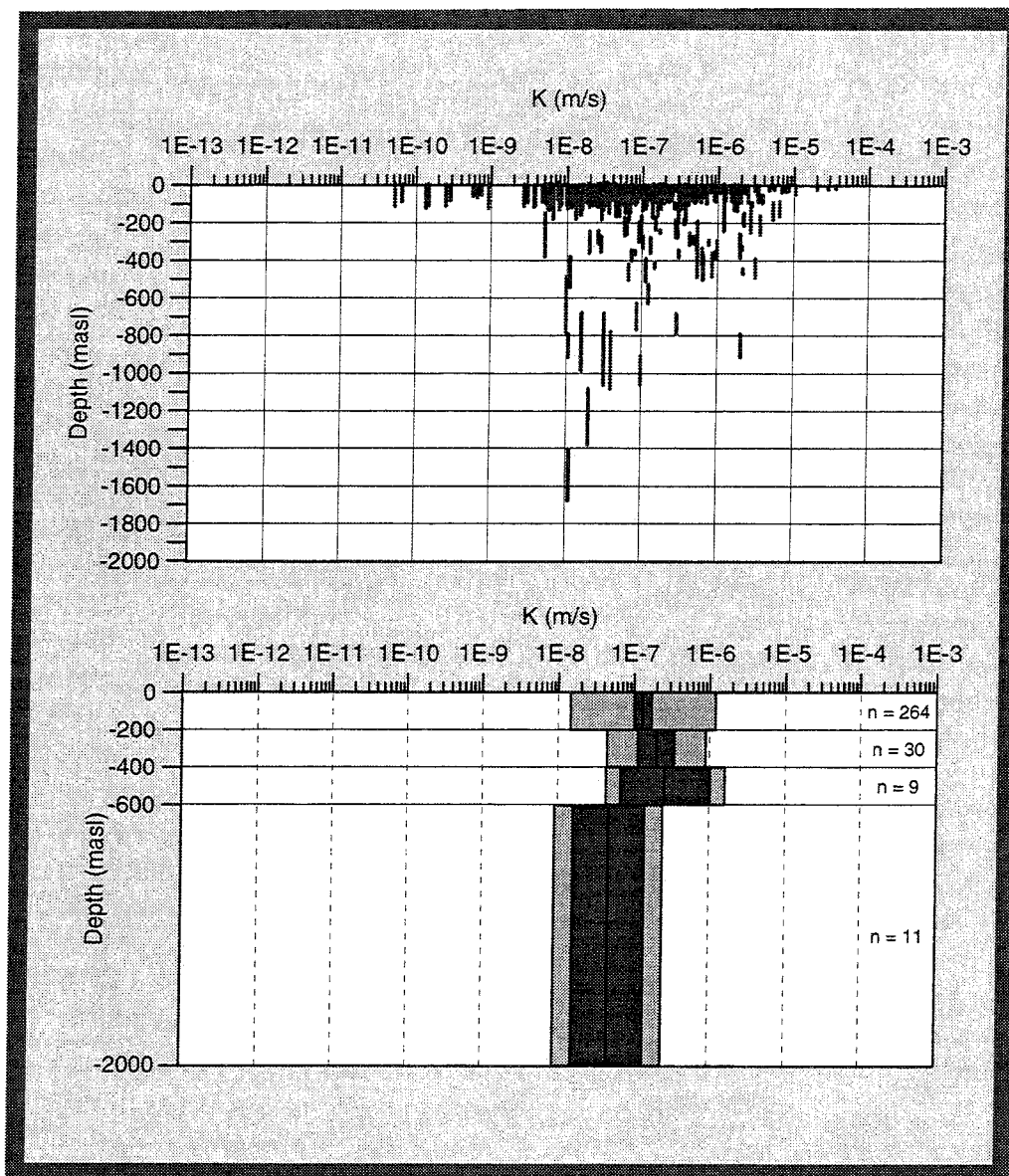
Figure A-1. *Aberg regional depth zonation of hydraulic conductivity (from Rhén et al., 1997).*
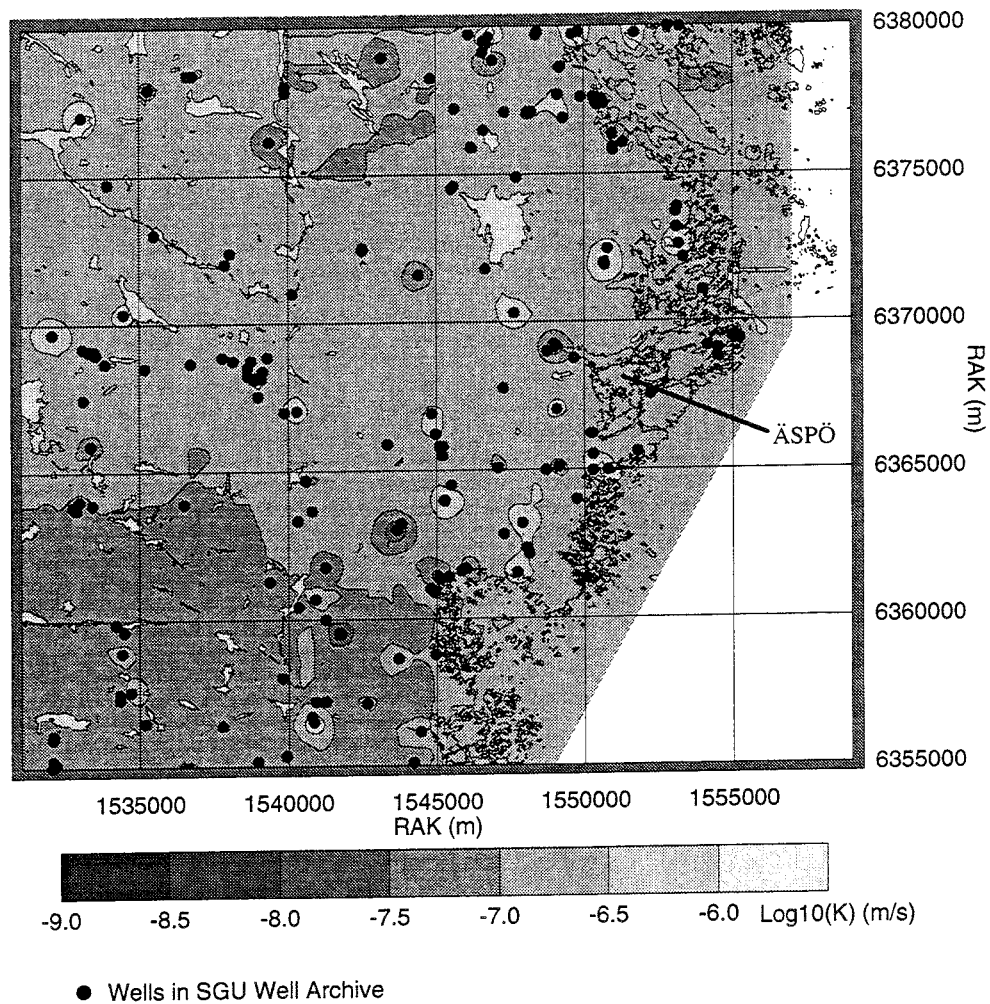
Figure A-2. Aberg Regional log hydraulic conductivity *Filled circles : location of SGU well. (All data included in the kriging)*. (from Rhén et al., 1997).

Table A-1. Sample statistics for $Log_{10}(Q/s)$ – Aberg regional scale - SGU wells covering an area of 25x25 km. (Scale = test length- median value, m = arithmetic mean, s = standard deviation, n = sample size).

Sample	Scale	m($Log_{10}(Q/s)$)	s($Log_{10}(Q/s)$)	$Log_{10}(Q/s)$ 95% confidence range of mean	n
	(m)	$Log_{10}(m^2/s)$	(-)	$Log_{10}(m^2/s)$	
Äspö HRL	100	-5.8	1.34	-6.15 to -5.42	54
SGU wells	64	-5.51	0.75	-5.61 to -5.40	193

A-3

A.2 ÄSPÖ PACKER TEST DATA

The principal source of data for hydraulic properties on the site scale is the double packer tests performed in the cored boreholes on Äspö and Laxemar. These tests were performed in boreholes KLX01, and KAS02 through KAS08 (Appendix A.5). This analysis emphasises the 3m packer tests, as these have the smallest test interval and the most thorough coverage of the cored boreholes. It is important to note that this study uses the interpreted hydraulic conductivities as used by Rhén et al. (1997). The chief difference between this and previous interpretations of the 3m data (Nilsson, 1989, 1990; Geier et al., 1996) is that the Rhén et al. interpretation is not truncated by a lower measurement limit. Where previous interpretations classified failed hydraulic tests as being below a measurement limit, Rhén et al. reinterpreted such tests using specific capacity to assign values to such tests. It is therefore possible that the inferences made regarding depth trends, spatial correlation, etc. made in this study might differ from those of previous studies of Liedholm (1991a), Niemi (1995), and La Pointe (1994).

In addition to the 3m packer tests, this analysis uses several other types of hydraulic tests. For example, the 3m packer tests are used with 30m, 100m and full-length tests in the same cored boreholes to construct the empirical scaling relationships for hydraulic conductivity (Appendix D.5). Hydraulic tests in the tunnel probeholes are used infer hydraulic properties of the area south of Äspö (e.g., SRD4). A series of interference pumping tests provided data for the interpreted transmissivity and storage properties of the deterministic conductors.

The data has been divided into two populations based on the site structural model (Rhén et al., 1997):

Rock Domain (RD) - borehole sections outside the deterministic hydraulic conductors.

Conductor Domain (CD) - borehole sections judged to be within the deterministic hydraulic conductors.

A.2.1 Rock Mass Domain

At the site scale, Aberg is divided into five rock mass domains (SRD) with different hydraulic properties:

- SRD 1: Northern part of Aberg, bounded to the south by the northern part of EW-1.

- SRD 2: Volume bounded by the northern and southern parts of EW-1.

- SRD 3: Southern part of Aberg bounded to the north by the southern part of EW-1 and to the south by EW-3.

- SRD 4: South of EW-3.

- SRD 5: a fine-grained granite body in the middle of the tunnel spiral at about 350m depth.

Outside of the site, SRD1-4 are assumed to be valid within an area bounded by EW-7 to the south and some 100 m outside of the site to the west, north and east (see Figure A-3). The SRD properties might reasonably be extrapolated to the hydraulic conductor domains limiting the rock mass domains to the north, south and to the model borders in Figure A-3. The exceptions to this are the Laxemar and Mjälen areas. Although these would fall into SRD4, these areas may be less fractured than the remainder of SRD4. The properties in the Laxemar and Mjälen areas should taken as the mean of SRD1, SRD2 and SRD3.

Tunnel observations and geostatistical modelling suggest that one or more bodies of fine-grained granite might exist at a depth of 300 to 400m within the tunnel spiral (Rosen and Gustafson, 1996). These fine-grained granites with relatively high hydraulic conductivity are represented by SRD5. This subdomain is a single elliptical body centred in the HRL tunnel spiral at a depth of 350 m, with major axis length of 150m (E-W), and minor axes of 75m. The volume and shape of SRD5 should be considered uncertain.

The hydraulic conductivities for domains SRD1-3 are based on the interpreted hydraulic conductivities of the 3m packer tests. No such 3m tests are available for within SRD4 (south of NE-1). However, during construction of the tunnel, 20m horizontal probeholes were drilled approximately every 16m into the left- and right-hand tunnel walls, angled 20 degrees outward from the tunnel centreline. As well as providing information for the tunnelling operations, single-packer pressure build-up tests were conducted in the probeholes. The test section length during hydraulic tests was approximately 15 m. The interpreted hydraulic conductivities from the probehole tests for tunnel chainage 700-1475m were used to infer hydraulic conductivities for SRD4.

There are only a limited number of hydraulic tests below -600 masl in the Äspö region, with very few below -800 masl and none below -1700 masl. The properties given in for depths below −600 masl inferred from the deeper portions of KLX01 and KAS02.

The statistics for the rock mass domains SRD1-5 based on the test data are given in Table A-2.

Rhén et al (1997) had suggested an arithmetic mean Log_{10} hydraulic conductivity of -6.46 for SRD4 based on the tunnel probehole data. However, it is possible that the mean of the probehole data might be biased because of the differences in test methods. Subsequent numerical modelling of the Äspö site indicates that, in order to match observed heads, the geometric mean of hydraulic conductivity for SRD4 should be an order of magnitude lower than that of the probehole data (Svensson, personal communication, 1997). That is, the calibrated value of the arithmetic mean Log_{10} K for SRD4 is -7.6 at the 20m scale, more similar to SRD2.
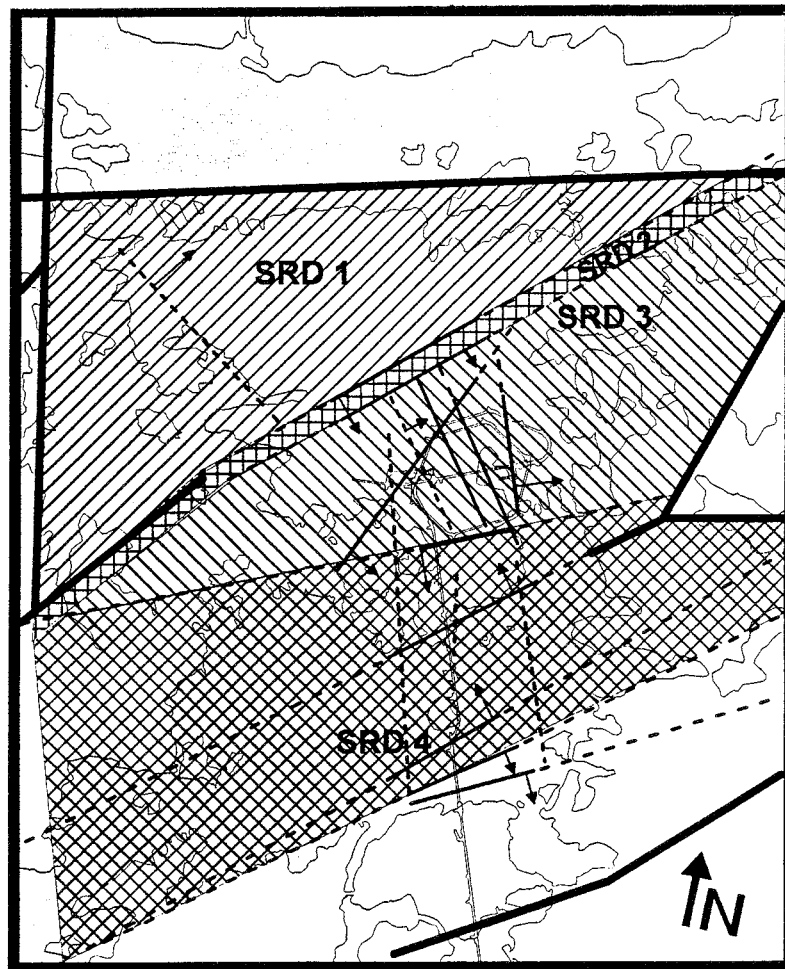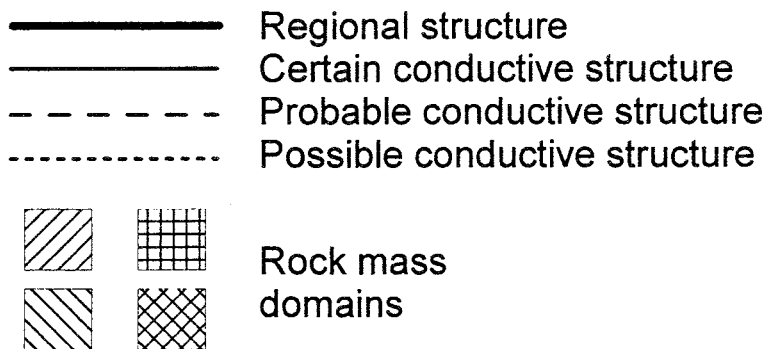
Figure A-3. Model of the Aberg hydraulic rock mass domains (SRD).

Table A-2. Statistics for Aberg rock domain hydraulic conductivity, based on 3m (and 15m) packer tests (from Rhén et al., 1997).

Group of domains	Depth range (m)	Scale (m)	Arithm. $(Log_{10}(K))$ $Log_{10}(m/s)$	Variance $(Log_{10}(K))$ (-)	Comment
SRD1	0-600	3	-8.74	1.32	KAS03-"rock"
SRD2	0-600	3	-7.82	1.79	KAS04-"rock"
SRD3	0-600	3	-9.47	1.63	KAS02,05-08-"rock"
SRD4*	0-600	15*	-6.46	1.61	Probe holes-700-1475m
SRD1-4	600-d_b	300	-7.33	0.72	Acc to regional model
SRD5	See text	3	-8.32	1.99	Fine-grained granite

* based on 15m probehole data; see text.

As discussed in Section 2.3.1, the rock mass appears to be preferentially fractured along a subvertical, NW-SE plane. This suggests that the hydraulic conductivity for a continuum model might be anisotropic with a major axis parallel to this direction. Although there have been no rigorous tests for anisotropy conducted at the site (i.e., no tests of the type advocated by Hsieh and Neuman, 1985), Rhén et al. (1997) did compare the interpreted conductivities from probeholes and boreholes of different orientations. Using the argument that tests in boreholes orthogonal to a major axis of anisotropy would yield higher transmissivities, their results suggested a NW-SE axis of anisotropy in the horizontal plane at the 10 to 20m scales (Table A-3 and Figure A-4). The simple ratio of horizontal major : horizontal minor : vertical provides a suggestion of anisotropy ratio of 100:1:10. Rhén et al. (1997) suggest that these values are approximate, given the differences in testing methods and the broad assumptions for test interpretations.

Table A-3. Estimates of transmissivities in different directions within the tunnel spiral at the Äspö HRL.

Probe holes Strike of plane perpendicular to the probe hole directions (^{O}) (Äspö co-ordinate system)	Scale (m)	T (m^2/s)
120-140	15	$8 \cdot 10^{-7}$
20 - 80	15	$4.5 \cdot 10^{-9}$

Cored boreholes Direction of plane perpendicular to the probe hole directions	Scale (m)	T (m^2/s)
$\approx$Horizontal	15	$5 \cdot 10^{-8}$
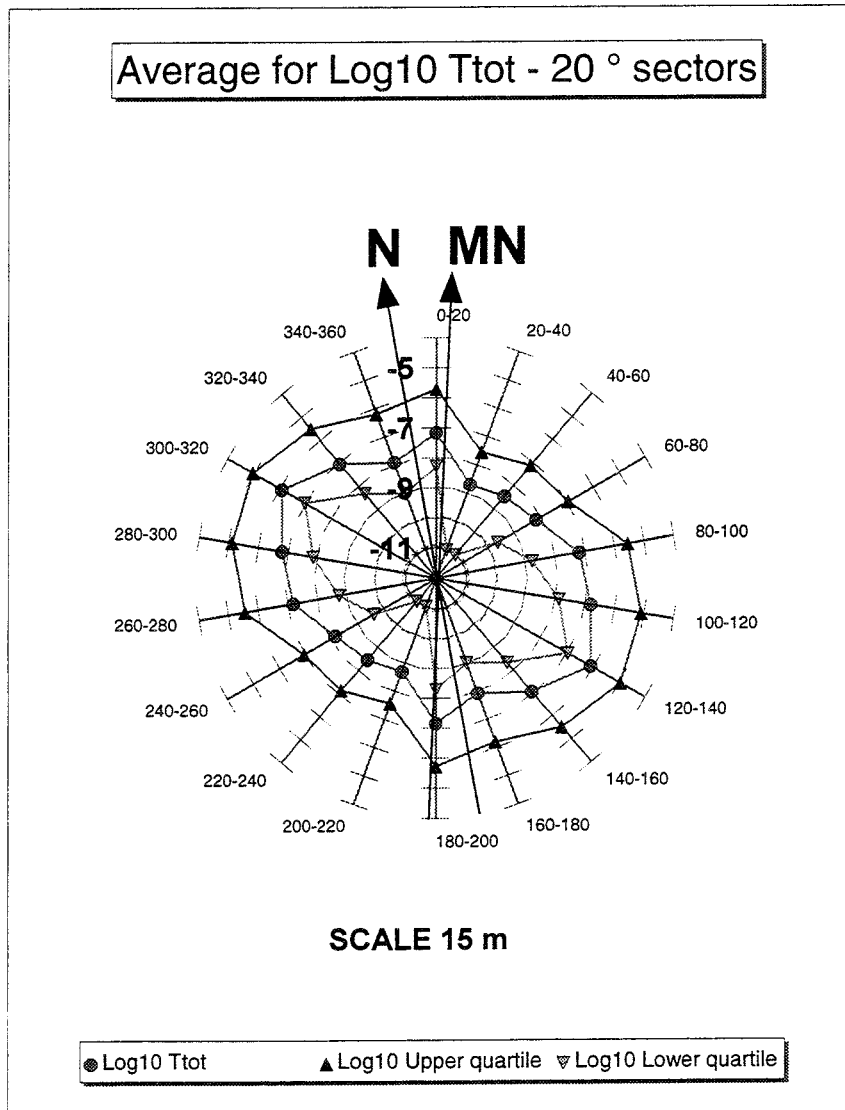
Figure A-4. Estimated transmissivities (T) in directions orthogonal to probeholes in HRL tunnel spiral, based on 15m probe holes in tunnel section 1400-3600m. Directions relative to Äspö coordinate system. Arithmetic mean, upper quartile and lower quartile of Log_{10} (T) shown in the figure for planes within a 20° sector in the horizontal plane. N= North in the Äspö co-ordinate system.

Laboratory tests of the permeability (k) of rock cores and also hydraulic tests in boreholes on the 5cm scale indicate that more or less unfractured rock at Äspö has a k value of about 10^{-20} to $10^{-19} m^2$ (Olsson et al, 1996). However, re-evaluation of the data indicated that the permeability should be approximately 10 times greater (Rhén et al., 1997). This suggests a lower limit of the Aberg hydraulic conductivity of approximately $K=10^{-12}$ to 10^{-11} m/s.

A.2.2. Conductor Domain

The geometries of the hydraulic conductor domains are defined by the major discontinuities observed in the host rocks. A simplified discontinuity model was made by fitting a plane to the observations at ground level and in the boreholes (Figure A-5; Appendix A.4 provides a set coordinates for three points on the plane). Note that one deterministic hydraulic conductor, NNW-8, is not shown in Figure A-5 because it is not thought to reach the surface. The position and extent of NNW-5 and NNW-6 are indicated only by surface geophysical measurements and must be considered uncertain.

Some of the hydraulic conductors are also defined as discontinuities in the geological model. Some of the discontinuities have a clear increase of fracture density while others are rather diffuse (fracture swarms). The hydraulic conductors called NNW strike approximately N 35°W are believed to be a fracture swarm consisting of mainly subvertical fracture sets striking NW and N-S.

The hydraulic conductors EW-1 and EW-3 are complex structures. Although some the outer parts of these structures are quite conductive, interference tests and tunnel data indicate that the cores of EW-1 and EW-3 have relatively low hydraulic conductivities. This suggests that the average conductivities of EW-1 and EW-3 is anisotropic with a major axis in the E-W direction

Several types of hydraulic tests have been performed in borehole sections corresponding to the individual conductive structures. These include double packer injection tests, airlift tests, and full-length borehole pump tests in combination with flow metre logging. Interference tests in selected conductors were also made. Most of the conductors had at least one test, some with multiple tests in several zones. In a few cases several tests from different parts of the discontinuities are available and make it possible to assign the variability within the zone. The exceptions of to this are NNW-6, which was not tested, and NNW-3 and NNW-5, whose single test results are considered unreliable. In such cases, expert judgement was used to assign material properties.

The properties for each conductor are given in Table A-4 (from A2-7 and A2-8 of Rhén et al., 1997). Values for NNW-3 and NNW-6 are taken from the average of all tested conductors. Measurement scale for these tests is approximately 50 to 100m (Rhén, 1988 and 1990).
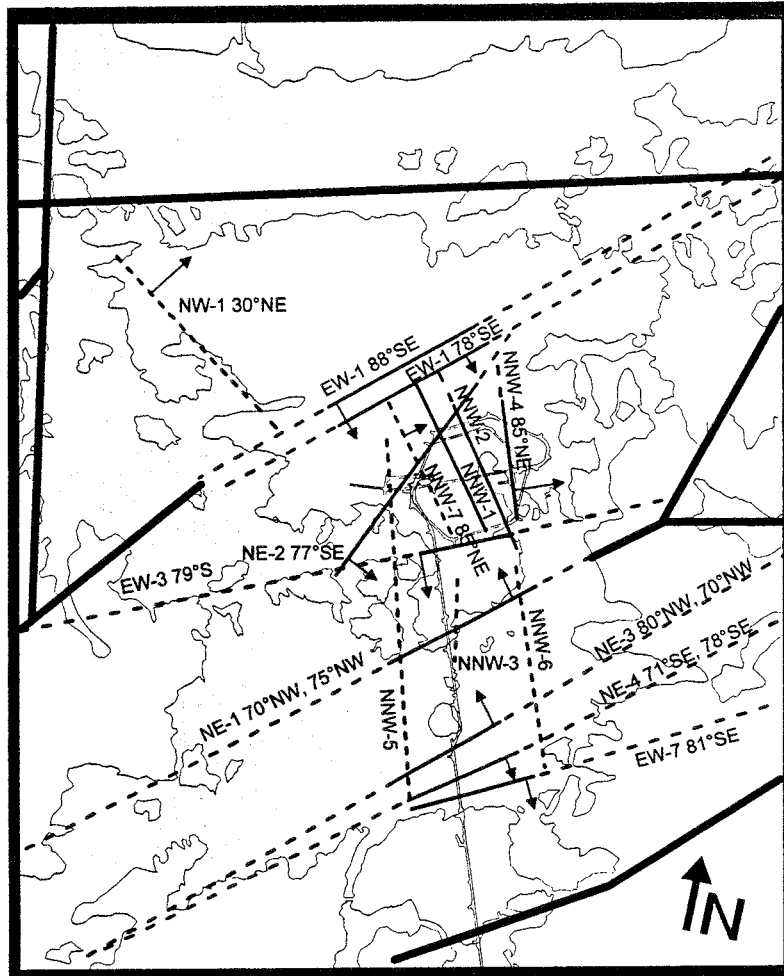
Figure A-5. *Aberg site-scale hydraulic conductors (SCD).*

Table A-4. Statistics for Aberg conductor domain transmissivity based on interference tests. Approximate measurement scale of 100m (from Rhén et al., 1997).

Zone	Geom. Mean T (m2/s)	Median T (m2/s)	Variance LogT	Width (m)	Sample size
EW-1N	5,20E-07	1,50E-06	2,56	30	4
EW-1S	1,20E-05	2,20E-05	1,37	30	4
EW-3	1,70E-05	2,40E-05	0,29	15	4
EW-7	1,50E-05	6,80E-05	1,61	10	3
NE-1	2,20E-04	3,00E-04	0,26	30	16
NE-2	1,20E-07	4,10E-07	4,58	5	12
NE-3	3,20E-04	2,90E-04	0,21	50	9
NE-4	3,10E-05	3,00E-05	0,62	40	8
NNW-1	8,60E-06	1,10E-05	0,67	20	7
NNW-2	2,40E-05	5,60E-05	1,12	20	4
NNW-4	6,50E-05	1,50E-04	2,25	10	8
NNW-5	4,00E-06	2,00E-06	0,71	20	3
NNW-7	7,50E-06	4,80E-06	0,76	20	5
NNW-8	8,40E-06	1,00E-05	0,02	20	3
NW-1	4,10E-07	1,70E-07	1,17	10	3

A.3 GEOSTATISTICAL MODELLING

This model of spatial correlation for Aberg site-scale hydraulic conductivity uses the previously defined divisions of SRD1 through 5, SCD1 and the elevation zones. The model is developed for the SKB stochastic continuum model HYDRASTAR, which assumes that hydraulic conductivity has a multivariate lognormal distribution. The elevation zones, SRD, and SCD treated as step changes in the mean of Log_{10} conductivities. A single variogram model is inferred for the entire domain (i.e., the same variogram for SRD and SCD). This model of trend and spatial correlation is inferred using the iterative generalised least squares estimation (IGLSE) approach to universal kriging suggested by Neuman and Jacobsen (1984). The SKB program INFERENS, which includes the HYDRASTAR regularisation algorithm (Appendix D.4), automates the IGLSE fitting algorithm.

As discussed in Section 1.6.1, the correct approach to the upscaling of hydraulic conductivities to the numerical grid block is not known. As an interim approach, this study uses the Äspö scaling relationships of Rhén et al. (1997) to determine the geometric mean of hydraulic conductivity in each SRD and depth zone (Appendix D.5). The effect of upscaling on the variogram is determined by applying the HYDRASTAR regularisation algorithm and fitting a variogram–trend model to the regularised data via INFERENS. The final model recommendation must be regarded as

uncertain and should be evaluated via deterministic sensitivity analysis. The geometric means of K_b require adjustment to insure that the subdomain boundary fluxes are consistent with the regional model boundary fluxes (Section 1.6).

A.3.1 Exploratory Data Analysis

The analysis is based on the Rhén et al. (1997) interpretation of the 3m packer tests. The 3m data is divided into the rock domain (RD) and conductor domain (CD) defined by Rhén et al. (1997). Exploratory data analysis via several software tools (Appendix D.4) reveals a skewed data distribution for the $\log_{10}$ transform of hydraulic conductivity for both RD and CD data sets (Figures A-6 and A-7). The skewness suggests that the data is not a promising candidate for a multivariate lognormal simulation method (e.g., the method used in HYDRASTAR). Preliminary variography using a median indicator variogram suggests that the RD data is spatially correlated out to a practical range of approximately 100 to 150m, with a large nugget effect (Figure A-8). The median indicator variogram of the CD data shows some spatial correlation structure but is not promising (Figure A-9).

The borehole spacing is such that for lag spacing of less than 50m, the variogram estimates are computed along the boreholes. This borehole spacing and the borehole plunge of 60 to 90° (various azimuths) inadvertently creates a *directional* variogram estimate for lags < 50m, in the direction of 60 to 90° plunge. Cross-hole pairs are gradually added for lags > 50m, so that the sill of the variogram is estimated for all directions (Figure A-10, for example). This severely limits attempts at directional variography, and is not pursued farther. The variogram is assumed to be isotropic (see notes concerning anisotropic covariance and anisotropic hydraulic conductivity tensor in Section 1.6). The maximum separation distance between data pairs is approximately 1900m. The rule of thumb choice for the maximum fitted lag is therefore approximately 600m.

Program restrictions of HYDRASTAR and INFERENS limit the geostatistical model to one variogram model for both domains. Because the RD data is more abundant and more promising, the geostatistical model will be developed from the RD data.

Aspo 3m data, all boreholes
Rock Domain (file KASrd.eas)

S t a t i s t i c s

N Total : 1170
N Miss : 0
N Used : 1170

Mean : -9.264
Variance: 2.558
Std. Dev: 1.599
% C.V. : 17.264
Skewness: .960
Kurtosis: 3.295

Minimum : -12.200
25th % : -10.400
Median : -9.720
75th % : -8.410
Maximum : -3.890

Relative Frequency

.30
.25
.20
.15
.10
.05
.00

-16. -14. -12. -10. -8. -6. -4. -2. 0.

Log_10(K_Rhen) (m/s)
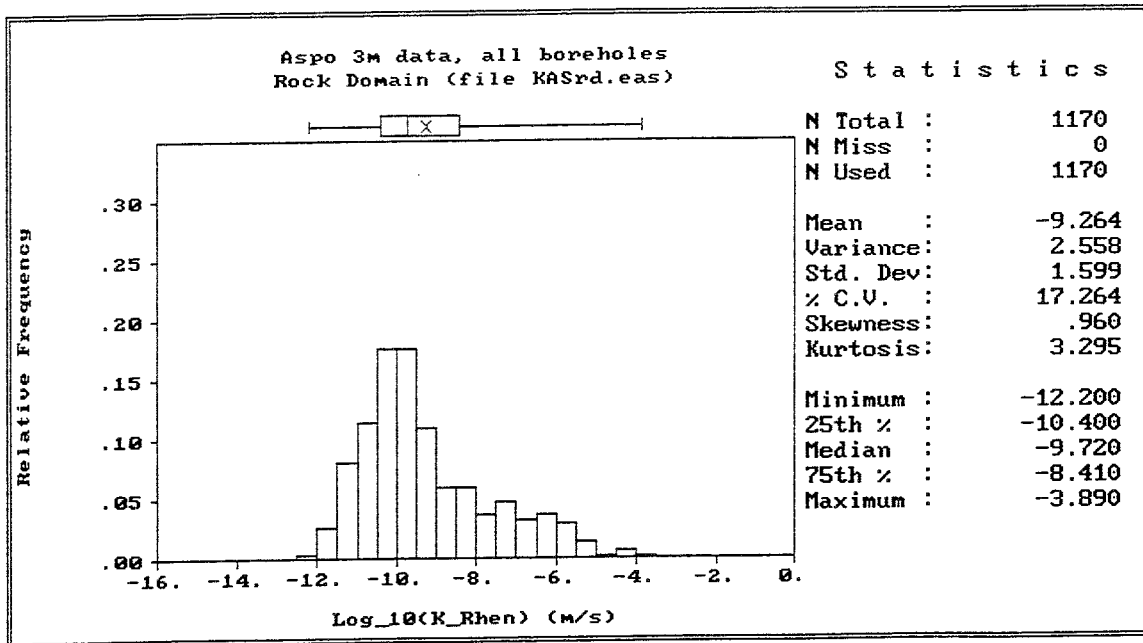
Figure A-6. Histogram of Aberg hydraulic conductivity from 3m packer test in rock domain (RD).

Aspo 3m data, all boreholes
Conductor Domain (file KASCD.eas)

S t a t i s t i c s

N Total : 130
N Miss : 0
N Used : 130

Mean : -7.454
Variance: 3.923
Std. Dev: 1.981
% C.V. : 26.572
Skewness: -.199
Kurtosis: 1.925

Minimum : -11.600
25th % : -9.180
Median : -7.460
75th % : -5.825
Maximum : -4.030

Relative Frequency

.30
.25
.20
.15
.10
.05
.00

-16. -14. -12. -10. -8. -6. -4. -2. 0.

Log_10(K_Rhen) (m/s)
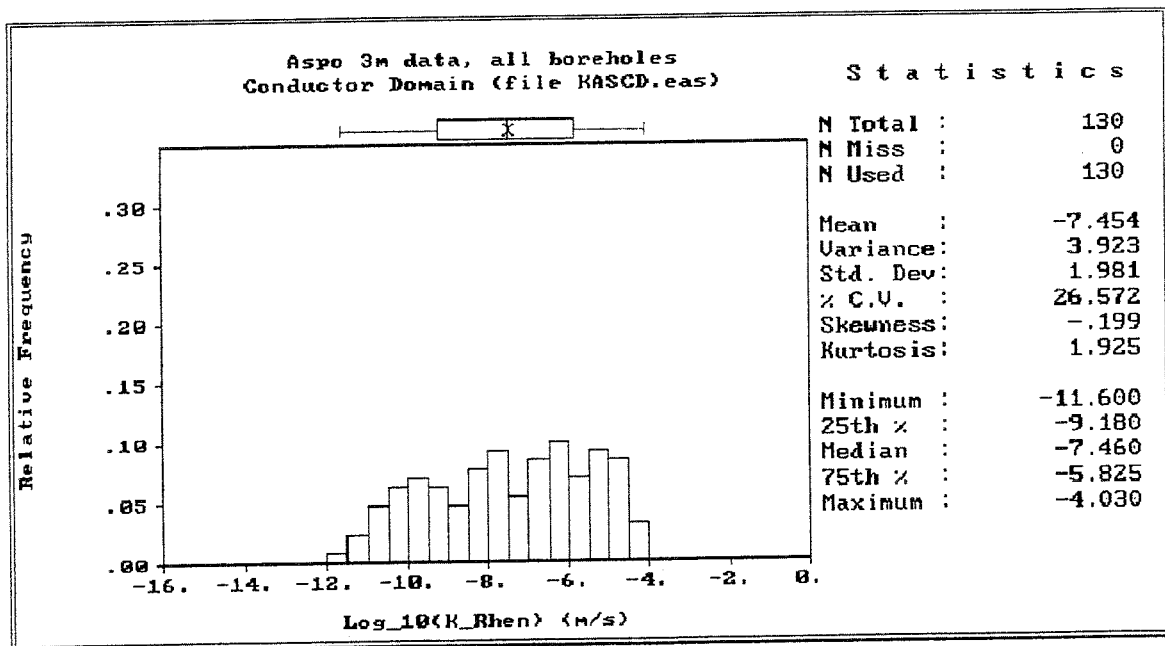
Figure A-7. Histogram of Aberg hydraulic conductivity from 3m packer test in conductor domain (CD).

A-13
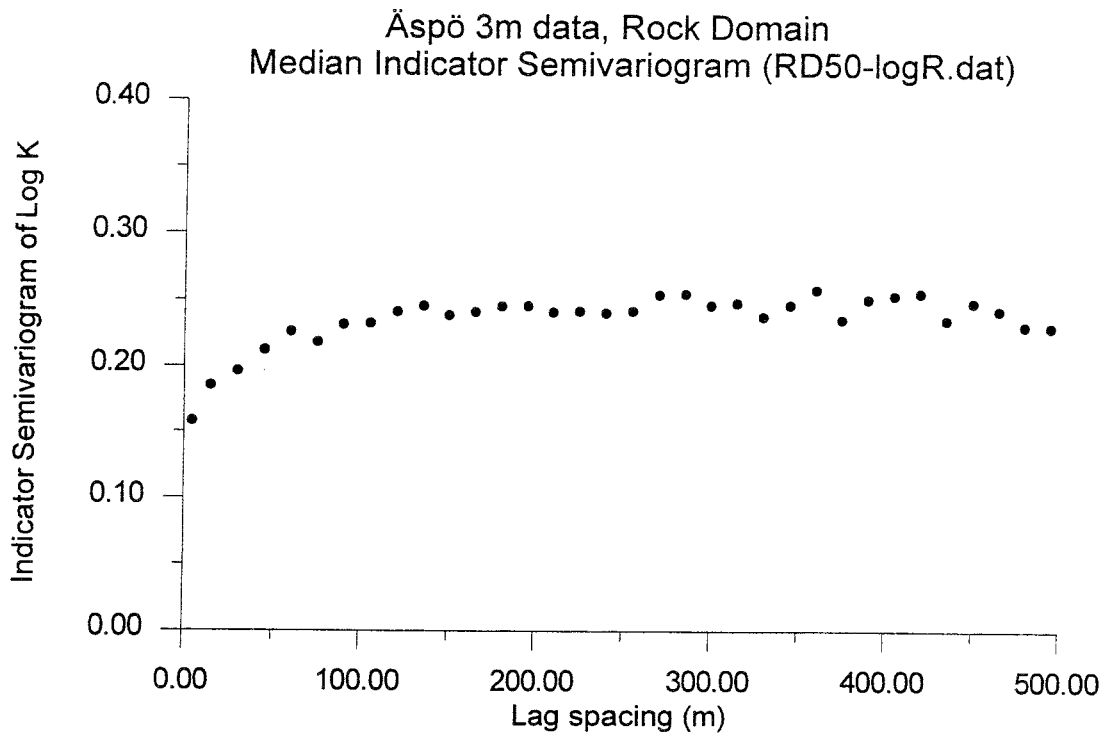
Figure A-8. *Median Indicator variogram for Aberg hydraulic conductivity from 3m packer test in rock domain (RD).*
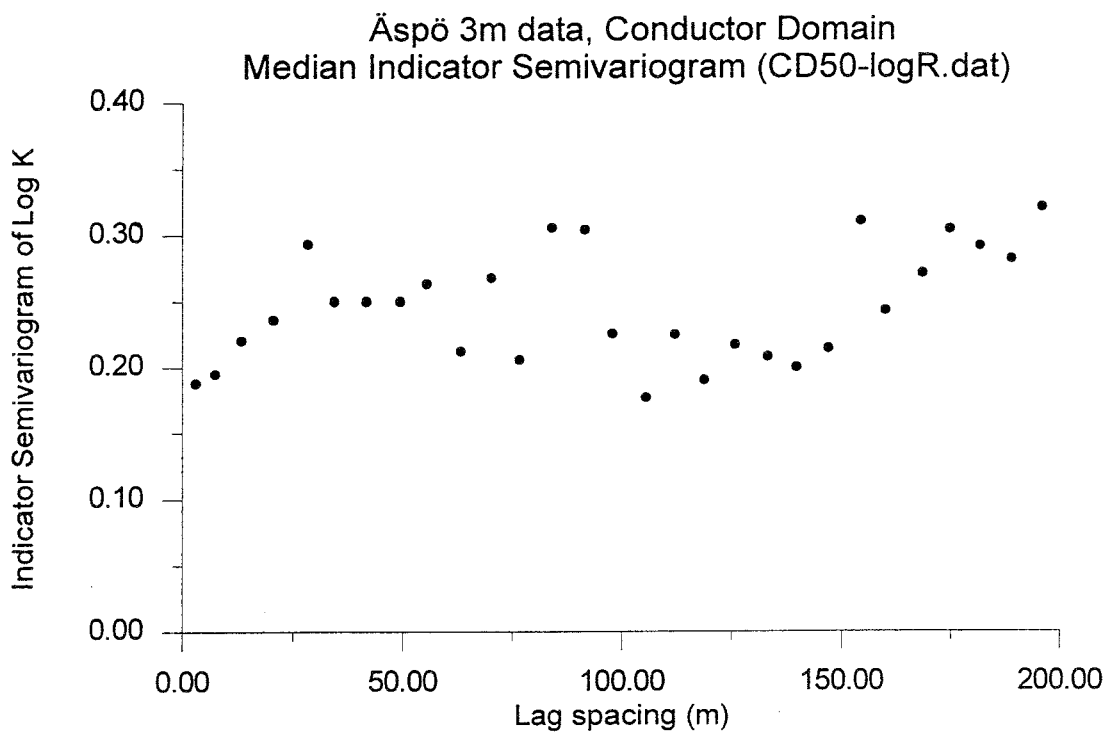
Figure A-9. *Median Indicator variogram Aberg hydraulic conductivity from 3m packer test in conductor domain (CD).*

A.3.2 Variography and Trends

The variography begins by using INFERENS to fit a variogram with and without trends for the 3m RD data. The purpose of this step is to determine the basic structure of the 3m RD data without the complications of upscaling/regularisation. Figure A-10 presents the experimental variogram and INFERENS-fitted exponential model for the 3m data without trends. Figure A-11 presents a similar result for the same analysis but using the SRD trends. The fitted set of SRD trends includes only SRD1, SRD2, SRD3, and a background value. This is because no 3m data is available for SRD4, and SRD5 is defined by tunnel observations of fine-grained granites. These SRD means must be taken directly from Rhén et al. (1997). As expected, including the trends decreases the practical range and the total variance $(C0 + C1)$.

The fitting is repeated using the data regularised to 24m, the proposed HYDRASTAR grid resolution (Hans Widén, personal communication, 1997) to estimate the possible effects of upscaling. The resulting experimental and model variograms are shown in Figure A-12. The obvious change is the effect on the experimental variogram at lag classes less than regularisation scale (24m). The total variance of the fitted model decreases slightly, but the practical range changes little in comparison to the 3m case (Figure A-11).

The more noticeable change for the three fitted models is in the fitted trends. Table A-5 summarises the INFERENS-fitted parameters for these models for comparison. It includes the SRD means for the 3m data from Rhén et al. (1997) and the upscaled means. Note that the Äspö 24m upscaling results in approximately the same contrasts as in INFERENS 24m upscaling, but approximately ½ order of magnitude lower. (i.e., INFERENS yields higher hydraulic conductivities). The suggested geostatistical model for Aberg is the model shown in bold in Table A-5, with the SCD values of Table A-4 scaled to 24m via the Äspö regression relationships.

Uncertainties:

The lognormal distributional assumption for this data is not well supported, and suggests that an alternative approach be used (e.g., other data transforms or nonparametric methods). Because this assumption may result in underestimating the variance, an alternative model with a higher sill (i.e., a higher variance) could be used for sensitivity analysis. The effect of the INFERENS upscaling algorithm for lag classes less than the regularisation scale is not well understood. An alternative variogram model with a nonzero nugget might be fitted to the estimates using lag classes greater than the regularisation scale

Äspö 3m data, INFERENS fit
No SRD trends (Anot.dat)
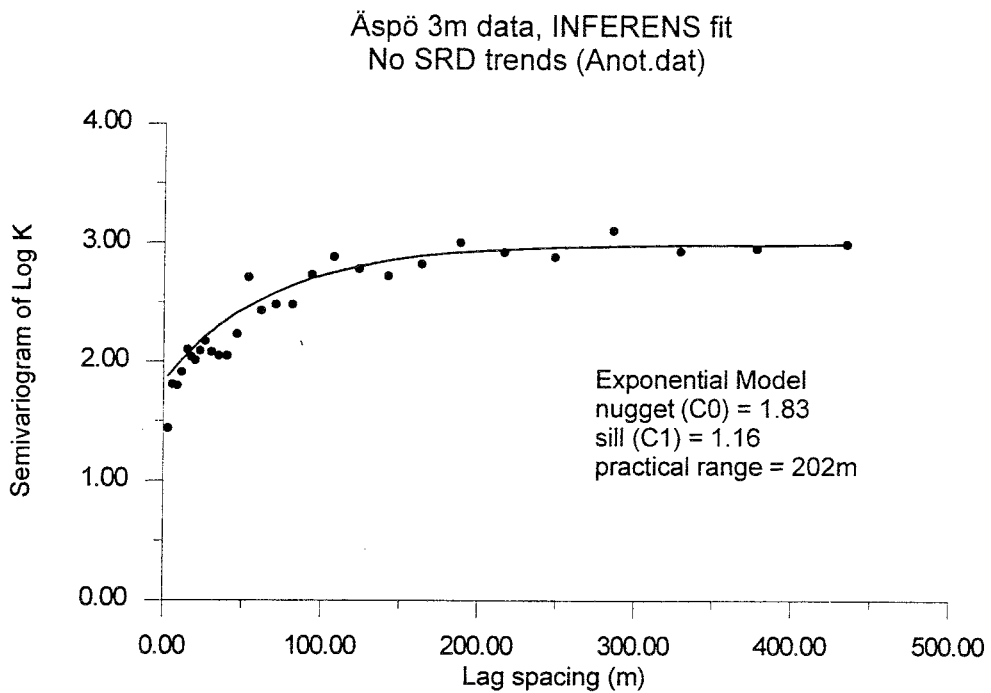
Figure A-10. Variogram for Aberg hydraulic conductivity from 3m packer test in rock domain (RD). No trends or regularisation.

Äspö 3m data, INFERENS fit
Constant SRD + background (Atrn2)
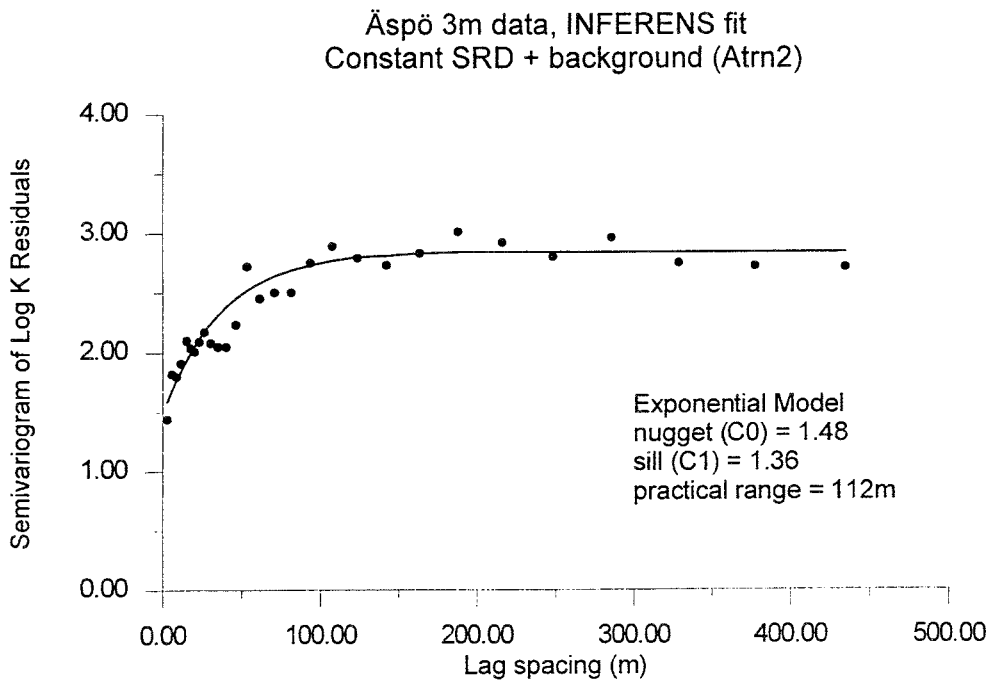
Figure A-11. Variogram for Aberg hydraulic conductivity from 3m packer test in rock domain (RD). With SRD trends, no regularisation .

A-16
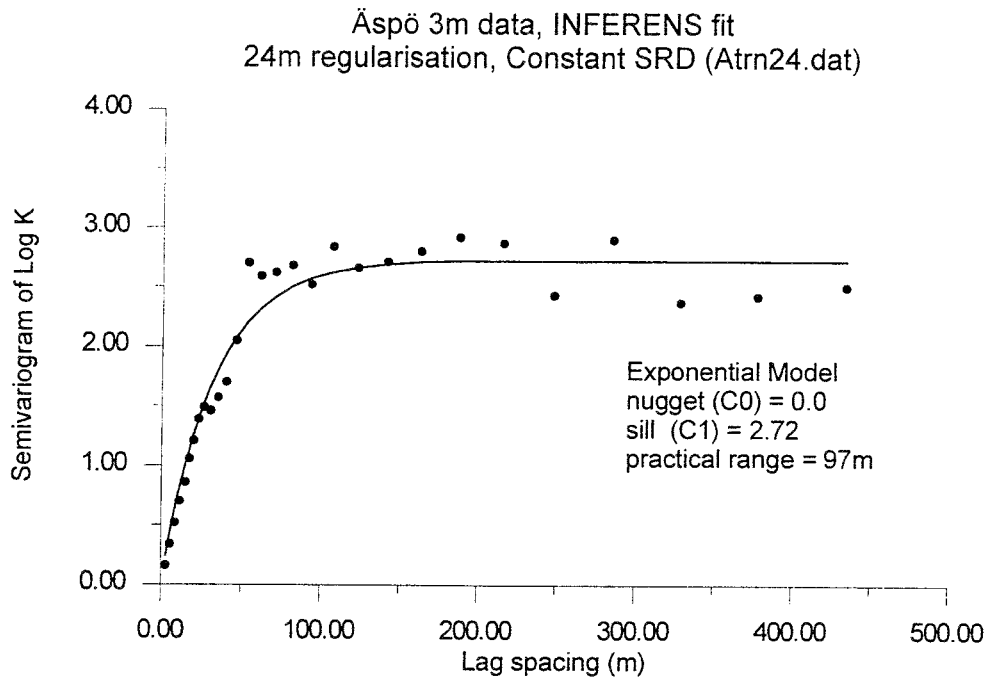
Figure A-12. *Variogram for Äspö hydraulic conductivity from 3m packer test in rock domain (RD). With SRD trends and regularisation to 24m.*

Table A-5. **Variography results for Aberg rock domain hydraulic conductivity. Exponential variogram model for all fitted models. Suggested Aberg model in bold.**

Parameter			INFERENS		
Arithm. Mean of $Log_{10}K$	3m data	Äspö upscaling to 24m	3m, No SRD	3m, SRD	24m, SRD
SRD1	-8.74	**-8.03**	-	-8.87	-7.49
SRD2	-7.82	**-7.11**	-	-8.34	-6.48
SRD3	-9.47	**-8.76**	-	-9.34	-7.98
Background*	-9.26	**-8.56**	-9.26	-9.52	-8.38
Nugget C_0	-	-	1.83	1.48	**0.0**
Sill C_1	-	-	1.16	1.36	**2.72**
Practical Range (m)	-	-	202	112	**97**

* all 3m data in SRD1, 2 and 3.

A.4 SITE-SCALE CONDUCTOR DOMAIN COORDINATES

From Rhén et al. (1997).

Table A2-4. Location of hydraulic conductors. The hydraulic conductors are in this table approximated to planes. Assumed extension of each plane is discussed in *Table A5-5*. Coordinates for zones are given in the local Äspö-system. w = water bearing structure. p = predicted structure */Wikberg et al, 1991/*. r = revised structure */Stanfors et al, 1994/*. n= new structure.

Zone		X-coordinate (m)	Y-coordinate (m)	Z (masl)
EW-1$_r$	88°SE	7482.0	1811.5	0
		7698.3	2197.1	0
		7575.4	2000.0	-327.4
EW-1$_r$	78°SE	7433.6	1838.7	0
		7649.8	2224.3	0
		7500.0	2110.9	-369.5
EW-3$_r$	79°S	7093.0	2047.7	0
		7143.1	2289.2	0
		7010.0	2166.5	-542.2
EW-7$_r$	81°SE	6418.9	2023.7	0
		6504.7	2343.8	0
		6428.2	2200.0	-231.8
NE-1$_r$	70°NW	6807.6	1967.2	0
		7005.9	2350.7	0
		7135.2	2054.6	-689.1
NE-1$_r$	75°NW	6807.6	1967.2	0
		7005.9	2350.7	0
		7081.0	2082.6	-708.4
NE-2$_r$	77°SE	7038.5	1829.9	0
		7540.7	2194.8	0
		7250.0	2083.3	-349.4
NE-3$_r$	80°NW	6495.5	1984.3	0
		6650.7	2253.1	0
		6610.0	2094.7	-233.2
NE-3$_r$	70°NW	6499.7	1983.1	0
		6654.9	2251.9	0
		6650.0	2076.0	-221.9
NE-4$_r$	71°SE	6443.0	2016.6	0
		6569.3	2300.2	0
		6440.0	2197.9	-224.5
NE-4$_r$	78°SE	6448.8	2010.3	0
		6596.9	2283.1	0
		6480.0	2169.6	-232.2
NW-1$_{wp}$	30°NE	7882.0	1257.6	0
		7510.3	1600.0	0
		7934.5	1790.0	-246.6
NNW-1$_{wp}$	(vertical)	7538.9	2039.4	
		7151.9	2218.6	

Table A2-4. continued

Zone		X-coordinate (m)	Y-coordinate (m)	Z (masl)
NNW-2$_{wr}$	(vertical)	7484.1	2134.6	
		7106.1	2300.2	
NNW-3$_{wp}$	(vertical)	7025.4	2143.6	
		6812.9	2136.9	
NNW-4$_{wr}$	85°NE	7391.8	2275.3	0
		7184.0	2301.7	0
		7300.0	2325.5	-436.7
NNW-5$_{wp}$	(vertical)	7394.1	1962.8	
		6421.1	2020.8	
NNW-6$_{wp}$	(vertical)	7058.1	2298.7	
		6529.1	2373.7	
NNW-7$_{wn}$	85°NE	7492.2	1967.6	0
		7129.2	2135.7	0
		7299.3	2074.7	-185
NNW-8$_{wn}$	(vertical)	8060	1540	-300
		7570	2030	-300
		8060	1540	-700
		7570	2030	-700

A.5 SICADA LOGS FOR ÄSPÖ SITE DATA

A.5.1 For coordinates and previous interpreted K values

Date: 970324 18:02:21

Table(s): transient_inj_cd

Columns :transient_inj_cd.idcode, transient_inj_cd.start_date, transient_inj_cd.stop_date, transient_inj_cd.seclen, transient_inj_cd.secup, transient_inj_cd.bc, transient_inj_cd.k_steady_state, transient_inj_cd.k_injection, transient_inj_cd.k_fall_off, transient_inj_cd.k_jacob, transient_inj_cd.k_prel, transient_inj_cd.k, transient_inj_cd.skinfactor_i, transient_inj_cd.skinfactor_t, transient_inj_cd.spec_cap, transient_inj_cd.goodness, transient_inj_cd.test_date, transient_inj_cd.comment

New Columns: midpoint

Condition: Expr=secup+(seclow-secup)/2

Criteria: (transient_inj_cd.idcode ='KAS02' OR

transient_inj_cd.idcode ='KAS03' OR transient_inj_cd.idcode ='KAS04' OR

transient_inj_cd.idcode ='KAS05' OR transient_inj_cd.idcode ='KAS06' OR

transient_inj_cd.idcode ='KAS07' OR transient_inj_cd.idcode ='KAS08' OR

transient_inj_cd.idcode ='KLX01') AND transient_inj_cd.seclen =3

Result: 1300 rows written

Filename: trans_1.csv

Fileformat: CSV

Coordinate system: Local

Coordinate calculation column: midpoint

A.5.2 For rock/conductor codes and Rhén K values

Date   :970324 18:05:05

Tables :sic_dba.transient_inj_cd

Columns :transient_inj_cd.idcode, transient_inj_cd.start_date, transient_inj_cd.stop_date, transient_inj_cd.seclen, transient_inj_cd.secup,   transient_inj_cd.bc,   transient_inj_cd.k_steady_state,   transient_inj_cd.k_injection, transient_inj_cd.k_fall_off,   transient_inj_cd.k_jacob,   transient_inj_cd.k_prel,   transient_inj_cd.k, transient_inj_cd.skinfactor_i, transient_inj_cd.skinfactor_t, transient_inj_cd.spec_cap, transient_inj_cd.goodness, transient_inj_cd.test_date, transient_inj_cd.comment

New Columns: midpoint

Condition: Expr=secup+(seclow-secup)/2

Criteria: (transient_inj_cd.idcode ='KAS02' OR

transient_inj_cd.idcode ='KAS03' OR transient_inj_cd.idcode ='KAS04' OR

transient_inj_cd.idcode ='KAS05' OR transient_inj_cd.idcode ='KAS06' OR

transient_inj_cd.idcode ='KAS07' OR transient_inj_cd.idcode ='KAS08' OR

transient_inj_cd.idcode ='KLX01') AND transient_inj_cd.seclen =3

Result: 1300 rows written

Filename: trans_r.csv

Fileformat: CSV

Coordinate system: RT

Coordinate calculation column: midpoint

Output to: File

Date   :970606 15:31:46

Table(s) :sic_dba.zone_model96

Columns :zone_model96.site, zone_model96.idcode,

zone_model96.borehole, zone_model96.sub_secup,

zone_model96.sub_seclow,

zone_model96.zone_name, zone_model96.rocktype,

zone_model96.k,

zone_model96.k_source, zone_model96.qc_ok,

Criteria :1=1

Result   : 1300 rows written to file.

Filename   : /home/skbee/rhen_k.csv

File format : csv

A.6 ABERG PARAMETER SOURCES

	Source	Treatment	Availability
REGIONAL			
Geology			
Rock type	SKB TR 97-06 SKB TR 91-22	Compilation	(1)
Lineaments	SKB TR 97-06	Compilation	(1)
Land rise	SKB TR 92-38	Interpolation	(1)
Geochemistry and Salinity	Laaksoharju et al. 1997 (SKB R 97-X)	Compilation	(1)
Hydrology			
Recharge pattern and rates	SKB PR 25-87-09 SKB TR 97-06	Compilation	(1)
Groundwater flow patterns	SKB PR 25-91-03	Compilation	(1)
Hydraulic Parameters			
Rock Mass K	SGU 1996 SKB TR 97-06	Compilation, rescaling	(1)
Conductor Location, K	SKB TR 97-06	Compilation, rescaling	(1)
Anisotropy	SKB TR 97-06	Compilation	(1)
Scale relationships	SKB TR 97-06	Compilation	(1)
Stochastic Param.	SKB TR 97-06	Compilation	(1)
SITE			
Geology	SKB TR 97-06 SKB TR 91-22	Compilation	(1)
Hydrology			
Surface Hydrology	SKB PR 25-87-09 SKB TR 97-06	Compilation	(1)
Groundwater Flow Patterns	SKB PR 25-91-03	Compilation	(1)
Hydraulic properties			
Rock Mass K	SICADA 1997 SKB TR 97-06, Svensson, 1997 (personal communication)	Compilation, rescaling	SICADA
Conductor Location, K	SICADA 1997 SKB TR 97-06	Compilation, rescaling	SICADA Appendix A
EDZ	SKB ICR 96-03, Olsson and Winberg, 1997 (unpublished SKB PM)	Compilation	(1)
Anisotropy	SICADA 1997 SKB TR 97-06	Compilation	(1)
Geostatistics, Scale relationships	SICADA 1997 SKB TR 97-06	Variography, Universal Kriging on 3m data, rescaling	(1)

(1) See the source report

A-21

APPENDIX B. BEBERG

B.1 ANALYSIS OF SGU DATA IN FINNSJÖN REGION

Swedish Geological survey (SGU) provided well data from the SGU well archive for wells in the Finnsjön area, loosely defined as a 25 km radius around the Lake Finnsjön. As discussed in Appendix D.1, it is possible to estimate a well's specific capacity, Q/dh, and use the Äspö regression of T versus Q/dh (Rhén, et al., 1997) to determine the approximate hydraulic conductivities represented by the SGU data.

Axelsson et al. (1991) examined SGU well data in the immediate area of Finnsjön and found it to be statistically similar to the 3m data from the upper 100m of the Southern rock block. However, their study involved only a small data set (15 SGU wells) and did not examine spatial correlation. This study reanalysed the SGU well data, as described in the following sections. Note that the depth dependence of hydraulic conductivity is inferred from the on-site packer test data, as discussed in section B.2.1.

B.1.1 Selecting a uniform subset of the data

The initial set of SGU data consisted of 414 wells within 25km radius of Finnsjön (Figure 4-15), but not all the data is considered valid. 18 wells had reported water capacities of 0 litres/hr. Since this was a relatively small censored proportion, these were simply discarded. Two more observations were discarded when preliminary variogram analysis indicated them as being extreme relative to neighbouring wells. As described in Appendix D.2, a consistent subset of the data was selected, resulting in a data set with the following characteristics:

- 192 measurements

- Arithmetic Mean of $Log_{10}K$ (m/s): -6.948

- Median of $Log_{10}K$: -6.950

- Variance of $Log_{10}K$: 0.268

- Median Depth: 67 m

The univariate histogram of the $Log_{10}K$ data is slightly skewed about the mean (Fig B-1), suggesting a weakly normal probability distribution.

B.1.2 Regional lineaments and clustering

Although the data is spatially clustered in communities, this does not necessarily indicate that they are preferentially clustered in areas of high hydraulic conductivity. If the data were preferentially clustered, this would bias the estimates of the global mean and possibly the variance of the data.
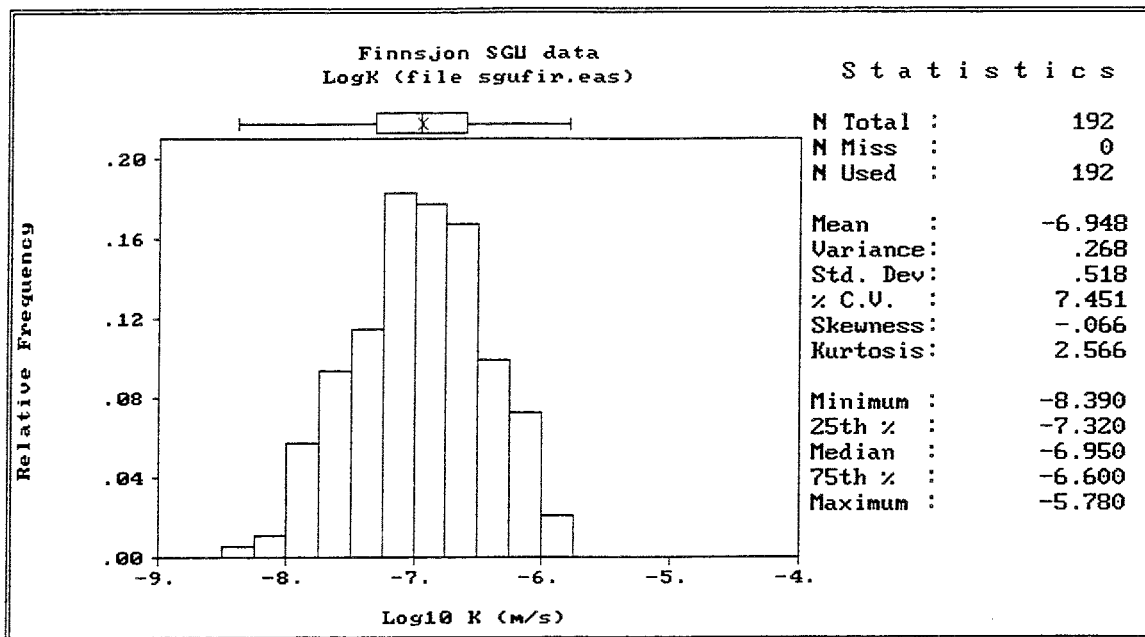
Figure B-1. Histogram of SGU data in the Beberg region.

Two simple calculations are performed to evaluate the possibility of clustering and consequent bias. The first is to use the regional lineaments to identify those wells which were in or near fracture zones, and compare the resulting subpopulations (similar to Ericsson and Ronge, 1986). Several sorting patterns were tested, using lineament widths from 50 to 200m and several lineament orientations. In general, none of the subpopulations associated with lineaments were showed an increased hydraulic conductivity; some even had decreased mean hydraulic conductivity relative to the global mean. That is, separating the data in or near lineaments had no apparent effect. Therefore the data was considered to be a single population of hydraulic conductivity measurements from the rock mass domain. This is also consistent with conclusions drawn from the SGU data at the Äspö site (Rhén et al., 1997).

The second calculation was to apply a cell declustering algorithm (Deutsch, 1989) to see if the any cell size would reduce or increase the global mean. The algorithm does indicate that a cell size of approximately 700m would maximise the mean Log_{10} K to -6.932, but this is little different than the untreated mean of -6.948 (Figure B-2). The data may be clustered, but its effect is minimal enough to be neglected.
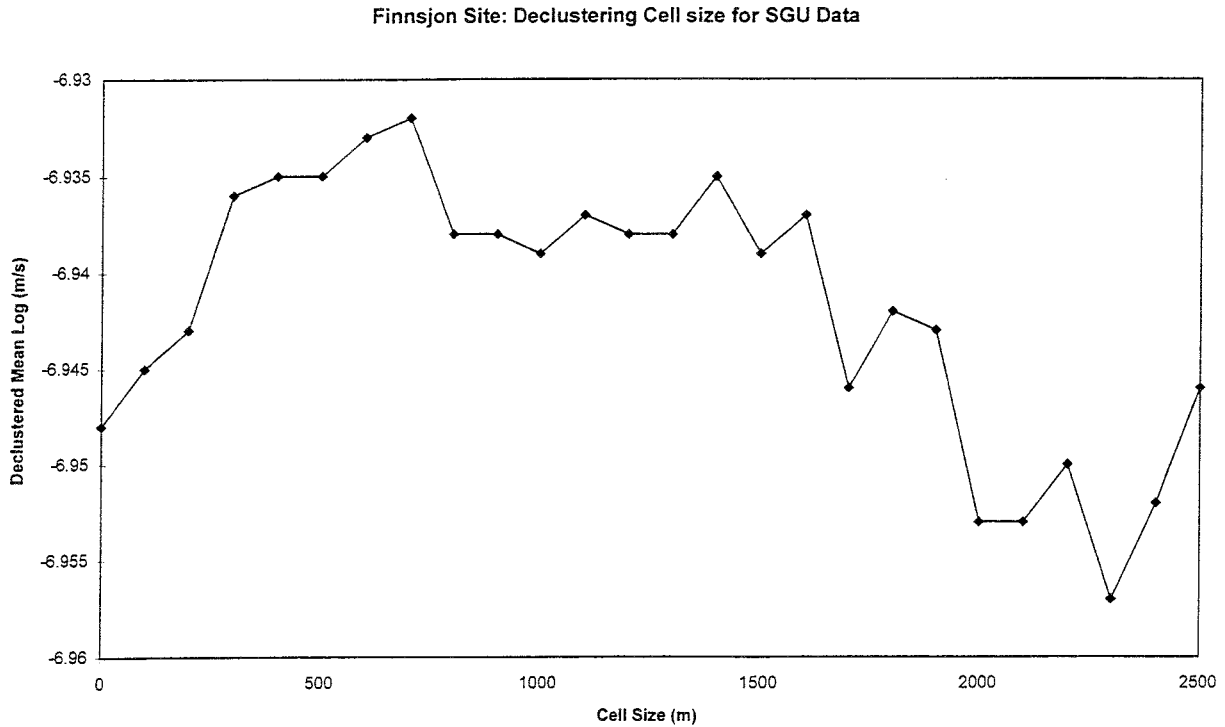
Figure B-2. Declustering cell size versus declustered mean of SGU data for Beberg.

B.1.3 Analysis of Spatial Correlation

In an attempt to infer a model of spatial correlation for the SGU data, several geostatistical software packages were used (Appendix D.3). This involved calculating the experimental semivariogram of the SGU data using several lag intervals and a maximum lag interval of approximately 10 km. This was repeated using the traditional semivariogram estimator and several robust estimators for the isotropic and anisotropic models. Three possible models were found:

1. Isotropic, low sill: $\gamma(h) = 0.144 + 0.131 \, Sph(2279)$

2. Isotropic, low sill: $\gamma(h) = 0.144 + 0.195 \, Sph(3300)$

3. Isotropic, low nugget: $\gamma(h) = 0.100 + 0.170 \, Exp(2200)$

All three of these models were cross validated using Ordinary and Simple kriging with various neighbourhood search criteria. Model 1 (above and Figure B-3) was found to be the most appropriate for the observed data (having the lowest crossvalidation error of KRMSE = 0.512), using simple kriging with mean = -6.948, an octant search over the entire domain, and 8 observations maximum.

However, a plot of observed value versus estimated value (Figure B-4) indicates that the quality of the estimation is very poor. This is reflected in the crossvalidation error that is only 1.2% lower than the sample standard

B-3

deviation, indicating that the kriged estimates are little better than using the mean of the data. This can be explained in part by the relatively high nugget (over 40% of the total variance) which indicates that the spatial correlation is relatively weak.

We can therefore conclude that, although the hydraulic conductivities of the SGU wells may be spatially correlated, including spatial correlation has little effect on the estimation.

B.2 FINNSJÖN PACKER TEST DATA

Packer test data for the site was taken from the SKB SICADA database and consisted of the hydraulic conductivity versus the RAK X, Y coordinates, and the elevation of the centre of each test section. Several scales of packer test data are available at this site, but the 3m data are the exhaustive set and are the basis of the following analysis. Table B.1 summarises the boreholes used in this study and their measurement limits. The measurements of KFI02 were not used because their measurement limit was much higher than comparable data in the other holes. It should be noted that many of the measurements are reported as being below a measurement limit of $K = 1.9 \times 10^{-10}$ m/s (i.e., $Log_{10}K = -9.72$). Preliminary analysis of the entire data set indicates that approximately 10% of the data are below this measurement limit, requiring corrections for the estimates of the means and variances (Figure B-5; Appendix D.4).

Finnsjon Site SGU data
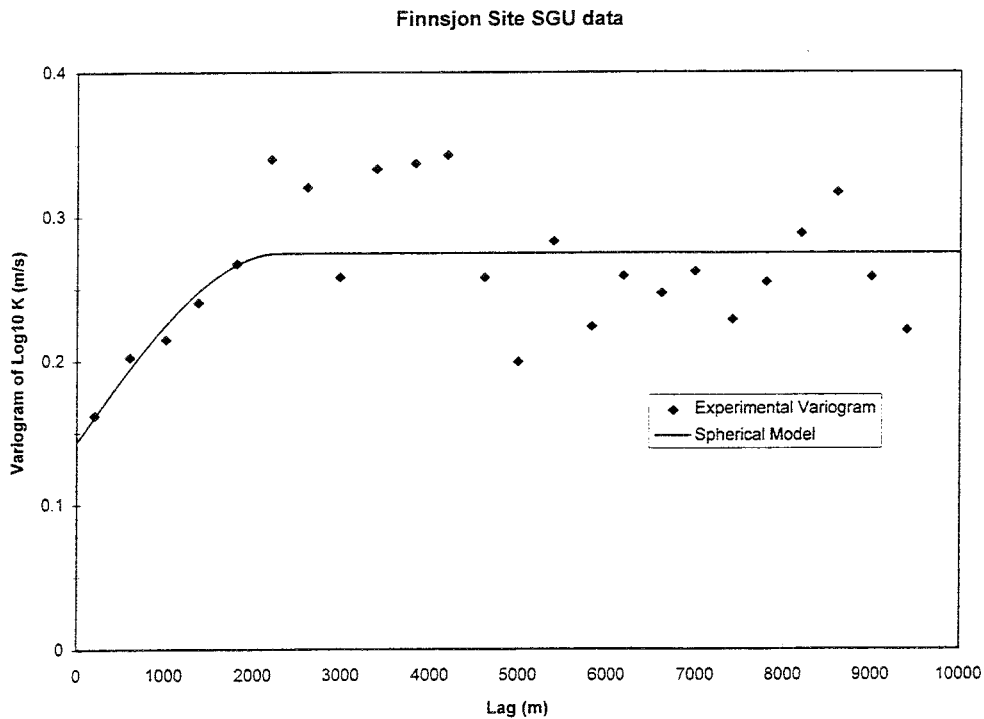
Figure B-3. Semivariogram for Log_{10} K from SGU data in Beberg region.

B-4
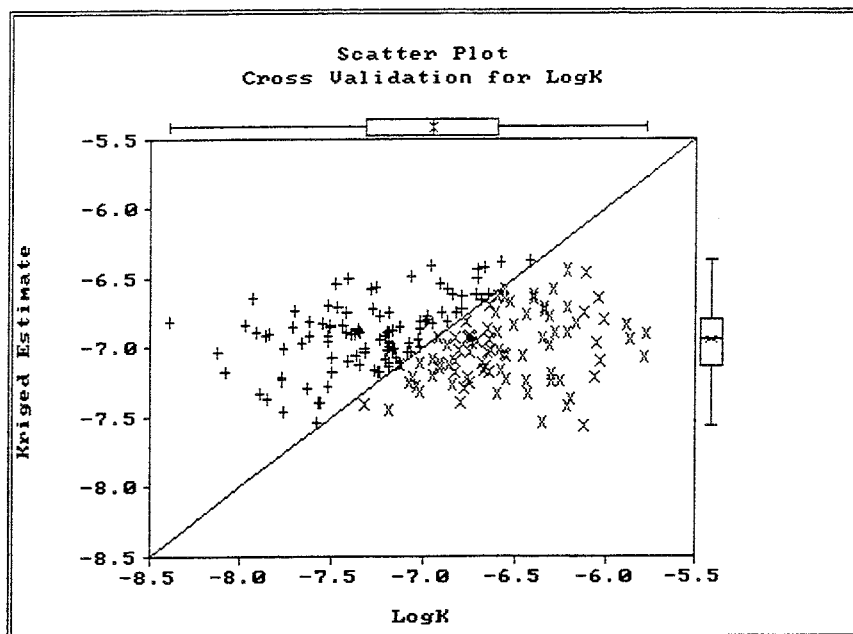
Figure B-4. *Crossvalidation results, kriged versus observed SGU log₁₀K in Beberg region.*

Table B-1. Finnsjön 3m data.

Borehole	Meas. Limit on K (m/s)
KFI03	3.3 E-10
KFI04	1.9 E-10
KFI05	1.9 E-10
KFI06	1.9 E-10
KFI07	1.9 E-10
KFI08	1.9 E-10

Figure B-6 shows the univariate histogram of all the 3m data. Based on the revised site structural model and designated fracture zone contacts (Andersson et al., 1991, Table 4.3) the 3m packer test data was separated into set of fracture zone data and a set of rock mass data. The following sections discuss the univariate statistics for each of those subsets.
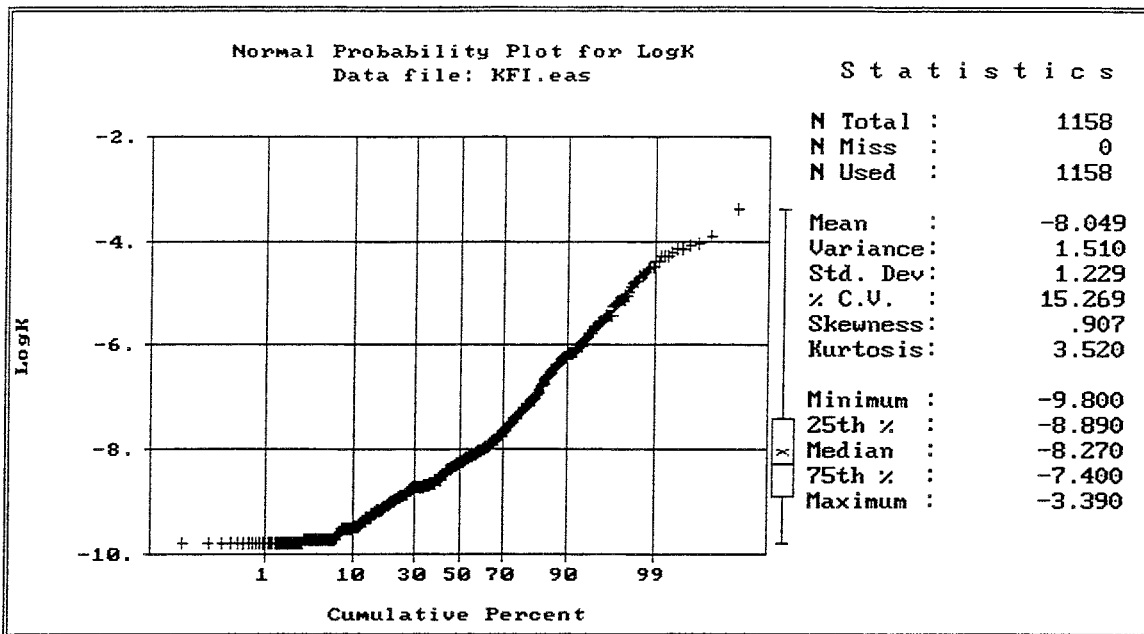
Figure B-5. *Lognormal probability plot for Finnsjön interpreted hydraulic conductivities from 3m packer test.*
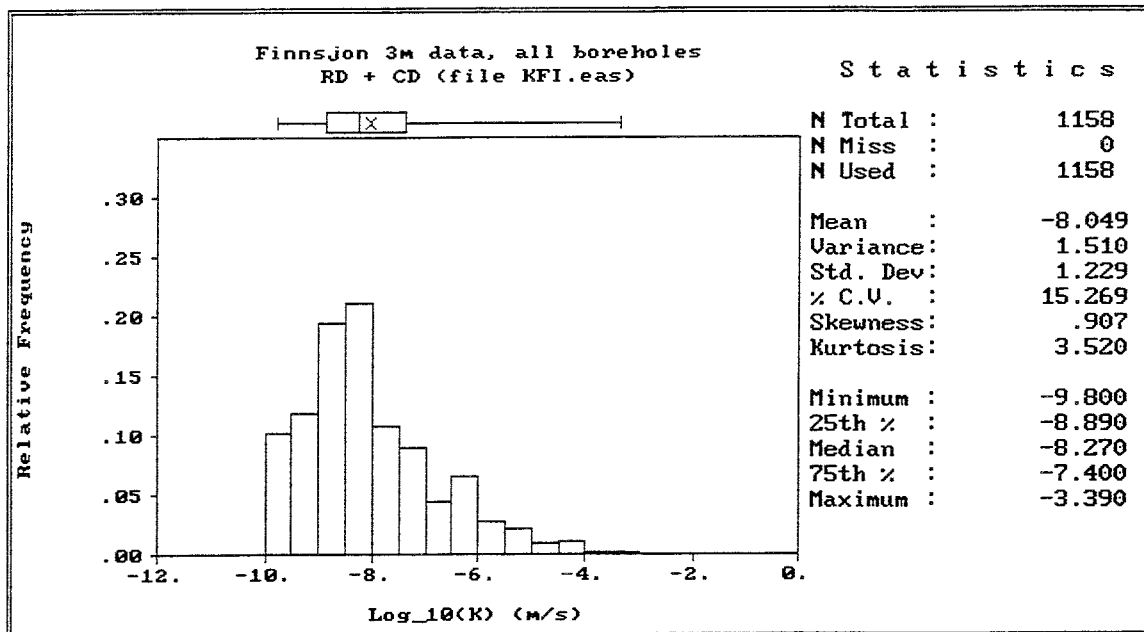
Figure B-6. *Histogram of Finnsjön interpreted Log₁₀ hydraulic conductivities from 3m packer test.*

B.2.1 Rock Mass Domain

The Finnsjön site 3m packer test hydraulic conductivities corresponding to the Rock mass domain (SRD1) have been previously analysed in several studies (Andersson et al., 1991; Winberg, 1989; Cvetkovic and Kung, Norman, 1992; Wen, 1994; Carlsson and Gidlund 1983). Although several authors have commented on the strong depth dependence of this data, attempts to regress models of hydraulic conductivity versus depth have been confounded by the measurement limits. Rather than regressing a continuous model of depth dependence, this study adopts a simpler depth zonation approach (Ahlbolm et al. 1983; Rhén, 1997). This study divides the data into elevation zones and determines the mean and variance of the packer tests falling into each elevation zone. These estimates are corrected for the measuring limit using the method of Wen (1994; Appendix D.4).

The statistics of these zones are relatively insensitive to the choice of intervals. The elevation zones are somewhat subjective, but can be delineated based on changes in the means and variances. These are:

above -100 masl: corresponds to the SGU data and has a relatively high variance.

-100 to -200 masl: begins at a large decrease in variance and ends just above another decrease in variance

-200 to -400 masl: relatively constant mean and variance, increased censoring; ends just above a decrease in variance.

below -400m masl: below the change in variance.

The means and variances for the hydraulic conductivities in these zones are presented in Table B-2. These elevation zones are determined using the 3m test data and will require scaling using the Äspö scaling regression equations when used at larger grid scale.

Table B-2. Beberg rock mass domain hydraulic conductivity values from 3m packer test data.

Elevation (masl)	Arith. Mean $\mathrm{Log_{10}}$ K(m/s)*	Variance $\mathrm{Log_{10}}$ K(m/s)*	Number of Samples	Censoring level (%)
above -100	-7.41	1.91	142	7.2
-100 to -200	-8.28	1.37	119	11
-200 to -400	-8.67	0.881	325	16
Below -400	-8.41	0.385	265	8.7

* corrected assuming normally distributed data, after Wen (1994)

It is interesting to compare the upper zone of the 3m data with the SGU data to check for consistency in concept RRD1. If these upper zone of Table B-2 is upscaled to approximately 67m (median borehole length of the SGU data), we can compare the upscaled on-site data to the SGU data:

above -100 masl: Mean LogK = -6.36, standard deviation = 0.564

SGU data: Mean LogK = -6. 95, standard deviation = 0.518

Although not an exact match, the upscaled 3m data and SGU data are at least similar. At Äspö the large-scale tests for the elevations above -100 masl were used to determine the pooled mean and variance, but there are no such large-scale tests in this elevation zone at Finnsjön. Axelsson et al. (1991) observed similar differences between the SGU well data and the on site data. They noted that the Northern Rock Block had an order of magnitude higher hydraulic conductivity than the Southern rock block. This would result in approximately one-half an order of magnitude increase in the site-wide mean of the 3m packer test data. They concluded that the Southern rock block was more representative of the region as a whole, as represented by the SGU data. It therefore seems reasonable to use the geometric mean of the SGU data for the upper zone in RRD1, with depth dependence described by the relative changes in the onsite data given in Table B-2.

No separation of the rock mass domain is made on the basis of rock type, as the rock is essentially all one type (Andersson et al., 1991).

B.2.2 Fracture Zone Domain

The hydraulic conductivities for the fracture zones are inferred from the interpreted hydraulic conductivities for the 222 3m packer corresponding to the mapped fracture zones. This inference provides hydraulic conductivities for both the site-scale and regional scale models for the conductor domains (SCD1 and RRD1). Figure B-7 presents the histogram of these data, which have the following statistics, corrected using the method of Wen (Appendix D.4):

Arithmetic Mean $Log_{10}K$ (m/s) = -7.13, variance = 2.62

As with the rock domain data, the data are divided into elevation zones for the conductor domain as shown in Table B.3. Note that there is no trend in the mean with depth, unlike the rock domain hydraulic conductivity. Therefore, no trend with depth is suggested for the base-case models SCD1 and RCD1 of Beberg.

Unlike Gideå, the fracture zones of Finnsjön have been thoroughly investigated and several of the regional scale conductive fracture domains cross the site. Additional information is provided by the SFR site characterisation studies. Andersen, et al. (1991) and Tirén (1992) have inferred the properties of the remaining lineaments based on orientation and similarity to other lineaments in the region. Table B-4 summarises the properties of these lineaments.
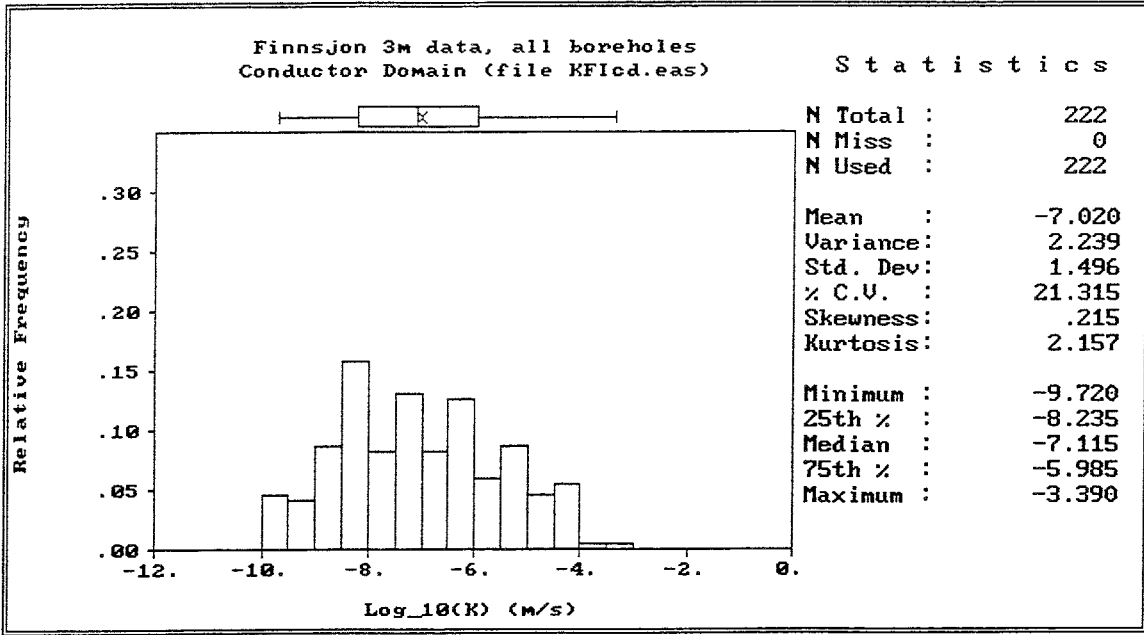
Figure B-7. Histogram for conductor domain (CD), Beberg interpreted Log_{10} hydraulic conductivities from 3m packer tests.

Table B-3. Beberg conductor domain hydraulic conductivity values from 3m packer test data.

Elevation (masl)	Arith. Mean Log_{10} K(m/s)*	Variance Log_{10} K(m/s)*	Number of Samples
above -100	-7.14	2.10	70
-100 to -200	-7-18	3.39	94
-200 to -400	-6.87	1.82	55
Below -400	-8.30	-	3

* corrected assuming normally distributed data, after Wen (1994)

Table B-4. Properties of Beberg Lineaments, based on 3m packer tests.

Zone	Inferred from	Dip	Width	Median Log K (m/s)	Variance Log K	Sample Size
1*	2 boreholes	75SE	20	-5.66	0.945	14
2**	9 boreholes	16SW	100	-6.34	2.72	82
3	1 borehole	80SW	50	-6.82	1.64	37
4	zone 5	60SW	10	-6.35	1.11	15
5	3 boreholes	60SW	5	-6.35	1.11	15
6	1 borehole	60SW	5	-8.39	2.62***	2
7	Ave. 5,6,10	70SW	5	-7.39	1.18	19
8	Ave. 5,6,10	90	5	-7.39	1.18	19
9	1 borehole	15SW	50	-7.94	1.19	18
10	1 borehole	85SW	5	-8.34	2.62***	2
11	4 boreholes	35SW	100	-7.22	1.87	100
12	Singö	90	25	-6.10	2.62***	
13	zone 1	90	20	-5.66	0.945	
14	Singö	90	100	-6.10	2.62***	
Skogbo	zone 5	90	100	-6.35	1.11	15
Giboda	zone 5	90	100	-6.35	1.11	15
Giboda S.	Giboda & 4	90	50	-6.35	1.11	15
Imundbo	zone 5	90	100	-6.35	1.11	15
Gräsbo	Singö	90	100	-6.10	2.62***	
Dannemora	Singö	90	100	-6.10	2.62***	
Källviken	zone 1	90	100	-5.66	0.945	14
Örbyhus	Singö	90	100	-6.10	2.62***	
Sillbö	Singö	90	100	-6.10	2.62***	
NS1	Singö	90	50	-6.10	2.62***	
NS2	Singö	90	25	-6.10	2.62***	
Singö	SFR	90	100	-6.10	2.62***	

*also known as the Brändan fracture zone

**the subject of many interference tests

***variance inferred from all Finnsjön 3m data in CD

Note that for Zone 1, no 3m test data are available to determine a comparable set of statistics. As the next-best alternative, the 2m data of KFI10 are used to infer properties for Zone 1.

The hydraulic conductivities for RCD1 and SCD1 should be upscaled from the statistics given above. As stated above, no trend with depth is indicated, but alternative cases for depth dependence are appropriate for both regional and site-scale.

B.3 GEOSTATISTICAL MODEL

The Beberg site-scale geostatistical model of hydraulic conductivity uses the previously defined divisions of SRD6, SCD1 and the elevation zones. The model is developed with HYDRASTAR in mind, which assumes that hydraulic conductivity has a multivariate lognormal distribution, with the elevation zones, Rock Blocks, and SCD treated as step changes in the mean of Log_{10} conductivities. A single variogram model is assumed for the entire domain (i.e., the same variogram for SRD and SCD). This complex model of trend and spatial correlation is inferred using the iterative generalised least squares estimation (IGLSE) approach to universal kriging suggested by Neuman and Jacobsen (1984). INFERENS is a computer program developed by SKB to automate the IGLSE fitting algorithm (Appendix D.3).

As discussed in Section 1.6.1, the correct approach to the upscaling of hydraulic conductivities is not known. As an interim approach, this study uses the Äspö scaling relationships of Rhén et al. (1997) to determine the geometric mean of hydraulic conductivity in each Rock Block and depth zone (Appendix D.5). The effect of upscaling on the variogram is determined by applying the HYDRASTAR regularisation algorithm and fitting a variogram–trend model to the regularised data via INFERENS. The final model recommendation must be regarded as uncertain and should be evaluated via deterministic sensitivity analysis. The geometric means of K_b require adjustment to insure that the subdomain boundary fluxes are consistent with the regional model boundary fluxes (Section 1.6).

B.3.1 Exploratory Data Analysis

The analysis is based on the interpreted hydraulic conductivities of the 3m packer tests as recorded in the SICADA database. The 3m data is divided into the rock domain (RD) and conductor domain (CD) defined by Andersson et al.(1991, Table 4.3). Exploratory data analysis via several software tools (Appendix D.3) reveals a skewed data distribution for the Log_{10} transform of hydraulic conductivity for both RD and CD data sets (Figures B-7 and B-8). The skewness and the censoring level of approximately 10% suggest that the data is not a promising candidate for a multivariate lognormal simulation method (e.g., the method used in HYDRASTAR). Preliminary variography using the median indicator variogram suggests that the RD data are spatially correlated out to a practical range of approximately 200 to 250m, with a large nugget effect (Figure B-9). A similar median indicator analysis for the CD data shows little spatial correlation structure (Figure B-10).

Finnsjon 3m data, all boreholes
Rock Domain (file KFIrd.eas)

Statistics

N Total :	936
N Miss :	0
N Used :	936
Mean :	-8.293
Variance:	1.029
Std. Dev:	1.014
% C.V. :	12.230
Skewness:	.756
Kurtosis:	3.270
Minimum :	-9.800
25th % :	-9.000
Median :	-8.420
75th % :	-7.820
Maximum :	-4.640
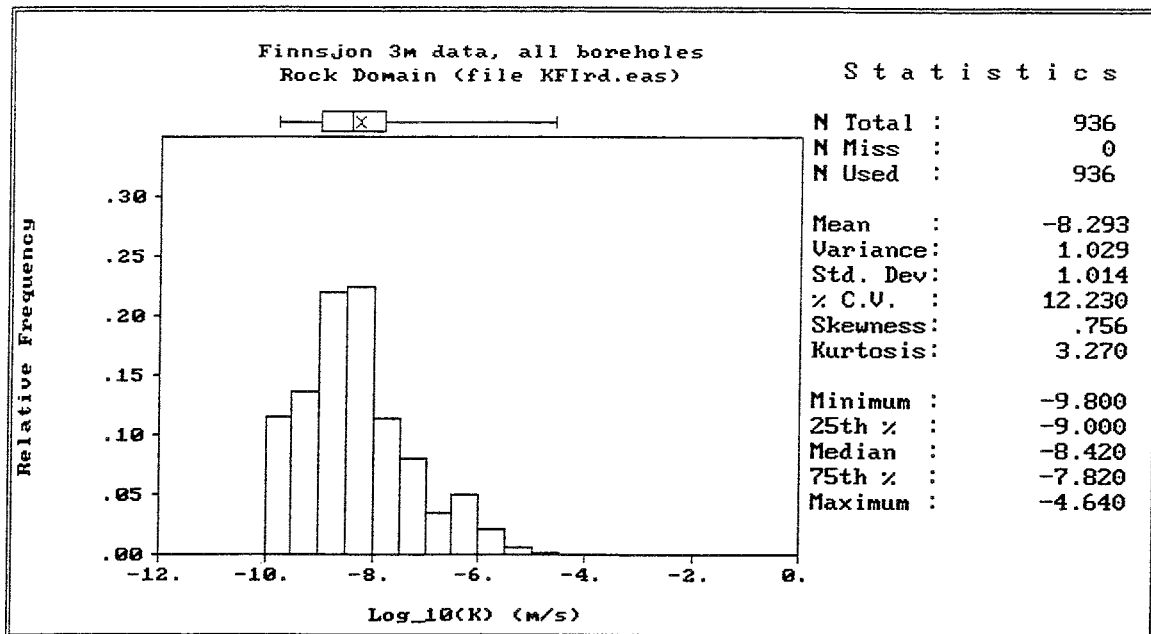
Figure B-8. Histogram of Beberg hydraulic conductivity from 3m packer test in rock domain (RD).
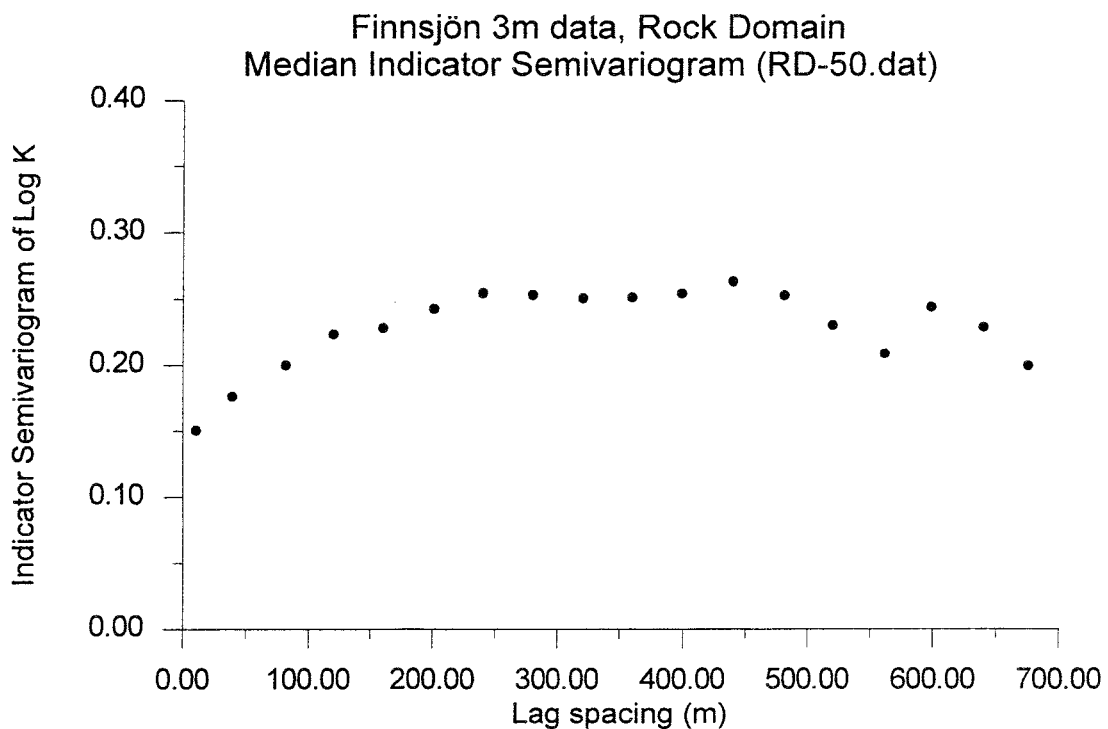
Figure B-9. Median Indicator variogram for Beberg hydraulic conductivity from 3m packer test in rock domain (RD).

B-12
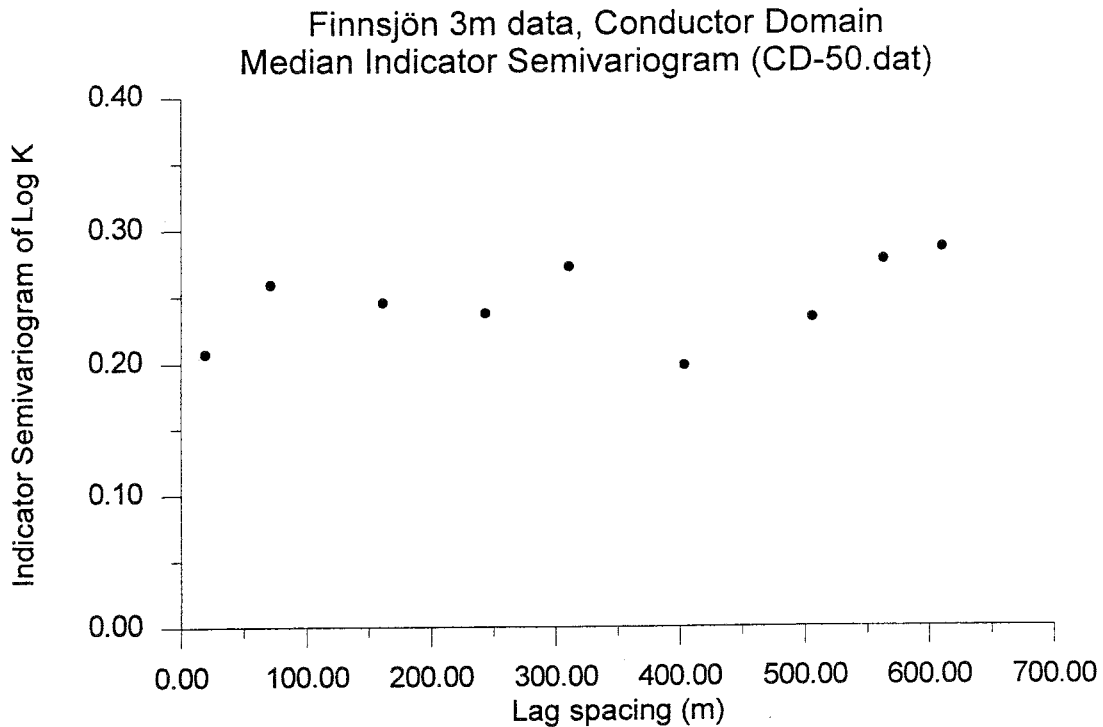
Figure B-10. Median Indicator variogram Beberg hydraulic conductivity from 3m packer test in conductor domain (CD).

The borehole spacing is such that for lag spacing of less than 50m, no cross-hole pairings of data occur. Consequently, the variogram estimates are computed from data pairs along the same boreholes until approximately 100m lag separation. This borehole spacing and the borehole plunge of 60 to 90° (various azimuths) results in the variogram estimate becoming a directional variogram estimate for lags < 50m, in the direction of 60 to 90° plunge. Cross-hole pairs are gradually added for lags > 50m, so that the sill of the variogram is estimated for all directions (Figure B-11, for example). This severely limits attempts at directional variography, and is not pursued farther. The variogram is assumed to be isotropic (see notes concerning anisotropic covariance and anisotropic hydraulic conductivity tensor in Section 1.6). The maximum separation distance between data pairs is approximately 2100 m. By rule of thumb, the maximum fitted lag is therefore 700m.

Program restrictions of HYDRASTAR and INFERENS limit the geostatistical model to one variogram model for both domains. Because the RD data is more abundant and more promising, the geostatistical model will be developed from the RD data.

B.3.2 Variography and Trend

The variography begins by using INFERENS to fit a variogram with and without trends directly to the unscaled 3m data in the Rock Domain (RD). The purpose of this step is to determine the basic structure of the 3m RD data without the complications of upscaling/regularisation. Figure B-11 presents the experimental variogram and INFERENS-fitted exponential model for the 3m data without trends. Figure B-12 presents a similar result for the same analysis but using the SRD6 trends (Northern Block, Southern Block, each with 4 elevation zones). Somewhat unexpectedly, including the trends has little affect on the range and total variance (C0 + C1). This may be a result of the noise in the data, inappropriate trend specifications, incorrect designation of RD vs. CD, the data spacing, or a combination of these factors. For either model, the range of the variogram is nearly the same as the maximum lag fitted, lending little confidence to the assumption of stationarity. Experience suggests a simple alternative is to fit the experimental variogram to lags < 350m, as suggested by the range of the median indicator variogram (Figure B-9). Because the proposed site-scale domains are on the order 1000m side length, the effect of nonstationarity beyond 350m radius will be limited.

The variogram fitting is repeated using the data regularised to 24m, the proposed HYDRASTAR grid resolution (Hans Widén, personal communication, 1997) to estimate the possible effects of upscaling. The resulting experimental and model variograms are shown in Figure B-13. The obvious change is the effect on the experimental variogram at lags approximately on the same scale as the regularisation scale (24m). The total variance and the range of the fitted model decrease, but this is a consequence of fitting only experimental variogram for lags < 350m.

Table B-5 summarises the INFERENS-fitted parameters for these models for comparison. It includes the means for the depth zones from unscaled 3m data, the Äspö upscaled means and the INFERENS upscaled means. Similar to the INFERENS results, the Äspö 24m upscaling results decreasing hydraulic conductivity with depth. However, the hydraulic conductivity of the uppermost depth zone of the INFERENS results are noticeably lower than the Äspö results. The reason for this difference is not known. The suggested geostatistical model for Beberg is the model shown in bold in Table B-5, with the SCD values of Table B-4 scaled to 24m via the Äspö regression relationships.

Finnsjön 3m data, INFERENS fit
No SRD (Bnot1)
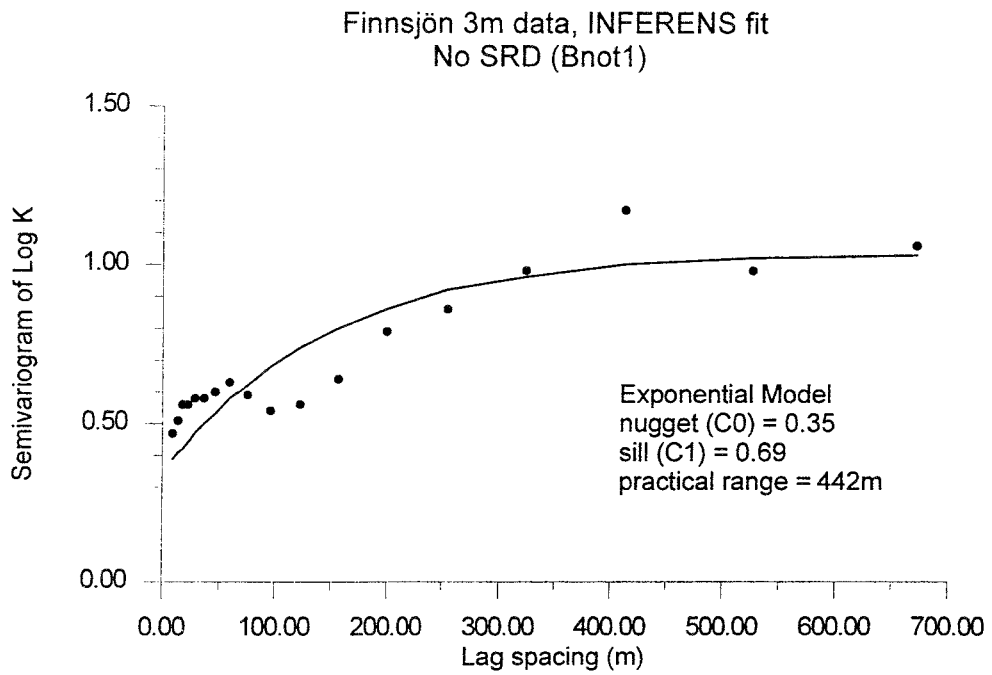
Figure B-11. *Variogram for Beberg hydraulic conductivity from 3m packer test in rock domain (RD). No trends or regularisation.*

Finnsjön 3m data, INFERENS fit
Constant SRD (Btrn1)
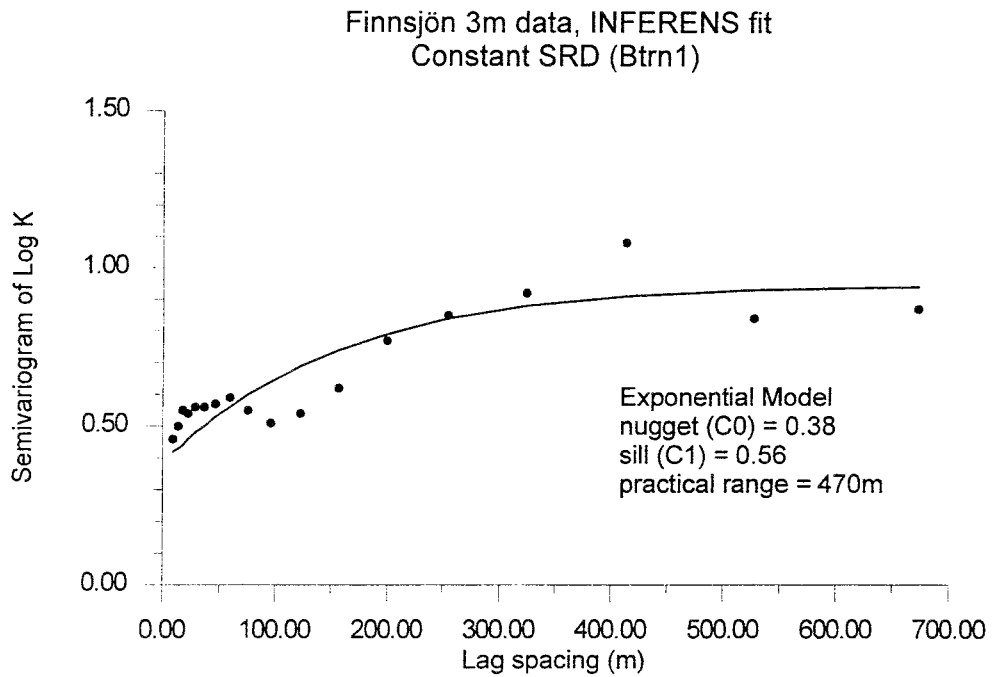
Figure B-12. *Variogram for Beberg hydraulic conductivity from 3m packer test in rock domain (RD). With SRD6 trends, no regularisation.*

B-15
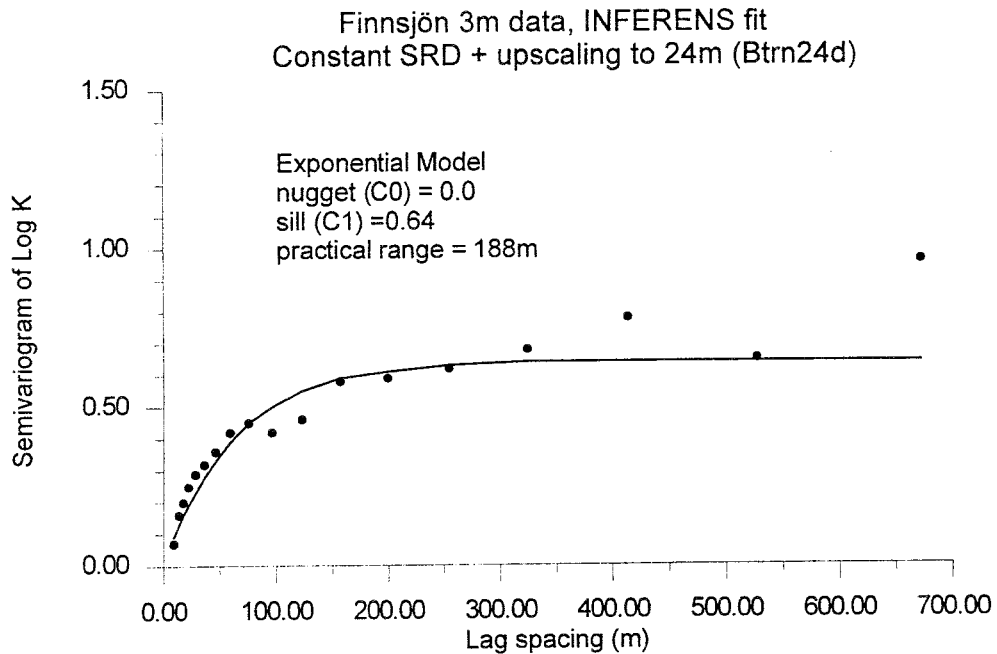
Figure B-13. *Variogram for Beberg hydraulic conductivity from 3m packer test in rock domain (RD). With SRD6 trends and regularisation to 24m.*

As noted in Appendix B.3.1, the 3m data is approximately 10% censored by a lower measurement limit. As well as affecting the mean and variance of the univariate distribution of the data, it will also affect the total variance (C0 + C1) of the experimental variogram estimates. Except for changing over to the Indicator approach to geostatistical analysis and simulation, there is no formal solution for this in the literature. A heuristic correction to the total variance would be to use the same relative corrections as was used for the univariate statistics (i.e., using the method of Wen, 1994; see also Appendix D.4). The Finnsjön 3m data is censored at approximately 10%, which results in a 10% correction of the standard deviation. This suggests that a similar correction to the sill of the variogram is appropriate. This translates (after working through the arithmetic) to a corrected total variance of 0.77.

Uncertainties:

The lognormal distributional assumption for this data is not well-supported, and suggests that an alternative approach be used (e.g., other data transforms or nonparametric methods). This weak assumption and the related corrections for the effects of censoring indicate that the geostatistical model is uncertain.

Table B-5. Variography results for Beberg rock domain hydraulic conductivity. Exponential variogram model for all fitted models. Suggested Beberg model in bold.

Parameter	Mean		INFERENS		
Arithm. Mean of $Log_{10}K$	3m data*	Äspö upscaling to 24m*	3m, No Depth Zones	3m, Depth Zones	24m, Depth Zones
Northern Block					
above -100	-7,35	**-6,64**	-	-7,70	-7,13
-100 to -200	-7,89	**-7,18**	-	-7,24	-7,43
-200 to -400	-8,50	**-7,79**	-	-8,11	-7,74
Below -400	-8,35	**-7,64**	-	-8,30	-7,78
Southern Block					
above -100	-7,50	**-6,79**	-	-7,53	-7,45
-100 to -200	-8,54	**-7,83**	-	-8,81	-7,74
-200 to -400	-8,80	**-8,09**	-	-8,61	-7,81
Below -400	-8,59	**-7,88**	-	-8,50	-7,90
All SRD, All depths	-8,47	-7,76	-8.28	-	-
Nugget C_0	-	-	0,35	0,38	**0,0**
Sill C_1	-	-	0,69	0,56	**0,64 (0.77) ****
Practical Range (m)	-	-	442	470	**188**

* corrected assuming normally distributed data, after Wen (1994)

**see text below regarding censoring and the variogram

B.4 SITE-SCALE CONDUCTOR DOMAIN COORDINATES

Table B-6. From Andersson et al. 1991.

Equations for planar approximations of upper and lower boundaries of fracture zones at the Finnsjön site.

The equations are given in the RAK coordinate system with offset in the point Y = .1600000, X = 6600000

Zone	Surface	Equation
1	Upper	Z = -149499 - 3.109502 * Y + 2.080344 * X
	Lower	Z = -149170 - 3.09981 * Y + 2.074301 * X
2	North	
	Upper	Z = -16684.9 + 0.2494731 * Y + 0.1298738 * X
	Lower	Z = -16828.4 + 0.2501056 * Y + 0.1301766 * X
	South	
	Upper	Z = -16629.3 + 0.2503358 * Y + 0.1303582 * X
	Lower	Not interpreted
3	Upper	Z = -235697.7 + 5.500286 * Y + 1.494558 * X
	Lower	Z = -234712.3 + 5.469382 * Y + 1.486729 * X
4		Z = -124628.9 + 0.8850448 * Y + 1.135518 * X
5		Z = -124149.6 + 0.8846424 * Y + 1.135257 * X
6	West	Z = -152429.4 + 0.9959893 * Y + 1.420884 * X
	East	Z = -162742.2 + 0.7204491 * Y + 1.574787 * X
7	West	Z = -149232.9 + 1.033854 * Y + 1.387761 * X
	East	Z = -155960.5 + 0.9015307 * Y + 1.480179 * X
8		Y = 123628.8 - 1.136259 * X (Vertical)
9	Upper	Z = -7756.7 + 0.2966286 * Y + 0.03280212 * X
	Lower	Z = -9423.1 + 0.2519771 * Y + 0.005668881 * X
10	West	Z = -993202.8 + 6.382012 * Y + 9.291836 * X
	East	Z = -3218997 + 20.24634 * Y + 30.18978 * X
11	Upper	Z = -16416.2 + 0.698822 * Y + 0.04800525 * X
	Lower	Z = -16533.8 + 0.6983383 * Y + 0.04800035 * X
12	East	Y = 25431.5 - 0.109049 * X (Vertical)
	West	Y = 25172.7 - 0.106779 * X (Vertical)
13	Upper	Z = -196108.6 - 2.575001 * Y + 2.556652 * X
	Lower	Z = -197471.8 - 2.587941 * Y + 2.572137 * X
14	Northeast	Y = 80832.3 - 0.689417 * X (Vertical)
	Southwest	Y = 88266.2 - 0.769231 * X (Vertical)

Boundary surface	Equation	
South	X = 93140	(Vertical)
East	Y = 17560	(Vertical)
North	Y = 234140.0 - 2.227273 * X	(Vertical)
West	Y = 14620	(Vertical)
Southwest	Y = 75009.8 - 0.630769 * X	(Vertical)
Top	Z = 30	(Horizontal)
Bottom	Z = -1000	(Horizontal)

B.5 SICADA LOGS FOR FINNSJÖN SITE DATA

B.5.1 For coordinates and previous 3m interpreted K values

Output to: File

Date   :970423 16:25:53

Table(s) :sic_dba.steady_state_inj_cd

Columns: steady_state_inj_cd.idcode,   steady_state_inj_cd.start_date,   steady_state_inj_cd.seclen, steady_state_inj_cd.secup, steady_state_inj_cd.k, steady_state_inj_cd.comment, steady_state_inj_cd.midpoint,

New column: midpoint=secup+seclen/2

Criteria : steady_state_inj_cd.idcode like'KFI%' AND

(steady_state_inj_cd.seclen =2 OR steady_state_inj_cd.seclen =2.05)

Result   : 678 rows written to file.

Coordinate calculations done.

Coordinate system : RT

Coordinate calculation column: secup

Filename   : /home/skbee/fi_secup.csv

File format : csv

Output to: File

Date   :970423 16:27:11

Table(s) :sic_dba.steady_state_inj_cd

Columns: steady_state_inj_cd.idcode,   steady_state_inj_cd.start_date,   steady_state_inj_cd.seclen, steady_state_inj_cd.secup, steady_state_inj_cd.k, steady_state_inj_cd.comment, steady_state_inj_cd.midpoint,

New column: midpoint=secup+seclen/2

Criteria: steady_state_inj_cd.idcode like'KFI%' AND

(steady_state_inj_cd.seclen =2 OR steady_state_inj_cd.seclen =2.05)

Result   : 678 rows written to file.

Coordinate calculations done.

Coordinate system : RT

Coordinate calculation column: midpoint

Filename   : /home/skbee/fi_mid.csv

File format : csv

B.5.2 For coordinates and previous 2m interpreted K values

Output to: File

Date   :970429 13:32:52

Table(s) :sic_dba.steady_state_inj_cd

Columns   :steady_state_inj_cd.idcode,   steady_state_inj_cd.start_date,   steady_state_inj_cd.seclen, steady_state_inj_cd.secup, steady_state_inj_cd.k, steady_state_inj_cd.comment, steady_state_inj_cd.midpoint,

New column: midpoint=secup+seclen/2

Criteria : steady_state_inj_cd.idcode ='KFI10' AND steady_state_inj_cd.seclen = 2

Result   : 81 rows written to file.

Coordinate calculations done.

Coordinate system : RT

Coordinate calculation column: secup

Filename   : /home/skbee/kfi10_s.csv

File format : csv

Output to: File

Date   :970429 13:33:57

Table(s) :sic_dba.steady_state_inj_cd

Columns: steady_state_inj_cd.idcode,   steady_state_inj_cd.start_date,   steady_state_inj_cd.seclen, steady_state_inj_cd.secup, steady_state_inj_cd.k, steady_state_inj_cd.comment, steady_state_inj_cd.midpoint,

New column: midpoint=secup+seclen/2

Criteria : steady_state_inj_cd.idcode ='KFI10' AND steady_state_inj_cd.seclen = 2

Result   : 81 rows written to file.

Coordinate calculations done.

Coordinate system : RT

Coordinate calculation column: midpoint

Filename   : /home/skbee/kfi10_m.csv

File format : csv

B-20

B.6 BEBERG PARAMETER SOURCES

	Source	Treatment	Availability
REGIONAL			
Geology			
Rock type	SKB TR 91-24 SKB TR 91-08 SGU Af nr. 166	Compilation	(1)
Lineaments	SKB TR 91-08	Compilation	(1)
Land rise	SKB TR 92-38	Interpolation	(1)
Geochemistry and Salinity	Laaksoharju et al. 1997 (SKB R 97-X) SKB TR 91-24	Compilation	(1)
Hydrology			
Recharge pattern and rates	SKBF KBS TR 83-56 SKB TR 91-24	Compilation	(1)
Groundwater flow patterns	SKB TR 91-24	Compilation	(1)
Hydraulic Parameters			
Rock Mass K	SGU 1996 SKB TR 91-24 SICADA 1997	Compilation, statistical analysis, rescaling	(1)
Conductor Location, K	SKB TR 91-24 SKB PR SFR 86-03 SICADA 1997	Compilation, statistical analysis, rescaling	(1)
Anisotropy	SKB TR 91-24 SKB PR SFR 86-03	Compilation	(1)
Scale relationships	SKB TR 97-06	Compilation	(1)
SITE			
Geology	SKB TR 91-24 SKB TR 91-08	Compilation	(1)
Hydrology			
Surface Hydrology	SKBF KBS TR 83-56 SKB TR 91-24	Compilation	(1)
Groundwater Flow Patterns	SKB TR 91-24 SKBF KBS TR 83-56	Compilation	(1)
Hydraulic properties			
Rock Mass K	SICADA 1997 SKB TR 91-24	Statistical analysis of 3m data, rescaling	SICADA
Conductor Location, K	SICADA 1997 Table 4.3 of SKB TR 91-24	Compilation, statistical analysis of 2 and 3m data, rescaling	SICADA Appendix B
EDZ	SKB ICR 96-03, Olsson and Winberg, 1997 (unpublished SKB PM)	Compilation	(1)
Anisotropy	SKB PR SFR 86-03 SKB TR 91-24	Compilation	(1)
Geostatistics, Scale relationships	SICADA 1997 SKB TR 97-06	Variography, Universal Kriging on 3m data, rescaling	(1)

(1) see the Source report

APPENDIX C. CEBERG

C.1 GIDEÅ REGIONAL LINEAMENTS

Previous lineament maps of the Gideå region were restricted to the area covered by LVM sheet 19J NV Husum (Ahlbom et al., 1983; Ahlbom et al., 1991). This area ends approximately 10km north of the site, leaving part of the area near the site undefined. For the purposes of this study, the lineament map of Ahlbom et al. (1983) was extended slightly north and south, using the interpretations of Askling (1997) and Lundqvist et al. (1990). Figure 4-4 presents that extended lineament map and Figures C-1 and C-2 present the same set of lineaments separated into well-expressed and less-well-expressed lineaments, respectively. These lineament maps are the basis of RCD1.
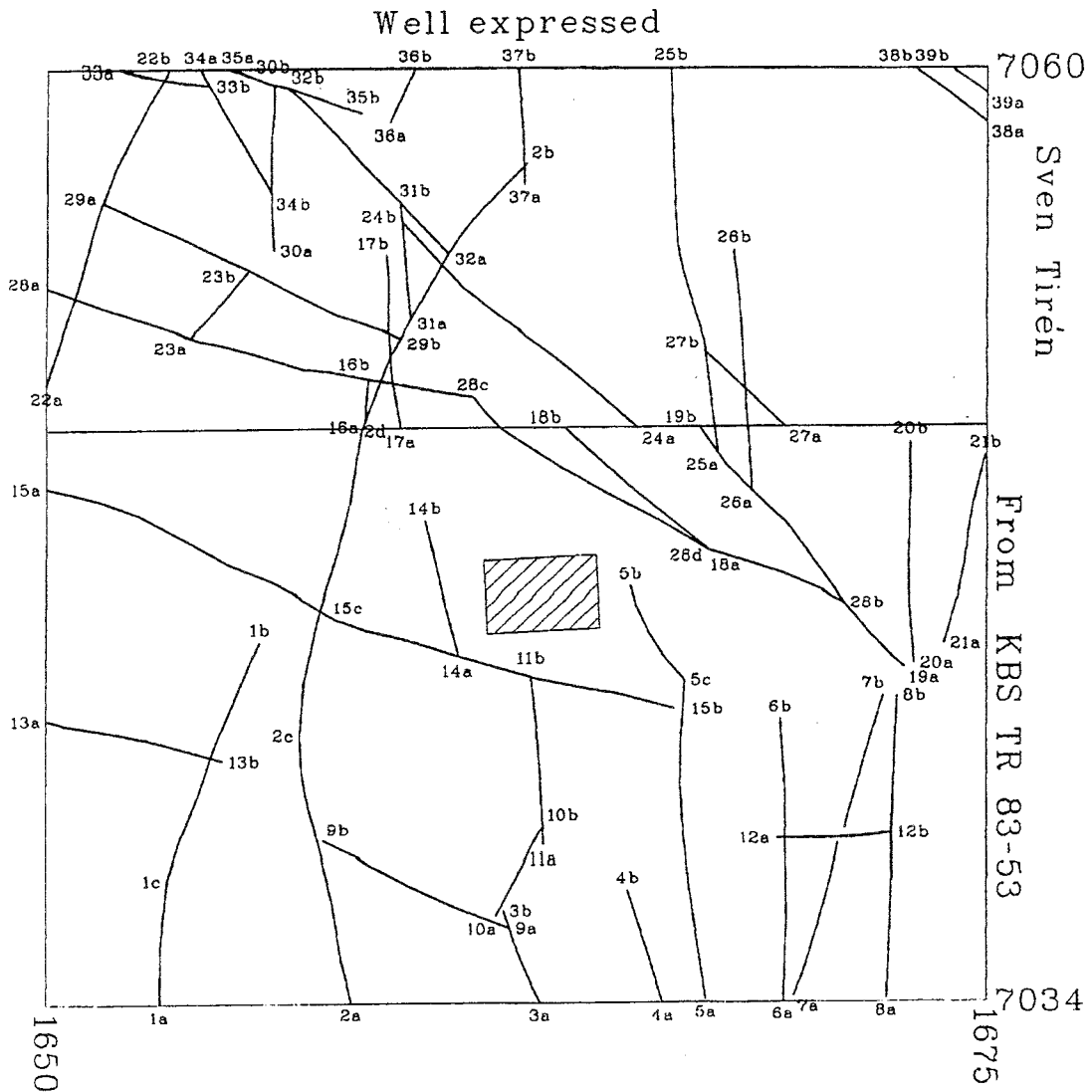
Figure C-1. Well expressed Gideå regional lineaments -- RCD1 (after Ahlbom et al., 1983). See also Figure 4-4.
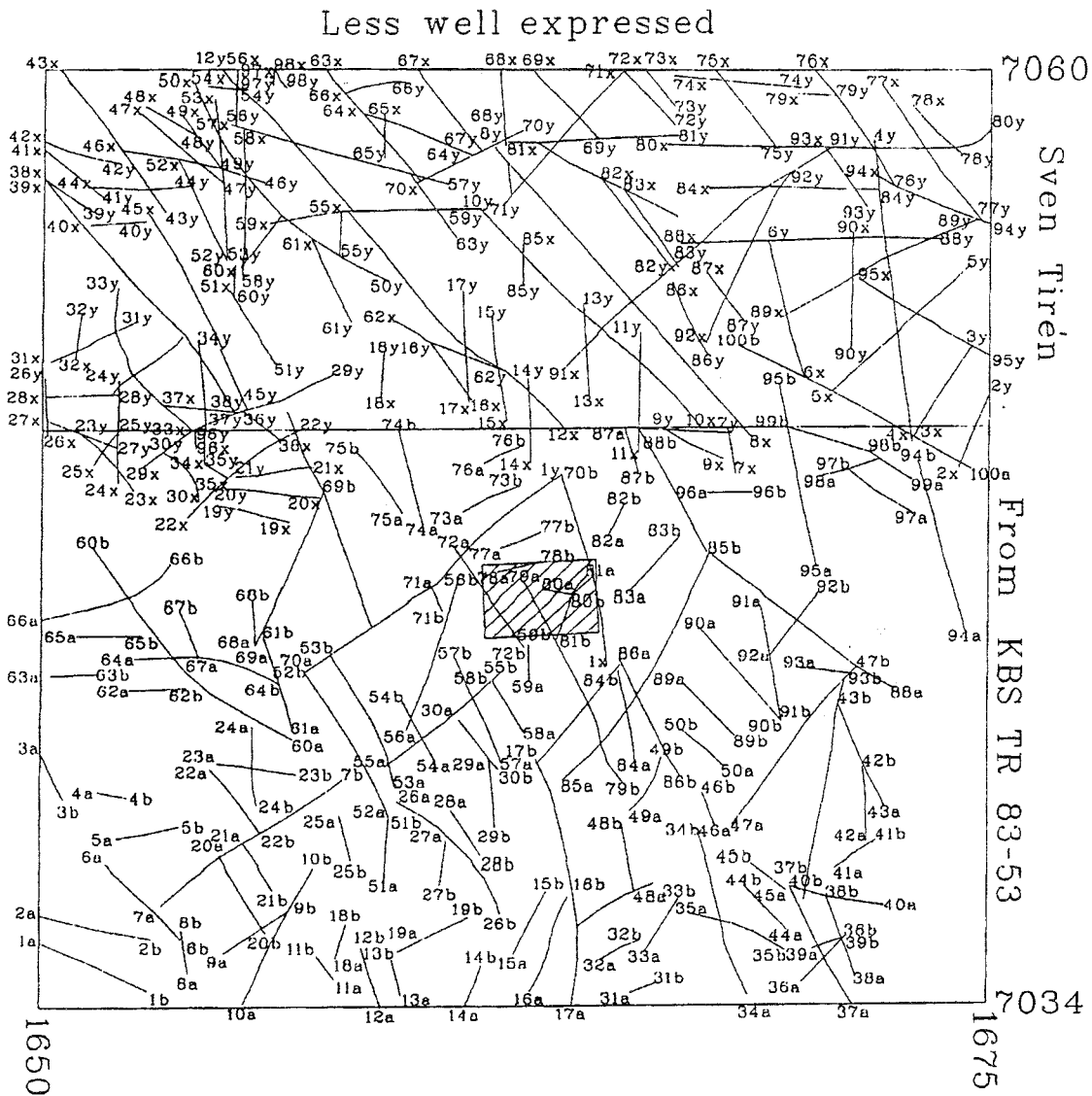
Figure C-2. *Less well expressed Gideå regional lineaments -- RCD1 (after Ahlbom et al., 1983). See also Figure 4-4.*

Hermanson et al. (1997) had updated the site structural model and created a 3-dimensional model for fracture zones and doleritic dikes within Gideå site. However, they did not reconcile the site scale structures with the regional lineaments. The regional lineaments can be correlated to site scale structures by comparing the maps and using a simple set of rules:

- Within the site, the site-scale structural model should be used over the regional lineaments. Because boreholes and geophysics generally confirm the site-scale structures, they should be regarded as more reliable than topographically interpreted lineament maps.

- Only the site-scale structures should be used within the site boundaries.

- Site-scale structures corresponding to regional lineaments should be extended outside site boundaries using the tabulated correlations (Table C-1 for RCD1 and Table C-2 for RCD3). Regional lineaments should

be moved as necessary to match the endpoints of the site scale structures. Dips of the site-scale structures should be used for these lineaments.

- Ideally, ALL lineaments (well expressed and less well expressed) should be included in the model. If the computational demands of including all the lineaments are excessive, one suggestion is to drop the less-well expressed lineaments EXCEPT for those in Table C-1 or C-2. Surface expression of a lineament is not necessarily related to the hydrogeologic importance of a fracture zone. Ignoring a lineament based on surface expression is subjective censoring and should be avoided.

Because of the uncertainties regarding the regional lineaments, a new lineament map was drawn in association with this study. Askling (1997) used LMV digital terrain models on a 50 X 50m resolution to create an alternative regional lineament map (Figure 4-5), which is the basis of RCD3, a variation case for the regional flow modelling. One of the well expressed northwest-southeast striking regional lineaments of this revised map crosses the northeast corner of the site, and may have important consequences for PA modelling. Figures C-3, 4, 5, and 6 present the less well expressed lineaments from RCD3 (Figure 4-5). Some thin, poorly expressed lineaments are quite extensive, striking east-west and northeast-southwest. Several of these thin lineaments cross the site, and correspond to site scale structures. (Askling, 1997, Hermanson, et al. 1997). Similar to the correlations cited above, the RCD3 lineament set can be correlated to the site structural map as shown in Table C-2.

Table C-1. Ceberg lineament correlations with site-scale structures (RCD1 and SCD1) (After Ahlbom et al., 1983). See also Figures C-1 and C-2.

Structure	Corresponding Regional Lineament
I	L.w. 81
II	None
III	L.w. 80 (does not extend beyond site boundaries)
IV	L.w. 78 (does not extend beyond site boundaries)
V	None
VI	None
VII	L.w. 79
VIII	L.w. 72
IX	None
X	None
XI	None
XII	None

Table C-2. Ceberg Lineament Correlations with Site structures (RCD3 and SCD2). (After Askling, 1997). See also Figures C-3, 4, 5, and 6.

Structure	Corresponding Regional Lineament
I	L.w. SW-NE 106 and 160
II	L.w. SW-NE 107
III	L.w. E-W 67
IV	L.w. E-W 99
V	L.w. E-W 98 (weak)
VI	L.w. SW-NE 92
VII	L.w. NW - SE 117, 118
VIII	L.w. NW - SE 119
IX	L.w. E-W 162
X	L.w. N-S 102
XI	L.w. E-W 120 (weak)
XII	L.w. E-W 161

Several onsite borings penetrate lineaments that are correlated to site structures, helping to document lineament properties. Although the surface expression of the lineaments is 100m to 200m wide, they correspond to fracture zones having widths between 5 to 50m. This is similar to such features found at other sites (e.g., Äspö, Finnsjön). Therefore, similar to Äspö, a reasonable assumption for the median width of all regional lineaments is 20m. The hydraulic properties are inferred from the rescaled, depth-dependent fracture zone values measured on site.

On-site data and the Gissjö hydropower tunnel data are used to infer dips of the fracture zones as 70 to 90 degrees.

In general, very little information is available for the regional lineaments. Consequently the regional scale conductor domain model for Ceberg is considered uncertain (Ahlbom et al., 1983; Askling, 1997, Hermanson, et al. 1997).
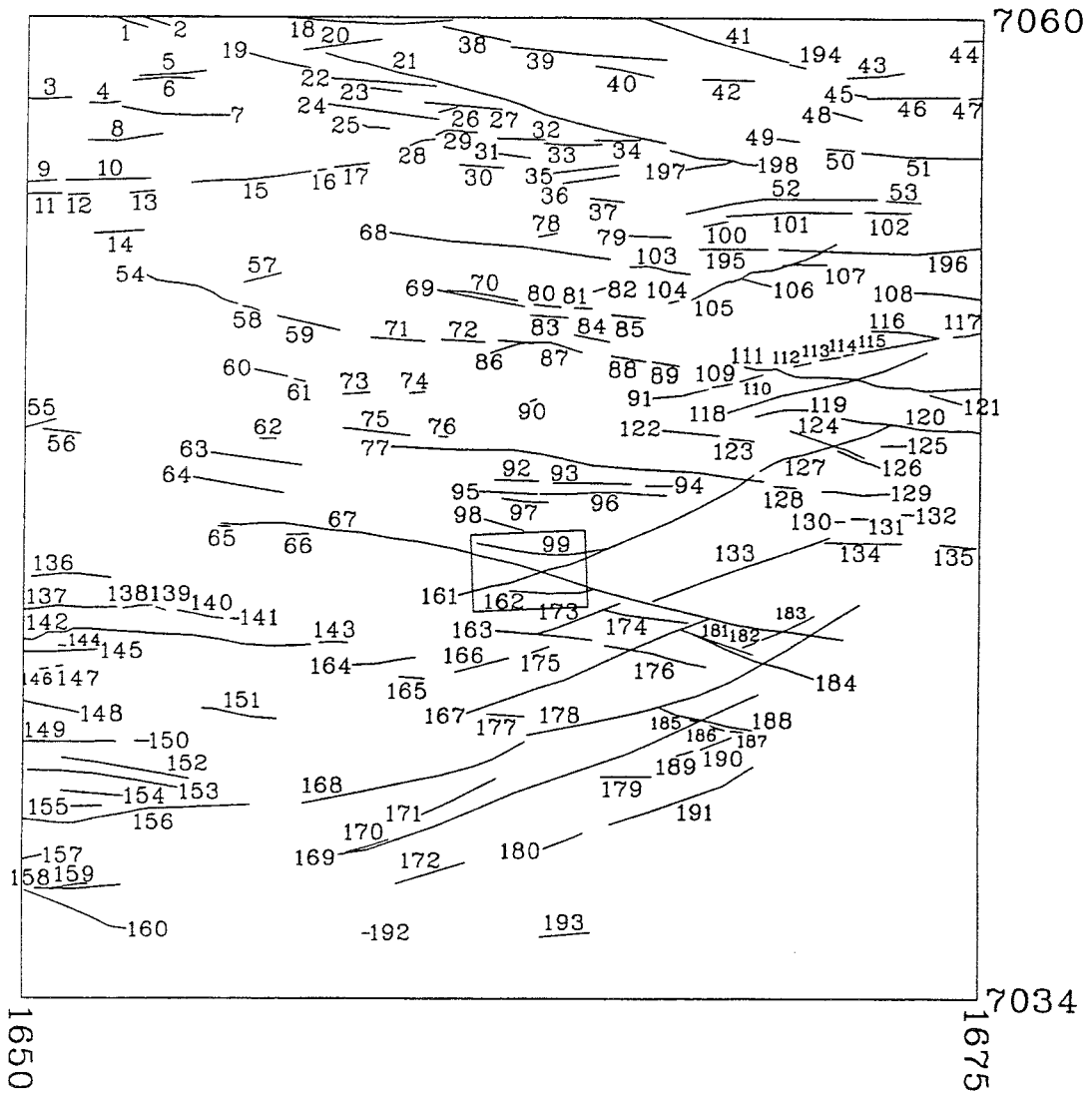
Figure C-3. *E–W Less-well expressed Gideå regional lineaments – RCD3 (from Askling, 1997). See also Figure 4-5.*
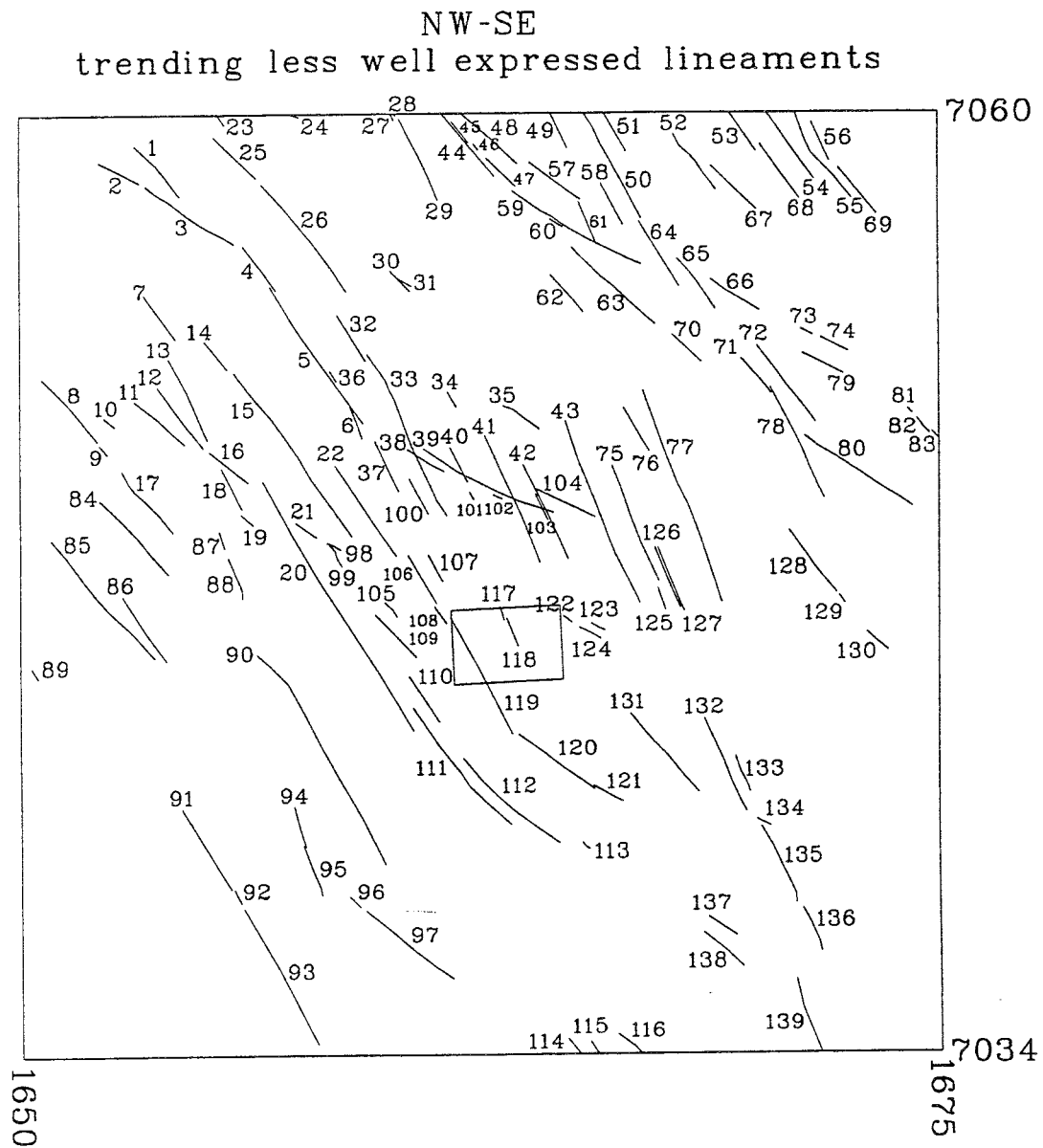
Figure C-4. *NW–SE Less-well expressed Gideå regional lineaments – RCD3 (from Askling, 1997). See also Figure 4-5.*
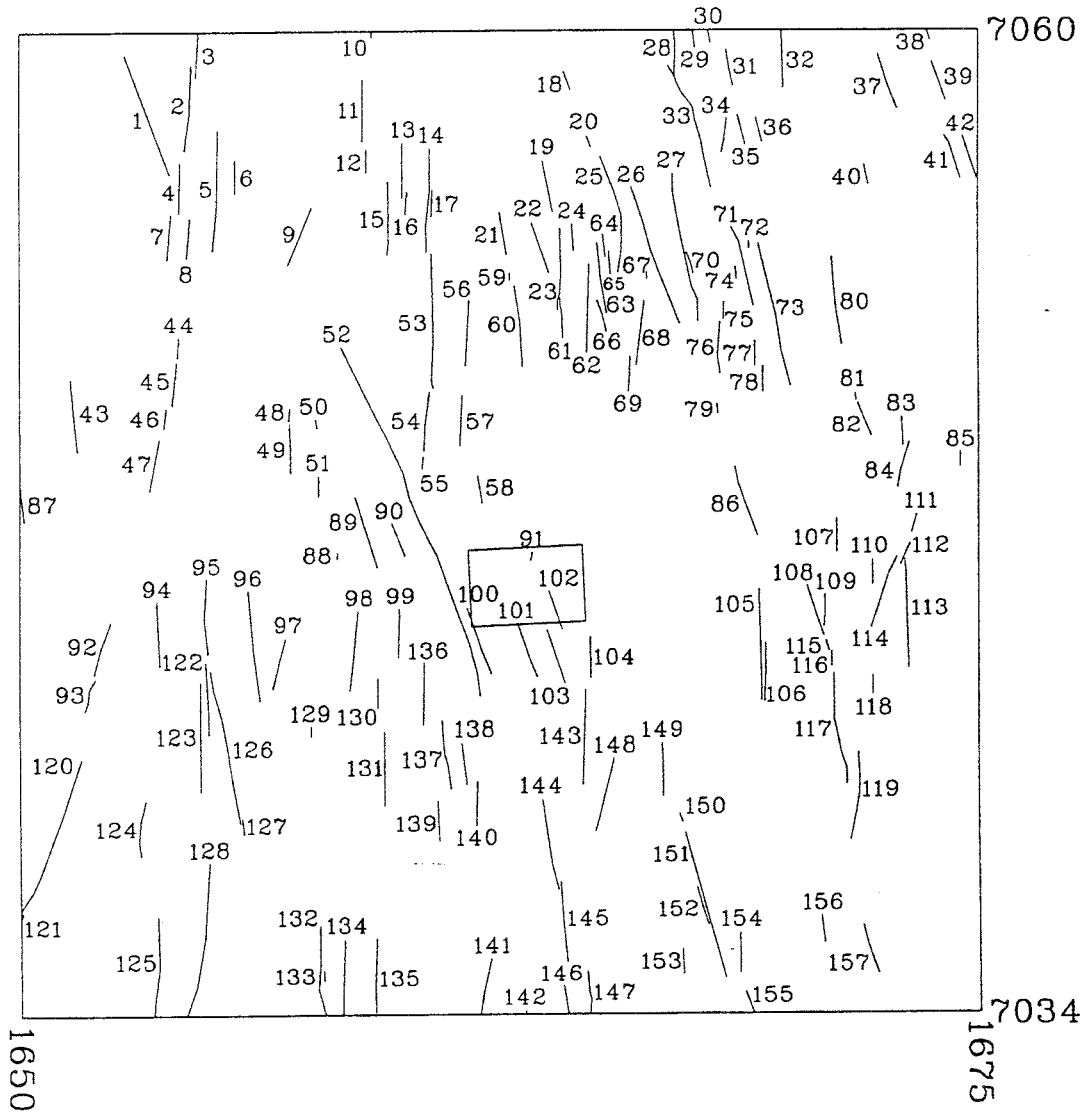
Figure C-5. *N–S Less-well expressed Gideå regional lineaments – RCD3 (from Askling, 1997). See also Figure 4-5.*
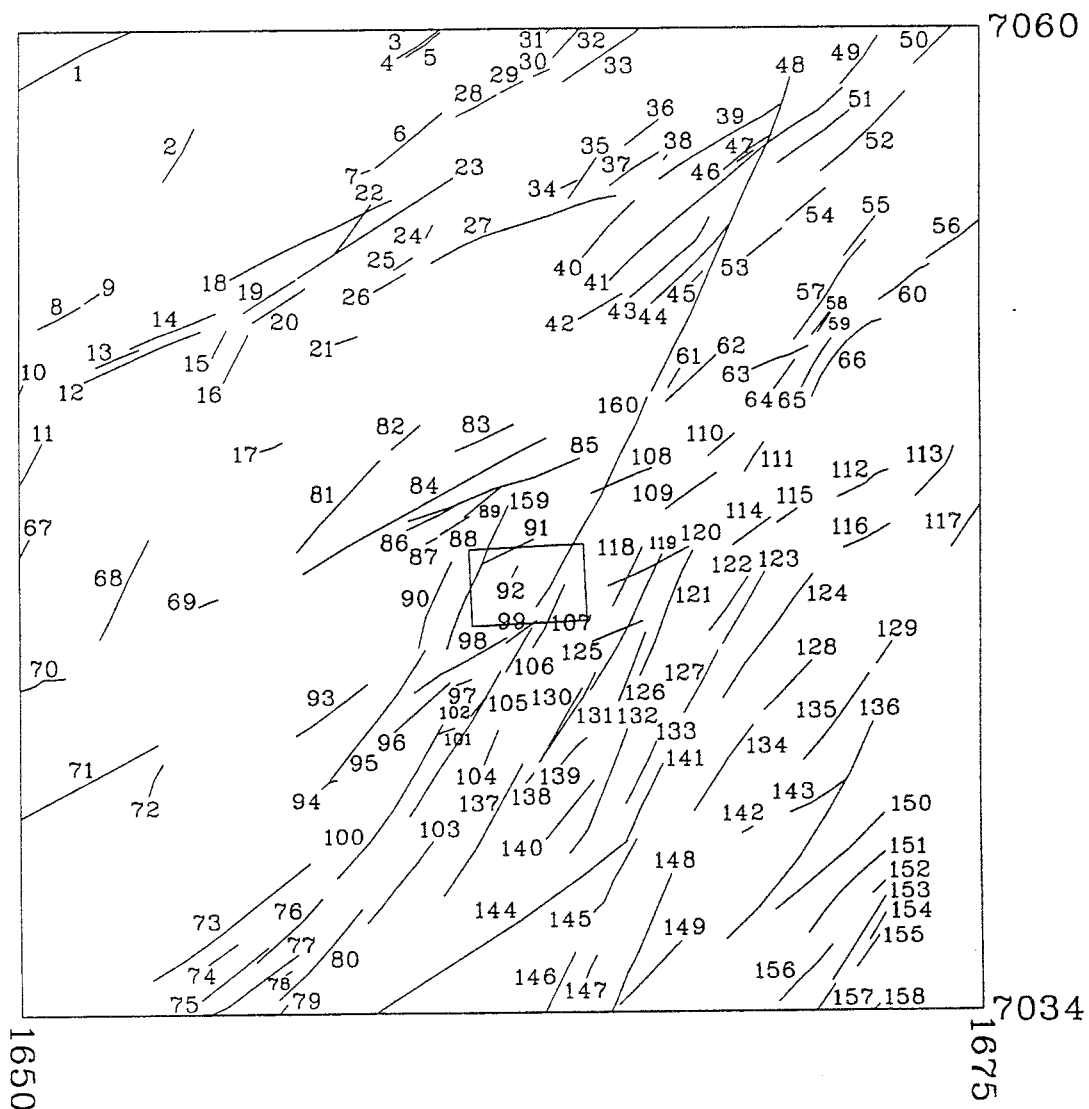
Figure C-6. NE–SW Less-well expressed Gideå regional lineaments – RCD3 (from Askling, 1997). See also Figure 4-5.

C.2 ANALYSIS OF SGU DATA IN GIDEÅ REGION

Swedish Geological Survey (SGU) provided well data from the SGU well archive for wells in the Gideå area, loosely defined as a 25 km radius around the town of Gideå. As discussed in Appendix D.1, it is possible to estimate the well's specific capacity, Q/dh, and use the Äspö regression relationship of T versus Q/dh of Rhén et al. (1997).

Previous studies of this data either ignored spatial correlation (Ericsson and Ronge, 1986) or ignored the regional lineaments (Jönsson et al., 1996). This study reanalysed the SGU well data to assess both of these effects.

C.2.1 Selecting a uniform subset of the data

The initial set of SGU data consisted of 218 wells within 25km radius of Gideå (Figure 4-15), but not all the data is considered valid. 8 wells had reported water capacities of 0 litres/hr. Since this was a relatively small censored proportion, these were simply discarded. As described in Appendix D.2, a consistent subset of the data was selected, resulting in a data set with the following characteristics:

- 148 measurements

- Arithmetic Mean of $Log_{10}K$ (m/s): -7.156

- Median of $Log_{10}K$: -7.215

- Variance of $Log_{10}K$: 0.219

- Median Depth: 100m

The univariate histogram of the SGU Log_{10} K is slightly skewed about the mean (Figure C-7), but might be modelled using a normal probability distribution.

Histogram
Data file: SGUgid.eas

Statistics	
N Total :	148
N Miss :	0
N Used :	148
Mean :	-7.156
Variance:	.219
Std. Dev:	.468
% C.V. :	6.543
Skewness:	.332
Kurtosis:	2.334
Minimum :	-8.030
25th % :	-7.490
Median :	-7.215
75th % :	-6.780
Maximum :	-5.980
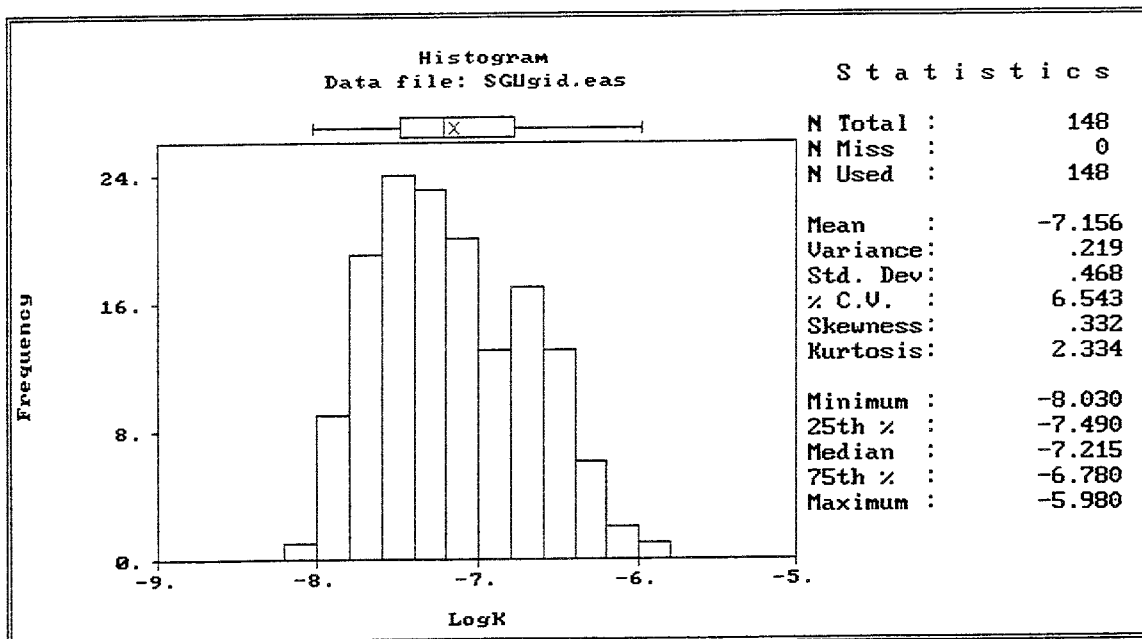
Figure C-7. *Histogram of Log_{10} hydraulic conductivity from SGU data in Gideå region.*

C.2.2 Regional lineaments and clustering

Jönsson et al. (1997) suggested that SGU data in the Gideå region were preferentially clustered in areas of high hydraulic conductivity. Although the data is spatially clustered in fault valleys and communities, this does not necessarily indicate that they are preferentially clustered. On the other hand, virtually all the data lies near or in a topographic lineament. If the

data were preferentially clustered, this would bias the estimates of the global mean and possibly the variance of the data.

Two simple calculations were performed to evaluate the possibility of clustering and consequent bias. The first was an approach similar to Ericsson and Ronge (1986), use the regional lineaments to identify those wells that were in or near fracture zones, and compare the resulting subpopulations. Several sorting patterns were tested, using lineament widths from 50 to 200m and several lineament orientations. None of the sorted data sets were appreciably different than the global data set. That is, separating the data that was in or near lineaments had no apparent effect, therefore the data was considered to be a single population of hydraulic conductivity measurements from the rock mass domain. This is also consistent with conclusions drawn from the SGU data at the Äspö site.

The second calculation was to apply a cell declustering algorithm (Deutsch, 1989) to see if any cell size would reduce or increase the global mean. The algorithm does indicate that a cell size of approximately 2.4km would maximise the mean $Log_{10}K$ to -7.092, but this is little different than the untreated mean of -7.156 (Figure C-8). The data may be clustered, but its effect is minimal enough to be neglected. Although the data does not appear to be preferentially clustered, it is possible that all the data lies within lineaments and thus is perfectly biased by the sampling. Subsequent comparison to the Gideå site 25m packer test data within the rock mass domain indicates that this is not the case, however (see appendix C.3).

Gideå Site: Cell Declustering of SGU data
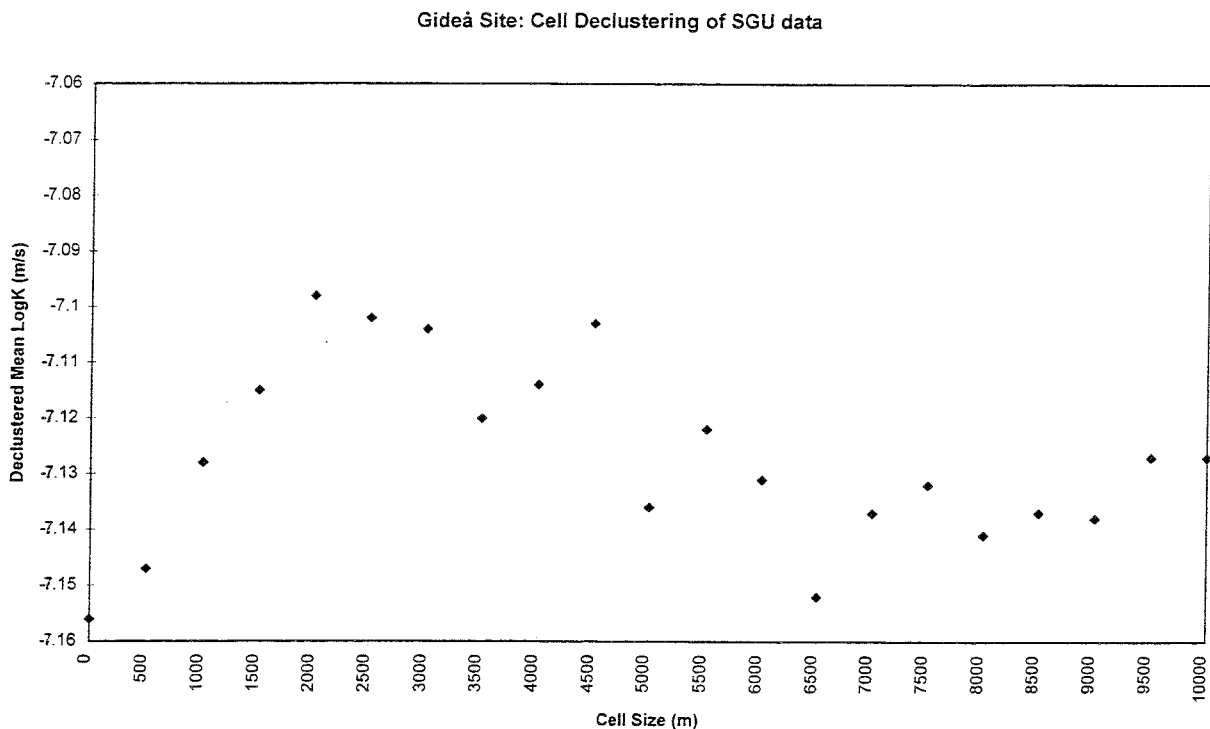
Figure C-8. Cell declustering results for Log_{10} hydraulic conductivity from SGU data in Gideå region.

C.2.3 Analysis of Spatial Correlation

In an attempt to infer a model of spatial correlation for the SGU data, several geostatistical programs were used (Appendix D.3). This involved calculating the experimental semivariogram of the SGU data using several lag intervals and a maximum lag interval of 10 km. This was repeated using the traditional semivariogram estimator and several robust estimators for the isotropic and anisotropic models. Three possible models were found:

1. Isotropic, high sill: $\gamma(h) = 0.095 + 0.145$ Sph(3500)

2. Isotropic, low sill: $\gamma(h) = 0.08 + 0.145$ Sph(2250)

3. Anisotropic: N: $\gamma(h) = 0.095 + 0.145$ Sph(5000)

                   E: $\gamma(h) = 0.095 + 0.130$ Sph(1000)

All three of these models were cross-validated using Ordinary and Simple kriging with various neighbourhood search criteria. A variant of model 2 was found to be the most appropriate for the observed data (having the lowest crossvalidation error of KRMSE = 0.448). That model was (Figure C-9):

Isotropic, low sill: $\gamma(h) = 0.09 + 0.13$ Sph(2000)

Simple Kriging, mean = -7.092, octant search, 8 observations maximum.

That is, simple kriging with a spherical variogram model whose range is 2km and with a nugget of over 40%. However, a plot of observed value versus estimated value (Figure C-10) indicates that the quality of the estimation is very poor. This is reflected in a crossvalidation error that is only 4% lower than the sample standard deviation. This indicates that the kriged estimates are little better than using the mean of the data. This can be explained in part by the relatively high nugget that indicates that the spatial correlation is relatively weak.

We can therefore conclude that, although the hydraulic conductivities of the SGU wells may be spatially correlated, including spatial correlation in the estimates has little effect.

C.3 GIDEÅ PACKER TEST DATA

Packer test data for the site was taken from the SKB SICADA database and consisted of the interpreted hydraulic conductivity, the RAK X, Y coordinates, and the elevation of the centre of each test section. The transient 25m test data had the most uniform coverage over the entire site, and are the basis of the following analysis. Figures C-11 and C-12 present summary statistics, histograms and lognormal probability plots for the Gideå 25m packer test data.

Figure C-9. Semivariogram for Log_{10} hydraulic conductivity from SGU data in Gideå region. (All directions).

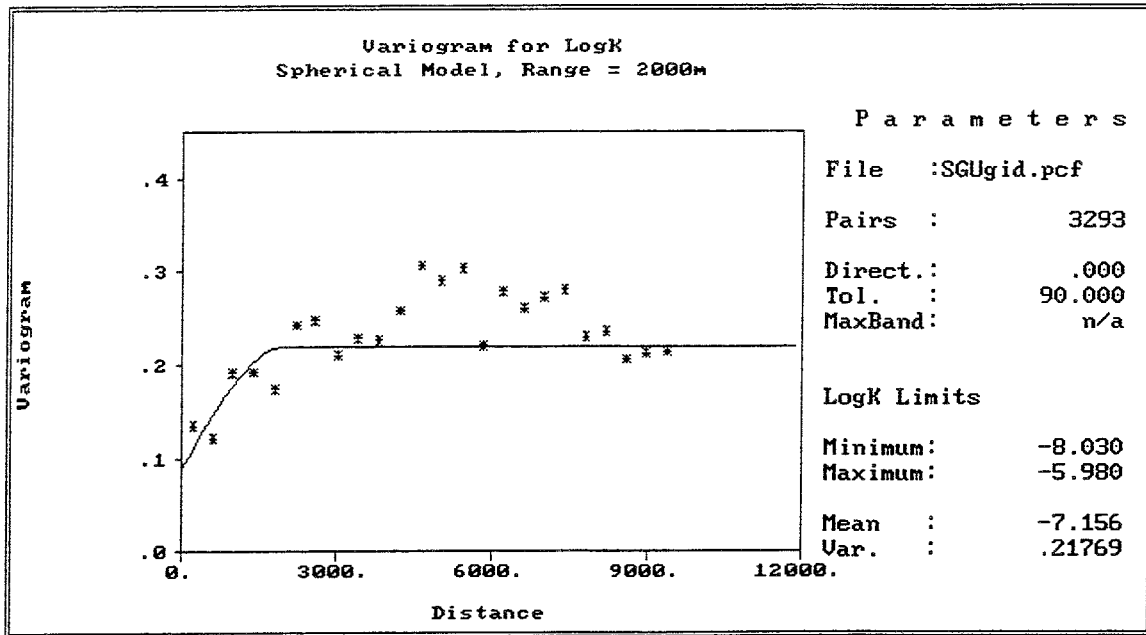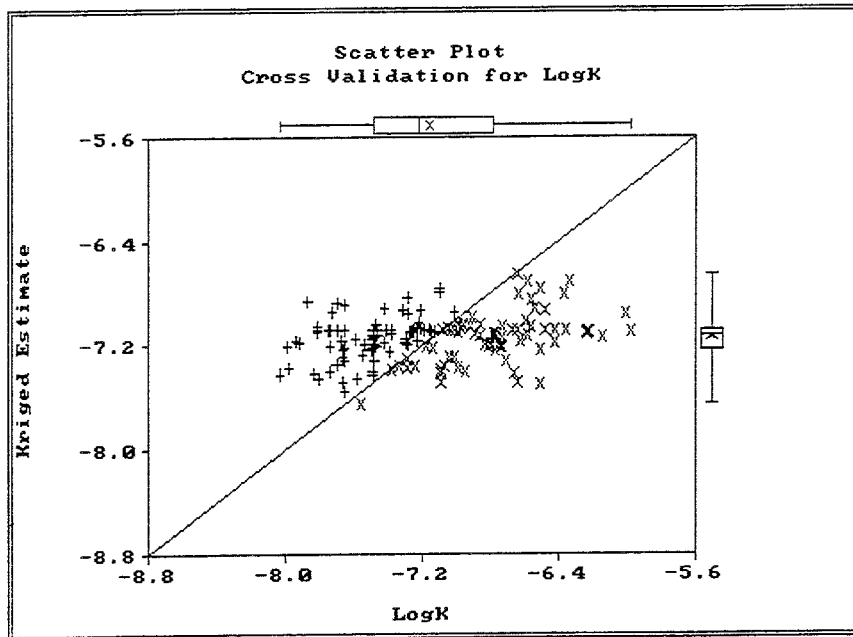**Figure C-10.** Crossvalidation results for kriging estimate versus observed Log_{10} hydraulic conductivity from SGU data in Gideå region.

C-12

Many of the measurements are reported as being below a measurement limit, which would censor the data and affect the estimates of the mean, variance and variogram. Unlike Äspö and Finnsjön, however, the interpreted hydraulic conductivities found in the SICADA database have not been coded to indicate which measurements are below the measurement limit. Although the reported measurement limit of Log_{10} K (m/s) is -11, the lognormal probability plot of the entire data set indicates a measurement limit of -10.25 (Ahlbom et al., 1991a; Figure C-12). This limit censors approximately 37% of the 25m data, similar to that cited by Winberg (1989). The effects of this censoring have been corrected using the method described in Appendix D.4.

Based on the revised site structural model and designated fracture zone contacts (Hermanson et al., 1997, Table 6-2) the 25m packer test data was separated into set of fracture zone data (SCD) and a set of rock mass data (SRD). Sections C.3.1 and C.3.2 discuss the univariate statistics for each of those subsets of the 25m test data.

Additional hydraulic test data is available at this site, but is of limited usefulness because of the incomplete coverage. The most useful are the 225 interpreted hydraulic conductivities from the 2m and 3m packer tests. Separating these data into SCD and SRD populations yields the univariate statistics given in Table C-3. This reveals an important characteristic of the Gideå site, that the identified conductors can have a lower hydraulic conductivity than the surrounding rock mass. The limited number of measurements and the limited coverage (portions of boreholes KGI07, KGI09 and KGI11) confound attempts to assess depth dependency or site-wide characteristics. The fracture zones intercepted by these boreholes are zones IIIa, IIIb and VI, reported to be of very low conductivity in comparison to other zones identified at the site. Although this data is not thought to be representative of the site, it does suggest an alternative site-scale conductor domain model, SCD4, which addresses the possibility that some of the fracture zones are more conductive. This is discussed further in Section C.3.2. Although it might be interesting to compare these short test intervals with the longer test intervals, 3 boreholes are insufficient to construct a scaling relationship for the Gideå site.

Table C-3. Gideå interpreted Log_{10} hydraulic conductivity from 2 and 3m packer tests.

Domain	Median Log_{10} K (m/s)	Number of Samples	Censoring Level (%)*
All 2 & 3m	-9.72	225	24
Rock (RD)	-9.66	197	24
Conductor (CD)	-10.11	28	29

* Censoring level is % of data below measurement limit.
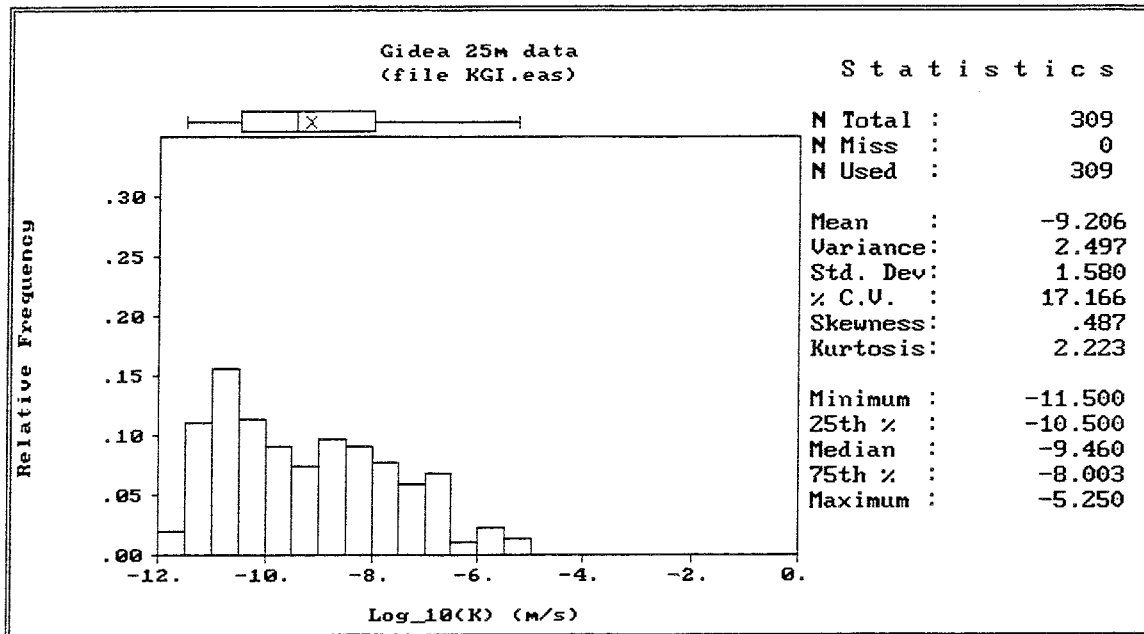
Figure C-11. Histogram of Gideå interpreted Log_{10} hydraulic conductivity from 25m packer tests.
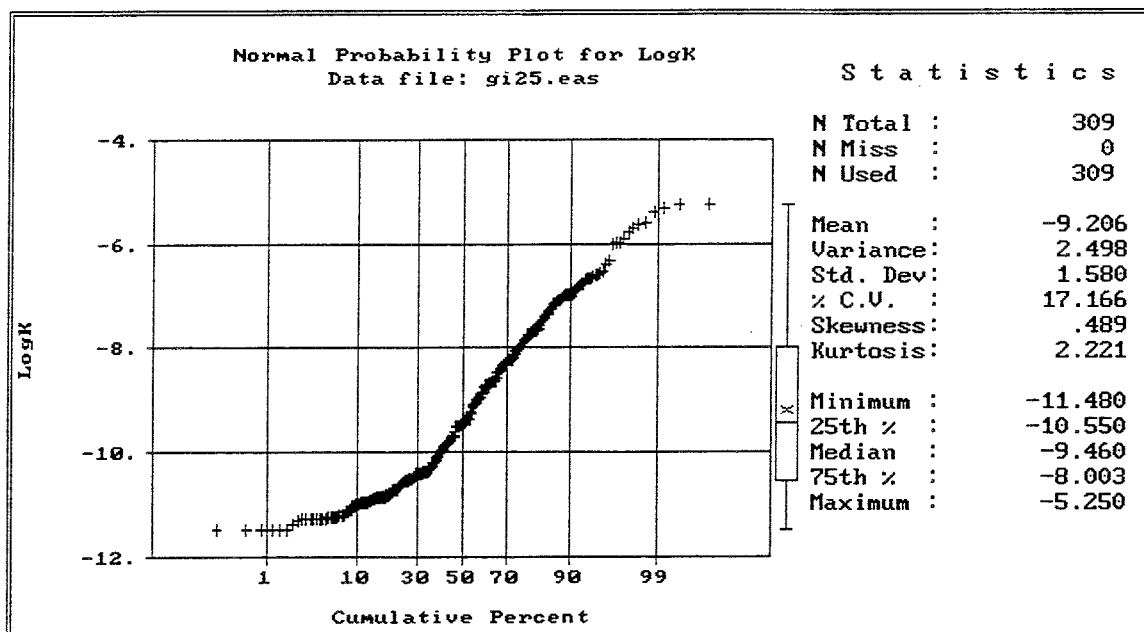
Figure C-12. Probability plot of Gideå interpreted Log_{10} hydraulic conductivity from 25m packer tests.

C-14

C.3.1 Rock Mass Domain

The Gideå site hydraulic conductivities corresponding to the site-scale rock mass domain (SRD) have been previously analysed in several studies (Ahlbom et al., 1983; Winberg, 1989; Hermanson et al., 1997). Although several authors have commented on the strong depth dependence of this data, attempts to regress models of hydraulic conductivity versus depth have been confounded by the measurement limits. Rather than regressing a continuous model of depth dependence, this study adopts a simpler depth zonation approach (Ahlbom et al. 1983; Rhén, 1997). Because the topographic relief is relatively large at Gideå, this study divides the data into elevation zones and determines the mean and variance of each. These estimates are corrected for the measuring limit using the method of Wen (1994).

The statistics of these zones are relatively sensitive to the choice of intervals, but the elevation zones can be delineated based on changes in fracture frequency and increases in the censoring level. These are:

- +110 to 0m masl: corresponds to the SGU data and has a relatively low variance.

- 0 to -100m masl: begins at a large increase in variance

- -100 to -300m masl: begins at an increase in the level of censoring.

- below -300m masl: begins at a large decrease in fracture frequency.

These elevation zones are the basis of SRD6, the site-scale conceptual model for the Ceberg rock domain. The means and variances for the hydraulic conductivities in these zones are presented in Table C-4. Note that the number of data values above the measurement limit is roughly the same for each of the zones, yielding estimators of comparable reliability for each zone.

Table C-4. Ceberg rock mass domain (SRD6) depth zonation for interpreted Log_{10} hydraulic conductivity from 25m packer tests.

Elevation (masl)	Arithm. Mean Log_{10} K (m/s)*	Variance Log_{10} K (m/s)*	Number of Samples	Censoring Level (%)
+110 to 0	-7.55	1.23	55	3.6
0 to -100	-9,04	2.27	50	16
-100 to -300	-10,03	2.28	86	49
Below -300	-10,25**	3.18	87	58

* corrected assuming normally distributed data, after Wen (1994). Censoring level is % of data below measurement limit.

** Since the censoring level is > 50%, this estimate amounts to the measurement limit

These elevation zones are determined using the 25m test data and will require scaling using the Äspö scaling regression equations when used at larger grid scales.

As a check on consistency, the upper 100m of the on-site data should be compared to the SGU data used for the regional model RRD1. The SGU data has an approximate measurement scale of 100m (median depth of 100m), so we upscale the on-site data in the upper elevation zone to 100m, then compare to the SGU data:

+110 to 0 masl: Mean Log_{10} K = -7.08, standard deviation = 0.616

SGU data: Mean Log_{10} K = -7.16, standard deviation = 0.468

Although not an exact match, it is reassuring that the values in this elevation zone are at least comparable.

No separation of the rock mass domain is made on the basis of rock type (Hermanson et al., 1997)

C.3.2 Fracture Zone Domain

This section provides hydraulic conductivities for both the site-scale and regional scale models for the conductor domains (SCD1 and RRD1). These are inferred from statistics computed from the 31 interpreted hydraulic conductivities of the 25m packer tests designated as representing the fracture zones. These statistics were corrected for the measurement limit (Wen 1994), since only 18 of these measurements were above the estimated measurement limit. Figure C-13 presents the histogram of these data, which have the following corrected statistics:

Arithmetic Mean Log_{10} K (m/s) = -8.8, variance = 5.07, Median = -8.87, IQR = 3.21

Various authors have noted that, where the zones have hydraulic tests at multiple depths, the data suggests that the hydraulic conductivity of the zones decreases with depth (Ahlbom et al., 1983). For example, the 25m tests in zones II and III indicate a decrease of ½ to 2 orders of magnitude with depth. However, there are only 31 measurements available, which are thought to be too few data to infer depth dependence for the fracture zones. However, for SCD1 it seems reasonable to assume that the above statistics are representative of the median elevation of these measurements, -130masl. The relative changes in the mean and variance for the rock mass elevation zones (as in Table C-4) can be used for the depth dependence of the conductive fracture domains. These statistics should be rescaled to the appropriate grid size.

As discussed in the beginning of Section C.3, some of the fracture zones may be clay-altered and consequently have relatively low hydraulic conductivity. Some authors have suggested that zones I, II, XI, and XII may be much more conductive than the other identified conductive zones at the site. An alternative case, SCD4, is proposed where the hydraulic conductivity of these zones have the same relative contrast to the

surrounding rock mass as at Aberg and Beberg (i.e., increased 2 orders of magnitude).

No data is known to exist for the regional scale conductive fracture domains (RCD1). Therefore the hydraulic conductivities for RCD1 should be taken as the upscaled elevation statistics described above.

Gidea 25m data
Conductor Domain (file KGIcd.eas)

S t a t i s t i c s

N Total :	31
N Miss :	0
N Used :	31
Mean :	-8.686
Variance:	3.661
Std. Dev:	1.913
% C.V. :	22.029
Skewness:	.391
Kurtosis:	1.904
Minimum :	-11.300
25th % :	-10.450
Median :	-8.870
75th % :	-7.235
Maximum :	-5.250
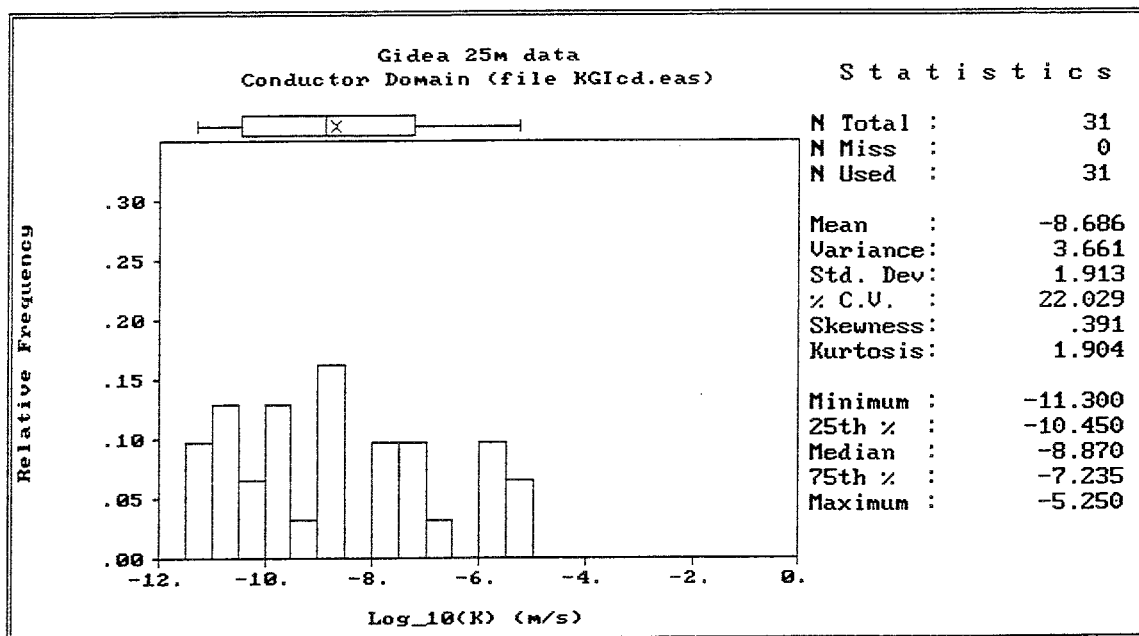
Figure C-13. Histogram of Conductor Domain, Gideå interpreted Log_{10} hydraulic conductivity from 25m packer tests.

C.4 GEOSTATISTICAL MODEL

The Ceberg site-scale geostatistical model of hydraulic conductivity consists of the previously defined divisions of SRD6, SCD1 and the elevation zones. The model is developed with HYDRASTAR in mind, which assumes that hydraulic conductivity has a multivariate lognormal distribution, with the elevation zones and SCD treated as step changes in the mean of Log_{10} conductivities. A single variogram model is inferred for the entire domain (i.e., the same variogram for SRD and SCD). This model of trend and spatial correlation inferred using the iterative generalised least squares estimation (IGLSE) approach to universal kriging suggested by Neuman and Jacobsen (1984). INFERENS is a computer program developed by SKB to automate the IGLSE fitting algorithm (Appendix D.3).

As discussed in Section 1.6.1, the correct approach to the upscaling of hydraulic conductivities is not known. As an interim approach, this study uses the Äspö scaling relationships of Rhén et al. (1997) to determine the geometric mean of hydraulic conductivity in depth zone (Appendix D.5). The effect of upscaling on the variogram is determined by applying the HYDRASTAR regularisation algorithm and fitting a variogram–trend

model to the regularised data via INFERENS. The final model recommendation must be regarded as uncertain and should be evaluated via deterministic sensitivity analysis. The geometric means of K_b require adjustment to insure that the subdomain boundary fluxes are consistent with the regional model boundary fluxes (Section 1.6).

C.4.1 Exploratory Data Analysis

The analysis is based on the interpreted hydraulic conductivities of the 25m packer tests as recorded in the SICADA database. The 25m data is divided into the rock domain (RD) and conductor domain (CD) as defined by Hermanson et al. (1997). Exploratory data analysis via several software tools (Appendix D.3) reveals a skewed data distribution for the Log_{10} transform of hydraulic conductivity for both RD and CD data sets (Figures C-13 and C-14). The skewness and the censoring level of approximately 37% suggest that the data is not a promising candidate for a multivariate lognormal simulation method (e.g., the method used in HYDRASTAR).
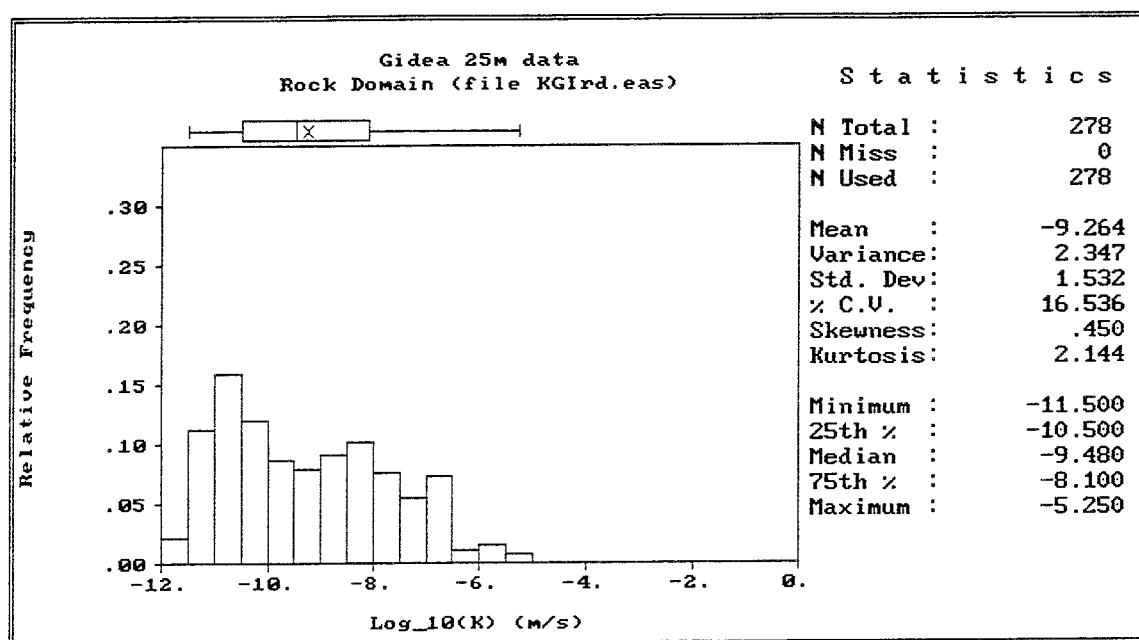
Figure C-14. Histogram of Gideå interpreted hydraulic conductivity from 25m packer test in rock domain (RD).

Preliminary variography reveals several important data characteristics. The median indicator variogram suggests that the RD data are spatially correlated out to a practical range of approximately 400m, with a moderate nugget effect (Figure C-15). A similar median indicator analysis for the CD data shows no spatial correlation structure. The censoring caused by the measurement limit should result in underestimating the total variance ($C_0 + C_1$), similar to the univariate cause (Wen,1994). An additional effect of censoring may arise from setting the censored measurements equal to the

measurement limit. If these censored measurements occur in sequence (e.g., in the lower elevations where the data is heavily censored) we should expect that censored sequence might artificially introduce correlation. Possible solutions to this (e.g., examining the variogram for only the upper levels, or indicator variography of de-trended data) have not been explored. Note that the median indicator variogram is unaffected by this measurement limit.

Unlike Äspö and Finnsjön, the borehole spacing is such that there are cross-hole data pairs at various lag spacings between boreholes KGI09 and KGI11, and also between KGI07 and KGI12. However, because the test interval is 25m there are relatively few measurements overall, which severely limits attempts at directional variography. The variogram is assumed to be isotropic, and statistical anisotropy is not pursued farther (see notes concerning anisotropic covariance and anisotropic hydraulic conductivity tensor in Section 1.6). The maximum separation distance between data pairs is approximately 2800m. By rule of thumb, the maximum fitted lag is therefore approximately 1000m.

Program restrictions of HYDRASTAR and INFERENS limit the geostatistical model to one variogram model for both domains. Because the RD data is more abundant and more promising, the geostatistical model will be developed from the RD data.
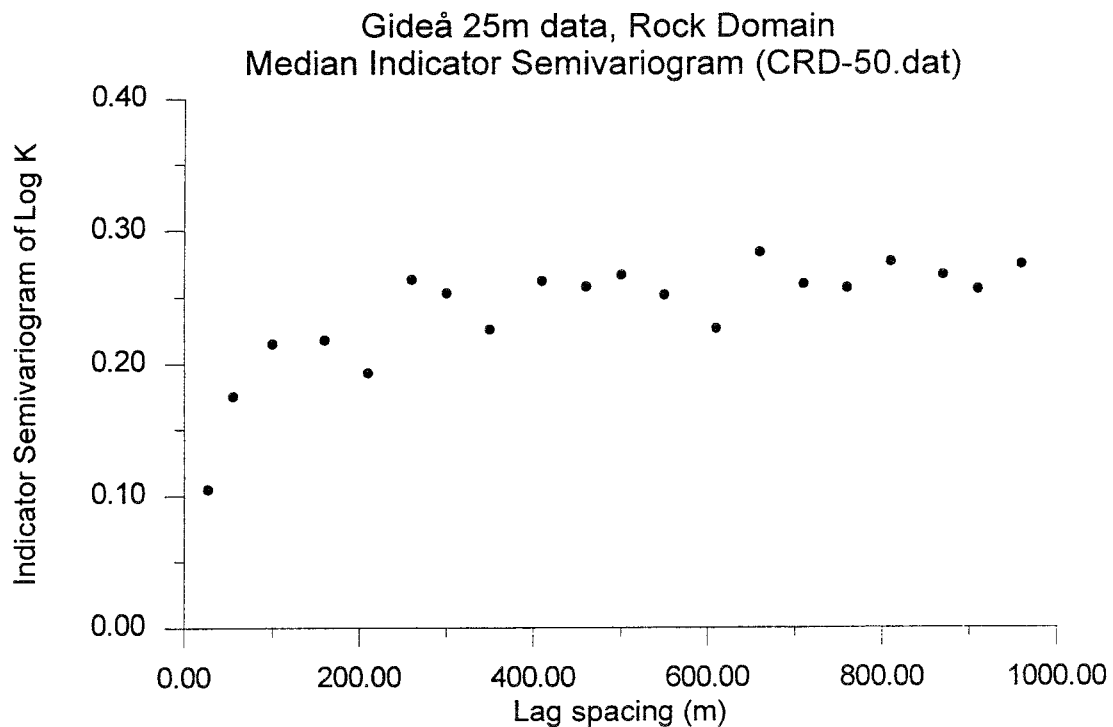

Figure C-15. Median Indicator variogram for Gideå hydraulic conductivity from 25m packer test in rock domain (RD).

C.4.2 Variography and trends

The variography begins by using INFERENS to fit a variogram with and without trends for the 25m RD data. The purpose of this step is to determine the basic structure of the 25m RD data without the complications of upscaling/regularisation. Figure C-16 presents the experimental variogram and INFERENS-fitted exponential model for the 25m data without trends. Figure C-17 presents a similar result for the same analysis but using the SRD6 trends (4 elevation zones as stepwise changes in the mean $\log_{10}$ hydraulic conductivity, i.e., 0 order trends). Including the trends in the fitting has a dramatic affect on the range, the nugget, and the total variance ($C_0 + C_1$). This suggests that much of the long-range correlation in the median indicator variogram (Figure C-15) may be the result of trend. The sill of the variogram is stable over most lags past the practical range of correlation.

One problem unique to the Gideå data is its relatively long test interval of 25m, which creates a special problem for the HYDRASTAR regularisation algorithm. This arises because the algorithm uses a corrected arithmetic mean of the adjacent measurements to upscale each measured value. The number of measurements to include in each upscaled value depends on the number of measurements that fall into a moving window representing the regularisation scale. Ideally, the number of measurements falling into this window is exactly an integer so that the measurement sections would not have to be split among upscaled measurements. Unfortunately, the proposed grid scales for SR 97 are 30 to 40m, which creates a mismatch of measurement scale and regularisation scale. Revision of the HYDRASTAR regularisation algorithm to address this problem is beyond the scope of this study. As an interim solution, this study performs the variogram/trend fitting for the measured and 50m scales. For intermediate scales, this study suggests linear interpolation between variogram model parameters at the 25 and 50m scales.

The fitting is repeated using the data regularised to 50m to estimate the possible effects of regularisation. The resulting experimental and model variograms are shown in Figure C-18. The regularisation results in small changes in the fitted model (decreased total variance and the increased range)

Table C-5 summarises the INFERENS-fitted parameters for these models for comparison. It includes the means for depth zones for both the 25m data and the upscaled data. Note that the Äspö upscaling to 50m results in different contrasts in depth zones in comparison to the INFERENS 25m results. This may be the effect of censoring on the INFERENS results, but is this is not been investigated further. At the time of writing this report, attempts to address censoring using ESTI, a variation of INFERENS (Lovius, 1994), have failed. The suggested geostatistical model for Ceberg is the model shown in bold in Table C-5, with the SCD values as discussed in Section C.3.2.

Gideå 25m data, INFERENS fit
No SRD (Cnot2)
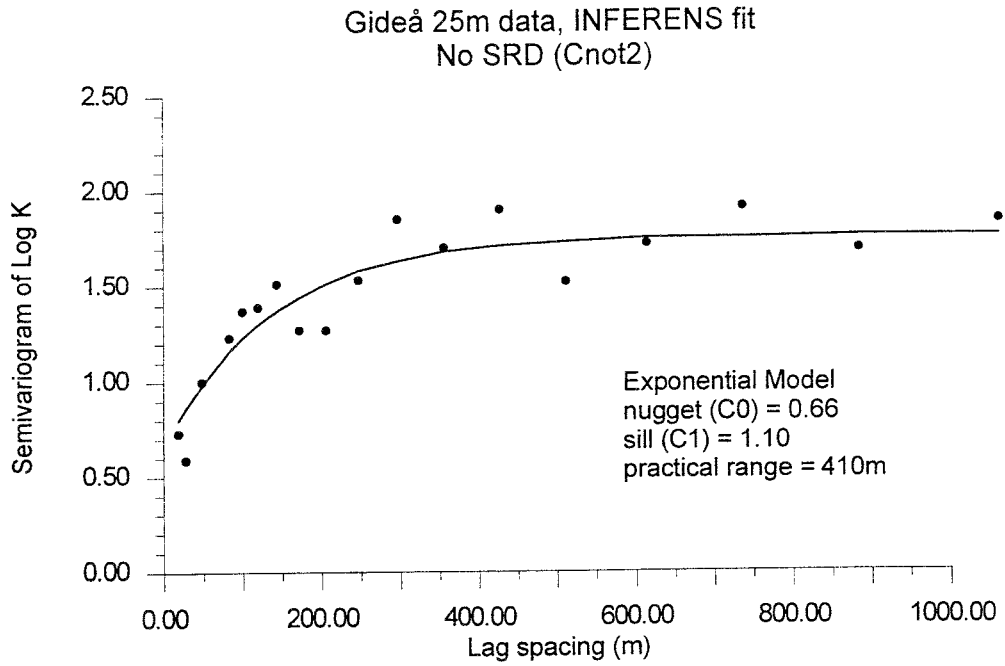
Figure C-16. Semivariogram for Ceberg hydraulic conductivity from 25m packer test in rock domain (RD). No trends or regularisation.

Gideå 25m data, INFERENS fit
Constant SRD (Ctrn3)
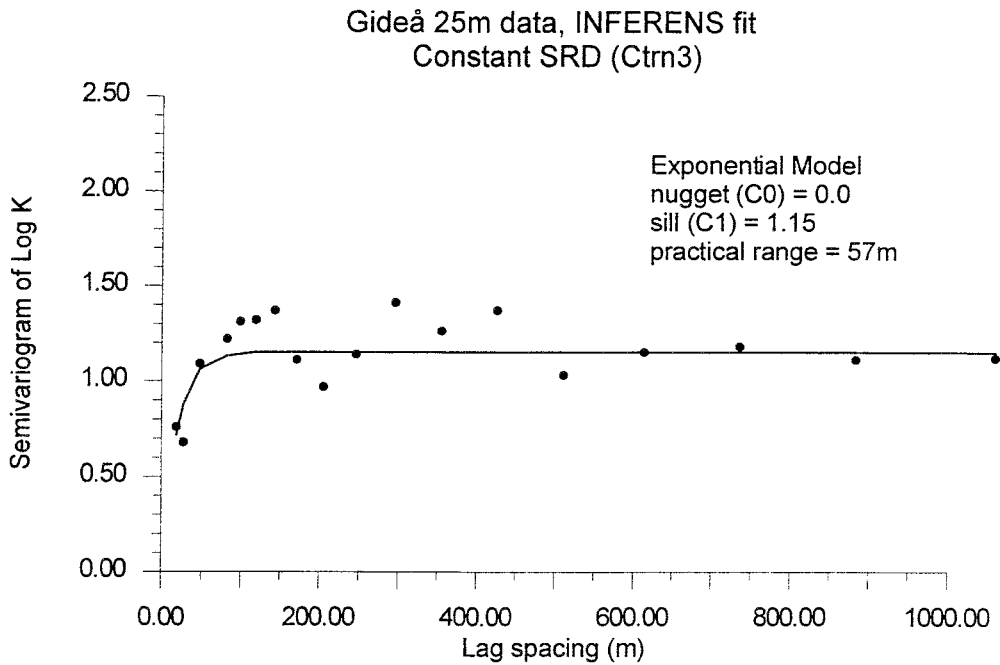
Figure C-17. Semivariogram for Ceberg hydraulic conductivity from 25m packer test in rock domain (RD). With SRD6 elevation zones as trends, no regularisation.
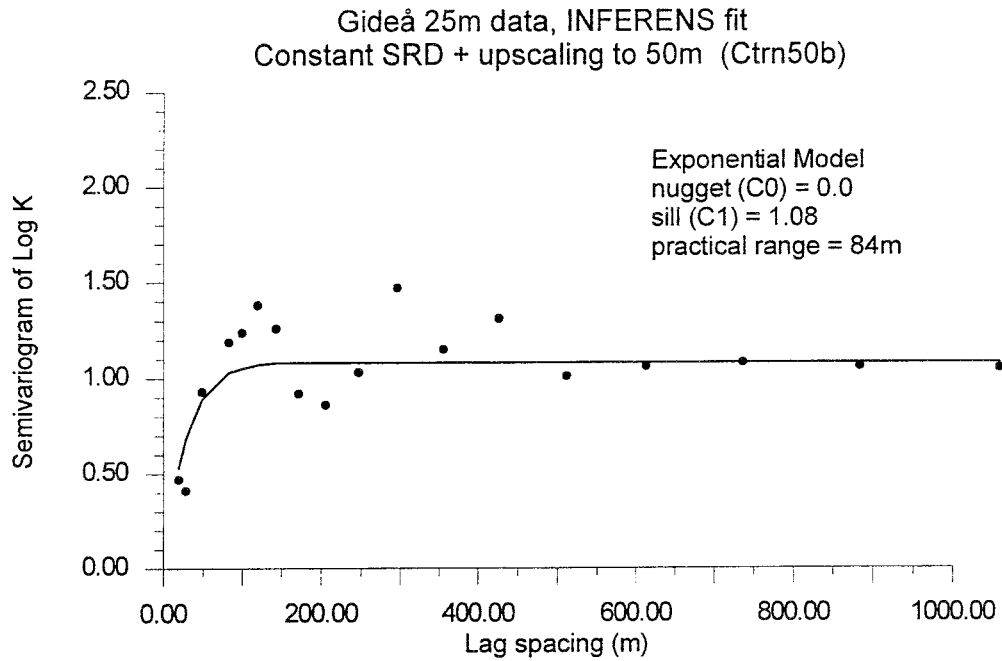
Figure C-18. *Semivariogram for Ceberg hydraulic conductivity from 25m packer test in rock domain (RD). With SRD6 elevation zones as trends and regularisation to 50m.*

Table C-5. Variography results for Ceberg rock domain hydraulic conductivity. Exponential semivariogram model for all fitted models. Suggested Ceberg model in bold.

Parameter			INFERENS		
Arithm. Mean of $Log_{10}K$	25m data*	Äspö upscaling to 50m*	25m, No Depth Zones	25m, Depth Zones	50m, Depth Zones
above 0	-7.55	**-7,32**	-	-7,70	-7,43
0 to -100	-9,04	**-8,80**	-	-8,66	-8,46
-100 to -300	-10,0	**-9,79**	-	-9,53	-9,25
Below -300	-10,3	**-10,0**	-	-9,68	-9,50
All depths	-9.69	-9,46	-9,07	-	-
Nugget C_0	-	-	0,66	0,0	**0,0**
Sill C_1	-	-	1,10	1,15	**1.08 (1.56) **
Practical Range (m)	-	-	410	57	**84**

* corrected assuming normally distributed data, after Wen (1994)
**see text below regarding censoring and the variogram

C-22

As noted in Appendix C.4.1, the data is approximately 37% censored by a lower measurement limit. As well as affecting the mean and variance of the univariate distribution of the data, it will also affect the total variance (C_0 + C_1) of the experimental variogram estimates. Except for changing over to the Indicator approach to geostatistical analysis and simulation, there is no formal solution to this problem in the literature. However, a typical correction to the standard deviation of this data is 20% (using Wen's method), which suggests a similar correction to the sill of the variogram. This translates (after working through the arithmetic) to a corrected total variance of 1.56.

Uncertainties:

The lognormal distributional assumption for this data is not well-supported, and suggests that an alternative approach be used (e.g., other data transforms or nonparametric methods). This weak assumption and the censoring effect of the measurement limit suggest that the assumed variance of 1.56 for the geostatistical model is uncertain.

C.5 CONDUCTOR DOMAIN COORDINATES

These may be found in digital form, appended to Hermanson, et al. (1997).

C.6 SICADA LOGS FOR GIDEÅ SITE DATA

C.6.1 For coordinates and 25m interpreted K values

Date   :970411 14:54:47

Tables :sic_dba.transient_inj_cd

Columns :transient_inj_cd.idcode, transient_inj_cd.seclen, transient_inj_cd.secup,

Criteria: (transient_inj_cd.idcode >='KGI01' AND

transient_inj_cd.idcode <='KGI13') AND transient_inj_cd.seclen =25

Result: 309 rows written

Filename: gi_tr.csv

Fileformat: csv

Coordinate system: RT

Coordinate calculation column: secup

C.6.2 For coordinates, 2m and 3m interpreted K values

Output to: File

Date   :970423 15:47:22

Table(s) :sic_dba.steady_state_inj_cd

Columns: steady_state_inj_cd.idcode,   steady_state_inj_cd.start_date,   steady_state_inj_cd.seclen, steady_state_inj_cd.secup, steady_state_inj_cd.k, steady_state_inj_cd.comment, steady_state_inj_cd.midpoint,

New column: midpoint=secup+seclen/2

Criteria: (steady_state_inj_cd.idcode='KGI07'OR steady_state_inj_cd.idcode='KGI09' OR

steady_state_inj_cd.idcode ='KGI11') AND (steady_state_inj_cd.seclen =2 OR

steady_state_inj_cd.seclen =3)

Result   : 225 rows written to file.

Coordinate calculations done.

Coordinate system : RT

Coordinate calculation column: secup

Filename   : /home/skbee/gi_secup.csv

File format : csv

Output to: File

Date   :970423 15:48:40

Table(s) :sic_dba.steady_state_inj_cd

Columns: steady_state_inj_cd.idcode,   steady_state_inj_cd.start_date,   steady_state_inj_cd.seclen,
steady_state_inj_cd.secup, steady_state_inj_cd.k, steady_state_inj_cd.comment, steady_state_inj_cd.midpoint,

New column: midpoint=secup+seclen/2

Criteria:(steady_state_inj_cd.idcode='KGI07'OR steady_state_inj_cd.idcode ='KGI09' OR

steady_state_inj_cd.idcode ='KGI11') AND (steady_state_inj_cd.seclen =2 OR

steady_state_inj_cd.seclen =3)

Result   : 225 rows written to file.

Coordinate calculations done.

Coordinate system : RT

Coordinate calculation column: midpoint

Filename   : /home/skbee/gi_mid.csv

File format : csv

C-24

C.7 CEBERG PARAMETER SOURCES

	Source	Treatment	Availability
REGIONAL			
Geology			
Rock type	SKBF KBS TR 83-53 SKB R-97-05 SGU ser. BA 31	Compilation	(1)
Lineaments	SKBF KBS TR 83-53 SKB PR U-97-05 SGU ser. BA 31	Compilation	(1)
Land rise	SKB TR 92-38	Interpolation	(1)
Geochemistry and Salinity	Laaksoharju et al. 1997 (SKB R 97-X)	Compilation	(1)
Hydrology			
Recharge pattern and rates	SKBF KBS TR 83-56 SKBF KBS TR 83-26	Compilation	(1)
Groundwater flow patterns	SKBF KBS TR 83-56 SKBF KBS TR 83-26	Compilation	(1)
Hydraulic Parameters			
Rock Mass K	SGU 1996 SICADA 1997	Compilation, statistical analysis, rescaling	(1)
Conductor Location, K	SKBF KBS TR 83-53 SKB R-97-05 SKB PR U-97-05 SICADA 1997	Compilation, statistical analysis, rescaling	(1), Digital
Anisotropy	SKB TR 86-19	Compilation	(1)
Scale relationships	SKB TR 97-06	Compilation	(1)
SITE			
Geology	SKBF KBS TR 83-53 SKB R-97-05	Compilation	(1)
Hydrology			
Surface Hydrology	SKBF KBS TR 83-56 SKBF KBS TR 83-26	Compilation	(1)
Groundwater Flow Patterns	SKBF KBS TR 83-56 SKBF KBS TR 83-26	Compilation	(1)
Hydraulic properties			
Rock Mass K	SICADA 1997	Statistical analysis of 25m data, rescaling	SICADA
Conductor Location, K	SICADA 1997 SKB R-97-05	Compilation, statistical analysis of 25m data, rescaling	SICADA Appendix C Digital
EDZ	SKB ICR 96-03, Olsson and Winberg, 1997 (unpublished SKB PM)	Compilation	(1)
Anisotropy	SKB TR 86-19	Compilation	(1)
Geostatistics, Scale relationships	SICADA 1997 SKB TR 97-06	Variography, Universal Kriging on 25m data, rescaling	(1)

(1) see the Source report

APPENDIX D. CALCULATION NOTES

D.1 SGU WELL ARCHIVE DATA REDUCTION

The Swedish Geological survey (SGU) maintains a database of water wells drilled throughout Sweden, which includes the RAK X,Y coordinates, total boring depth, soil depth (depth to bedrock) and the well's water capacity (vattenmangd). The well's water capacity is assumed to be the well's production capacity in litres per hour under maximum drawdown conditions. Assuming that the full length of the borehole is the drawdown, we can determine the well's specific capacity, Q/dh.

Although there are published methods for reducing specific capacity to transmissivity and hydraulic conductivity (e.g., Domenico and Schwartz, 1990), such methods require some information regarding the transient behaviour of the well. As an alternative approximation at Äspö, Carlsson and Gustafsson (1984) and Rhén et al. (1997) have constructed site-specific regression equations for transmissivity versus specific capacity for wells where both variables were measured (Figure D-1). This regression equation could then be used to estimate the transmissivity of SGU wells in the area. Unfortunately, such a regression of transmissivity versus specific capacity is not possible for the all three sites, since the well tests at Finnsjön and Gideå did not record specific capacity data (Ludvigsson, personal communication, 1997). This study consequently relies on the Äspö regression equations for 50 to 200m scale, provided by Rhén et al., 1997:

$$Log_{10}(T) = 0.16 + 0.93 Log_{10}\left(\frac{Q}{dh}\right)$$

where: T = transmissivity (m2/sec)

Q/dh = specific capacity (m3/sec*m)

This can be further reduced to hydraulic conductivity by dividing by the test section length, assumed to be the total borehole length. Note that many assumptions have been required to reduce the SGU water capacity to hydraulic conductivity reducing the reliability of this data.

D.2 SELECTING A CONSISTENT SUBSET OF SGU WELL DATA

The initial sets of SGU data are not all the data is considered valid for use in determining the regional hydraulic conductivity of the bedrock. Usually, a small number of wells have reported water capacities of 0 litres/hr. If the censored proportion is relatively small (order of 5% or less) these may be discarded without dramatically biasing the parameter estimates. Similar to Liedholm (1991) and Jönsson, et al. (1997), shallow wells dominated by surficial aquifers are also deleted from the sets since these were not

considered to be representative of the bedrock. Very long and very shallow wells are discarded to be consistent with the scale of the T vs. Q/dh regression equation of Rhén et al. (1997). All of the above conditions thus require discarding wells with:

- less than 10m total depth in bedrock

- less than 75% bedrock depth

- overburden depth greater than 20m

- total depth (the test section length) less than 50m

- total depth greater than 200m.

Duplicate measurements are also deleted, retaining the deepest well of the duplicated location. Additional wells may also be deleted if, by inspection of h-scattergrams, it is judged to be an outlier (extremely high relative to its neighbouring measurements).
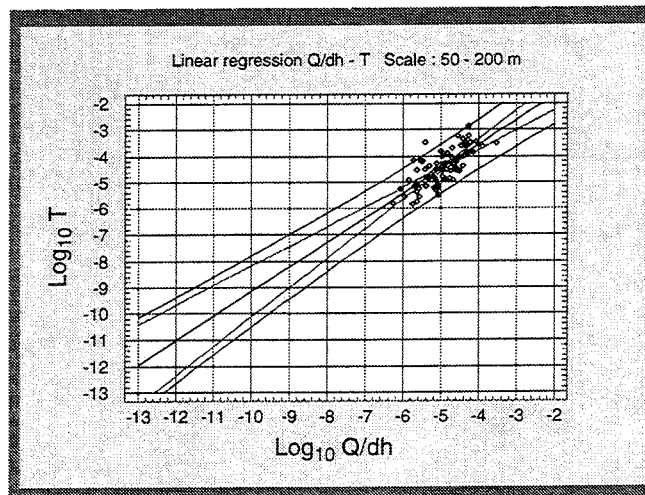
Figure D-1. Regression of $Log_{10}(T)$ versus $Log_{10}(Q/dh)$, based on Äspö data. Inner pair of lines is the 95% CI for the mean, outer pair of lines is the 95% CI for prediction.

D.3 GEOSTATISTICAL SOFTWARE

Several packages were used in the analysis of the data for this report, as listed below:

GeoEAS (Englund and Sparks, 1991). This is an MSDOS program developed by the U.S. Environmental Protection Agency and Stanford University to assist in Geostatistical Environmental Assessment. It is used in this study for exploratory data analysis, including univariate statistics,

2-D variography, outlier analysis and data manipulation. In the case of regional models for hydraulic conductivity, it is also used for cross-validation of model semivariograms. All SICADA data files are converted to GeoEAS format prior to analysis in this study.

VarioWin (Pannatier, 1997) a 2-D directional variography package that is used for exploratory data analysis (similar to GeoEAS).

EDAVar (INTERA, 1995). This is a 2-D variography and exploratory data analysis (EDA) package developed by INTERA. It is an enhanced version of GeoEAS with additional EDA tools and variogram fitting options. It is used in this study to assist in identifying directional anisotropy.

GSLIB (Deutsch and Journel, 1992). GSLIB is a comprehensive set of FORTRAN programs for geostatistical analysis, estimation and simulation. It provides the declustering algorithm used in this study, cited as Deutsch, 1989.

UNCERT (Wingle et al., 1996). This is a GeoEAS-like geostatistical software package for UNIX environments, which emphasises indicator geostatistics. It is used in this study for exploratory data analysis, 3-D variography, and indicator variography.

INFERENS (Norman, 1992a; Geier, 1993a). INFERENS is a FORTRAN program developed by SKB that incorporates the HYDRASTAR regularisation algorithm and Universal Kriging via iterative generalised least squares estimation (IGLSE). It is necessary in this study because each of the sites in SR 97 divide the model domain into a series of fracture zones, rock masses and depth zones that represent stepwise changes in the hydraulic conductivity. HYDRASTAR represents this complex hydraulic conductivity field as a multivariate lognormal regionalised variable with local trends in Log_{10} hydraulic conductivity. A single variogram model is inferred for the entire domain (i.e., the same variogram for SRD, SCD, etc.). Although not a restriction of HYDRASTAR itself, this study will consider the trends as constants within well-defined volumes in the domain (0 order trends in Log_{10} K_b). This complex model of trend and spatial correlation violates the assumptions of ordinary least squares estimation (i.e., fitting trends by simple least squares regression). This study instead uses the more versatile IGLSE for universal kriging suggested by Neuman and Jacobsen (1984). INFERENS is an SKB computer program for geostatistical inference that automates the IGLSE fitting and data exploration (Norman, 1992a). INFERENS is unique in that includes the same regularisation algorithm as HYDRASTAR to upscale the data and apply universal kriging.

Thus the resulting model of trends and covariance are compatible with the conditioning data and the chosen grid scale.

A programming bug prohibited using the crossvalidation option in INFERENS for this study. Alternative methods that met QA standards were not readily available during this study, therefore crossvalidation was omitted.

D.4 CORRECTING UNIVARIATE STATISTICS FOR MEASUREMENT LIMITS

Measurement limits are common in observed data, and are present in most of the interpreted hydraulic conductivity data examined in SR 97. Measurement limits are important because they censor the data set, which can result in biased estimators of the mean and variance of the data. Consider, for example, when the data have a symmetric probability distribution function (e.g., the normal distribution) and are censored by a lower measurement limit. In such a case, the sample mean will tend to overestimate the true mean and the sample variance will tend to underestimate the true variance. The magnitude of the bias increases with the degree of censoring (Gilbert, 1987; Wen, 1994; Kroll and Stedinger, 1996)

For the simple univariate case (i.e., the data are uncorrelated) with known underlying probability distribution, censoring can be addressed with the Maximum Likelihood Estimator (MLE) approach. Cohen (1959), for example, presents a series of tables for the univariate normal case, and Gilbert (1987) presents an example of this technique. However, the calculations of the MLE approach are sufficiently cumbersome that the method is not widely used in hydrogeology. Wen (1994) assumed an underlying univariate normal distribution and found an analytical solution for the true mean and variance given the mean and variance estimated from the data above the measurement limit. Wen's solution is not exact, because it requires an iterative solution for finding the roots of a quadratic equation. However, it yields results virtually identical to the MLE approach and does not require the use of tables. Wen (1994) applied this method to Finnsjön Log_{10} hydraulic conductivity data and showed that the mean and variance were badly estimated if the censoring effects of the measurement limit were ignored.

In the case of spatially correlated data, it is common to look at the histogram of the data and conclude that it is normally distributed. This is misleading, since the geostatistical simulation algorithms used in SR 97 actually require that the *estimation errors* at each location in the domain to be normally distributed. Furthermore, the spatial correlation in the data requires that the error distribution be a function of (conditional to) the surrounding data. In such a case, it is more correct to describe the data as having a *multivariate* normal distribution. (Norman, 1992a; Deutsch and Journel, 1992). In this case, corrections to the mean and variance assuming a *univariate* normal distribution (e.g., Wen, 1994) may be inappropriate, depending on the strength of the spatial correlation.

The literature presents two possible solutions for dealing with censored, spatially correlated data. The most direct method is to use the indicator approach to geostatistical analysis and simulation. This approach easily incorporates a measurement limit as an indicator cutoff level and simultaneously avoids the unrealistic assumption of multivariate normality. (Deutsch and Journel, 1992; Kung, et al., 1992; Tsang, 1996). Unfortunately, the approach has not been incorporated into HYDRASTAR, the stochastic continuum groundwater flow simulation program proposed for SR 97.

A second alternative is suggested by Lovius (1994), to use conditional simulation to estimate the value of the censored data, followed by re-estimation of the variogram. This iterative approach has been coded as ESTI, which uses INFERENS to iteratively estimate, simulate and re-estimate the variogram. At the time of writing this report, only a few experimental results are available, and it is not known if the approach is stable.

D.5 ÄSPÖ SCALE RELATIONSHIPS

The models for hydraulic conductivity at each site are based on injection tests with a fixed packer interval. However, such hydraulic tests are apparently scale dependent, suggesting that an empirical upscaling might be constructed by regressing hydraulic conductivity versus scale using the multi-scale injection tests, air-lift tests and pump tests of the entire borehole. Such multi-scale data are available at Äspö, but not at Finnsjön or Gideå. Even at Äspö, there are generally neither all test scales in neither all boreholes nor all test scales along an entire borehole length. Consequently, the scale relationships are evaluated using just the Äspö data, and only for borehole sections where injection tests with 3 m packer spacing were performed along with longer test intervals.

The empirical relationship between the test scale and hydraulic conductivity presented in Wikberg et al (1991) was re-evaluated by Rhén et al. (1997) and the result is shown in Figure D-2 and Table D-1. The arithmetic mean, geometric mean and standard deviation for each borehole are also shown in Figure D-2. For each borehole the statistics for the equivalent hydraulic conductivity (K) was calculated for each test scale (equivalent hydraulic conductivity = transmissivity/length of tested section). The statistical measures were the mean of Log_{10} (K) and the standard deviation of Log_{10} (K).

The mean of Log_{10} (K) and the standard deviation of Log_{10} (K) for a rock or conductor domain is given for a specified test scale in this report. When generating the hydraulic conductivity field in a numerical model, the cell size in the model should be used to scale the values of the statistical distribution to be used for generating the field.
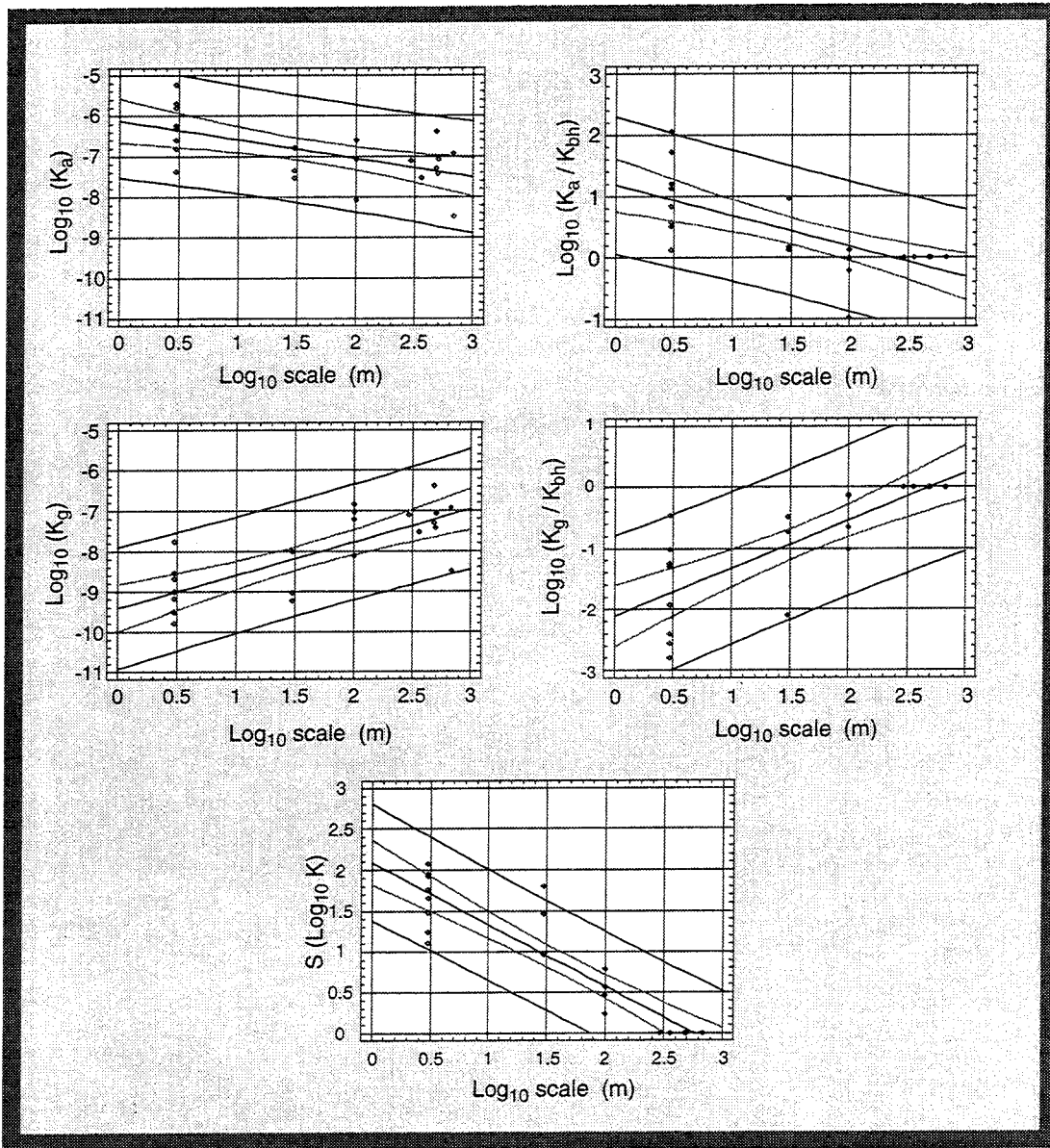
Figure D-2. Regression of Y versus Log_{10} (scale). $Y=Log_{10}$ (K_a/K_{bh}), Log_{10} (K_g/K_{bh}) or $s(Log_{10}(K))$. K=hydraulic conductivity (m/s), K_a =arithmetic mean, K_g =geometric mean. K_{bh}= mean K of entire borehole with correction for test sections outside the range for other test scales. Note that values of K appear to stabilise at measurement scale of approximately 300 to 500m; this is an artifact, since that scale is the entire borehole length. Standard deviations at this last scale are set to zero. Boreholes: KAS02-08, KLX01.
Inner pair of lines : 95 % confidence band on mean of Y.
Outer pair of lines: 95% prediction band on Y as a function of $Log_{10}(scale)$.

Such multi-scale data are not available at Gideå and Finnsjön in sufficient density to establish similar relationships. Therefore, the Äspö regression equations will be used for all three sites, adapted for use as relative scaling functions as:

$$Log_{10}K_{gu} = Log_{10}K_{gm} + 0.782(Log_{10}L_u - Log_{10}L_m)$$

$$s(Log_{10}K)_u = s(Log_{10}K)_m\left(\frac{Y_u}{Y_m}\right)$$

where:

$$Y_u = 2.089 - 0.758Log_{10}L_u$$

$$Y_m = 2.089 - 0.758Log_{10}L_m$$

K_g = geometric mean of hydraulic conductivity (m/s)

$s(Log_{10}K)$ = standard deviation of $Log_{10}K$ (m/s)

L = length scale (m/s)

and the subscripts m and u refer to the measurement and upscaled values, respectively.

Note that the use of the arithmetic mean of Log_{10} (K) (i.e., the geometric mean of the hydraulic conductivity, in m/s) implies the use of the lognormal probability distribution for stochastic simulation. The base cases presented here assume lognormally distributed hydraulic conductivities after Freeze (1979). This not a necessity, since other transforms and approaches might be more appropriate.

Table D-1.   The linear relationship between Y and Log_{10} (scale). Y=Log_{10} (K_a / K_{bh}), Log_{10} (K_g / K_{bh}) or s(Log_{10} (K)). K=hydraulic conductivity, K_a =arithmetic mean, K_g =geometric mean, K_{bh} = equivalent hydraulic conductivity for the entire borehole, s(Log_{10} (K))= standard deviation of Log_{10} (K), Entire borehole length length≈ 500 m. Y=a+b·Log_{10}(scale). ρ=Correlation coefficient .

Y	a	b	ρ
$Log_{10}(K_a/K_{bh})$	1.184	-0.50	-0.70
$Log_{10}(K_g/K_{bh})$	-2.107	0.782	0.80
s($Log_{10}(K)$)	2.089	-0.758	-0.92

D.6 COMPARISION OF SCALE RELATIONSHIPS FOR EFFECTIVE HYDRAULIC CONDUCTIVITY

This report discusses several relationships that attempt to address the apparent scale dependency of K_e, the effective hydraulic conductivity, and also that of K_b, the block hydraulic conductivity. Although this study emphasises the regression relationships developed from the Äspö hydraulic tests (Appendix D.5), it is reasonable to ask if the Äspö regression relationships are comparable to other approaches. This appendix briefly compares several possible approaches to the problem of scale dependency. The theory and definitions of these approaches are summarised in Section 1.6; readers interested in more detail are referred to Gelhar, (1986 and 1993).

The three approaches considered in this study include:

- The Äspö regression relationships developed by Wikberg, et al., (1991) and Rhén et al., (1997) (Appendix D.5)

- The analytical solutions of Gutjahr, et al. (1978), based on stochastic continuum theory.

- The HYDRASTAR regularisation algorithm of Norman (1992a).

Each of the above-named approaches is used to estimate K_b, the geometric mean block hydraulic conductivity for a numerical stochastic continuum model. The Äspö data is used as an example, assuming a cubic grid block, 30m on each side, is assumed.

For this comparison, the first step is to estimate K_e. As was discussed in Section 1.6, this is nontrivial since even the existence of K_e may be difficult to establish. If K_e exists for a particular domain, the domain must be large, statistically homogeneous and under uniform flow conditions. In practice, domains of size $L > 10\lambda$ are sufficiently large for K_e to exist (where λ is the integral scale of K). For the 3m data at Äspö, various authors have given a range of 10 to 30m for λ (Liedholm, 1991b; LaPointe, 1994; Niemi, 1995). This study found that for 3m data in the rock domain, the practical range of an exponential variogram model could be between 100 and 200m (Appendix A.3). With a 50% nugget variance, this results in a λ between 15 and 30m. Therefore, it is possible that K_e can exist at 100 to 300m. Large scale borehole tests at Äspö indicate that the value of K begins to stabilise at approximately 100m test scale, with a mean $Log_{10} K = -7.2$ (i.e., geometric mean $K = 6.3 \times 10^{-8}$ m/s) (Nilsson, 1989; Niemi 1995; Appendix D.5). We will assume $K_e = 6.3 \times 10^{-8}$ m/s to exist at $L_e = 100$ to 300m.

The next step is to determine K_b, the geometric mean hydraulic conductivity of a block in a stochastic continuum model represented by K_e. If we assume a 30m block and use the above value of K_e and range of L_e, the Äspö regression relationships yield a range of $1.0 \times 10^{-8} \leq K_b \leq 2.5 \times 10^{-8}$ m/s.

Gutjahr et al. (1978) assumed that the fields were multivariate lognormal fields and used a perturbation approach to derive several analytical solutions for K_e for various flow regimes. For 3-D, isotropic hydraulic conductivity (statistically isotropic and with an isotropic tensor), Gutjahr et al. (1978) found:

$$K_e = K_g \left(1 + \frac{\sigma^2_{\ln K}}{6}\right)$$

If we want to determine K_b at 30m, we rearrange the above equation to solve for $K_g = K_b$. The variance of the natural log of K, $\sigma^2_{\ln K}$ should be taken from the observed variability of the 30m data, given by Nilsson (1989) as $\sigma^2_{\ln K} = 10$. After substitution, this yields $K_b = 2.4 \times 10^{-8}$ m/s. Note, however, that this analytical solution is only thought to be valid for $\sigma^2_{\ln K}$ on the order of 1.0.

Both the 3m packer test data and the large-scale tests in the Laxemar boreholes suggest that the flow system is 2-D, not 3-D (Sven Follin, personal communication, 1997; Geier et al., 1996). For the perfectly stratified, 2-D isotropic case, Gutjahr et al.(1978) give:

$$K_e = K_g \left(1 + \frac{\sigma^2_{\ln K}}{2}\right)$$

If we rearrange, substitute and solve as before, this yields $K_b = 1.05 \times 10^{-8}$ m/s. Again this analytical solution is only thought to be valid for $\sigma^2_{\ln K}$ on the order of 1.0.

The third and final approach to compare is the HYDRASTAR regularisation algorithm. In this case, we use INFERENS to regularise the 3m data up to the 30m scale. Unlike the geostatistical analyses in Appendices A, B and C, we do not separate the data into rock and conductor domains, since the K_e of the large boreholes have not been separated. Thus the mean $Log_{10} K = -9.1$ of the Rhén interpretation of the 3m hydraulic conductivity data is regularised to a 30m $Log_{10} K_b = -7.59$. That is, the HYDRSTAR regularisation algorithm yields $K_b = 2.6 \times 10^{-8}$ m/s.

Table D-2 summarises the results of this comparison. Although all results are within a factor of 3 of each other, none of them satisfactorily predict the observed 30m geometric mean. As discussed in Section 1.6, this may be a result of violating of the underlying assumptions when applying these approaches to the Äspö site. It may also be the result of misinterpreting a 30m packer test as having a 30m measurement scale. Regardless of the cause, this study suggests resolving this ambiguity by calibrating the final choice of K_e and K_b to observed data.

Table D-2. Summary of results for alternative approaches to the scale dependency of hydraulic conductivity at Äspö.

Approach	Assumption	K_b (m/s)
Äspö Regression	$L_e = 100m$	2.5×10^{-8}
	$L_e = 300m$	1.0×10^{-8}
Gutjahr et al. (1978)	3-D	2.4×10^{-8}
	2-D	1.1×10^{-8}
HYDRASTAR/ INFERENS	-	2.6×10^{-8}
Observed (Nilsson, 1989)	-	4×10^{-9}

D.7 CONVERTING SALINITY TO DENSITY

The relationship between the water density and electrical conductivity for Äspö at 25°C was estimated for waters sampled during the pre-investigation phase (Nilsson 1989). This relationship was later slightly modified (Rhén et al. 1994b) and the relationship between the electrical conductivity (C), salinity (S) and the density of pure water (ρ_0) and the density of saline water (ρ) can be estimated using:

$$\rho = \rho_0(T) + 0.00467 * C$$
$$\rho = \rho_0(T) + 0.741 * S$$

ρ	=	Density of saline water	(kg/m^3)
ρ_0	=	Density of pure water	(kg/m^3)
C	=	Electrical conductivity of water	(mS/m)
S	=	Salinity	(g/L)
T	=	Temperature	$(°C)$

D.8 EXCAVATION DISTURBED ZONE (EDZ)

Construction of the repository necessitates the excavation of extensive tunnels, shafts and vaults. Such construction may involve drilling, blasting, boring, and grouting, all of which could affect the hydraulic, mechanical and thermal properties of the surrounding host rock. One commonly held view is that the combination of stress relief and excavation damage will decrease the hydraulic conductivity perpendicular to the tunnel axis, and increase the hydraulic conductivity parallel to the tunnel axis (Olsson and Winberg, 1996). If this model is true, such changes in the excavation disturbed zone (EDZ) could influence groundwater flow and radionuclide transport. A summary of EDZ experiments world wide, at Stripa and at the Äspö HRL tentatively agreed with that commonly-held model (Olsson, et al., 1996). However, Olsson and Winberg (1996) re-evaluated those experiments and concluded that:

- There is little evidence to support an increased hydraulic conductivity parallel to the long axis of the tunnel

- There is some evidence of increased hydraulic conductivity in the floor of a blasted drift, but this zone is restricted to within one metre of the tunnel floor.

- The significance of the EDZ as a pathway is overestimated.

Therefore, the base case model for the excavation disturbed zone, EDZ1, has no change in the hydraulic conductivity of the surrounding host rock. However, Olsson and Winberg (1996) also indicated that the current understanding of the hydraulic conductivity of the EDZ is poorly understood. This study suggests evaluating the uncertainty with an alternative model, EDZ2, which allows for an order of magnitude increase of the host rock hydraulic conductivity parallel to the tunnel axis, extending 25cm into the rock surrounding the tunnel.

List of SKB reports

Annual Reports

1977-78
TR 121
KBS Technical Reports 1 – 120
Summaries
Stockholm, May 1979

1979
TR 79-28
The KBS Annual Report 1979
KBS Technical Reports 79-01 – 79-27
Summaries
Stockholm, March 1980

1980
TR 80-26
The KBS Annual Report 1980
KBS Technical Reports 80-01 – 80-25
Summaries
Stockholm, March 1981

1981
TR 81-17
The KBS Annual Report 1981
KBS Technical Reports 81-01 – 81-16
Summaries
Stockholm, April 1982

1982
TR 82-28
The KBS Annual Report 1982
KBS Technical Reports 82-01 – 82-27
Summaries
Stockholm, July 1983

1983
TR 83-77
The KBS Annual Report 1983
KBS Technical Reports 83-01 – 83-76
Summaries
Stockholm, June 1984

1984
TR 85-01
**Annual Research and Development
Report 1984**
Including Summaries of Technical Reports Issued
during 1984. (Technical Reports 84-01 – 84-19)
Stockholm, June 1985

1985
TR 85-20
**Annual Research and Development
Report 1985**
Including Summaries of Technical Reports Issued
during 1985. (Technical Reports 85-01 – 85-19)
Stockholm, May 1986

1986
TR 86-31
SKB Annual Report 1986
Including Summaries of Technical Reports Issued
during 1986
Stockholm, May 1987

1987
TR 87-33
SKB Annual Report 1987
Including Summaries of Technical Reports Issued
during 1987
Stockholm, May 1988

1988
TR 88-32
SKB Annual Report 1988
Including Summaries of Technical Reports Issued
during 1988
Stockholm, May 1989

1989
TR 89-40
SKB Annual Report 1989
Including Summaries of Technical Reports Issued
during 1989
Stockholm, May 1990

1990
TR 90-46
SKB Annual Report 1990
Including Summaries of Technical Reports Issued
during 1990
Stockholm, May 1991

1991
TR 91-64
SKB Annual Report 1991
Including Summaries of Technical Reports Issued
during 1991
Stockholm, April 1992

1992
TR 92-46
SKB Annual Report 1992
Including Summaries of Technical Reports Issued
during 1992
Stockholm, May 1993

1993
TR 93-34
SKB Annual Report 1993
Including Summaries of Technical Reports Issued
during 1993
Stockholm, May 1994

1994
TR 94-33
SKB Annual Report 1994
Including Summaries of Technical Reports Issued
during 1994
Stockholm, May 1995

1995
TR 95-37
SKB Annual Report 1995
Including Summaries of Technical Reports Issued
during 1995
Stockholm, May 1996

1996
TR 96-25
SKB Annual Report 1996
Including Summaries of Technical Reports Issued
during 1996
Stockholm, May 1997

List of SKB Technical Reports 1997

TR 97-01
**Retention mechanisms and the flow
wetted surface – implications for safety
analysis**
Mark Elert
Kemakta Konsult AB
February 1997

TR 97-02
**Äspö HRL – Geoscientific evaluation
1997/1. Overview of site characterization
1986–1995**
Roy Stanfors[1], Mikael Erlström[2],
Ingemar Markström[3]
[1] RS Consulting, Lund
[2] SGU, Lund
[3] Sydkraft Konsult, Malmö
March 1997

TR 97-03
**Äspö HRL – Geoscientific evaluation
1997/2. Results from pre-investigations
and detailed site characterization.
Summary report**
Ingvar Rhén (ed.)[1], Göran Bäckblom (ed.)[2],
Gunnar Gustafson[3], Roy Stanfors[4], Peter Wikberg[2]
[1] VBB Viak, Göteborg
[2] SKB, Stockholm
[3] VBB Viak/CTH, Göteborg
[4] RS Consulting, Lund
May 1997

TR 97-04
**Äspö HRL – Geoscientific evaluation
1997/3. Results from pre-investigations
and detailed site characterization.
Comparison of predictions and
observations. Geology and
mechanical stability**
Roy Stanfors[1], Pär Olsson[2], Håkan Stille[3]
[1] RS Consulting, Lund
[2] Skanska, Stockholm
[3] KTH, Stockholm
May 1997

TR 97-05
**Äspö HRL – Geoscientific evaluation
1997/4. Results from pre-investigations
and detailed site characterization.
Comparison of predictions and observa-
tions. Hydrogeology, groundwater
chemistry and transport of solutes**
Ingvar Rhén[1], Gunnar Gustafson[2], Peter Wikberg[3]
[1] VBB Viak, Göteborg
[2] VBB Viak/CTH, Göteborg
[3] SKB, Stockholm
June 1997

TR 97-06
**Äspö HRL – Geoscientific evaluation
1997/5. Models based on site character-
ization 1986–1995**
Ingvar Rhén (ed.)[1], Gunnar Gustafson[2],
Roy Stanfors[4], Peter Wikberg[4]
[1] VBB Viak, Göteborg
[2] VBB Viak/CTH, Göteborg
[3] RS Consulting, Lund
[4] SKB, Stockholm
October 1997

TR 97-07
**A methodology to estimate earthquake
effects on fractures intersecting canister
holes**
Paul La Pointe, Peter Wallmann, Andrew Thomas,
Sven Follin
Golder Associates Inc.
March 1997

TR 97-08
**Äspö Hard Rock Laboratory
Annual Report 1996**
SKB
April 1997

TR 97-09
**A regional analysis of groundwater flow
and salinity distribution in the Äspö area**
Urban Svensson
Computer-aided Fluid Engineering AB
May 1997

TR 97-10
On the flow of groundwater in closed tunnels. Generic hydrogeological modelling of nuclear waste repository, SFL 3–5
Johan G Holmén
Uppsala University/Golder Associates AB
June 1997

TR 97-11
Analysis of radioactive corrosion test specimens by means of ICP-MS. Comparison with earlier methods
R S Forsyth
Forsyth Consulting
July 1997

TR 97-12
Diffusion and sorption properties of radionuclides in compacted bentonite
Ji-Wei Yu, Ivars Neretnieks
Dept. of Chemical Engineering and Technology, Chemical Engineering, Royal Institute of Technology, Stockholm, Sweden
July 1997

TR 97-13
Spent nuclear fuel – how dangerous is it? A report from the project "Description of risk"
Allan Hedin
Swedish Nuclear Fuel and Waste Management Co,
Stockholm, Sweden
March 1997

TR 97-14
Water exchange estimates derived from forcing for the hydraulically coupled basins surrounding Äspö island and adjacent coastal water
Anders Engqvist
A & I Engqvist Konsult HB, Vaxholm, Sweden
August 1997

TR 97-15
Dissolution studies of synthetic soddyite and uranophane
Ignasi Casas[1], Isabel Pérez[1], Elena Torrero[1], Jordi Bruno[2], Esther Cera[2], Lara Duro[2]
[1] Dept. of Chemical Engineering, UPC
[2] QuantiSci SL
September 1997

TR 97-16
Groundwater flow through a natural fracture. Flow experiments and numerical modelling
Erik Larsson
Dept. of Geology, Chalmers University of Technology, Göteborg, Sweden
September 1997

TR 97-17
A site scale analysis of groundwater flow and salinity distribution in the Äspö area
Urban Svensson
Computer-aided Fluid Engineering AB
October 1997

TR 97-18
Release of segregated nuclides from spent fuel
L H Johnson, J C Tait
AECL, Whiteshell Laboratories, Pinawa, Manitoba, Canada
October 1997

TR 97-19
Assessment of a spent fuel disposal canister. Assessment studies for a copper canister with cast steel inner component
Alex E Bond, Andrew R Hoch, Gareth D Jones, Aleks J Tomczyk, Richard M Wiggin, William J Worraker
AEA Technology, Harwell, UK
May 1997

TR 97-20
Diffusion data in granite. Recommended values
Yvonne Ohlsson, Ivars Neretnieks
Department of Chemical Engineering and Technology, Chemical Engineering, Royal Institute of Technology, Stockholm, Sweden
October 1997

TR 97-21
Investigation of the large scale regional hydrogeological situation at Ceberg
Anders Boghammar[1], Bertil Grundfelt[1], Lee Hartley[2]
[1] Kemakta Konsult AB, Sweden
[2] AEA Technology, UK
November 1997

TR 97-22
**Investigations of subterranean
microorganisms and their importance
for performance assessment of
radioactive waste disposal. Results
and conclusions achieved during the
period 1995 to 1997**

Karsten Pedersen
Göteborg University, Institute of Cell and
Molecular Biology, Dept. of General and Marine
Microbiology, Göteborg, Sweden

November 1997